ISTANBUL TECHNICAL UNIVERSITY ★ GRADUATE SCHOOL OF SCIENCE ENGINEERING AND TECHNOLOGY

FABRICATION AND CHARACTERIZATION OF NANOCOMPOSITE FLAT-SHEET POLYMERIC MEMBRANES

M.Sc. THESIS

Merve ŞİLE

Graduate School of Science Engineering and Technology

Nanoscience and Nanoengineering Programme

JUNE 2013

ISTANBUL TECHNICAL UNIVERSITY ★ GRADUATE SCHOOL OF SCIENCE ENGINEERING AND TECHNOLOGY

FABRICATION AND CHARACTERIZATION OF NANOCOMPOSITE FLAT-SHEET POLYMERIC MEMBRANES

M.Sc. THESIS

Merve ŞİLE
(513101030)

Graduate School of Science Engineering and Technology

Nanoscience and Nanoengineering Programme

Thesis Advisor: Prof. Dr. İsmail KOYUNCU

JUNE 2013

İSTANBUL TEKNİK ÜNİVERSİTESİ ★ FEN BİLİMLERİ ENSTİTÜSÜ

POLİMERİK NANOKOMPOZİT DÜZ PLAKA MEMBRANLARIN ÜRETİMİ VE KARAKTERİZASYONU

YÜKSEK LİSANS TEZİ

Merve ŞİLE
(513101030)

Fen Bilimleri Enstitüsü

Nanobilim ve Nanomühendislik Programı

Tez Danışmanı: Prof. Dr. İsmail KOYUNCU

HAZİRAN 2013

Merve Şile, a **M.Sc.** student of ITU **Graduate School of Science Engineering and Technology** student ID 513101030, successfully defended the **thesis** entitled "**FABRICATION AND CHARACTERIZATION OF NANOCOMPOSITE FLAT-SHEET POLYMERIC MEMBRANES**", which she prepared after fulfilling the requirements specified in the associated legislations, before the jury whose signatures are below.

Thesis Advisor :	**Prof. Dr. İsmail KOYUNCU** İstanbul Technical University	.....
Jury Members :	**Prof. Dr. İsmail KOYUNCU** İstanbul Technical University	.....
	Prof. Dr. Halil HASAR Fırat University	.....
	Prof. Dr. Mehmet KİTİŞ Süleyman Demirel University	.....

Date of Submission : 03 May 2013
Date of Defense : 05 June 2013

FOREWORD

The membrane processes have been increasingly used for drinking water and wastewater treatment. In spite of the advantages of membrane systems, the fouling can be accepted as the main problem and the biggest obstacle to their broader application of membrane technologies. In recent years, the new techniques have been applied for fouling control such as the production of fouling resistant new generation membrane materials or the modification of membrane surfaces using nanoparticles.

I own a great dept of thanks to Prof. İsmail Koyuncu who supported me by providing a very efficient work environment and mentoring me during my graduate education, to very dear Dr. Derya İmer, the executiveof the TUBITAK project I've been working on, who not only supported me during the project and thesis studies but also helped and be there for me since I started to work with her, to my very dear fiance Çağatay Yüksel who, as always, was my most important supporter and moral source during the thesis studies with his endless love and patience, to my very dear family for their support and love, to my very dear confidant and project partner Bahar Taş who eased the stresful and hard working days with her company, to MEMTEK Research Center where I have been working during my graduate education and thesis studies and its employees.

This study was financially supported by the TUBITAK-ÇAYDAG (The Scientific and Technological Research Council of Turkey) (Project No: 111Y095).

June 2013 Merve ŞİLE

TABLE OF CONTENTS

Page

ABBREVIATIONS

PS : Polysulfone
PES : Polyethersulfone
CA : Cellulose acetate
PVDF : Polyvinylidene fluoride
CN :Cellulose nitrate
CTA : Cellulose triacetate
PA : Aromatic polyamides
PC : Polycarbonate
PAN : Polyacrylonitrile
MWCO :Molecular weight cut off
BSA :Bovin serum albümin
RO : Reverse osmosis
NF : Nanofiltration
UF : Ultrafiltration
MF : Microfiltration
∆P : Pressure difference
∆C : Concentration difference
∆Y : Electrical potential difference
∆T : Temperature difference
NPs : Nanoparticles
AgNP : Silver nanoparticle
SiNP : Silicon oxide nanoparticle
AlNP : Aluminum oxide nanoparticle
TiNP : Titanium oxide nanoparticle
CNT : Carbon nanotube

LIST OF TABLES

Page

LIST OF FIGURES

Page

FABRICATION AND CHARACTERIZATION OF NANOCOMPOSITE FLAT-SHEET POLYMERIC MEMBRANES

The membrane filtration systems have now become an attractive option for the water and wastewater treatment and reuse of industrial and municipal wastewaters. However, the filtration performance inevitably decreases with time due to membrane fouling. Different polymers (Polyethersulfone (PES), polysulfone (PS), cellulose acetate (CA), polyvinylidene fluoride (PVDF) etc.) could be selected as membrane material according to its good physical and chemical characteristics such as good heat-aging resistance and environmental endurance as well as easy processing. However, the inherent hydrophobicities of some polymers due to its structure leads to a low membrane flux and poor anti-fouling properties, which have a great impact on its application and useful life. There have been few studies about the membrane characteristics because the commercial membranes types have been limited and these membranes have been used at many studies. The last membrane fouling studies have concerned with the physical or chemical modification of membrane material for low fouling properties. These studies were divided into three titles; the modification of membrane surface with physical and chemical treatment, the coating of membrane with spacer having low fouling properties and the production of membrane with adding nanomaterials (nanocomposite membranes). So far especially the membrane modification studies using nanotechnological methods have given the useful results. The nanoparticles (NPs) are defined as the particles having the size of 1-100 nm and they have unique magnetic, electrical, optical, mechanical and structural properties. Moreover, some nanoparticles such as silver (Ag), copper (Cu), zinc oxide (ZnO), and titanium oxide (TiO_2) etc. have antibacterial properties and thus show high toxicity to a broad spectrum of microorganisms including bacteria, fungi, viruses and yeasts and have been studied as antibacterial agents in different areas. The combination of membrane chemistry and antibacterial properties of NPs may solve the fouling problem in membrane systems. At the prevention of fouling problem, NPs can be applied by directly coating on the surface of the membranes or by blending in the polymer matrix of the membrane during phase inversion technique.

This study has focused on identifying the relationship between physical characteristics and fouling resistances of bare and nanocomposite membranes. Therefore, the main objective of this study is to investigate the production of membranes with nanomaterials and the examination of these membranes at the filtration systems. The experiments were performed at three stages. Firstly, the polymer concentration was optimized using three different membrane polymers (PS, PES and CA). Secondly, the amounts of five nanomaterials (silver (Ag), titanium oxide (TiO_2), aluminium oxide (Al_2O_3), silicon dioxide (SiO_2) and carbon nanotubes (CNT)) in membrane dope solutions were optimized. Finally, the filtration performances of fabricated bare and nanocomposite membranes were tested at dead-end filtration using model solutions.

POLİMERİK NANOKOMPOZİT DÜZ PLAKA MEMBRANLARIN ÜRETİMİ VE KARAKTERİZASYONU

ÖZET

Membran filtrasyon sistemleri artık su ve atık su arıtma ve endüstriyel ve yerel atıksuların yeniden kullanımı için cazip bir seçenek haline gelmiştir.Bununla birlikte, filtrasyon performansı kaçınılmaz şekilde membran kirlenmesi nedeniyle zamanla azalır.Farklı polimerler (Polietersulfon (PES), polisülfon (PS), selüloz asetat (SA), polyvinilydene florid (PVDF) vs.) iyi ısı direnci ve kimyasal direnci, çevresel etkilere dayanıklılık, kolay işleme ve iyi fiziksel ve kimyasal özellikleri göz önünde bulundurularak membran malzemesi olarak seçilebilir.Ancak, yapısı nedeniyle bazı polimerlerin doğal hidrofobisiteleri düşük membran akısı ve çabuk tıkanma özellikleri nedeniyle uygulama ve faydalı ömrü üzerinde büyük bir etkiye sahiptir. Membran özellikleri hakkında az sayıda çalışma yapılmıştır çünkü membranlar ticari membran türleri sınırlı kalmış ve bu membranlar birçok çalışmalada kullanılmıştır.Son membran kirlenme çalışmaları, membralara düşük tıkanma özellikleri kazandırmak için membran malzemesinin fiziksel veya kimyasal modifikasyonunu içermektedir.Son membran kirlenme çalışmaları kirlenme önleyici özellikler kazandırmak için membran malzemesinin fiziksel veya kimyasal modifikasyonu üzerinedir. Bu çalışmalar üç ana başlıkta toplanabilir; fiziksel ve kimyasal işleme ile membran yüzey modifikasyonu, yeni malzemeler ekleyerek membran üretimi, düşük kirlenme özellikleri için spacer kullanarakmembran kaplaması.Şimdiye kadar membran modifikasyon çalışmaları yararlı sonuçlar vermiştir.Bu nedenle, bu çalışmanın temel amacı nanomalzemeler ile membran üretimi ve bu membranların karakterizasyon deneylerinin ardından filtrasyon performanslarının belirlenmesidir.

Tez çalışmasında 1970'li yıllardan beri kullanılmakta olan evre dönüşümü (phase inversion) yöntemi ile nanoparçacık ve nanotüp kullanılarak tabaka halinde membranların üretilmiş ve bu membranların karakterizasyonu yapılmıştır. Bu kapsamda üç (3) farklı membran polimeri ve beş (5) farklı nanomateryal kullanılarak membran üretimi gerçekleştirilmiştir. Membran malzemesi olarak polisülfon (PS), Polietersülfon (PES) ve selüloz asetat (SA) polimerleri kullanılmıştır. Nanoparçacık olarak metal (gümüş (Ag)) ve metal oksitler (titanyum oksit (TiO_2), alüminyum oksit (Al_2O_3) ve silikon dioksit-silika (SiO_2)), nanotüp olarak ise karbon nanotüp kullanılmıştır. Dolayısıyla her bir polimerik membran malzemesi ile beş (5) farklı nanomateryalin kullanılması ile toplam onbeş (15) farklı membran malzemesi üretilmiştir. Çalışmalar iki ana başlık altında özetlenebilir; (i) evre dönüşüm yönteminde, saf polimerik membranların hazırlanmasının optimizasyonudur (polimer/solvent/ıslatıcı madde(PVP) oranları, buharlaştırma ve koagülasyon süreleri), (ii) ilk aşamada belirlenmiş olan polimer/solvent/PVP oranında nanomateryallerin optimum miktarlarının belirlenmesi ve klasik filtrasyon sisteminde

model EPS, model *E.coli* bakterisi filtrasyonlarında performanslarının tespit edilmesidir.

Deneylerin ilk aşamasında nanomateryal olmadan saf membranların hazırlanması için sabit PVP (%8) ve farklı polimer/solvent oranlarında membranlar hazırlanmıştır. Farklı polimer oranları literatür araştırması yapılarak istenilen filtrasyon türüne göre literatürde en çok kullanılan oranlar arasından belirlenmiştir. Kullanılan polimer oranları %14, %16 ve %18 olarak seçilmişdir. Üretilen bu membranlarda başta geçirgenlik deneyleri olmak üzere karakterizasyon çalışmaları yapılmıştır. Bu aşamadaki deneyler en az üç kere tekrar edilmiştir. Membranlar dökülmeden önce hazırlanan membran çözeltilerinde (dope çözelti) viskozite ölçümleri yapılmıştır. Deneyler sonunda geçirgenliği ve moleküler ağırlık kesme değeri (MWCO) ultrafiltrasyona yakın, çekme derecesi ve pürüzlülüğü düşük, boşluk oranı, hidrofilikliği, protein ve karbonhidrat tutma kapasitesi yüksek membranların üretim şartları seçilerek nanomateryalli membran üretimine geçilmiştir. Nanomateryalli membran üretiminde üç (3) faklı nanomateryal oranı kullanılmıştır. Kullanılan nanomateryal oranları yine literatür çalışması ile belirlenmiştir. Her bir nanomateriyal için kullanılan nanomateriyal oranları %0.4-0.8-1.2 olarak seçilmişdir. Yine üretilen bu membranların karakterizasyon testlerinin ardından optimum nanomateryal miktarı belirlenmiştir.

Düz plaka halinde saf polimerli ve nanomateryalli membranların dökümünde evre dönüşüm (phase inversion) yöntemi kullanılmıştır. Bu yöntemde nanomateryalli ve saf polimerli membranların döküm işlemleri aynı şartlar altında gerçekleştirilmiştir. Membran dökümünde ilk olarak homojen dağılımı sağlanmış membran çözeltisi cam yüzey üzerine belirli hacimde dökülmüş ve dökme bıçağı (casting knife) sabit kalınlığa ayarlanarak bu çözeltinin üzerine yerleştirilmiştir. Ardından laboratuar ölçekli dökme makinesinin gerekli ayarlamaları yapılarak sabit hızda (100 mm/s) cam yüzeyinde polimer film oluşturulmuştur. Bu esnada oluşturulmak istenen membranın özelliğine bağlı olarak polimer filmler belirli bir solvent buharlaşma süresinde bekletilmişlerdir. Bu çalışmada buharlaşma süresi 10 sn. olarak sabit tutulmuştur. Buharlaşmanın ardından polimer filmlerinin olduğu camlar destile suyun bulunduğu koagülasyon banyosuna daldırılmışlardır. Bu esnada en az 5 dakika membranın oluşması beklenmiş ve ardından oluşan membranlar destile suyun bulunduğu temiz bir kaba aktarılmışlardır. Biyolojik büyümenin olmaması ve reaksiyona girmeyen polimer veya solventin membrandan uzaklaşması için üretilen membranlar en az 1 hafta süre ile $+4^0$C'de soğuk odada saklanmışlardır.

Karakterizasyon deneylerindeilk olarak membranların kalınlıkları mikrometre yardımı ile hassas bir şekilde ölçülmüş kalınlığı yaklaşık 180-200 µm aralığında olan membranlar deneylerde kullanılmak üzere seçilmişlerdir.Karakterizasyon deneylerinde manyetik karıştırmalı klasik filtrasyon hücresi kullanılarak geçirgenlik, moleküler kesme değeri (MWCO), protein (Bovin serum albümin-BSA) ve karbonhidrat (Dextran, Mw=70.000 Da) tutunumları belirlenmiştir. Cihazlar kullanılarak yapılan karakterizasyon ölçümlerinde boşluk oranı ve çekilme değeri, temas açısı, SEM-EDS ve AFM analizleri, yüzey yükü (pH 6.0-6.5 aralığında zeta potansiyeli) ve XRD analizlerigerçekleştirilmiştir. Üretilen membranlar filtrasyon performansları (geçirgenlik, model çözeltiler) öncesi ilk olarak literatürde sıkıştırma deneyi olarak isimlendirilen ön işleme tabi tutulmuştur. Bu işlemde, yüksek basınç altında membranların saf su ile yıkanması sağlanmış ve bu esnada reaksiyona girmemiş polimer/ıslatıcı/solvent kalıntılarının membranlardan yıkanması ve membran gözeneklerinin son halini alması sağlanmıştır. Bu deneyin ardından klasik

filtrasyon deneyleri sırayla gerçekleştirilmiştir. Cihaz analizleri için membran numunelerinin hazırlanmasında sıkıştırma ön işlemi yapılmayan membranlar kullanılmıştır. Membranların filtrasyon hücresinde ilk olarak geçirgenlik değerleri bulunmuş ardından protein ve karbonhidrat tutunum ve filtrasyon performansları model çözeltiler kulllanılarak tespit edilmiştir. Bu filtrasyon deneylerinde geçirgenlik değerleri belirlenmiş olan membranlar kullanılmıştır. Kirlenme mekanizmasını belirlemek için ise filtrasyon deneyi sonrası membranların yüzeyi fiziksel olarak temizlenip tekrar geçirgenlik değerleri tespit edilmiştir. Membranların por yoğunluğunun göstergesi olan boşluk oranı ve fiziksel deformasyonunu veren çekilme oranı deneyleri de yine tüm saf ve nanomateryalli membranlar için bulunmuştur. Membranların yüzey ıslanabilirliğinin bir göstergesi olan hidrofilik veya hidrofobik özelliğin ölçümü için temas açısı cihazı kullanılmış ve damlatma yöntemi kullanılarak analizler en az üç tekrarlı olarak gerçekleşitirilmiştir. Membranların yüzey özelliklerini ve maddesel analizlerini gözlemlemek amacıyla SEM-EDS cihazı ve yüzey pürüzlülük değerinin belirlenmesi için de AFM cihazı kullanılmıştır.Saf ve nanomateryalli membranların yüzey yükleri, elektrokinetik ölçer ile sabit pH'da (6.0-6.5 aralığında) KCI tampon çözeltisi kullanılarak ölçülmüştür. Cihaz iki ara yüzeye sabitlenmiş membran parçalarının karşılıklı zeta potansiyeli ölçüm prensibine dayanmaktadır. Malzemelerin X ışını geçirimliliğini ölçen XRD cihazı ile saf ve nanomateryalli membranların yüzeylerinde bulunan bileşenler analiz edilmiştir.

Tez çalışmasının son aşamasında ilk aşamada gerçekleştirilmiş olan optimizasyon çalışmaları sonucunda en iyi performansları göstermiş nanoparçacık oranlarında tekrar PS (polisülfon), PES (polietersülfon) ve SA (selüloz asetat) membranları üretilmiştir. Daha sonra bu membranlar kullanılarak klasik filtrasyon sisteminde model EPS çözeltisi (*Xhantan gum*) ve model *E.coli* bakterisi ile membran kirlenmesi deneyleri aşamalı olarak gerçekleştirilmiştir. Deneyler sırasında, giriş süspansiyonlarından ve süzüntülerden numuneler alınarak tutunum değerleri tespit edilmiştir. *E.coli*bakterisi ile gerçekleştirilen çalışmalarda mikrobiyal üremenin olup olmadığının tespiti için agar-plateler kullanılarak canlılık testleri de gerçekleştirilmiştir. Tüm deneyler sonucunda, kirlenme performansı en düşük olan optimum polimer/nanoparçacık kombinasyonları belirlenmiştir.

1. INTRODUCTION

In recent years, polymer–nanoparticle composite materials have attracted the interest of a number ofresearchers, due to their synergistic and hybrid properties such as unique mechanical, electrical, optical and thermal properties.Nanomaterials could provide high functionality and performance for conventional materials such as membranes used in environmentalapplications. Membrane filtration properties can becontrolled for each specific application by the proper choice of the polymer, the solvent, additives (like nanoparticles, pore forming agents etc.) andother fabrication parameters. Moreover, especially at recent years, the membrane fouling problems can be avoid with different membrane fabrication components. Membrane fouling can be defined as the deposition of particles, colloids, macromolecules or salt molecules in feed solution at the membrane surface or inside the pores. It is a severe problem for membrane materials used in pressure-driven processes such as reverse osmosis (RO), nanofiltration (NF), ultrafiltration (UF), and microfiltration (MF) and also for other membrane processes. The fouling causes the decreasing of membrane performance either temporarily or permanently. The fouling mechanism included the interaction between the membrane surface and the foulants (inorganic, organic, and biological substances at many different forms). The foulant molecules not only physically interact with the membrane surface but also chemically degrade the membrane material.Various approaches have been studied in order to reduce membrane fouling either by improving oroptimizing the membrane surface properties. One of these approaches were the fabrication of organic-inorganic composite membranes. Thesecomposite membranes are formed by the addition of inorganic oxide particles having micrometer or nanometer sizesto the polymeric casting solution or by in situ generation. Over thepast few years, the rapid growth in nanotechnology has gainedsignificant interest the using of nanomaterials in membrane applications.More recently, several natural and engineerednanomaterials have also been shown to have properties, including chitosan, silver nanoparticles

(nAg), photocatalytic TiO_2, fullerol, aqueous fullerene nanoparticles (nC60), and carbon nanotubes (CNT).

1.1 Purpose of Thesis

The main objective of this study is to investigate the production of nanocomposite membranes with nanomaterials and the examination of these membranes at the filtration systems. This study was carried out different polymer and nanomaterial combinations and was aimed to establish the interactions of optimum polymer/nanomaterial type and ratio. Experiments to be carried out together with the membrane characterization and fouling performance achieved important results in terms of membranes fabrication at low fouling characteristics. Comprehensive fouling tests of the model solutions(protein, carbohydrate, model EPS and *E. coli* bacteria medium) provided the determination of the best-performing types of nanocomposite membranes.

1.2 Scope of Thesis

In this thesis stduy, the experiments were performed at three stages. Firstly, the polymer concentration was optimized using three different membrane polymers (PS, PES and CA). Secondly, the amounts of five different nanomaterials (silver (Ag), titanium oxide (TiO_2), aluminium oxide (Al_2O_3), silicon dioxide (SiO_2) and carbon nanotubes (CNT)) in membrane dope solutions were optimized. Finally, the filtration performances of fabricated bare and nanocomposite membranes were tested at dead-end filtration using model solutions (protein, carbohydrate, model EPS and *E. coli* bacteria medium). As a result of this thesis, new nanocomposite membrane materials contributed to literature for membrane fabrication studies.

2. LITERATURE REVIEW

2.1 Nanomaterials

Nanotechnology is a general description that includes every science and technology on a nano scale. The Royal Society's definition for nanotechnology is: Nanotechnology is the design, characterisation, production and application of structures, devices and systems by controlling shape and size at nanometer scale (The Royal Society & The Royal Academy of Engineering, 2004a). Nanoparticles have different optical, magnetic or electrical properties properties than bulk particles. These properties have potential to be used in a wide range of areas such as in energy production and storage, materials, medicine, information technologies, manufacturing and environmental applications.

Two main fabrication techniques of nanoscale materials are the top-down and the bottom-up techniques. The top-down method is making large materials smaller to nanoscale by nano fabrication techniques. The bottom-up approach is making nanostructures from individual atoms.

2.1.1 Physical and chemical properties of nanomaterials

Nanomaterials are naturally occurring from forest fires and volcanos. They also generated from anthropogenic sources as a by-product of combustion or can be produced deliberately.

There are two main features that make nanoparticles have diffirent properties than larger particals: in nanoscale quantum effects become predominant and surface area to volume ratio is increased (Holister et al., 2003).

While the particles get smaller, the surface area to volume ratio increases, which makes the atoms on the outside of the particle become dominant to the ones inside

the particle. The particle's individual properties also interactions with other particles around it change by this. The greater surface area to volume ratio makes the particles important for the industries. This may let some products perform better as batteries, besides minimize usage of resource in catalytical processes resulting the decrease the waste amount. In addition, interaction with surrounding materials increases as a result of the larger surface area and this is advantageous for materials like composites.

While the particles getting smaller, quantum mechanical behaviour become dominant. For large objects, classical mechanics can explain the relation between theory and observation; on the other hand, for objects as small as electrons just quantum mechanics can explain the behavior.

Various materials used to make nanoparticles, the most widely used is ceramics which can be split into metal oxide ceramics, such as titanium, zinc, aluminium and iron oxides, and silicate nanoparticles (silicates, or silicon oxides are also ceramics), generally in the form of nanoscale flakes of clay (Holister et al., 2003).

2.1.2 Application areas

Nanotechnology generaly combines different disciplines. This interdisciplinary approach shows promise to contribute to innovations to solve many of the problems in society today. A part of the nanoparticle applications are discussed here.

In commercial products, nanotechnology is already being used. For example, nanoparticles are used in sunscreens to increase transparency and in cosmetic products for deeper absorption by body. The commercial companies to develop their products are actively using nanotechnology, for example, L'Oreal has many nanotechnology patents (Wood et al., 2003). Furtermore, nanomaterials are used as fillers in the composite materials which is a great market. The material's properties are changed by the nanoparticles such as; soften ceramics, harden metals or change properties of alloys as needed. Clay nanoparticles make the materials stronger, lighter, more durable and more transparent by adding. These properties have potentials in many industries like, aerospace industry, packaging and the car industry. The car industry is already using this technology in the GM Motors Safari and Chevrolet Astro vans (Wood et al., 2003).

Other applications that uses nanotechnology includes solar energy collection (photovoltaics), medical diagnostic tools and sensors, flexible display technologies and e-paper, glues, paints and lubricants, various optical components, and new forms of computer memories and electronic circuit boards (Twist, 2004).

One of the products of nanotechnology is smart textiles, which are expected to be able to make change in their physical futures depending on the conditions (Holister, 2002). Using nanoparticles in textile industry is promising to production of very light and durable and also water, stains and wrinkling resistant fabrics.

Among nanotechnology applications, medical applications are one of the most expected due to human welfare. By combining nanotechnology and biotechnology, it may be possible to generate artificial organs, tissues and implants through cell growth (Wood et al., 2003). Moreover, interdisciplinary working of information technology and nanotechnology could make for example diagnosis for personal health monitoring also provide better precision and quick response time to the diagnosis tests.

Drug-delivery is another promising usage area of nanotechnology due to the better solubility and absorption potential of nanoparticles. Drugs can be carried by nanoparticles directly to the targeted area and may release it in required doses in a long-term period, eliminating the side effects of the classical drugs.

Nanotechnology have also environmental applications, which are promising better solutions for environmental issues than the traditional ones. For example, energy storage for hydrogen is possible with carbon nanotubes for renewable energy. Using nanoparticles for bioremediation is another application field.

2.2 Membrane Systems

Membrane can be defined as a selective barrier between two phases. Membrane technology is an emerging technology because it can be used in every separation processes with its multi-disciplinary characteristics (Mulder, 1996). Membrane processes have diversified amount of applications and the numbers are increasing. Especially for water and wastewater treatment technologies, membrane technology is painting a promising picture. Many types of membranes are used for water and wastewater treatment. Fundamentals of membrane processes are shown in Figure 2.1.

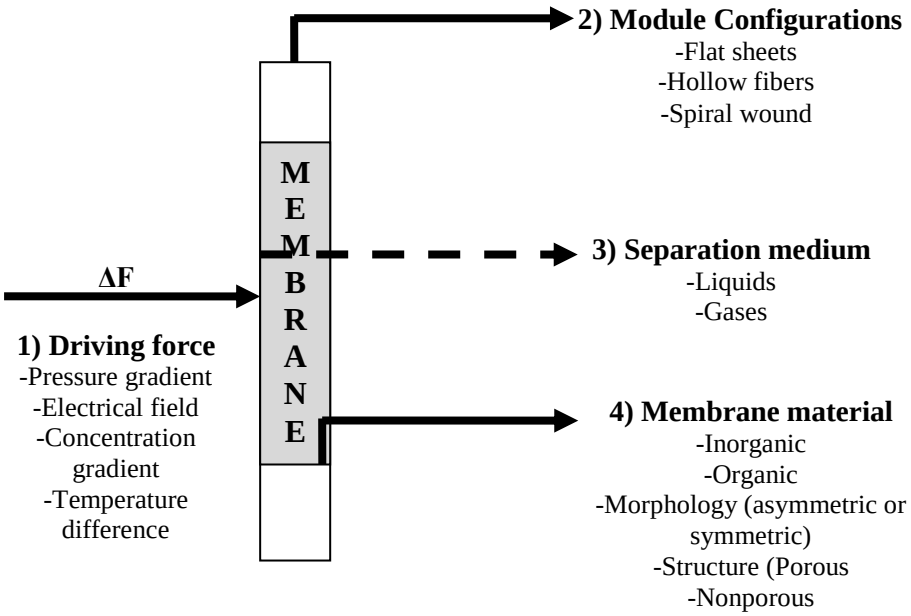

Figure 2. 1. Fundamentals of membrane and membrane processes.

Membranes can be classified by considering different aspects. The first classification is about genesis, biological or synthetic membranes. This is first differentiation point. These two types of membranes differ completely from each other in structure and functionality(Mulder, 1996). Biological membranes is an different issue which is not relevant with this thesis. About synthetic membranes, they can be subdivided into organic and inorganic membranes. The most important class of membrane material is organic which are mainly polymers. The inorganic membranes can be ceramic, glass or metallic. Although the inorganic membranes generally have better chemical and thermal stability than polymeric membranes, as membrane material their use are limited. Ceramic membrane is a specific genre of microporous membranes, which is used for microfiltration and ultrafiltration applications where resistance to solvent and thermal stability is necessary. Dense metal membranes, particularly palladium membranes, are being considered for the separation of hydrogen from gas mixtures, and supported liquid films are being developed for carrier-facilitated transport processes (Takao, 1983). Another classification of membranes is based on morphology or structure. Because the separation mechanism of membranes depends on the membrane structure, this is a very revealing margin (Mulder, 1996). There are two types of membranes can be subdivided by morphology; symmetric and asymmetric membranes. Symmetric membranes can be porous or dense. As

functionality and structure, symmetric microporous membrane resembles to commercial filters. It has rough, voided configuration and randomly dispersed, interdependent pores. The difference from commercial filters is having very small pores that are between 0.01 to 1 micrometers in diameter (Baker, 2004). Particles larger than the largest pore of the membrane rejected and smaller particles than largest pore of membrane are relatively rejected depend on the distribution of membrane's pore size. Also, much smaller particles than smallest pore of the membrane traverse the membrane. Therefore, microporous membrane's separation of solutes depend on molecular size. Nonporous membrane compromise of a dense film. Driving forces are pressure, concentration or electrical potential which allow diffusion for transportation of permeants. Diffusivity and solubility in the membrane material determines the separation of several components of a mixture which has direct relationship with transport rate within the membrane. Dense membranes are used for mostly gas separation, RO (reverse osmosis) and pervaporition membranes for separation. Generally these membranes have an anisotropic structures to enhance flux. Another symmetric membrane type is electrically charged membranes that can be found as microporous or dense but principally they are microporous which have positively or negatively charges ions on pore walls. A membrane with preset positively charges ions are an anion-exchange membrane that binds anions from fluid. In a similar vein, a membrane with fixed negatively charge ions are a cation-exchange membrane which bind cations from fluid. Electrically charged membranes are used for processing electrolyte solutions in electrodialysis. Schematic diagram of the principal types of membranes is shown inFigure 2. 2.

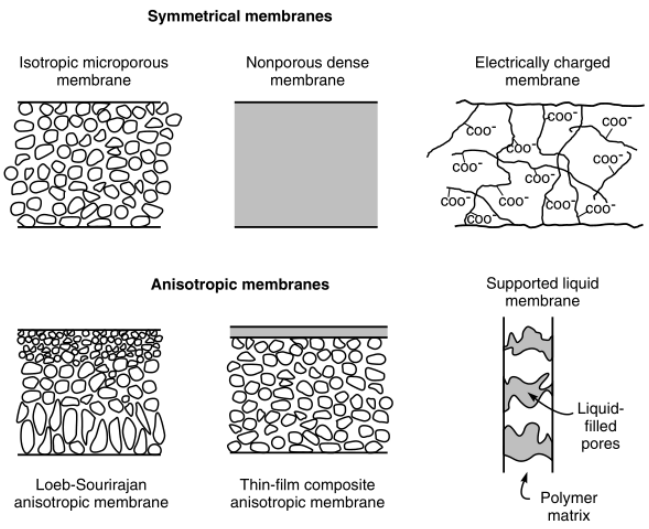

Figure 2. 2. Schematic diagram of the principal types of membranes. (Mulder, 1996)

Asymmetric membranes thickness and the transport rate of species are inversely proportional. Over 30 years, it was one of the major novelty for membrane technology to develop newfangled membrane fabrication techniques for anisotropic membrane structures. Anisotropic membranes are composed of intensely thin surface layer which backed on much thicker, porous basis. In a single operation the layer and substructure can be formed or they can be formed separately. Layers are generally made of discrete polymers in composite membranes. The surface layer designate the separation features and permeation rates and the subsurface is only for mechanical backing. For higher flows, anisotropic membranes are very advantageous that nearly all commercial processes use them (Baker, 2004).

There is also composite membranes which are actually skinned asymmetric membranes but in composite membrane, the top layer and sublayer are formed of different polymeric materials (Mulder, 1996).

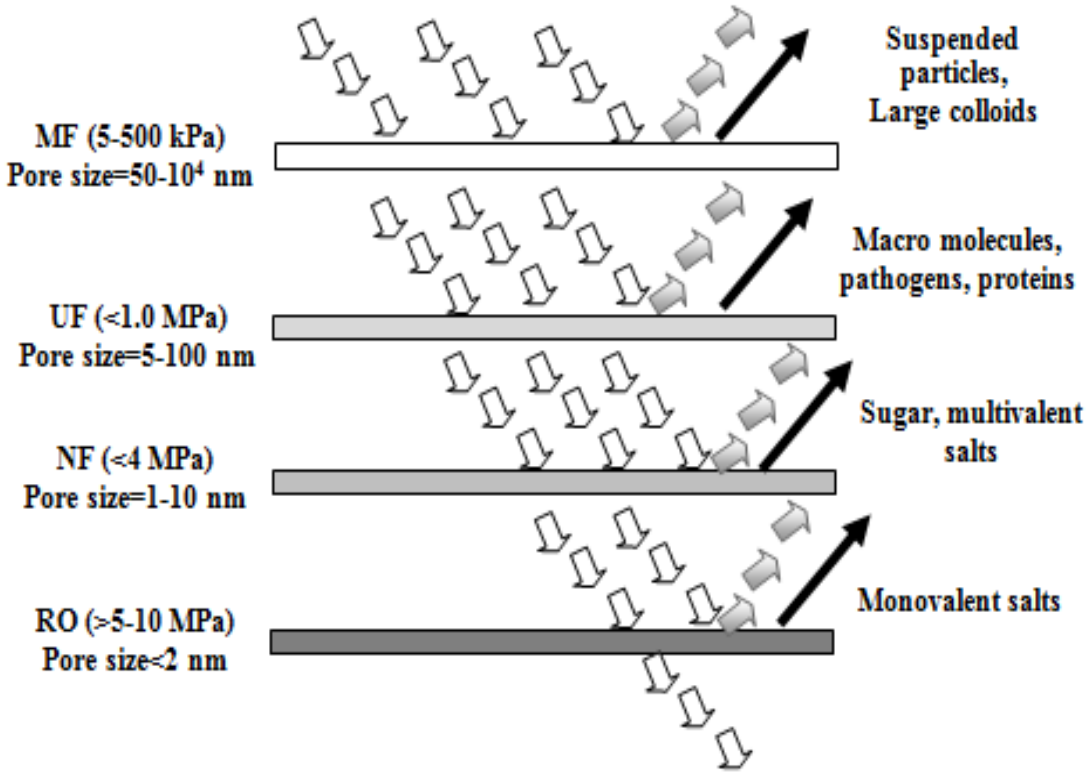

Figure 2. 3. Pressure driven membranes for water and wastewater treatment (Wang and Chan, 2007)

Membranes can also classify as porous or nonporous. Porous membranes enable separation by differentiation between particle sizes. These membranes are used in microfiltration and ultrafiltration. Membranes can be highly selective when the pore size is greatly smaller than solute size (Mulder, 1996). Membranes have pore size greater than 50 nm called as macroporous, membranes have pore size 2 to 50 nm called as mesoporous and membranes have pore size smaller than 2 nm called as microporous. Membranes, which do not have pores, also called nonporous or dense membranes. These types of membranes have the capacity of separating molecules at same size. These membranes are used in pervaporation and gas separation.

Another classification can be done by driving force. Driving force of reverse osmosis (RO), nanofiltration (NF), ultrafiltration (UF) an microfiltration (MF) membranes is pressure (ΔP). Pervaporation and dialysis membranes' driving force is concentration (ΔC). Electrodialysis and electrodialysis reversal membranes driving force is electrical potential (ΔY). Also there are membranes which the driving force is temperature (ΔT) (Drioli and Giorno, 2010). Pressure driven membranes for water and wastewater treatment are schematically shown in Figure 2. 3.

Module types are an alternate division for membranes. Wide membrane areas are necessary to apply membranes on a technical scale. Module is the smallest unit that membrane area is packed.

2.3 Membrane Materials

Various materials are used for membrane production. Synthetic polymers often is preferred, however,inorganic membranesknown as ceramic or mineral membranes can also be used.The most preferred polymeric membrane materials for water and wastewater treatment and their properties are as follows (Nath, 2008)

Cellulose derivatives, cellulose is the most important natural polymer used in membrane production. High structural order and hydrogen bonds between molecules with hydroxyl groups make cellulose resistant to dissolving. The most widely used types of cellulose in membrane systems are inorganic (nitrate) and organic (acetate) esters. Cellulose nitrate (CN) is the first synthetic polymer produced for filtration.Cellulose acetate (CA) produced as a lower cost alternative to the cellulose nitrate.The biggest advantage of cellulose acetate is the production of different pore sizes for required high fluxes. Cellulose triacetate (CTA) is a derivative of cellulose membrane the which has acetyl content greater than 42.3%. Cellulosic membranes known as hydrophilic membranes and advantageous in particular for membrane fouling.A major drawback of cellulosic membranes are haveing a narrow rangeof operating temperature (30-40^{0}C), low pH range (pH 3-6) andlow durability of chlorinated species (Nath, 2008).

Aromatic polyamides (PA), are membranes that can be used at high temperature and have the characteristics of high resistance to organic solvents. They are characterized bythe amide (-CONH-) linkage in structure. Thay cope with many disadvantage of cellulose acetate membranes (such as pH and temperature influence), but the resistance to chlorine species is worse than cellulosic membranes. Chlorine increase the selectivity and reduces the permeability of the membrane by damaging the the aromatic rings of polyamide (Nath, 2008)..

Polysulfone (PS), a concentrated product of bisphenol-A and diclorodifenil sulfone.These membranes contain-SO_2 group. Polysulfones and poly-ethersulfone membranes have high molecular and dimensional stability, hard and resistant structure. They are suitable for operation in a wide temperature range. Polysulfone

membranes can be operated at 75◦C and polietersülfon membrane can be oparated at 125^0C.pH ranges of these membranes is wide, can be used in the range of pH 1-10. Chlorine resistance higher than other membranes.Sulfone groups, provides the electrons confined in the aromatic groups that increases the resistance of the membranes. Electrons to provide aromatic groups, sulfone groups that membranes increase resistance in the confined.These membranesare often preferred for microfiltration, ultrafiltration and reverse osmosis systems in order to be prepared at the desired pore size and have use as the tubular or layer(Nath, 2008).

Polycarbonate (PC), these membranes contain -OCOO-group. Their structures are usually amorphous. In order to thin thickness (~ 10 mm) and higher molecular weight, they can also be used in the preparation of other membranes.Unlike other amorphous polymers, they are smooth and high flexibility. Due to the nature of thermoplastic they can be prepared in different shapes and layers.With polyethylene glycol, and silicon, they especially used in the preparation of membranes used in hemodialysis(Nath, 2008)

Polyacrylonitrile (PAN),PAN membranes are membranes that have co-monomers such as methylmethacrylate. They are usually produced by the method of phase inversion and high stability membranes. In some cases they can also be used for the production of composite membranes in order to increase hydrophilicity(Scott, 1999).

2.4 Membrane Production Techniques

There are several varied techniques exist to prepare synthetic membranes. Some of them are possible to use to prepare both organic or inorganic membranes. The most important techniques are sintering, stretching, track-etching, phase invention and coating (Mulder, 1996).

2.4.1 Sintering

Sintering is a simple technique which enable porous membranes to be derived from both organic and inorganic materials. The method comprise pressing a powder containing given sized particles. Next step is sintering at high temperature. The temperature requirement belongs to used material. Interface between contacting particles disappears in the course of sintering. Different materials can be used in this method such as powders of polymers, metals, ceramics, graphite or glass. Powder's

particle size distribution specified the pore size of membrane. With this technique, 0.1 to 10 μm of pore size can be obtained (Mulder, 1996).

2.4.2 Stretching

This technique places crystalline regions to the extrusion direction by stretching an extruded film or foil made from a partially crystalline polymeric material perpendicular to that direction. Pore size 0.1 μm to 3μm can be obtain when small ruptures occurred by mechanical stress. Only material can be used for this method is semi crystalline polymeric material. Prepared membranes with this technique have much higher porosity than the membranes manufactured by sintering (Mulder, 1996).

2.4.3 Track-etching

A membrane's most basic pore geometry is assembled by parallel cylindrically shaped pores of uniform dimension. Track-etching method allows this kind of structures to be made. A film or foil is exposed to high energy particle radiation adopted perpendicular to the film in this technique and polymer matrix is devastated by the particles to cause tracks. Then to create uniform cylindrical pores with narrow pore size distribution the film is immersed in an acid or alkaline bath and along these tracks the polymeric material is etched. The pore sizes can be obtained 0.02 to 10μm by this method. However, the surface porosity is not high which is about maximum 10% (Mulder, 1996).

2.4.4 Template leaching

Leaching out one of the components from a film is another production method for porous membranes. This technique allow to make porous glass membranes. A three component system's homogeneous melt is heated until the system separates in to two phases which one phase is soluble and the other is not soluble. The soluble phase is leached out by acid or base. Then a broad range of pore sizes can be procured. The minimum size is about 0.05 μm (Mulder, 1996).

2.4.5 Phase inversion

Phase inversion technique is mainly used for production of commercially available membranes. This method is highly multipurpose and can be used for all types of

morphologies (Mulder, 1996). Phase inversion technique is used for production of membranes used for this thesis so it is explained detailed in other section.

2.4.6 Coating

Low fluxes are occurred in dense membranes. Reduction of membrane's effective thickness is necessary to increase the flux. Preparing composite membranes can solve this problem. Composite membranes are made from two different materials. Many coating methods are possible to used for preparation of these kind of membranes such as dip coating, plasma polymerization, interfacial polymerization and in-situ polymerization (Mulder, 1996).

2.5 Fabrication of Nanocomposite Membranes

Material properties are major limit for the performance of membranes. Thriving attempts have been made to use nanoparticles or nanotubes as additive to polymers for membrane synthesis. Partical sizes range from 4 to 100 nm. Due to the fouling problem is one of the main problems of membrane, low-fouling membrane improvement is an important research area in membrane separation technology (Helin et al., 2008; Ji-xianget al., 2009; Suet al., 2009).For the removal of various contaminants from water and wastewater membranes have many applications but the fouling problem is the main limitation for commercial polymeric and ceramic membranes. Because of rejected colloids, chemicals and bacteria membrane fouling occurs. Fouling problem can cause high energy demand, expensive cleaning and replacement of membranes so it need considerable attention (AWWA, 2005).For making low-fouling or anti fouling membranes many attempts have been done by modifying the membrane surface with chemical modification such as grafting hydrophilic monomers on the membrane but the results still is not satisfying. Recent developments on nanotechnology provide new opportunities to improve membrane technologies. Especially for membrane fouling, it has been reported from many research communities that usage of nanoparticles has beneficial effects (AWWA, 2005; Li et al., 2007; Liet al., 2009a).Membrane production with nanoparticles provides high control over membrane fouling, moreover it allows to manufacturing membranes with desired structure and functionalities (Li et al., 2009b; Cortalezziet al., 2002, 2003). Nanocomposite membranes can be improved by blending them with

polymeric or inorganic membranes (Bottinoet al., 2002) or by assembling engineered nanoparticles into porous membranes (Li et al., 2009a; Kimet al., 2003; Taurozzi et al., 2008).

Membranes with metal oxide nanoparticles or carbon nanotubes have been produsedby researchers for the purpose of increase the permeability, resistance to fouling, material properties and also quality of permeate (Li et al., 2009a,b; Cortalezzi et al., 2002, 2003; Kimet al., 2003; Taurozzi et al., 2008; Bottino et al., 2002).Some of the metal oxide nanoparticles (mainly TiO_2) have catalytic properties that using them with membranes can reduce the fouling by providing a built-in oxidative functionality. Due to decomposition of organic matter by catalytic effects of membrane, permeate quality can also be improved (Kimet al., 2008).

It is also reported that using carbon based nanoparticles have effects on inactivation of bacteria and viruses (Chaeet al.,2009). Additionally, higher water permeailities than bare polymeric membranes are observed when using carbon-based nanomaterials (Verweji et al., 2007).

Using nanoparticles in the fabrication of polymeric membranes has taken considerable attention lately, especially as a new viewpoint in flux enhancement and fouling reduction. Hybrid membranes including inorganic fillers in polymer matrix are well known. Common fillers are oxides like SiO_2, and zeolites (Luo et al.,2005). Filler concentration can be very high without losing physical properties of membrane. The membrane is called mixed matrix membrane that both phases have a positive mutual in fluence (Luo et al., 2005; Choi et al., 1994; Bae and Tak, 2005; Mansourpanahet al., 2009).In these mix matrix membranes, the inorganic material is usually used as bulk material and not as additive. Using similar material with nano sizes is a newer idea. This approach provide better interaction between the two phases and well distribution of smaller particles, resulting the usage of nanoparticles more effectively for flux improvement and fouling reduction.

Fabrication process is the first challenge of nanoparticle based membrane development. Adding well-chosen amount of nanoparticles to the casting solution is the simplest approach.

2.5.1 Polymeric nanocomposite membranes with silver nanoparticles (AgNPs)

At fabrication of nanocomposite membranes with AgNP, the different pathways can be used to incorporate silver particles in the membrane structure such as ex-situ synthesis (subsequent addition to the casting solution), or in-situ reduction of ionic silver by the polymer solvent (Taurozzi et al., 2008).Furthermore, the silver can be applied by coating nAg^0 (AgNP) directly on the surface ofmembranes or by embedment in the polymer matrix ofmembrane itself (Yang et al., 2009; Zodrow et al., 2009).Zodrow et al. (2009) have prepared nAg^0 incorporatingmembranes by using the phase inversion technique, in other words the 'immersionprecipitation'method was applied, in which the dope solution containing the polymer and nAg^0 was casted on a support and then immersed in a waterbath to effect polymer precipitation. Zodrow et al. (2009) have found that the addition of silverprevented bacterial attachment and biofilm formation on membrane surface. Moreover, theauthors suggested the release of ionic silver to be the main mechanism.

At recent years, a combination of polymeric materials with AgNPs in nanocomposite membrane fabrication has attained much attention dueto the outstanding optical, high conductivity and antibacterialproperties of silver (Hirano et al., 2003, Chou et al. 2005). The combination of polymer and AgNPs may enhance the filtration properties due to the preventing of particle deposition (Babu et al., 2010). Therefore, AgNPs have the high antibacterialactivity and this property may provide the long-term stability and efficient operationof these composites in membrane filtration especially at the prolonged operational time periods. In literature there have been a number of studies to improve AgNPs distribution and its stability. Cellulose acetate (CA),chitosan, polyacrylonitrile (PAN) and polysulfone (PS) were themost popular polymeric materials studied (Basri et al, 2011). However,CA, chitosan and PAN polymers have disadvantages such as poorsolubility in common organic solvent and were relatively expensive;therefore, PES has appeared to be a more promising material because it isan easy handling polymeric material, good solubility in the most of organic solventsand resistant to chemical attack (Wang et al., 2005, Susanto and Ulbricht,2009).

2.5.2 Polymeric nanocomposite membranes with silica nanoparticles (SiNPs)

The use of silica nanoparticles in membrane fabrication has not yet been studied to a large extent, inspite of the wide availability of different types with a wide range of

particle sizes. Jadav and Singh (2009) incorporated two types of silica nanoparticles in situ into polyamide films caston PS supports. One type of SiNP was commercial Ludox®HS 40 (particle size of 16 nm); the other type of SiNP was a lab-synthesized colloid prepared from controlled hydrolysis of tetraethylortho silicate (TEOS) (0.4 wt% suspension in water). They studied that SiNPs was trapped into the polymer film with high temperature curing. It was observed that the effective pore radius of the nanocomposite membranes increased when the silica concentration in the casting solution is increased. Furthermore, the number of pores in the membrane to also increased.

2.5.3 Polymeric nanocomposite membranes with carbon nanotubes (CNT)

In polymeric nanocomposite membranes having CNTs, the membrane fabrication processes may not be so easy. The size and uniformity of CNTs are very important parameters because they may cause the stability problems in membranes(Ismail et al. 2009). There have been a lot of studies about the nanocomposite membranes with CNTs and they are given at Table 2. 1.

Table 2. 1. Studies about the nanocomposite membranes with CNTs.

Membrane type	Fabrication Methods	References
CNTs in polyvinylidene fluoride (PVDF-CNT) membrane	CNTs were immobilized in the membrane pore structure	Sae-Khow and Mitra, (2009)
Multi-walled carbon nanotubes (MWCNT, 4%w/w) into polysulfone ultrafiltration membranes	Membranes were fabricated using the wet phase inversion method	Brunet et al., (2008)

Multi-walled carbon nano-tubes (MWNTs) in polysulfone blend membranes	Membranes were fabricated by the phase inversion process with MWNTs dispersed in NMP. Before membrane fabrication, MWNTs were first treated with strong acid to make them well dispersed inorganic solvents such as NMP for the preparation of homogeneous MWNTs/PSf blend solutions.	Choi etal., (2006)
Multi-walled carbon nano-tubes (MWNTs) in PVA membranes for pervaporation	Membranes were fabricated using the wet phase inversion method	Choi etal., (2007)

2.5.4 Polymeric nanocomposite membranes with alumina nano particles

One of the nanoparticles used in polymeric membranes is Al_2O_3 nanoparticle. The comprehensive study about fabrication of nanocomposite membrane with Al_2O_3 was carried out by Yan et al.(2005). They fabricated PVDF membranes including nano-sized alumina. Dimethylacetamide (DMAC) was used as the solvent and the dope solution consisted 19% (wt.) PVDF polymer, 0-4% (wt.) nano-sized alumina particles and additional additives (hexad-sodium phosphate, and polyvinylpyrrolidone(PVP)).They found a remarkable change on the contact angle values that the bare PVDF membrane had a contact angle of 84^0 but this value decreased to $57\text{-}59^0$ for membranes with 2-4% Al_2O_3. Only the membrane with the lowest concentration of Al_2O_3 still had a higher contact angle (68^0). The porosity and rejection values remain unchanged in all experiments. Interestingly, they observed at SEM images that the addition of nano-sized aluminadid not affect the structure of surface and crosssection. Furthermore, the mechanical properties of nanocomposite membranes have improved: the tensile strength increased remarkably, whereas the break elongate ratio reached a maximum at 2% Al_2O_3 added. From these studies, it can be said that nano-sized alumina increased the membrane hydrophilicty.

2.5.5 Polymeric nanocomposite membranes with TiO_2 nano particles

At membrane fabrication studies, TiO_2 was one of the most preffered nanoparticles. Li et al. (2009a) produced polyether sulfone (PES)-TiO_2 composite membranes using combined vapor induced phase separation/immersion precipitation process. The casting solution consisted of 15wt% PES dissolved in a mixture of equal amounts of N,N dimethyl acetamide and diethylene glycol and 0-15% TiO_2. The form of TiO_2 was anatase and had a mean particle size of 21 nm. Wu et al. (2008) used a similar approach with the lower concentration (0-0.7 wt%) of TiO_2. N,Ndimethyl acetamide (DMAc) was used as solvent with addition of 5 wt% PVP and 5wt% water. Commercial rutile TiO_2 nanoparticles with a size of 30 nm were used. PES concentration was selected as 15wt%.The requirement of TiO_2 surface modification is remarked by authors to cope with aggregation and to increase dispersibility of particles in the casting solution. This was possible by adding 5g TiO_2 into100 ml ethanol in the presence of 0.1g γ-aminopropyltriethoxysilane. Yang et al. (2007) also reported this by observing aggregation of TiO_2 nanoparticles at the concentration above 2w %. In this study, the surface of TiO_2 nanoparticleswas modified using 1 g of nanoparticles with the particle size of 20-30 nm to a 200 ml aqueous solution which contains 0.7% sodium dodecyl sulfate (SDS). A solution of 18wt% polysulfone (PS) in a 4:1 mixture of N,N'dimethylacetamide and N-methyl-2-pyrrolidone (NMP) was casted on to a glass plate with a 200 mm knife.Bae et al. (2006) applied the dipping procedure (1% TiO_2 aqueous solution, with 20 nm particle size) forthe fabrication of poly acrylonitrile (PAN) and polyvinylidene fluoride (PVDF) and polsulfone (PS) polymeric membranes. In this study, entrapment of nanoparticles was also applied, but the concentration of TiO_2 in the casting solution is not mentioned.

Rahimpour et al. (2008) studied the effect of dipping time in a 0.03wt % TiO_2 colloidal suspension by comparing 15, 30 and 60 min of dipping. They concluded that 15 min yielded the best performance in terms of permeability, and hypothesized that longer dipping times led to more pore plugging. Rahimpour et al. (2008) combined both TiO_2 nanoparticle entrapment (in the casting solution) and subsequent dipping in TiO_2 suspensions for PS membranes. Rahimpour et al. (2008) also explained that for the nanoparticle entrapped membranes, a longer time was needed for the exchange between the non-solvent bath and the polymer casting film before

gelation and vitrification. About 1 min was needed for a film containing TiO_2 nanoparticles (with indicated size 25 nm), compared to a few seconds in the absence of nanoparticles. This is attributed to the higher affinity between TiO_2 and water compared to PES/PS, and results in a more developed polymer-lean phase growth and coalescence, and thus larger finger-like pores. They concluded that TiO_2-entrapped membranes should have a larger pore size and porosity, based on SEM images of the surfaces and crosssections.

2.6 Membrane Fouling Mechanism

Nowadays the membrane processes are preffered in chemical, biotechnology, food, water,wastewater treatment and many other fields of industries because these technology have high removal capacity and ability to meetmultiple treatment objectives. However, one of the main barriersto greater use of membrane technology is membrane fouling. When membrane fouling occurs, a thick gel layer (which canbe both biological or chemical in composition) is formed onto the membrane surface and into the membrane pores,which causes the permeate flux to decline quickly (Yu et al., 2005).As fouling progresses,membrane performance declines; more energy must be expended because of higher pressures to achieve the desiredthroughput. Cleaning procedure must be implemented to removefoulant material and restore membrane productivity. In many cases, however,the fouling is irreversible and the membrane elementsmust be replaced (Ba et al, 2010). There are many factors contributing to fouling such as surfaceproperties (chemistry, morphology, etc.), hydrodynamic conditions, ionic strength, and solute concentration (Kim et al., 2002).

The fouling is formed by the interaction between the membrane surface and the foulants, which includeinorganic, organic, and biological substances in many differentforms. The foulants not only physically interact with the membrane surface but also chemically degrade themembrane material. For example, colloidal particles, suchas natural organic matter (NOM), are considered as the mainreason for membrane fouling, which could be controlled bythe permeation hindrance and electric double layer repulsion.The formation of biofilms with extra-cellular polymericsubstances (EPSs) and microbial cells matrix is the example of biofouling (Rana and Matsuura, 2010). Biological fouling (biofouling) results from assimilable organics accumulation, biofilm formation and the regrowth of microorganismson the

membrane surface. Among all types ofmembrane fouling, biofouling is themost complicated one anddifficult to eliminate since inorganic fouling and scaling could be more easily predicted by monitoring feed characteristicsand prevented by chemical or physical pretreatments (Yanget al., 2009).Typical side effects of biofouling aregiven following (Kochkodanet al., 2006);

1. A reduction of theperformance of membranes because of the formation ofa biofilm on their surfaces,
2. The rise in the level ofconcentration polarization,
3. The biodegradation ofthe membrane material,
4. The secondary pollution ofthe purified water by bacterial cells and products oftheir metabolism,
5. An increase in the power consumptiondue to the necessity to raise the operatingpressure in order to exclude the drop in the membraneflux.

Membrane characteristics such as pore size, porosity, surface charge, roughness, and hydrophilicity/hydrophobicity, etc.,have been proven to impact onmembrane fouling.The determination of suitable membrane characteristics has been extensively investigated at recent years. The development of newmembrane material reduces the high cost of investment for the membranemodules or to enhance and maintain membrane flux. So it is necessary to improve the characteristics (especially hydrophilicity) of membranes through versatile methods,i.e. surface coating, surface grafting and blending. Surface coatingis usually unstable and might be washed away during theoperation process. Surface grafting usually needs an extra step tomodify the surface chemistry of the membrane, such as high energyelectron beam, plasma, surface living/controlled grafting method, which makes surface grafting not suitablefor an industrial scale production. Themembranewith the desirableproperties can be modified simultaneously using blending methodduring the membrane preparation process. Blending method can be considered as a single-step method for preparing a hydrophilic and anti-fouling membrane, indicating a potential application forlarge scale production (Liuet al., 2009).

3. EXPERIMENTAL METHOD

3.1 Materials

Brands and product codes of solvent(s), polymer(s) and the nanomaterials are indicated in Table 3. 1.Chemicals are used without extra purification.

Table 3. 1. Brands and product codes of materials used for the experiment.

Chemical Name	Brand	Code
Polysulfon (PS, Mw=10000 Da)	BASF	Ultrason S6010
Polyethersulfon (PES, Mw=10000 Da)	BASF	Ultrason E6020P
Cellulose acetate (CA, Mw=50000 Da)	Sigma-Aldrich	419028
Polyvinylpyrrolidone (PVP, Mw=10000 Da)	Sigma-Aldrich	PVP10
1-Methyl-2-pyrrolidinone (NMP)	Sigma-Aldrich	328634
Dimetilformamide (DMF)	Sigma-Aldrich	D4551
Silver nanoparticles (Ag)	NanoAmor	0476JY
Silicon dioxide (SiO_2)	NanoAmor	4830HT
Titanium dioxide (TiO_2) anatase	NanoAmor	5420HT
Short multiwalled carbon nanotube (CNT) with COOH	NanoAmor	1259YJF
Alumium oxide (Al_2O_3) gama	NanoAmor	1020MR
Bovine serum albumine (BHR)	Sigma-Aldrich	A9617
Dextran (Mw=70000 Da)	Sigma-Aldrich	31390
PEG (Mw=4400 Da)	Sigma-Aldrich	373001
PEG (Mw=10000 Da)	Sigma-Aldrich	309028
PEG (Mw=20000 Da)	Sigma-Aldrich	81300
PEG (Mw=35000 Da)	Sigma-Aldrich	81310

3.2 Preparation of the Membrane Solutions

3.2.1 Preparation of the membrane (dope) solutions with bare polymer

For the preparation of bare polymer solutions, addition rate of the materials are determined according to the weight percentage (% weight). Weight percentage ratios of the polymer, PVP and solvent for the prepared membranes are indicated in the Table 3. 2. For PS and PES polymers NMP is used as a solvent while DMF solvent is used for the CA polymer.

Table 3. 2. Polymer/PVP/solvent rates of the dope solution for the preparation of membranes.

Membrane code	Polymer ratio (%)	PVP ratio (%)	Solvent ratio (%)
PS-14	14	8	78
PS-16	16	8	76
PS-18	18	8	74
PES-14	14	8	78
PES-16	16	8	76
PES-18	18	8	74
CA-14	14	8	78
CA-16	16	8	76
CA-18	18	8	74

Pictures of the dope solution preparation process (for bare membranes) are shown inFigure 3. 1. In the first step of solution preparation, PVP is added to the solvent and stirred for 20 min with a magnetic stirrer until it is completely dissolved. As the CA dope solutions are prepared at 60^0C, PVP ingredient is also added to the solution at 60^0C. PS and PES dope solutions are prepared at room temperatures. After the PVP is completely dissolved in the solvent, polymer is added and stirred with a magnetic stirrer for 24 h in order to obtain homogeneous solutions. Solutions are kept in an ultrasonic bath for 20 h before membrane preparation.

Figure 3. 1. Dope solution preparation steps for pure membranes.

For the preparation of nanomaterial containing membranes, nanomaterial ratio is determined according to the weight percentage (% weight). Nanomaterial ratios are

adjusted as 0.4, 0.8 and 1.2% for all membranes. Silver-Ag (AgNP, 35nm), silicon oxide - SiO_2 (SiNP, 80 nm), multiwalled carbon nanotube-MWCNT (CNT, 30-50 nm),aluminum oxide-Al_2O_3 (AlONP, 20-30 nm), and titanium oxide-TiO_2 (TiNP, 10-30 nm) are used as nanomaterials.Images of the nanomaterials are shown in Figure 3. 2.

Figure 3. 2. Nanomaterials, used for producing the nanocomposite membranes (a) AgNP (b) SiNP (c) CNT (d) AlONP (e) TiNP.

Nanomaterial, polymer, PVP and solvent ratios for the preparation of nanomaterial containing dope solutions are indicated in the Table 3. 3. Nanomaterial concentration was changed while the polymer, PVP and solvent ratios were kept constant.

Table 3. 3. Nanomaterial/polymer/PVP/solvent ratios for the preparation of nanomaterial containing dope solutions.

Membrane code	Nanomaterial	Nanomaterial (%)	Polymer (%)	PVP (%)	Solvent (%)
1.2AgNP-PS	Silver (Ag)	1.2	14	8	78
0.8AgNP-PS	Silver (Ag)	0.8	14	8	78
0.4AgNP-PS	Silver (Ag)	0.4	14	8	78
1.2AgNP-PES	Silver (Ag)	1.2	14	8	78
0.8AgNP-PES	Silver (Ag)	0.8	14	8	78
0.4AgNP-PES	Silver (Ag)	0.4	14	8	78
1.2AgNP-CA	Silver (Ag)	1.2	14	8	78
0.8AgNP-CA	Silver (Ag)	0.8	14	8	78
0.4AgNP-CA	Silver (Ag)	0.4	14	8	78
1.2SiNP-PS	Siliconoxide (SiO_2)	1.2	14	8	78
0.8SiNP-PS	Siliconoxide (SiO_2)	0.8	14	8	78
0.4SiNP-PS	Siliconoxide (SiO_2)	0.4	14	8	78
1.2SiNP-PES	Siliconoxide (SiO_2)	1.2	14	8	78
0.8SiNP-PES	Siliconoxide (SiO_2)	0.8	14	8	78
0.4SiNP-PES	Siliconoxide (SiO_2)	0.4	14	8	78
1.2SiNP-CA	Siliconoxide (SiO_2)	1.2	14	8	78
0.8SiNP-CA	Siliconoxide (SiO_2)	0.8	14	8	78
0.4SiNP-CA	Siliconoxide (SiO_2)	0.4	14	8	78
1.2CNT-PS	Carbon nanotube (CNT)	1.2	14	8	78
0.8CNT-PS	Carbon nanotube (CNT)	0.8	14	8	78
0.4CNT-PS	Carbon nanotube (CNT)	0.4	14	8	78
1.2CNT-PES	Carbon nanotube (CNT)	1.2	14	8	78
0.8CNT-PES	Carbon nanotube (CNT)	0.8	14	8	78
0.4CNT-PES	Carbon nanotube (CNT)	0.4	14	8	78
1.2CNT-CA	Carbon nanotube (CNT)	1.2	14	8	78
0.8CNT-CA	Carbon nanotube (CNT)	0.8	14	8	78
0.4CNT-CA	Carbon nanotube (CNT)	0.4	14	8	78
1.2AlONP-PS	Aluminumoxide (Al_2O_3)	1.2	14	8	78
0.8AlONP-PS	Aluminumoxide (Al_2O_3)	0.8	14	8	78
0.4AlONP-PS	Aluminumoxide (Al_2O_3)	0.4	14	8	78
1.2AlONP-PES	Aluminumoxide (Al_2O_3)	1.2	14	8	78
0.8AlONP-PES	Aluminumoxide (Al_2O_3)	0.8	14	8	78
0.4AlONP-PES	Aluminumoxide (Al_2O_3)	0.4	14	8	78
1.2AlONP-CA	Aluminumoxide (Al_2O_3)	1.2	14	8	78
0.8AlONP-CA	Aluminumoxide (Al_2O_3)	0.8	14	8	78
0.4AlONP-CA	Aluminumoxide (Al_2O_3)	0.4	14	8	78
1.2TiNP-PS	Titaniumoxide (TiO_2)	1.2	14	8	78
0.8TiNP-PS	Titaniumoxide (TiO_2)	0.8	14	8	78
0.4TiNP-PS	Titaniumoxide (TiO_2)	0.4	14	8	78
1.2TiNP-PES	Titaniumoxide (TiO_2)	1.2	14	8	78
0.8TiNP-PES	Titaniumoxide (TiO_2)	0.8	14	8	78
0.4TiNP-PES	Titaniumoxide (TiO_2)	0.4	14	8	78
1.2TiNP-CA	Titaniumoxide (TiO_2)	1.2	14	8	78
0.8TiNP-CA	Titaniumoxide (TiO_2)	0.8	14	8	78
0.4TiNP-CA	Titaniumoxide (TiO_2)	0.4	14	8	78

Images of the nanomaterial containing dope solution preparation process are shown in theFigure 3. 3. In the first step of the dope solution preparation, nanomaterials

were added to the solvent and dissolved completely by using a sonication probe for 20 min. To be able to compare the produced nanocomposite membranes, same amount of nanomaterials were treated with the same procedures while the preparation of dope solutions. When the nanomaterials were dissolved completely, PVP was added to the solution and dissolved by stirring for 20 min. Dope solution of the CA membrane is prepared again at 60°C. After the PVP and nanomaterials are completely dissolved, polymers were added and stirred again with a magnetic stirrer for 24 h in order to obtain homogeneous solutions. Before the membrane preparation, these solutions were also kept in an ultrasonic bath for 20 min like the dope solutions of the bare membranes.

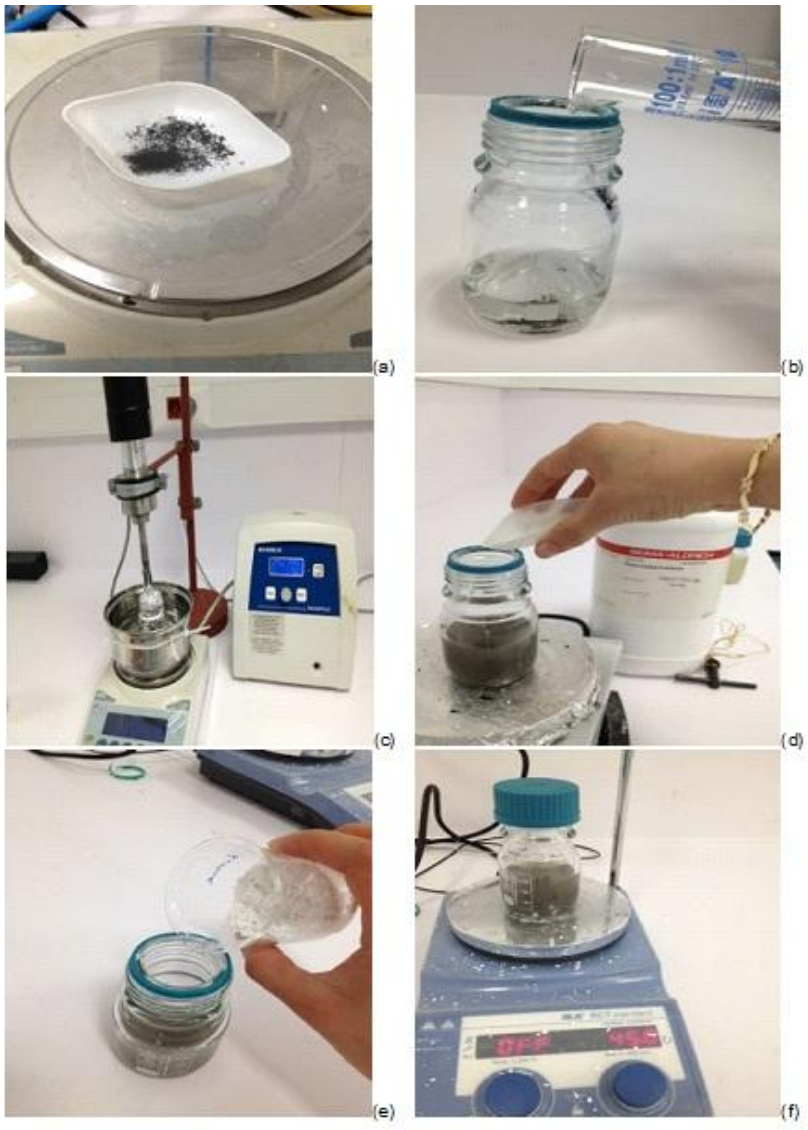

Figure 3. 3. Steps of the dope solution preparation process for nanocomposite membranes.

3.2.2 Viscosity measurements for the dope solutions

Viscosity values of the polymers were measured before the membrane preparation by using an AND - Vibro Viscometer-SV10 (measures the viscosity by using wave lengths) in the National Membrane Technologies Research Center (MEMTEK). Viscosity measurements were carried out at room temperature by using approximately 30 ml of dope solutions. Images of the device and the measurements are shown in theFigure 3. 4.

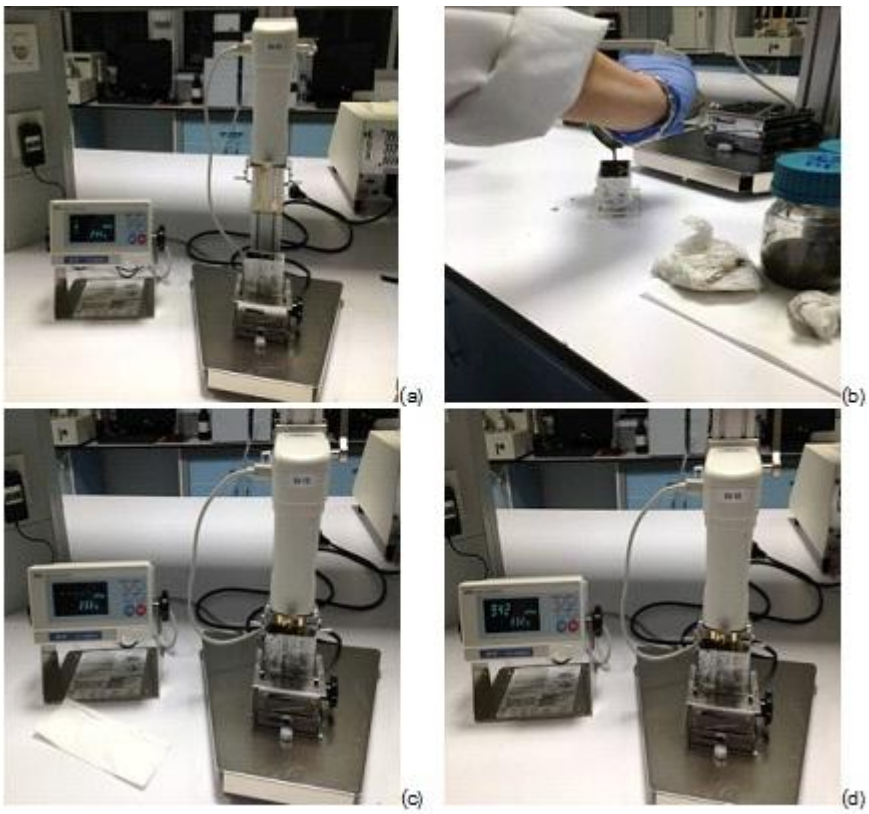

Figure 3. 4. Images of the viscosimetry measurement process and the viscosimeter.

3.2.3 Preparation processes of the flat sheet membranes

Phase inversion method is used to prepare the polymer, nanomaterial containingflat sheet membranes. Images of the membrane preparation by using phase inversion method are shown in theFigure 3. 5. Nanomaterial containing membrane preparation and bare membrane preparation processes were carried out under the same conditions. In the first step, a specific volume (Figure 3. 5– a) of homogeneous dope solution was poured on a glass surface and an aluminum casting knife which was arranged to a constant thickness (Sheen branded) was put on that solution (Figure 3. 5-b,c). Then the laboratory scaled automatic film applicator machine in the National

Membrane Technologies Research Center (MEMTEK) was adjusted to a constant velocity (100 mm/s) and a thin film was formed on the glass surface (Figure 3. 5-d). In the next step, solvent was evaporated from the polymer films for a specific time interval, in order to obtain the desired properties for produced membranes (Figure 3. 5-e). Evaporation time was set to 10 seconds for this step. After the evaporation process, polymer film coated glasses were put in a distilled water containing coagulation bath (Figure 3. 5-f). Polymer film coated glasses were kept in the coagulation bath for 5 min for membrane production. Then, the produced membranes were transformed into a clean medium filled with distilled water (Figure 3. 5-g, h). Produced membranes were kept in a cold room at $+4^{0}$C for one week to prevent the biological growth and to eliminate the unreacted polymer and solvent.

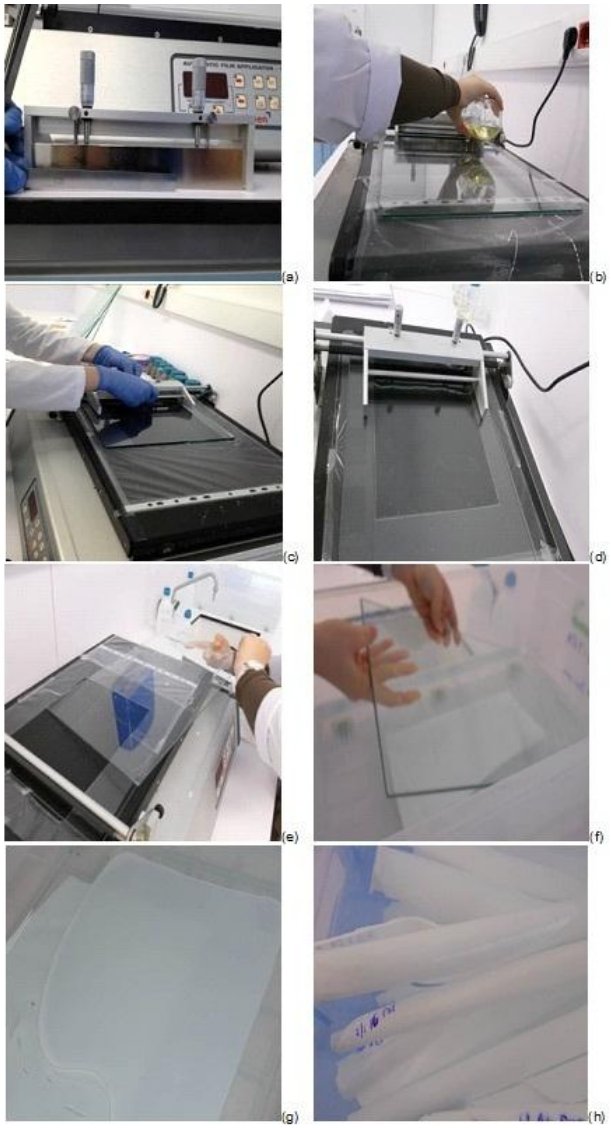

Figure 3. 5. Preparation processes of the flat sheet membranes.

3.3 Membrane Characterization Techniques

Characterization experiments of the bare and nanocomposite membranes were done after keeping the membranes for 1 week in the cold room. Thicknesses of the membranes were measured by using a micrometer before the characterization experiments as shown in theFigure 3. 6. Membranes between the thickness ranges of 180 – 200 µm were chosen for the experiments.

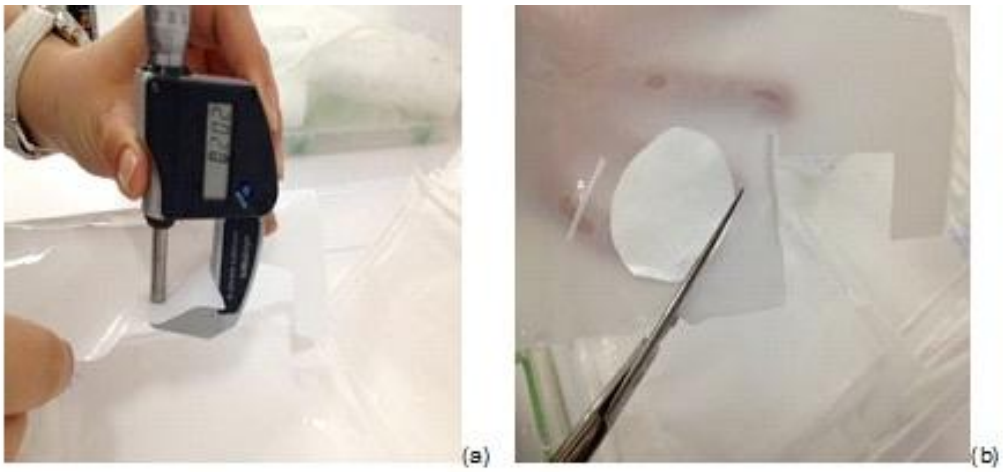

Figure 3. 6. Measurement of the membrane thickness.

Sterlitech HP4750 branded, magnetic stirrer containing classical filtration cell was used for the characterization experiments to determine permeability, molecular weight cut off (MWCO), protein (Bovin serum albumin-BSA) rejection rates and the carbohydrate (Dextran, Mw=70.000 Da) rejection rates. Instrumental analysis such as membrane porosity and shrinkage ratio value determination, contact angle, SEM-EDX and AFM measurements, surface charge (zeta potential in the pH range of 6.0 – 6.5) and XRD measurements are explained below in details.

3.3.1 Filtration system

As stated above, Sterlitech HP4750 branded magnetic stirrer containing classical filtration cell was used for the filtration experiments. Pressure in the device was adjusted by using nitrogen gas while the cross flow on the membrane surface was provided by stirring. Properties of the filtration system are indicated in the Table 3. 4. as stated by the producer company.

Table 3. 4. Technical properties of the filtration system.

Parameter	Value
Membrane diameter	49 mm
Active membrane area	14.6 cm^2
Volume	300 ml
Maximum pressure	69 bar
Maximum temperature	121^0C

Preparation steps of the filtration process are shown in theFigure 3. 7. Experiments in the filtration cell are explained below in details.

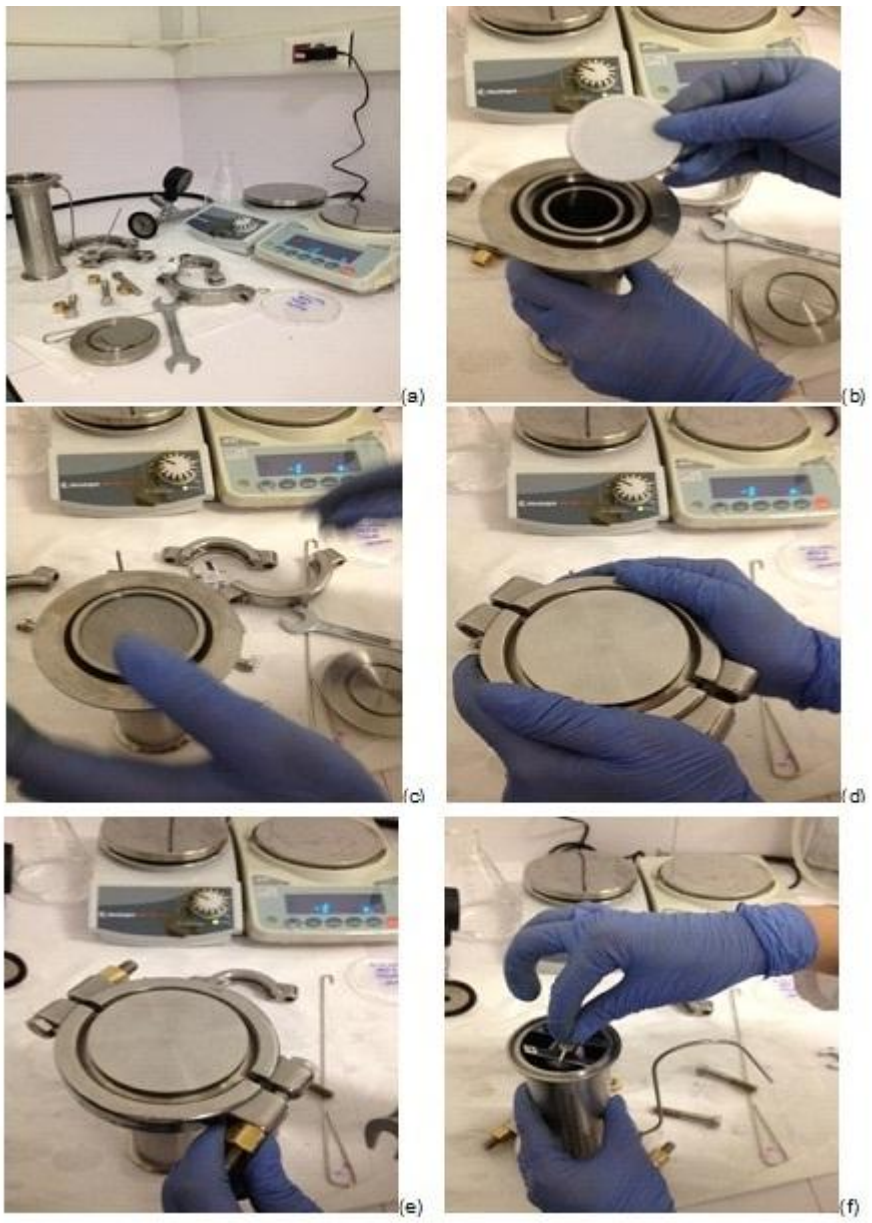

Figure 3. 7. Preparation of the filtration cell.

3.3.2 Calculation of the permeability value

Permeability values (R) of the membranes are defined as the amount of water passing through per unit area in a unit time and under a unit pressure. Calculation is done by using the equation**(3.1)** below;

$$R = \frac{J}{\Delta P} \quad \textbf{(3.1)}$$

R: Permeability, L/m^{2}h.bar

J: Flux, L/m^{2}h

ΔP: Pressure, bar

A process called compaction with distilated water filtration under high pressure, is applied to the membranes for at least 1 h to clean the membranes and to open the pores before the permeability experiment. In this process, membrane was put in a filtration cell that is filled with approximately 300 ml distilled water. Then pressure was set to a certain amount and water flow was provided for at least 1 h. Flux rates were not recorded for this process. Then, distilled water was added again to the cell and filtration was carried out for 10 min under 3 different pressure values. Flux rates for every pressure value were recorded while this process.

Afterwards, pressure – flux Graph was drawn by using Microsoft Excel and a line equation was obtained. Slope of the line shows the permeability value for the membrane. Same procedure is repeated at least 3 times for the membrane pieces obtained from the different parts of the membrane sheet and permeability values were calculated separately. Hereby, mean values of the permeability were obtained for every membrane and results could be given with mean values and standard deviation.

TiO_2 nanoparticle containing membranes were kept under 160 Watt UV light in a UV system (Images of the system are shown inFigure 3. 8) for catalysis before permeability experiments, filtration experiments and characterization processes.

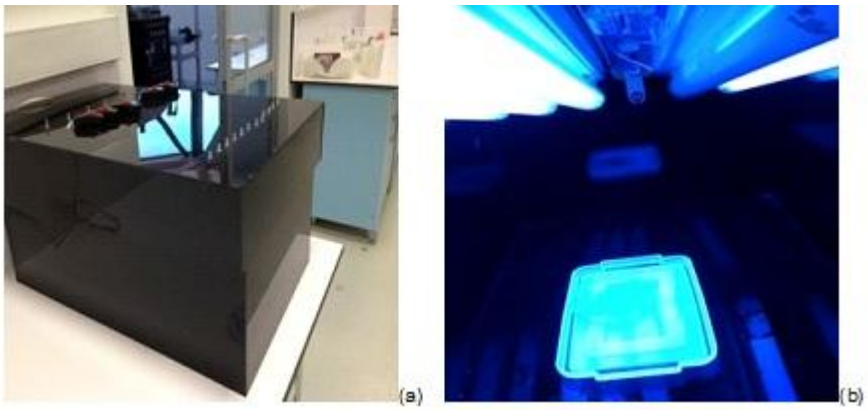

Figure 3. 8.UV system, used to activate the TiO_2 nanoparticle containing membranes.

3.3.3 Determination of the molecular weight cut off (MWCO) values for membranes

Molecular weight cut off values of the membranes were determined by the filtration of polyethylene glycol (PEG) solutions including polymers with different molecular weights. Solutions were prepared by using PEG's with 4.400, 10.000, 20.000 and 35.000 Da molecular weights as 100 mg/l. Afterwards 50 ml of the solutions were filtrated from every membrane. Compaction process was applied and one of the membranes with a calculated permeability value was used for the process. While changing the PEG solutions, membrane surfaces were cleaned and used again. Samples, obtained from the initial solution and the filtrate solution were used for TOC measurements. Measurements were done by using a Shimadzu branded VCPN model TOC device. Values obtained from the TOC device, were then used for the equations**(3.2)** given below and MWCO values for every membrane were calculated by using Excel.

$$f = \left(1 - \frac{C_p}{C_f}\right) x100 \quad \textbf{(3.2)}$$

f:% rejection

C_p: filtrate's TOC value (mg/l)

C_f: initial TOC value (mg/l)

$$a_{PEG} = 16.73x10^{-10} xM^{0.557}$$

a_{PEG}: stokes diameter of PEG (nm)

M: molecular weight of PEG (Da)

$$d_s = 2.a_{PEG}$$

d_s: diameter of PEG

It is accepted that, there is no stearic interaction between PEG and membrane. Thus, diameter of PEG (d_s) and pore diameter of the membrane (d_p) are accepted as equal.

$$d_s = d_p$$

d_p: Diameter of membrane (nm)

A Graph for f - $d_s$was drawn and slope of the line was used for the calculations given below.

$$\mu_s = d_s \ @ \ f(\%50)$$
$$\sigma_g = d_s \ @ \ f(\%84.13) / d_s \ @ \ f(\%50)$$

Average size μ_s (molecular weight) of PEG can be calculated when 50 is put instead of f value in the line equation that is obtained from the f - d_s graph. Calculated value is also equal to the pore size of the membrane. Geometric standard deviation σ_g can be calculated as the ratio of two d_s values obtained by putting 84.13 and 50.00 instead of f on the same line equation. Following the calculation of the membrane pore size, a final calculation should be done to obtain MWCO value. MWCO value represents the molecular weight of PEG with which 90% rejection rate can be achieved. Thus 90 should be put in the line equation, obtained from the f - $d_s$graph, instead of f in order to calculate the MWCO value. By using the calculated d_s value, stokes diameter of PEG and then M value can be calculated with the equations given above. Calculated value gives the molecular weight cut off value of the membrane.

3.3.4 Determination of the rejection capacity for proteins and carbohydrates

Rejection capacity for proteins and carbohydrates are determined. While BSA (Bovine serum albumin)was used for proteins, dextran was used for carbohydrates in the experiments. Solutions having 100mg/l concentration were prepared by using these materials and filtrated in a filtration cell under 1 bar pressure for 1 h to record the flux values with a computer. Protein and carbohydrate analysis were done for initial solution and the filtrate. TOC measurement was used for the analysis of carbohydrate and Lowry method was used for the analysis of protein. Three main

solutions (A,B and C solutions) were prepared for this method. 2.86 g NaOH and 14.31 g Na_2CO_3 were dissolved in distilled water and diluted to 500ml for preparation of the solution A. 1.42 g $CuSO_4.5H_2O$ was dissolved in 100 ml distilled water for preparation of the solution B. and, 2.85g Na_2tartarate.$2H_2O$ was dissolved in 100 ml distilled water for preparation of the solution C.

Lowry solution was prepared by mixing these three solutions with a specific rate of 100:1:1 (A:B:C) right before the analysis. 0.7 ml Lowry solution was added to 0.5 ml sample and stirred for 20 min at room temperature in a dark place. Folin solution was prepared during this stage. Then, 5 ml of 2N Folin solution was mixed with 6 ml of distilled water. 0.1 ml of folin solution was mixed with 0.5 ml of the sample and kept in a dark place for 30 min after vigorous stirring. Afterwards, samples were colored from dark blue to light blue according to their protein concentrations. Measurements were done by using a UV spectrophotometer, obtained from Hach Lange Company, at a constant wavelength (660 nm). Reference solution was also prepared under the same conditions for these measurements. Two similar solutions were prepared and measured for each solution in order to provide repeatability for the measurements. Protein and carbohydrate rejection rates for the initial solution and filtrate were calculated by using **(3.3)**as given below.

$$R(\%) = \left(1 - \frac{C_s}{C_g}\right) x100 \qquad \textbf{(3.3)}$$

R: % rejection

C_g: Initial protein and TOC concentration (mg/L)

C_s*:* Filtrate's protein and TOC concentration (mg/L)

In order to estimate the contamination on membranes after protein and carbohydrate filtration, flux of the distilled water and flux of the protein-carbohydrate filtration end were put in the equation**(3.4)** given below. Decrease rates were measured for each membrane.

$$FRR = \left(1 - \frac{J_{ss}}{J_{ds}}\right) x100 \qquad \textbf{(3.4)}$$

FRR: Decrease rate of flux (%)

J_{ds}: Equilibrium flux rate of the membrane for distilled water filtration (L/m^{2}h)

J_{ss}: Equilibrium flux rate of the membrane for protein or carbohydrate filtration (L/m^{2}h)

3.3.5 Determination of the porosity and shrinkage ratio values

Porosity parameter, presenting the pore density of the membrane, was calculated by subtracting the wet and dry weights of the membranes according to the equation**(3.5)** given below. Images of the experiment are shown inFigure 3. 9.

$$Porosity(\%) = \left(1 - \frac{M_2}{M_1}\right) x100 \quad \textbf{(3.5)}$$

M_1: weight of the wet membrane (g)

M_2: weight of the membrane after it was dried at 105^{0}C for 1 h (g)

Figure 3. 9. Images of the porosity experiment.

Shrinkage values were determined to examine the change of membrane forms after drying process. In the first step of shrinkage ratio experiment, membranes were cut as rectangles and their sizes were measured by using a micrometer. Later on, these membranes were dried at 105^0C for 1 h similar with the porosity experiment and their sizes were measured again by using a micrometer. Weight changes of these measurements were displayed as % difference to determine the form loss of the membranes. Images of the experiments are shown in theFigure 3. 10.

Figure 3. 10. Images of the shrinkage ratio experiment.

3.3.6 Contact angle measurements

Hydrophobicity and hydrophilicity properties that shows the wettability of the membranes were measured by using Theta model contact angle device (obtained

from KSV Attension Company) in the National Membrane Technologies Research Center (MEMTEK). Measurements were done by using the sessile drop technique. Images of the device and sample preparation process are shown inFigure 3. 11. Contact angles were measured for at least three membranes and the mean results were indicated with the standard deviation values.

Figure 3. 11. Contact angle measurement device and the sample preparation process.

3.3.7 SEM-EDS and AFM measurements

Quanta Feg250 model SEM device (obtained from the FEI Company) was used to examine the surface properties of membranes in the National Membrane Technologies Research Centre (MEMTEK). And surface roughness values were

determined in the GYTE-Materials Engineering Department Laboratory by a Digital Instruments labeled device. SEM device is shown in the Figure 3. 12and AFM device is shown in theFigure 3. 13. Samples were washed with ethanol and dried at room temperature before the analysis. Samples were coated with gold before the SEM analysis.

Figure 3. 12. SEM device.

Figure 3. 13. AFM device.

3.3.8 Measurement of the surface charge

Surface charge of bare and nanoparticle containing membranes were measured with Surpass model electrokinetic analyzer (obtained from Anto Paar company), in the National Membrane Technologies Research Center (MEMTEK). The device is shown in theFigure 3. 14. pH was kept constant (in the 6.0-6.5 pH range) for the measurements by using KCl buffer solution. Working principle of the device relies on the mutual zeta potential measurement of the membrane pieces which were set on two interfaces. Pressure, interlayer distance and flow rate arrangements were required a long time because of the high sensitivity of the device so, only one measurement could be done in a day. Thus, surface charge was only measured for the 14% polymer containing membrane and 1.2% nanoparticle containing membrane.

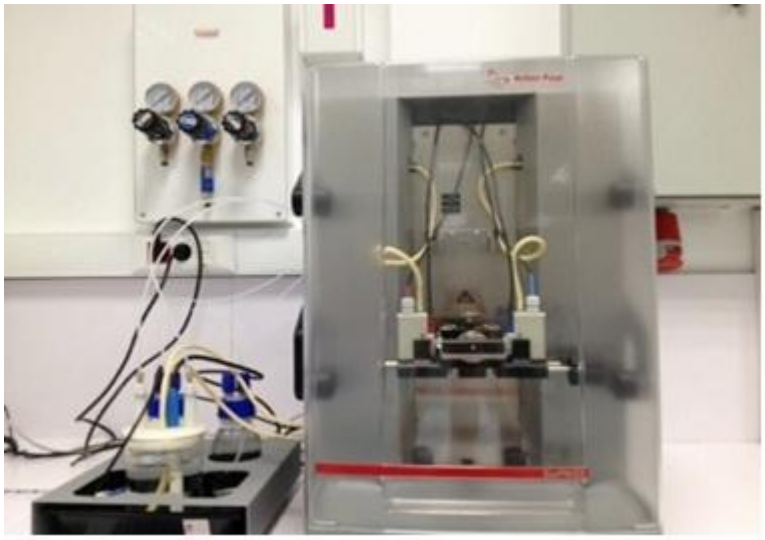

Figure 3. 14. Surface charge measurement device.

3.3.9 XRD measurement

X ray permeability of bare and nanomaterial containing membranes were measured by using an XRD device (obtained from Rigaku Company) in the GYTE-Materials Engineering department laboratory. Image of the device is shown in Figure 3.15. Two teta interval was arranged as 20-80 degrees and scanning interval was set as 2 degrees per minute.

Figure 3. 15. XRD measurement device.

3.4 Model EPS Filtration Experiment

Experiments were based on the filtration of *Xanthan gum* solution (with concentration of 100 mg/L) which was used as the model EPS in a filtration cell under 1 bar pressure for 1 h. Similarity of the rheological properties of Xanthan gum solution and activated sludge was indicated in the literature (Mayer et al., 2006). Xanthan is a microbial polysaccharide having extracellular cellulosic chains and it is used for the food industry as thickener (Homme et al., 1982). Purpose of using this material in the project is to examine the membrane behavior against bacterial products, in a medium without living bacteria. Protein and carbohydrate analysis were done for the samples which were obtained from the initial solution and the filtrate in order to determine the rejection capacities. Dubois method was used for the carbohydrate analysis while Lowry method was used for the protein analysis. Results for % rejection rates for proteins and carbohydrates were calculated by using the **(3.6)** given below.

$$R(\%) = \left(1 - \frac{C_s}{C_g}\right) x100 \qquad \textbf{(3.6)}$$

R: % rejection

C_g: Initial protein or carbohydrate concentration (mg/L)

C_s: Filtrate's protein or carbohydrate concentration (mg/L)

3.5 *E.coli* Filtration Experiment

Filtration and viability tests were applied under sterile conditions in order to examine the biological contamination of membranes by using a *Escherichia coli* (*E.coli*) strain and a filtration cell. *Escherichia coli* (*E.coli*) strain was obtained from Istanbul University ÇAPA Faculty of Medicine, Microorganism Culture Collections Research and Application Center (KÜKENS). First step was the preparation of *E.coli* suspension. Bacteria culture (as powder) was put in a liquid bacterial growth medium and spread on an agar-containing plate. Incubation temperature was 37ºC for all growth media. Sterile growth media and sterile agar-containing plates were used for the experiments. Used tools were also sterilized by using a bunsen spirit burner for this process with under necessary precautions. Regulations and steps for using lyophilizate ampoule are indicated below;

• Information written on the ampoule should be noted on a notebook.

• A cutt line should be marked 2.5-3 cm below the top of the ampoule with an ampoule cutter.

• Ampoule should be held with an alcohol containing cotton and vicinity of the cutt line should be decontaminated.

• Ampoule should be broken by holding with alcohol containing cottons from both sides.

• Top of the ampoule should be put in a disinfectant containing medium.

• Cutting edge of the ampoule must be closed with a piece of cotton.

• 0.2 cm^3 Liquid broth should be added to the ampoule by using a Pasteur pipette.

• Inoculation should be done in the liquid broth from suspension and in the solid medium by using serial dilution method.

Proliferation of Bacteria: After the dry and inactive organisms were activated in the growth media, they were proliferated according to the procedures on different plates in order to obtain required number of organisms for the experiments. Process was carried out under sterilized conditions. Used glass materials were kept in an autoclave for a while. Petri dishes and pipettes were obtained as sterilized. Metal

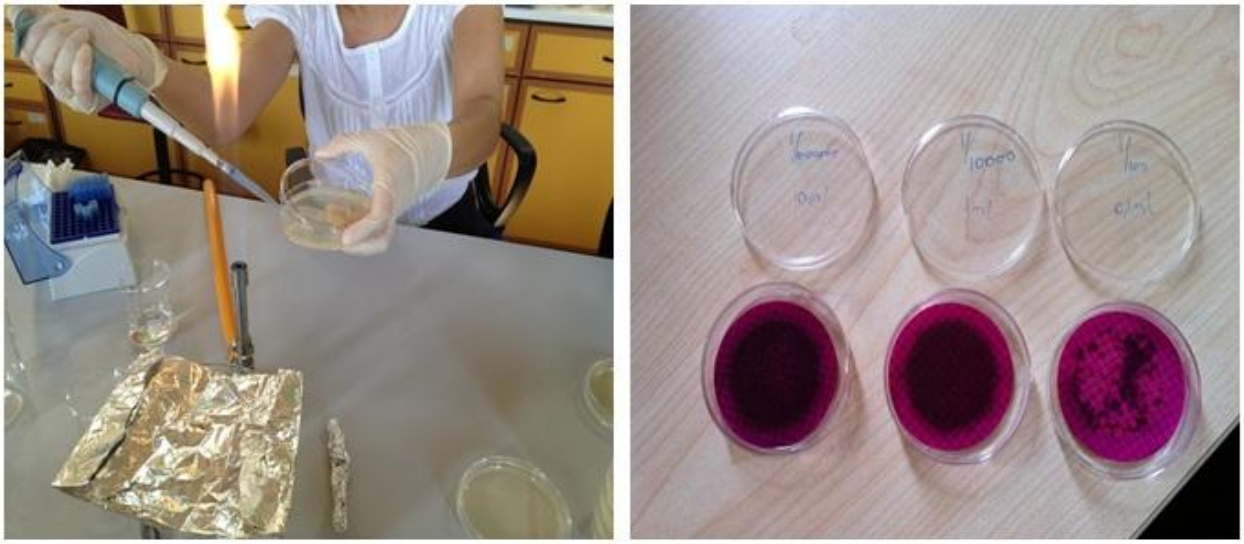

Figure 3. 16. Images of the *E.coli* inoculation and enumeration processes.

materials were incandesced by using a Bunsen spirit burner and cooled again before using.

Preparation of the liquid broth and solid growth medium: Determination of the amount and proliferation of the bacteria were required in order to be used for the filtration experiments.

Thus, obtained pure cultures were inoculated to the liquid broth and solid growth medium. Images of the inoculation and enumeration process are shown in Figure 3.16.

Prescription for solid growth medium (500 mL);

- 5 g Tripton
- 2.5 g yeast
- 7.5 g bactoagar
- 5 g NaCl

Chemicals were weighted and put to the autoclaved sterile solution dish in an order. After it was diluted to 500 mL, solution was heated and stirred until it became transparent. Growth medium was then autoclaved. Top of the plate was left partially open while keeping it in the autoclave. Autoclaving process was carried out under 121^0C and 1.06 bar pressure. A OT032 model, vacuum drier included, tabletop, steam-power sterilizer device (obtained from Nuve company) was used as the autoclave. Since agar-containing growth mediums freeze at room temperatures,

temperature of the solution was controlled (from outside of the glass) at certain time intervals to prevent freezing of agar-containing growth mediums and applied to the plates at 40-45^{0}C. Bacteria which were activated in the liquid broth were applied to the agar and kept at a cold room after preliferation. Solutions were prepared with the density of 2x10^{7}bacteria/mL by using these bacteria to be used for the filtration experiments. *E.coli* solutions were prepared and same solution was applied to every membrane. Filtration experiments were carried out again in a filtration cell under 1 bar pressure for 1 h and time-flux values were recorded. Samples, obtained from the initial and filtrate solutions, were used to determine the filtration rejection capacity for bacterial products. Filtration rejection capacities were determined by performing the protein and carbohydrate analysis after SMP segragation. Dubois method was used for carbohydrate analysis while Lowry method was used for protein analysis. Calculation of the % rejection of proteins and carbohydrates for initial and filtrate solutions were done by using the **(3.7)** given below.

$$R(\%) = \left(1 - \frac{C_s}{C_g}\right) x100 \qquad \textbf{(3.7)}$$

R: % rejection

C_g: Initial protein or carbohydrate concentration (mg/L)

C_s*:* Filtrate's protein or carbohydrate concentration (mg/L)

Used membranes were put in agar plates after filtration with and without applying the cleaning procedure and proliferation of the incubated bacteria were investigated after keeping at 37^{0}C for 24 h. Main purpose of the process was to understand if *E.coli*bacteria could stay alive in NP containing membranes.

3.6 Protein and Carbohydrate Analysis

Three main solutions (A,B and C solutions) were prepared for analysis of Lowry method. 2.86 g NaOH and 14.31 g Na_2CO_3 were dissolved in distilled water and diluted to 500ml for preparation of the solution A. 1.42 g $CuSO_4.5H_2O$ was dissolved in 100 ml distilled water for preparation of the solution B. And, 2.85g Na_2tartarate.$2H_2O$ was dissolved in 100 ml distilled water for preparation of the solution C. Lowry solution was prepared by mixing these three solutions with a

specific rate of 100:1:1 (A:B:C) right before the analysis. 0.7 ml Lowry solution was added to 0.5 ml sample and stirred for 20 min at room temperature in a dark place. Folin solution was prepared during this stage. Then, 5 ml of 2N Folin solution was mixed with 6 ml of distilled water. 0.1 ml of folin solution was mixed with 0.5 ml of the sample and kept in a dark place for 30 min after vigorous stirring. Afterwards, samples were colored from dark blue to light blue according to their protein concentrations. Measurements were done by using a UV spectrophotometer, obtained from Hach Lange Company, at a constant wavelength (660 nm). Reference solution was also prepared under the same conditions for the measurements. Two similar solutions were prepared and measured for each solution in order to provide repeatability for the measurements.

Bovin Serum Albuming (BSA) was used as the standard protein solution for protein calibration. Solutions having concentrations in the range of 0-100 mg/L were prepared by using the standard protein. Absorption values were measured at 660nm by using a UV spectrophotometer and an absorption-concentration graph was drawn with the obtained values. Calibration graph is given in theFigure 3. 17.

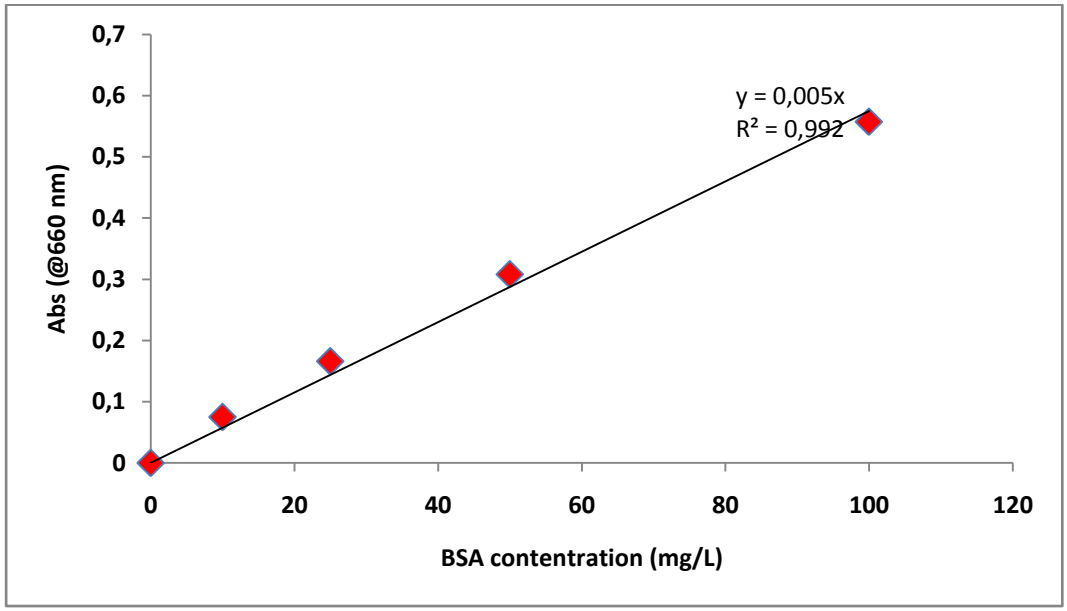

Figure 3. 17. Calibration curve for protein.

Modified "phenol-sulfuric acid method" (Dubois et al. 1956)was used for the carbohydrate analysis. Phenol solution with concentration of 80% and concentrated H_2SO_4 (95-97%) were used for the analysis. 25 µL of phenol and 2.5 mL of H_2SO_4 were added to 1 mL of sample at 30^0C and kept in a water bath for 15 min. Colors of

the samples were varied from light yellow to dark yellow according to their carbohydrate concentrations. Colors were investigated by using a UV spectrophotometer at 490 nm wave length. Glucose was used as the standard for calibration. Solutions having concentrations in the range of 2-80 mg/L were prepared by using the standard glucose. Calibration curve is shown in theFigure 3. 18.

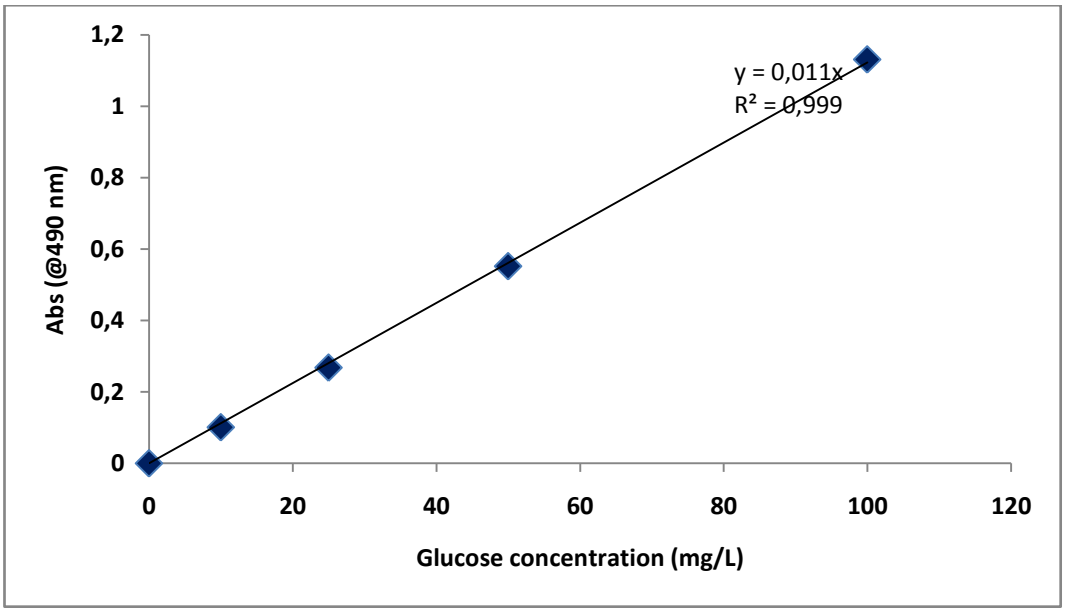

Figure 3. 18. Calibration curve for carbohydrate.

4. EXPERIMENTAL RESULTS

4.1 Viscosity Values of the Dope Solutions

Measured viscosity values of the dope solutions, prepared as the first set, containing 8% PVP, different types (PS, PES andCA) and different amounts (14-16-18%) of polymers are shown as a graph inFigure 4. 1. While measured viscosity values for PES and PS containing solutions were very similar, measured viscosity value for CA polymer containing solutions was quite high. Viscosity measurements proved that, viscosity of the solution increases as the polymer content of the solution increases.

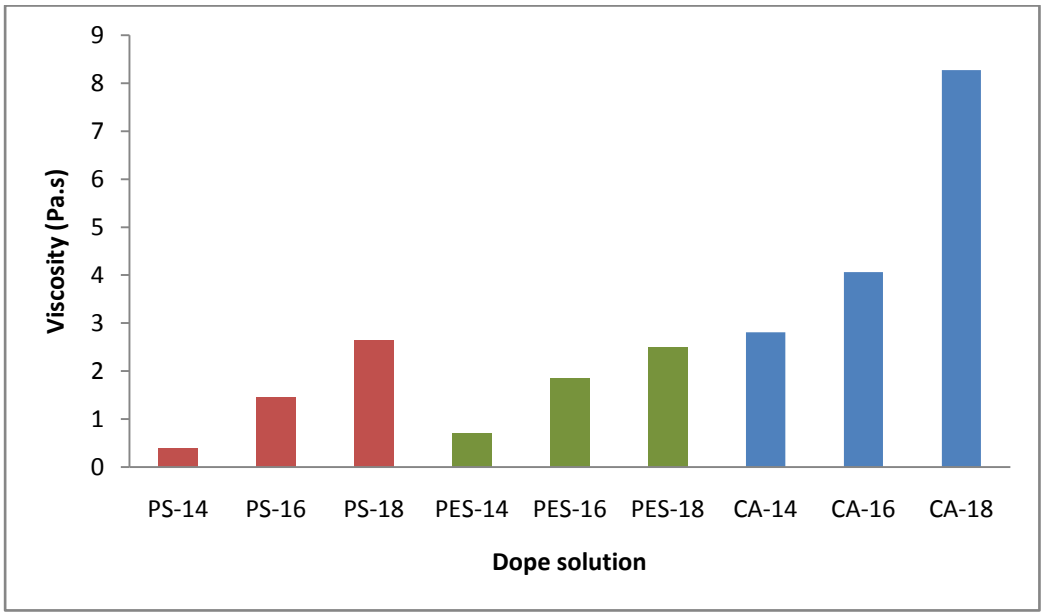

Figure 4. 1. Viscosity values of bare polymer containing dope solutions.

Measured viscosity values of the solutions, prepared as the second set, containing different amounts of silver nanoparticles (AgNP), certain amount of polymer (14%) and certain amount of PVP (8%) are shown in theFigure 4. 2. Values that are

remarked with the lines represent the viscosity amounts of 14% bare polymer containing dope solutions. As can be seen from the graph, addition of AgNP caused a little increase for the viscosity values, but amount of viscosity change is not significant for the increasing AgNP ratios.

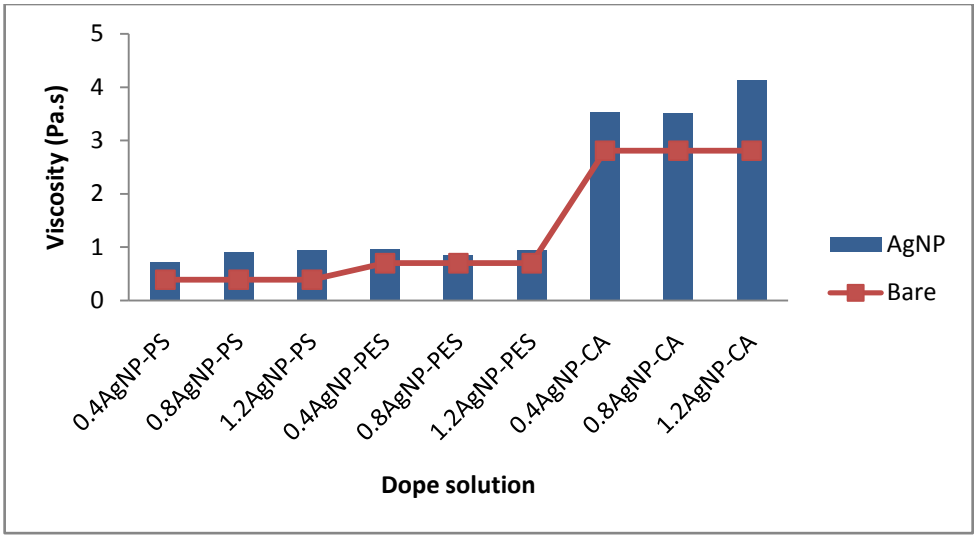

Figure 4. 2. Viscosity values of AgNP containing dope solutions.

Measured viscosity values of the dope solutions, prepared as the third set, containing different amounts of silicon oxide (SiO_2, SiNP) nanoparticle, certain amount of PVP (8%) and certain amount of polymer (14%) are shown in the Figure 4. 3. Values that are remarked with the lines represent again the viscosity amounts of 14% bare polymer containing dope solutions. As can be seen from the graph, addition of SiNP caused a larger increase for the viscosity values than the addition of AgNP, but amount of viscosity change is also not really significant for the increasing SiNP ratios.

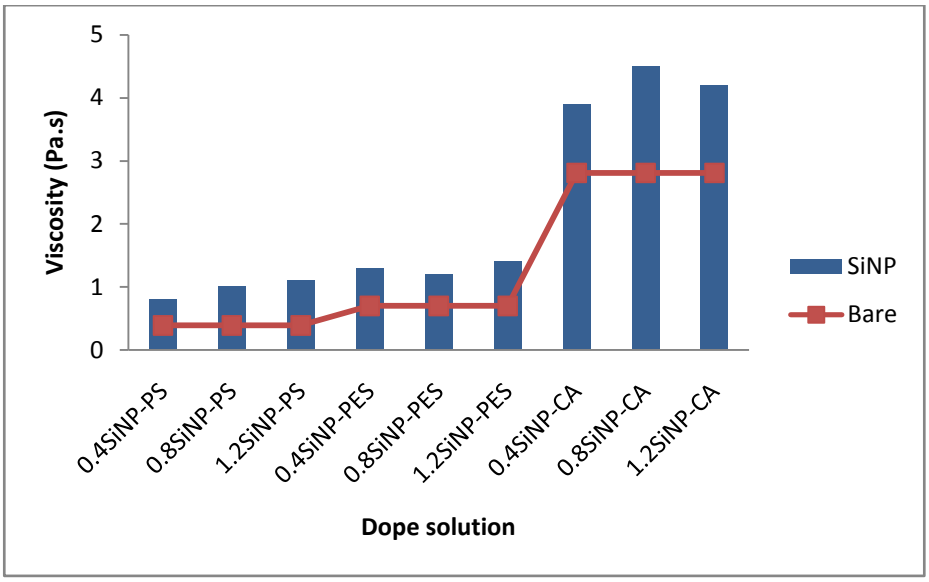

Figure 4. 3. Viscosity values of SiNP containing dope solutions.

Measured viscosity values for the dope solutions, prepared as the fourth set, containing different amounts of multiwalled carbon nanotubes (CNT) with $COOH^-$ funcitonal groups, certain amount of polymer (14%) and certain amount of PVP (8%) are shown in theFigure 4. 4. As can be seen from the graph, addition of CNT caused an increase for the viscosity values, but amount of viscosity change is not significant for the increasing CNT ratios. Highest viscosity values were obtained for CNT-CA membranes similar with the previous results.

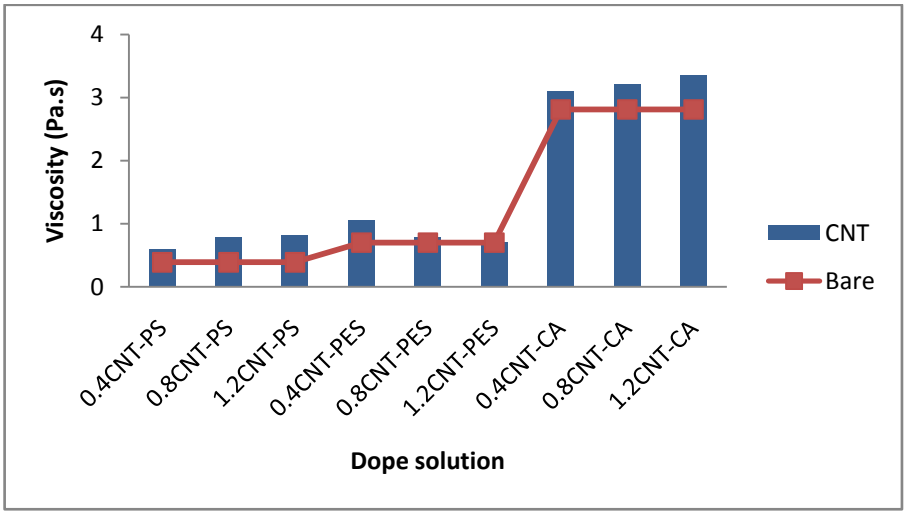

Figure 4. 4. Viscosity values of CNT containing dope solutions.

Measured viscosity values of the dope solutions, prepared as the fifth set, containing different amounts of aluminum oxide nanoparticles (Al_2O_3, AlONP), certain amount of polymer (14%) and certain amount of PVP (8%) are shown in theFigure 4. 5. As

can be seen from the graph, addition of AlONP caused an increase for the viscosity values, but amount of viscosity change is not significant for the increasing AlONP ratios.

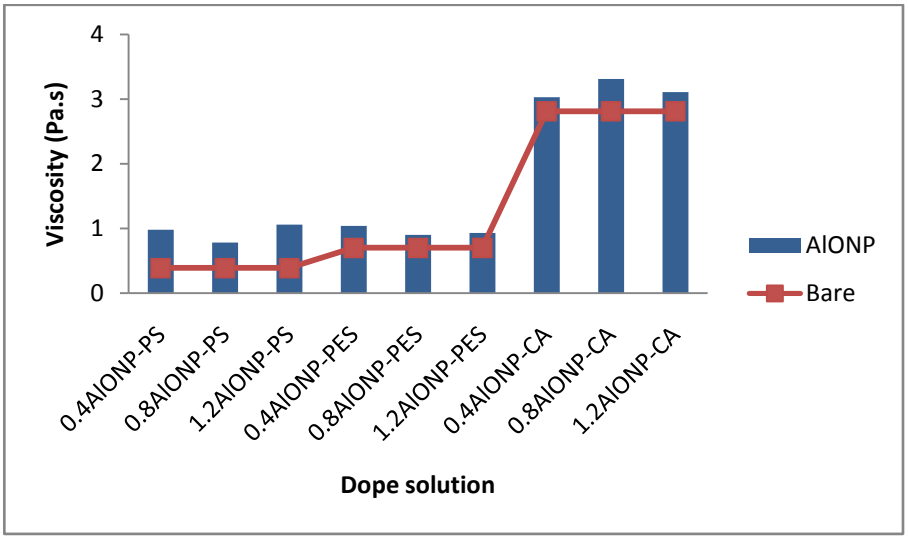

Figure 4. 5. Viscosity values of the AlONP containing dope solutions.

Measured viscosity values of the dope solutions, prepared as the sixth set, containing different amounts of titanium oxide nanoparticles (TiO_2, TiNP), certain amount of polymer (14%) and certain amount of PVP (8%) are shown in theFigure 4. 6. Similar results are also obtained for this set. Addition of TiONP caused an increase for the viscosity values but amount of viscosity change is not significant for the increasing TiONP ratios. Highest viscosity values were obtained for TiONP-CA membranes similar with the previous results.

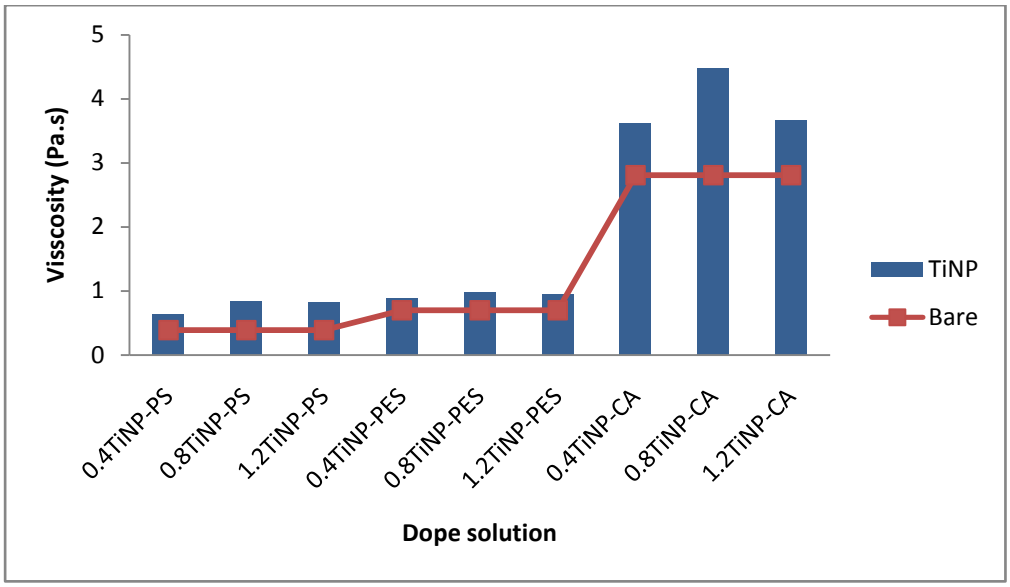

Figure 4. 6. Viscosity values of the TiNP containing dope solutions.

As a result, after consideration of the viscosity results one by one it can be said that highest viscosity increase for all membranes is caused by the addition of SiNP while the lowest viscosity increase is caused by addition of CNT nanoparticle for PS and PES membranes and addition of AlONP for CA membrane.

4.2 Permeability Values of the Membranes

Permeability tests were applied for at least 3 times to the first set of membranes produced by using different amounts of bare polymers (PS,PES and CA) and a certain amount of PVP. Results of the testsare shown as a graph in theFigure 4. 7. Permeability of the PS membranes are measured as; 154±20 L/m^{2}h.bar for PS-14, 95±3 L/m^{2}h.bar for PS-16 and 44±10 L/m^{2}h.bar for PS-18. Permeability of the PES membranes are measured as; 365±18 L/m^{2}h.bar for PES-14, 239±33 L/m^{2}h.bar for PES-16 and 135±19 L/m^{2}h.bar for PES-18. Finally, Permeability of the CA membranes are measured as; 79±6 L/m^{2}h.bar for CA-14, 35±4 L/m^{2}h.bar for CA-16 and 9±1 L/m^{2}h.bar for CA-18. As can be seen from the results, produced PES membranes have the highest permeability values while the produced CA membranes have the lowest permeability values. Increase in the polymer amount caused dramatic decrease for the permeability values. This situation is caused by the production of membranes with higher densities and less surface porosity because of the increase in the amount of polymers. As a result, it is proved that the higher permeability values can be obtained for the 14% polymer containing membranes.

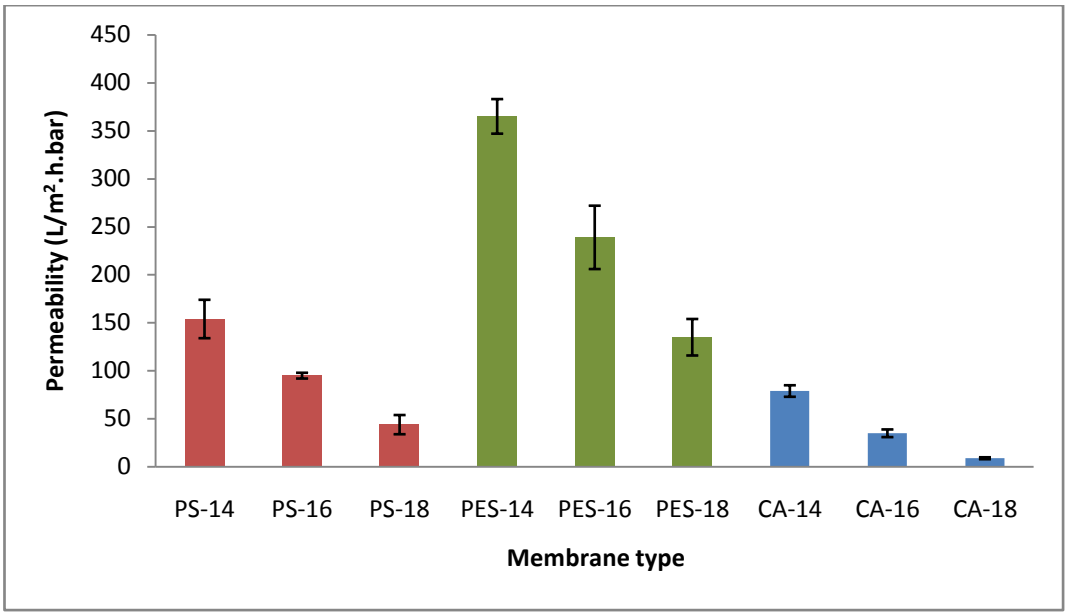

Figure 4. 7. Permeability values of the bare polymer containing membranes.

Permeability tests were applied for at least 3 times to the second set of membranes produced by using different amounts of AgNP (0.4-0.8-1.2%), a certain amount of PVP (8%) and a certain amount of polymer (14%). Results of the testsare shown as a graph in theFigure 4. 8. Values that are shown as lines represent the permeability values for 14% PS, PES and CA containing bare membranes. Permeability of the bare PS-14 membrane was measured as; 154±20 L/m^{2}h.bar before the AgNP addition, but the result changed as; 218±41 L/m^{2}h.bar for 0.4% AgNP content, 210±12 L/m^{2}h.bar for 0.8% AgNP content and 225±20 L/m^{2}h.bar for 1.2% AgNP content. Permeability of the bare PES-14 membrane was measured as; 365±18 L/m^{2}h.bar before the AgNP addition, but the result changed as; 327±33 L/m^{2}h.bar for 0.4% AgNP content, 248±21 L/m^{2}h.bar for 0.8% AgNP content and 220±30 L/m^{2}h.bar for 1.2% AgNP content. Finally, Permeability of the bare CA-14 membrane was measured as; 79±6 L/m^{2}h.bar before the AgNP addition, but the result changed as; 67±10 L/m^{2}h.bar for 0.4% AgNP content, 49±4 L/m^{2}h.bar for 0.8% AgNP content and 40±5 L/m^{2}h.bar for 1.2% AgNP content. As can be seen from results and the graph, AgNP addition caused an increase for the permeability values of PS membranes but caused a decrease for the permeability values of PES and CA membranes. With the increase of AgNP amount in the polymer, permeability value for the PS membrane did not change but permeability values for PES and CA membranes are decreased. It can be stated that, according to the permeability results, optimum AgNP ratio is 0.4% for all of the membranes.

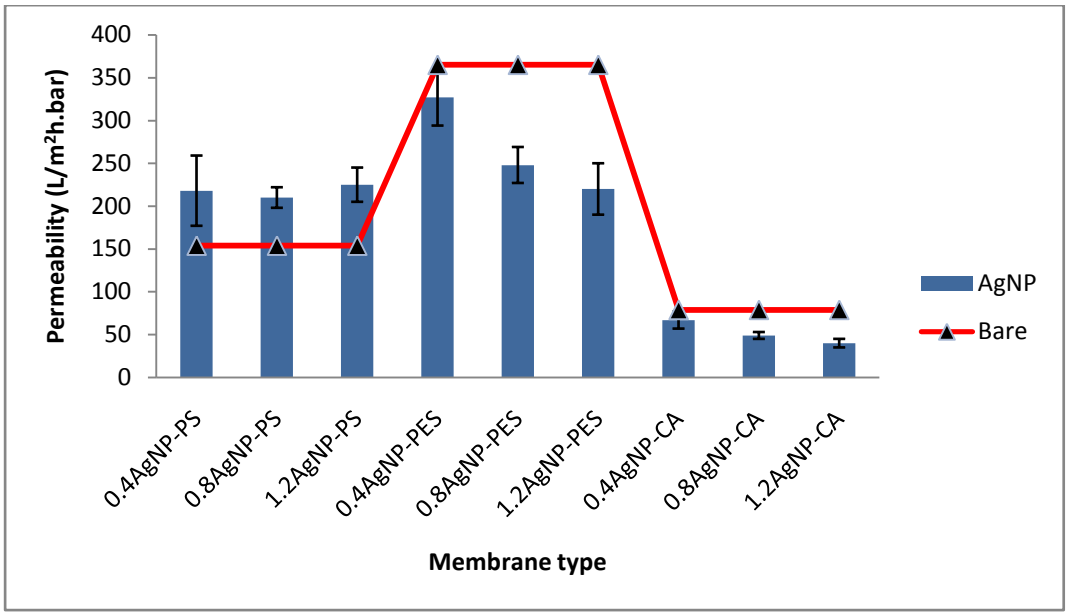

Figure 4. 8. Permeability values of AgNP containing membranes.

Permeability tests were applied to the third set of membranes produced by using different amounts of SiNP (0.4-0.8-1.2), 14% polymer and 8% PVP. Results are shown as a graph inFigure 4. 9. Values that are shown as lines represent the permeability values for bare membranes. Permeability of the bare PS-14 membrane was measured as; 154±20 L/m^{2}h.bar, before the SiNP addition, but the result changed as; 95±12 L/m^{2}h.bar for 0.4% SiNP content, 108±15 L/m^{2}h.bar for 0.8% SiNP content and 193±27 L/m^{2}h.bar for 1.2% SiNP content. Permeability of the bare PES-14 membrane was measured as; 365±18 L/m^{2}h.bar before the SiNP addition, but the result changed as; 110±27 L/m^{2}h.bar for 0.4% SiNP content, 260±14 L/m^{2}h.bar for 0.8% SiNP content and 297±20 L/m^{2}h.bar for 1.2% SiNP content. Finally, Permeability of the bare CA-14 membrane was measured as; 79±6 L/m^{2}h.bar before the SiNP addition, but the result changed as; 14±3 L/m^{2}h.bar for 0.4% SiNP content, 7±2 L/m^{2}h.bar for 0.8% SiNP content and 7±2 L/m^{2}h.bar for 1.2% SiNP content. As can be seen from results and the graph, SiNP addition caused a decrease for the permeability values of PS, PES and CA membranes compared with the permeability values of the bare polymeric membranes.

With the increase of SiNP amount in the polymer, permeability values are increased for the PS and PES membranes but permeability values did not change much for CA membranes. According to the obtained permeability values, optimum SiNP addition

rate is 1.2% for PS and PES membranes while optimum SiNP addition rate is 0.4% for CA membrane.

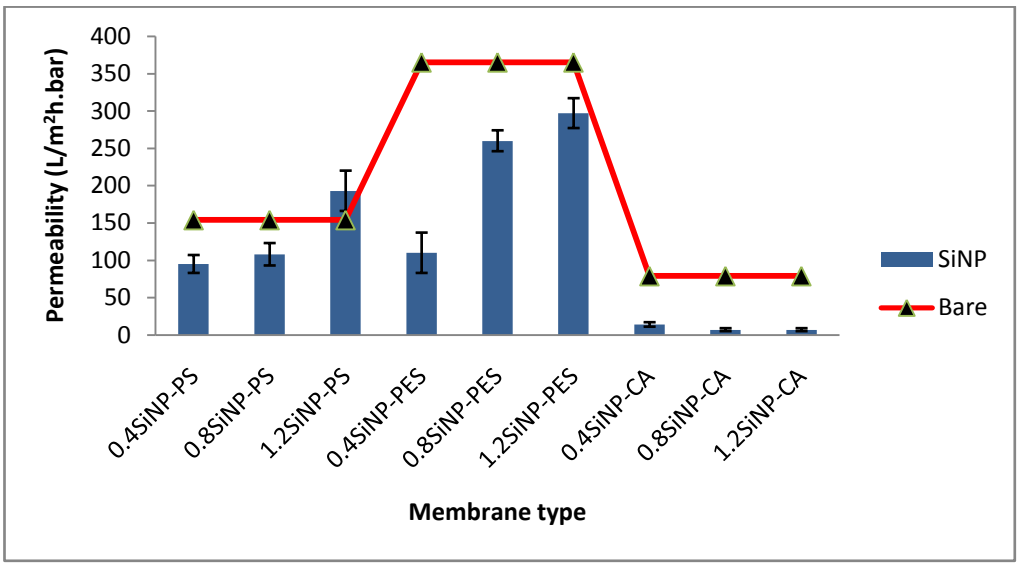

Figure 4. 9. Permeability values of SiNP containing membranes.

Permeability tests were applied for at least 3 times to the fourth set of membranes; produced by using different amounts of CNT, 14% polymer and 8% PVP. Results are shown as a graph in Figure 4. **10**. Permeability of the bare PS-14 membrane was measured as; 154±20 L/m^{2}h.bar before the CNT addition, but the result changed as; 140±9 L/m^{2}h.bar for 0.4% CNT content, 109±7 L/m^{2}h.bar for 0.8% CNT content and 150±27 L/m^{2}h.bar for 1.2% CNT content. Permeability of the bare PES-14 membrane was measured as; 365±18 L/m^{2}h.bar before the CNT addition, but the result changed as; 277±15 L/m^{2}h.bar for 0.4% CNT content, 371±37 L/m^{2}h.bar for 0.8% CNT content and 401±12 L/m^{2}h.bar with for 1.2% CNT content. Permeability of the bare CA-14 membrane was measured as; 79±6 L/m^{2}h.bar before the CNT addition, but the result changed as; 6.8±0.4 L/m^{2}h.bar for 0.4% CNT content, 9.5±0.3 L/m^{2}h.bar for 0.8% CNT content and 9±0.3 L/m^{2}h.bar for 1.2% CNT content. As can be seen from results and the graph, CNT addition caused a decrease for the permeability values of PS, CA and caused an increase for the permeability value of PES (except the 0.4% CNT containing PES) membranes, compared with the permeability values of the bare polymeric membranes.

It is observed that, with the increase of CNT amount in the polymer, permeability values are increased for PES membranes, decreased for CA membranes and did not

change much for PS membranes. It can be said that, optimum CNT ratio is 1.2% for all of the membranes according to the permeability values.

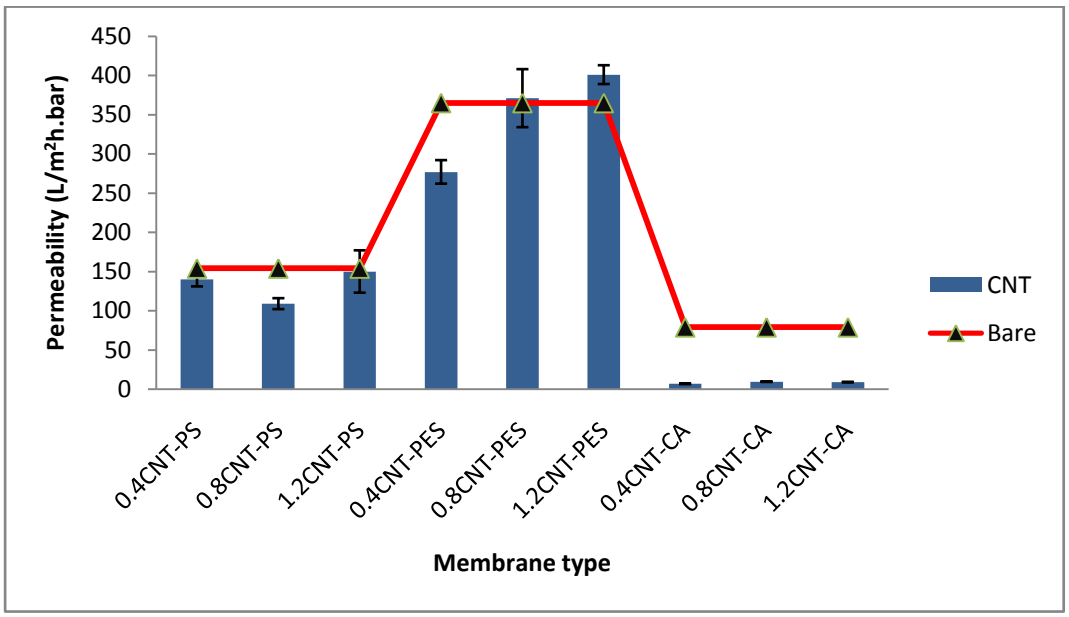

Figure 4. 10. Permeability values for CNT containing membranes.

Permeability tests were applied for at least 3 times to the fifth set of membranes; produced by using different amounts of Al_2O_3 (0.4-0.8-1.2%) nanoparticles (AlONP), 14% polymer and 8% PVP. Results are shown as a graph inFigure 4. 11. Permeability of the bare PS-14 membrane was measured as; 154±20 L/m^{2}h.bar before the AlONP addition, but the result changed as; 213±13 L/m^{2}h.bar for 0.4% AlONP content, 180±12 L/m^{2}h.bar for 0.8% AlONP content and 144±1 L/m^{2}h.bar for 1.2% AlONP content. Permeability of the bare PES-14 membrane was measured as; 365±18 L/m^{2}h.bar before the AlONP addition, but the result changed as; 324±8 L/m^{2}h.bar for 0.4% AlONP content, 257±26 L/m^{2}h.bar for 0.8% AlONP content and 338±29 L/m^{2}h.bar for 1.2% AlONP content. Permeability of the bare CA-14 membrane was measured as; 79±6 L/m^{2}h.bar before the AlONP addition, but the result changed as; 111±14 L/m^{2}h.bar for 0.4% AlONP content, 143±15 L/m^{2}h.bar for 0.8% AlONP content and 132±25 L/m^{2}h.bar for 1.2% AlONP content. As can be seen from results and the graph, AlONP addition caused an increase for the permeability values of PS and CA membranes and caused a decrease for the permeability value of the PES membrane, compared with the permeability values of the bare polymeric membranes.It is observed that, with the increase of AlONP amount in the polymer, permeability value is decreased for PS membrane, increased

for CA membrane and did not change much for the PES membrane. It can be said that, optimum AlONP addition rate is 0.4% for PS membrane while the optimum addition rate is 1.2% for PES and CA membranes according to their permeability values.

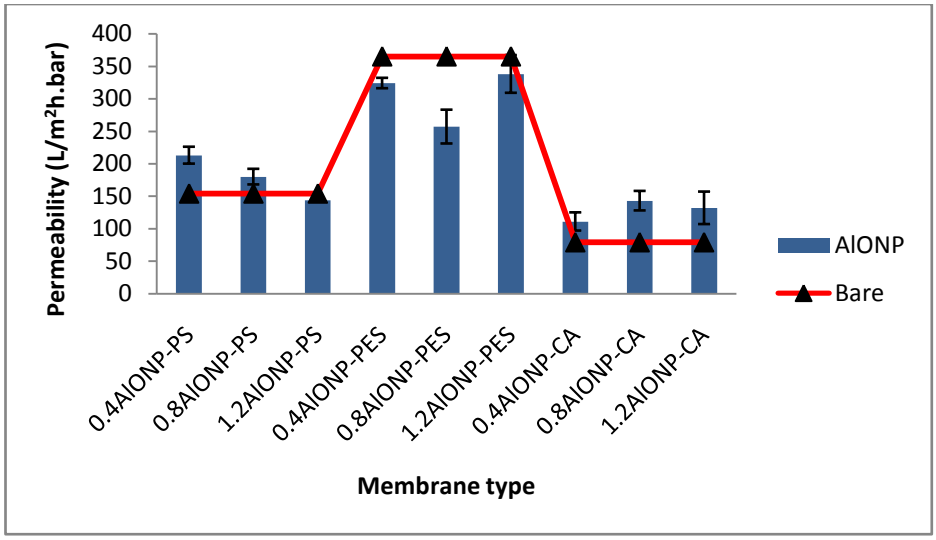

Figure 4. 11. Permeability values of AlONP containing membranes.

Permeability tests were applied for at least 3 times to the fifth set of membranes; produced by using different amounts of TiO_2 nanoparticles (TiNP), 14% polymer and 8% PVP. Membranes were activated with UV light before the experiments. Results are shown as a graph inFigure 4. 12. Permeability of the bare PS-14 membrane was measured as; 154±20 L/m^{2}h.bar before the TiNP addition, but the result changed as; 234±21 L/m^{2}h.bar for 0.4% TiNP content, 160±23 L/m^{2}h.bar for 0.8% TiNP content and 176±35 L/m^{2}h.bar for 1.2% TiNP content. Permeability of the bare PES-14 membrane was measured as; 365±18 L/m^{2}h.bar before the TiNP addition, but the result changed as; 235±19 L/m^{2}h.bar for 0.4% TiNP content, 307±32 L/m^{2}h.bar for 0.8% TiNP content and 321±10 L/m^{2}h.bar for 1.2% TiNP content. Permeability of the bare CA-14 membrane was measured as; 79±6 L/m^{2}h.bar before the TiNP addition, but the result changed as; 148±7 L/m^{2}h.bar for 0.4% TiNP content, 146±9 L/m^{2}h.bar for 0.8% TiNP content and 144±12 L/m^{2}h.bar for 1.2% TiNP content. As can be seen from results and the graph, TiNP addition caused an increase for the permeability values of PS and CA membranes and caused a decrease for the permeability value of the PES membrane, compared with the permeability values of the bare polymeric membranes. It is observed that, with the increase of TiNP amount in the polymer, permeability value is decreased for PS

membrane, increased for PES membrane and did not change much for the CA membrane. It can be said that, optimum addition rate of TiNP was 0.4% for PS and 1.2% for PES and CA according to their permeability values.

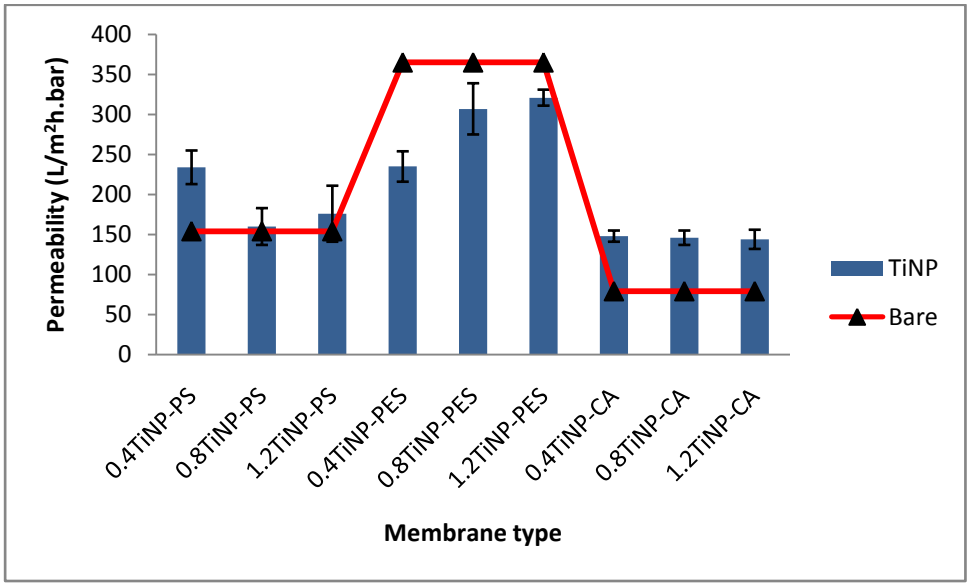

Figure 4. 12. Permeability values of TiNP containing membranes.

4.3 Molecular Weight Cut Off Values (MWCO)for Membranes

MWCO values for the first set of membranes (produced by bare polymers) are calculated by using PEG filtration method, and shown as a graph in Figure 4. 13. MWCO values for PS membranes were calculated as; 253560 Da for PS-14, 205347 Da for PS-16 and 93770 Da for PS-18. MWCO values for PES membranes were calculated as; 307025 Da for PES-14, 231712 Da for PES-16 and 95159 Da for PES-18. Finally, MWCO values for CA membranes were calculated as; 202563 Da for CA-14, 151162 Da for CA-16 and 86441 Da for CA-18. The results showed that, PES membranes have the highest MWCO values while CA membranes have the lowest MWCO values just like the permeability measurements. For all membranes, MWCO value was decreased as the polymer amount of membranes were increased.

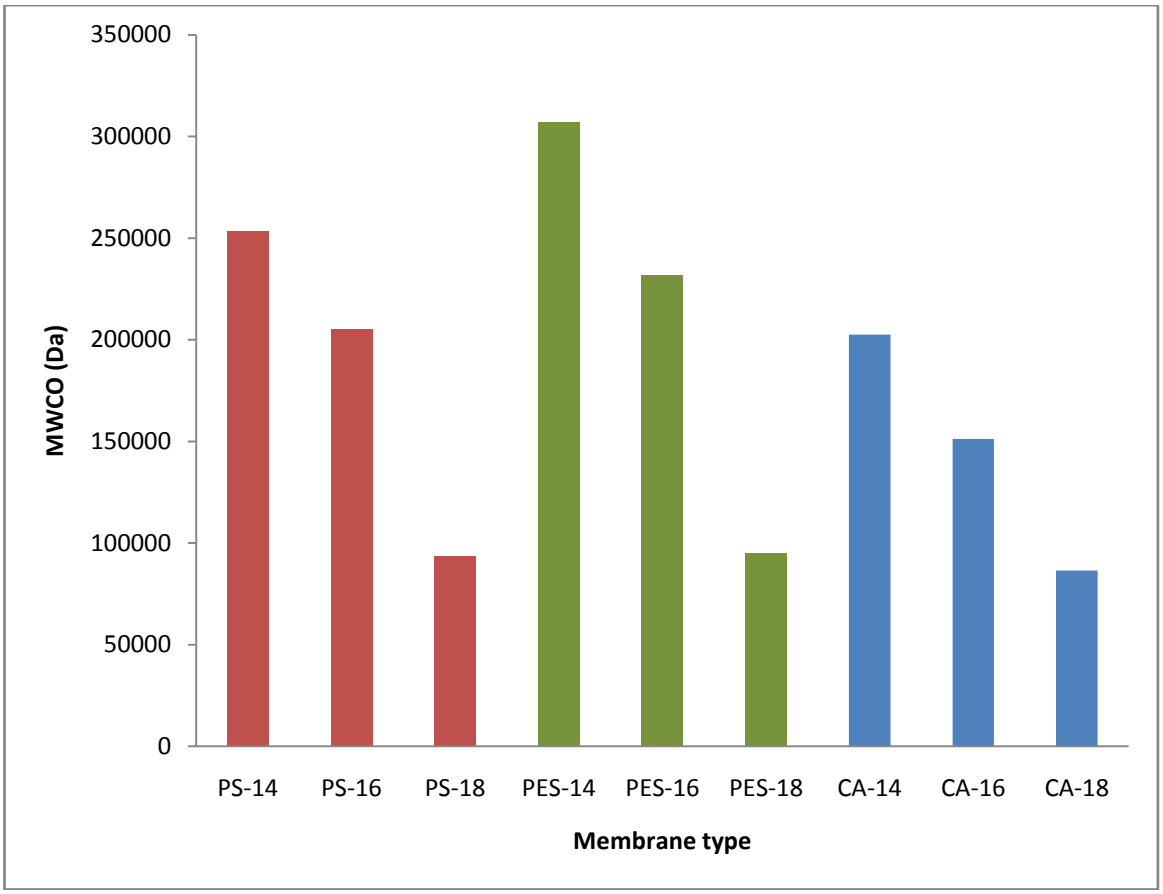

Figure 4. 13. MWCO values of bare polymeric membranes.

MWCO values for the second set of membranes (produced with AgNP) are calculated and shown as a graph inFigure 4. 14. MWCO values of the AgNP containing PS membranes are calculated as; 423362 Da for 0.4% AgNP content, 427547 Da for 0.8% AgNP content and 414556 Da for 1.2% AgNP content. These MWCO values are higher than that of the bare PS-14 containing membranes having MWCO value of 253560 Da.

MWCO values are calculated for the AgNP containing PES membranes as; 251748 Da for 0.4% AgNP content, 263948 Da for 0.8% AgNP content and 232314 Da for 1.2% AgNP content. These MWCO values are lower than that of the bare PES-14 containing membranes having MWCO value of 307025 Da.

MWCO values are calculated for the AgNP containing CA membranes as; 176967 Da for 0.4% AgNP content, 129087 Da for 0.8% AgNP content and 136021 Da for 1.2% AgNP content. These values are lower than that of the bare CA-14 containing membranes having MWCO value of 202563 Da.

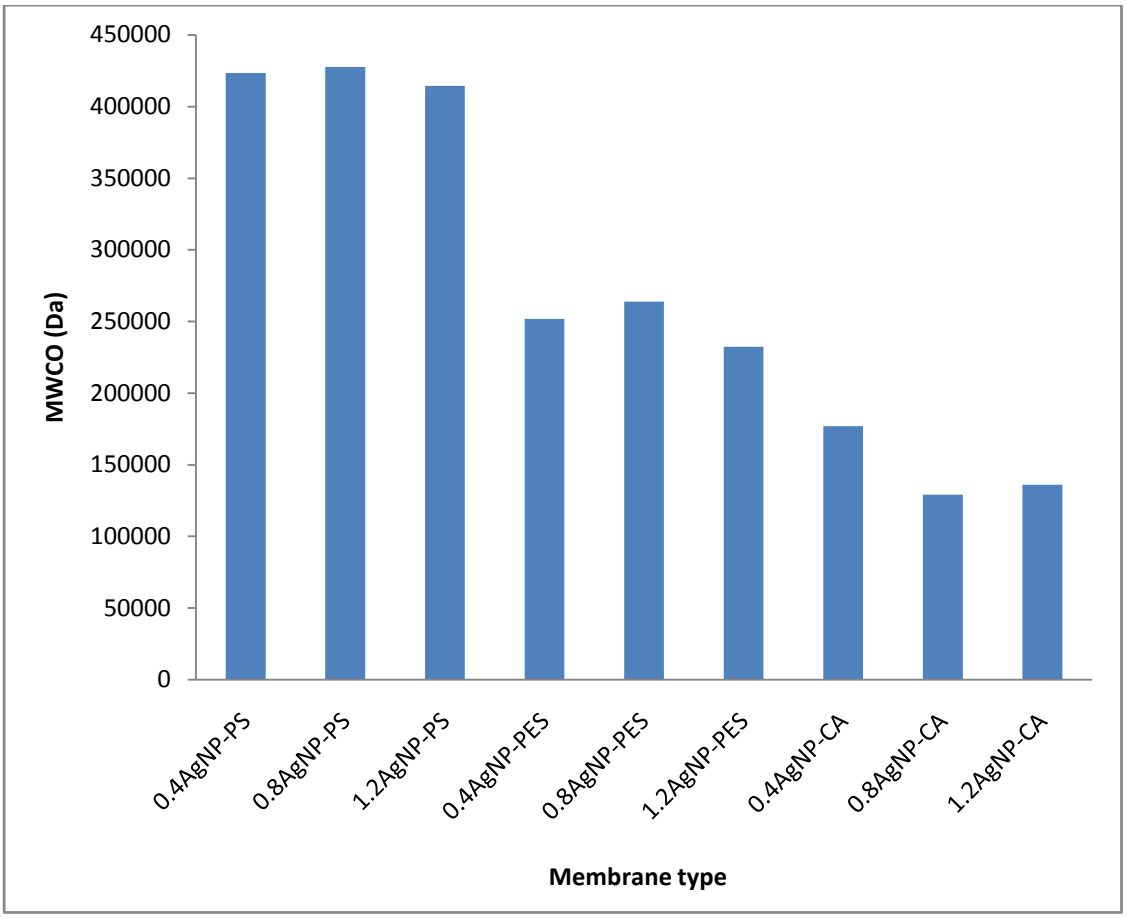

Figure 4. 14. MWCO values of AgNP containing membranes.

MWCO values for the third set of membranes (produced with SiNP) are calculated by using the PEG filtration method and shown as a graph inFigure 4. 15. MWCO values of the SiNP containing PS membranes are calculated as 121223 Da for 0.4% SiNP content, 112838 Da for 0.8% SiNP content and 117545 Da for 1.2% SiNP content. These MWCO values are higher than that of the PS-14 containing bare membranes having MWCO value of 253560 Da.

MWCO values of the SiNP containing PES membranes are calculated as; 81945 Da for 0.4% SiNP content, 152761 Da for 0.8% SiNP content and 188348 Da for 1.2% SiNP content. These MWCO values are lower than that of the bare PES-14 containing membranes having MWCO value of 307025 Da.

MWCO values of the SiNP containing CA membranes are calculated as; 120860 Da for 0.4% SiNP content, 42315 Da for 0.8% SiNP content and 31107 Da for 1.2% SiNP content. These MWCO values are lower than that of the bare CA-14 containing membranes having MWCO value of 202563 Da.

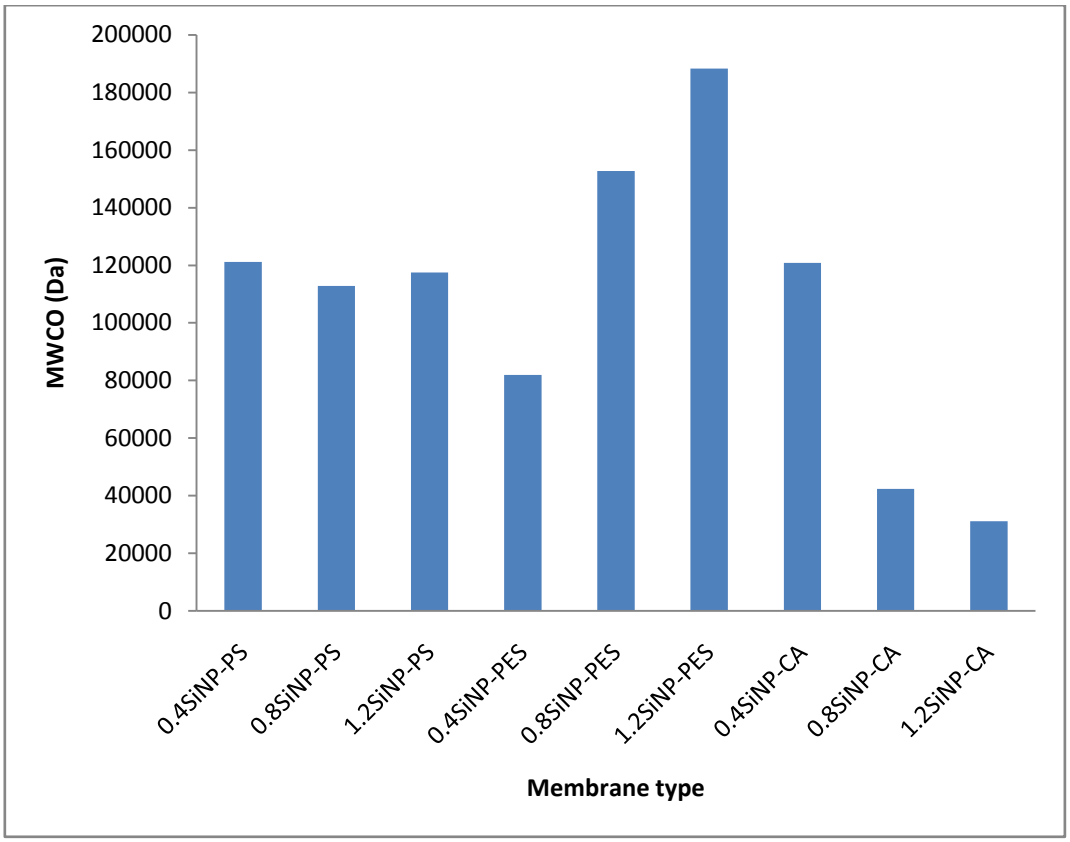

Figure 4. 15. MWCO values of SiNP containing membranes.

MWCO values for the fourth set of membranes (produced with CNT) are calculated by using the PEG filtration method and shown as a graph inFigure 4. 16. MWCO values of the CNT containing PS membranes are calculated as; 328688 Da for 0.4% CNT content, 403230 Da for 0.8% CNT content and 511198 Da for 1.2% CNT content. These MWCO values are higher than that of the bare PS-14 containing membranes having MWCO value of 253560 Da, except for the 0.4% CNT containing PS-14.

MWCO values of the CNT containing PES membranes are calculated as; 694495 Da for 0.4% CNT content, 797334 Da for 0.8% CNT content and 707167 Da for 1.2% CNT content. These MWCO values are much higher than that of the bare PES-14 containing membranes having MWCO value of 307025 Da.

MWCO values of the CNT containing CA membranes are calculated as; 81460 Da for 0.4% CNT content, 100665 Da for 0.8% CNT content and 133255 Da for 1.2% CNT content. These MWCO values are much lower than that of the bare CA-14 containing membranes having MWCO value of 202563 Da.

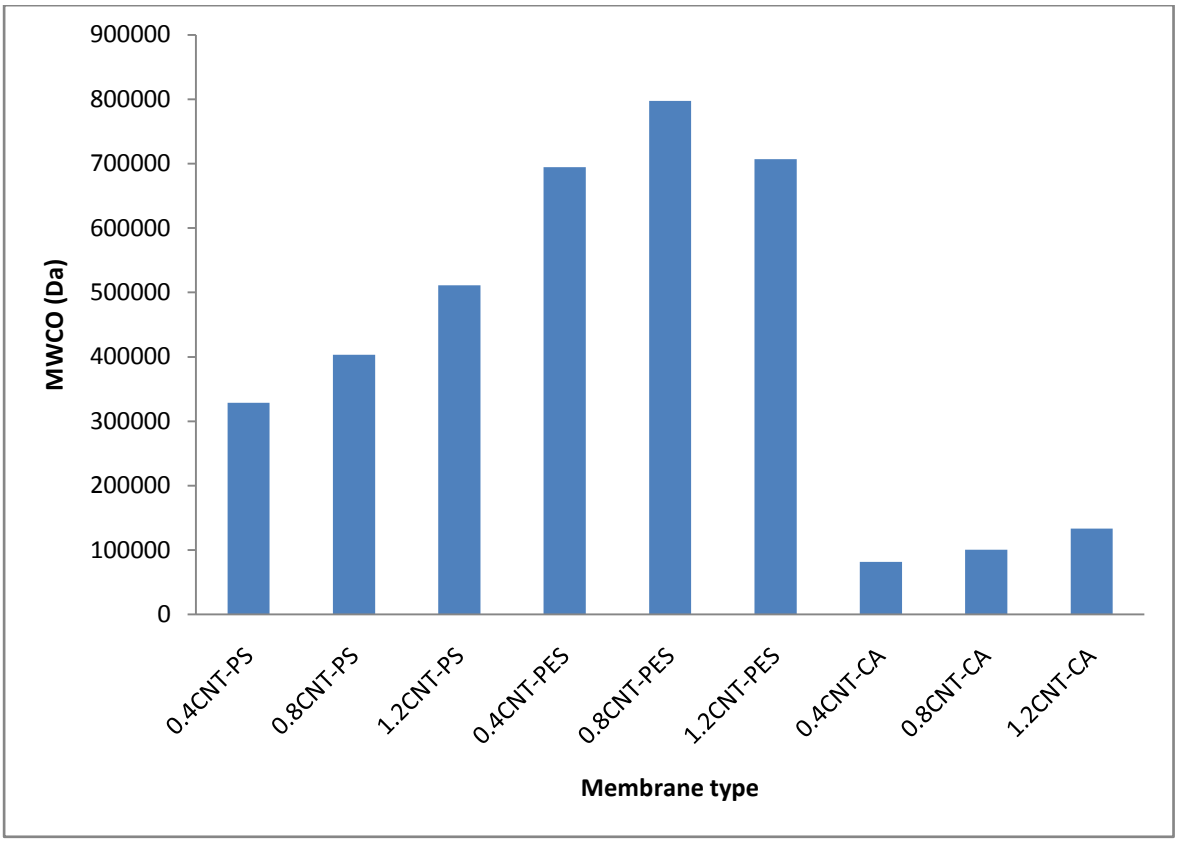

Figure 4. 16. MWCO values of the CNT containing membranes.

MWCO values for the fifth set of membranes (produced with Al_2O_3) are calculated by using the PEG filtration method and shown as a graph inFigure 4. 17. MWCO values for the AlONP containing PS membranes are calculated as; 734533 Da for 0.4% AlONP content, 528215 Da for 0.8% AlONP content and 925491 Da for 1.2% AlONP content. These MWCO values are higher than that of the bare PS-14 containing membranes having MWCO value of 25360 Da.

MWCO values of AlONP containing PES membranes are measured as; 487053 Da for 0.4% AlONP content, 504202 Da for 0.8% AlONP content and 702320 Da for 1.2% AlONP content. These MWCO values are much higher than that of the bare PES-14 containing membranes having MWCO value of 307025 Da.

MWCO values of the AlONP containing CA membranes are measures as; 144679 Da for 0.4% AlONP content, 169436 Da for 0.8% AlONP content and 180333 Da for 1.2% AlONP content. These MWCO values are lower than that of the bare CA-14 containing membranes having MWCO value of 202563 Da.

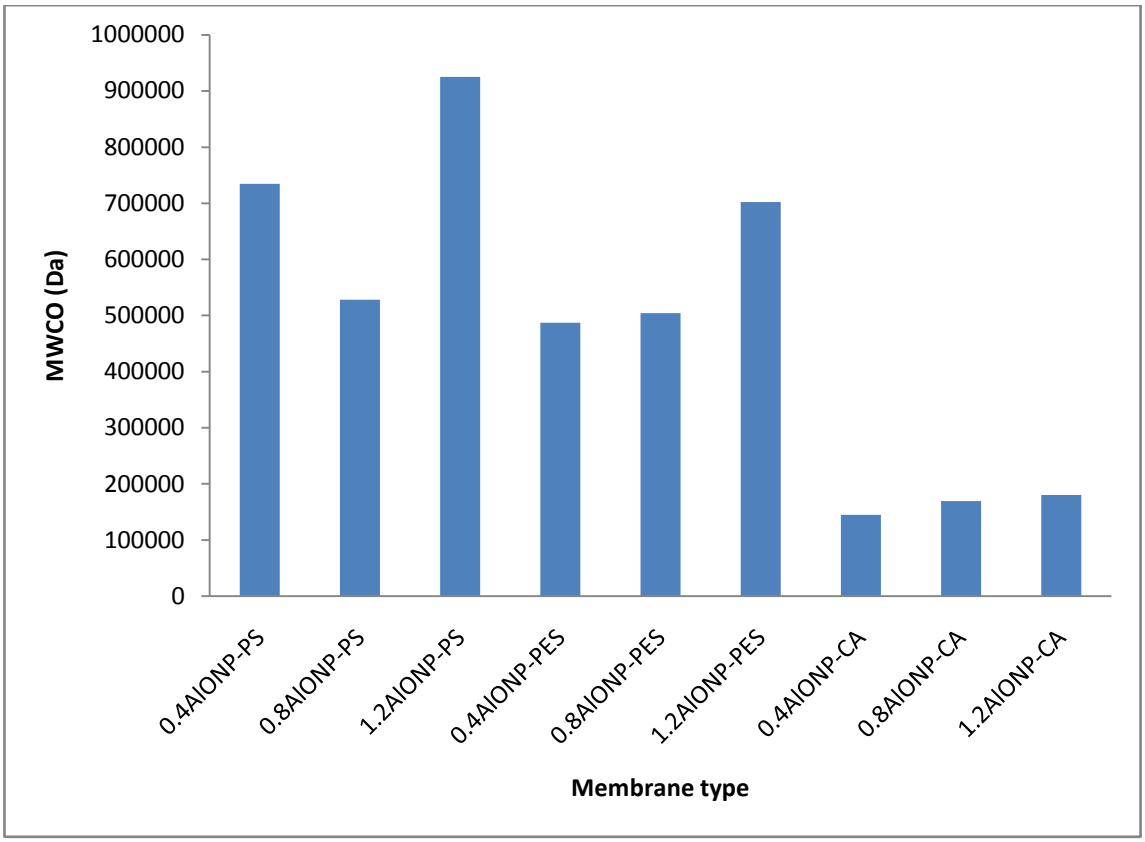

Figure 4. 17. MWCO values of AlONP containing membranes.

MWCO values for the sixth set of membranes (produced with TiO_2) are calculated by using the PEG filtration method and shown as a graph inFigure 4. 18. MWCO values of the TiNP containing PS membranes are calculated as; 641103 Da for 0.4% TiNP content, 843628 Da for 0.8% TiNP content and 1623693 Da for 1.2% TiNP content. These MWCO values are much higher than that of the bare PS-14 containing membranes having MWCO value of 253560 Da.

MWCO values pf TiNP containing PES membranes are calculated as; 367266 for 0.4% TiNP content, 503032 Da for 0.8% TiNP content and 2899728 Da for 1.2% TiNP content. These MWCO values are much higher than that of the bare PES-14 containing membranes having MWCO value of 307025 Da.

MWCO values of the TiNP containing CA membranes are calculated as; 294270 Da for 0.4% TiNP content, 490226 Da for 0.8% TiNP content and 1769891 for 1.2% TiNP content. These MWCO values are lower than that of the bare CA-14 containing membranes having MWCO value of 202563 Da.

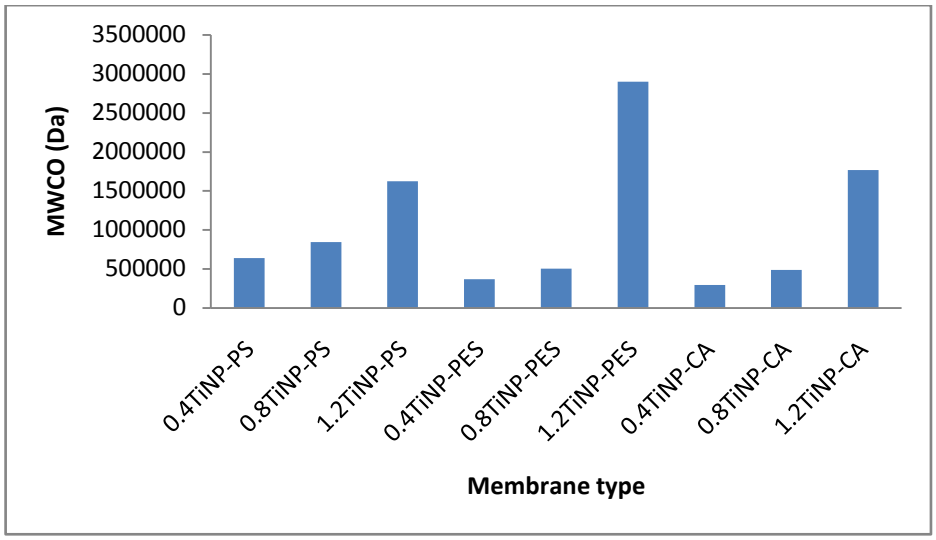

Figure 4. 18. MWCO values of TiNP containing membranes.

4.4 Porosity of the Membranes

Results of the porosity measurements are given inFigure 4. 19. Porosities were measured higher than 80% for all membranes. Porosities were slightly decreased with the increased amount of polymer. Measured porosity values were higher for CA membranes than other membranes.

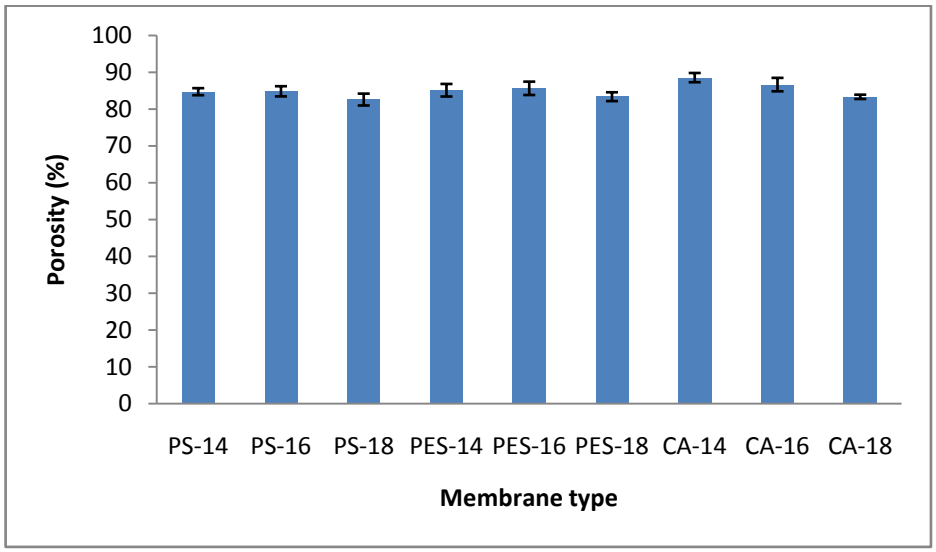

Figure 4. 19. Results of the porosity measurements of bare membranes.

Measured porosity values for the nanomaterial containing membranes are given inFigure 4. 20. It is observed that, when results are compared with the 14% polymer containing membranes; SiNP, CNT and AlONP nanomaterials increased the porosity of the membranes while AgNP and TiNP nanomaterials did not affect the porosities.

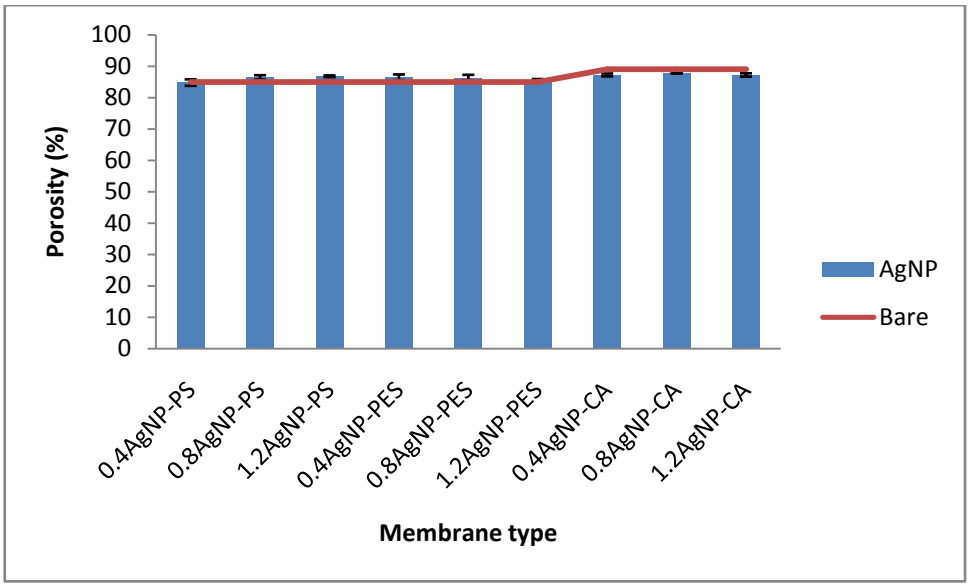
Porosity (%)
100
90
80
70
60
50
40
30
20
10
0
0.4AgNP-PS
0.8AgNP-PS
1.2AgNP-PS
0.4AgNP-PES
0.8AgNP-PES
1.2AgNP-PES
0.4AgNP-CA
0.8AgNP-CA
1.2AgNP-CA
Membrane type
AgNP
Bare

(a)

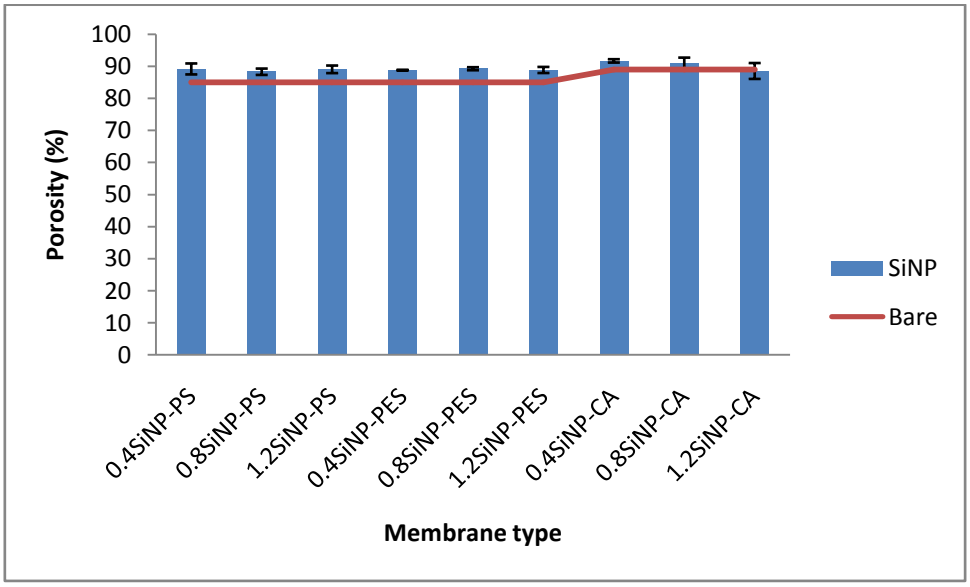
Porosity (%)
100
90
80
70
60
50
40
30
20
10
0
0.4SiNP-PS
0.8SiNP-PS
1.2SiNP-PS
0.4SiNP-PES
0.8SiNP-PES
1.2SiNP-PES
0.4SiNP-CA
0.8SiNP-CA
1.2SiNP-CA
Membrane type
SiNP
Bare

(b)

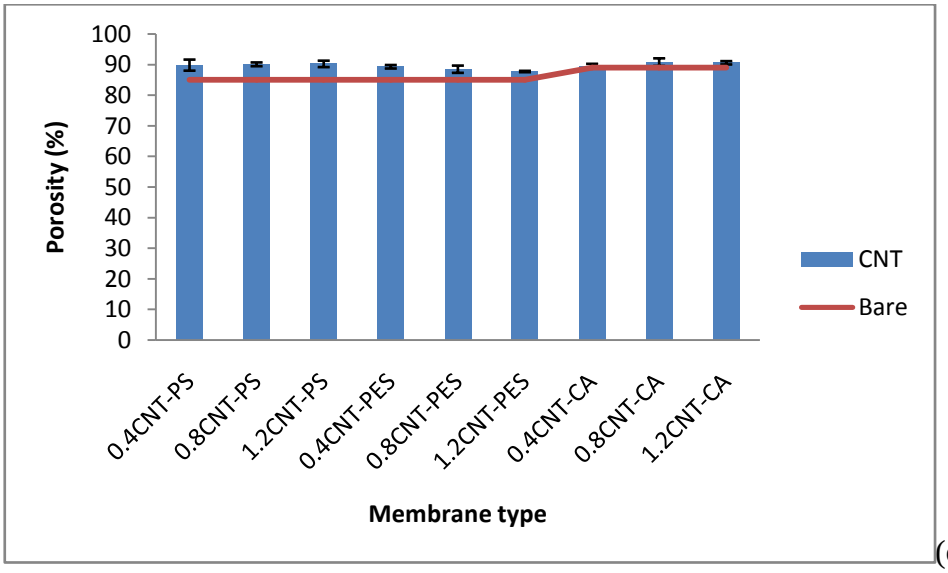
Porosity (%)
100
90
80
70
60
50
40
30
20
10
0
0.4CNT-PS
0.8CNT-PS
1.2CNT-PS
0.4CNT-PES
0.8CNT-PES
1.2CNT-PES
0.4CNT-CA
0.8CNT-CA
1.2CNT-CA
Membrane type
CNT
Bare

(c)

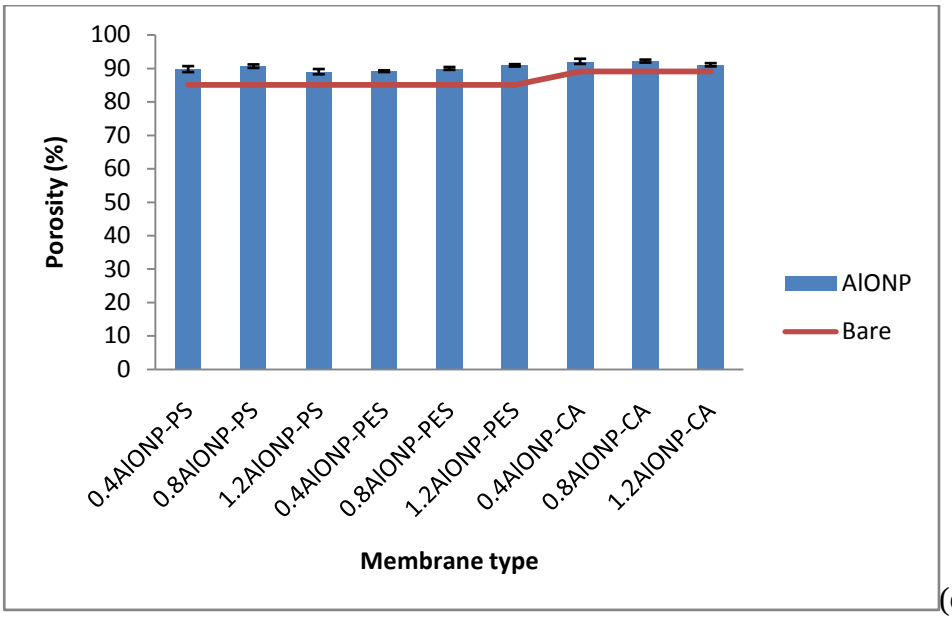

(d)

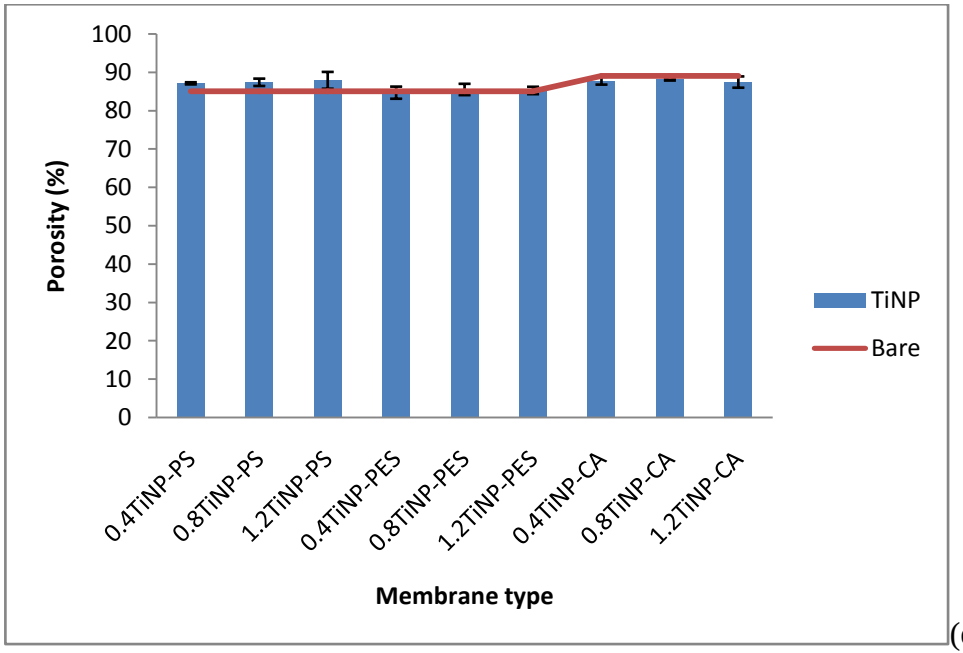

(e)

Figure 4. 20. Measured porosity results of the nanomaterial containing membranes (a) AgNP (b) SiNP (c) CNT (d) AlONP (e) TiNP.

4.5 Shrinkage Ratios of Membranes

Results of the shrinkage experiment for bare polymeric membranes are given in Figure 4. 21. Size change of the membranes after drying process was observed with shrinkage experiments. As can be seen from the graph, measured shrinkage ratios are much higher for CA membranes than shrinkage ratios of other membranes.

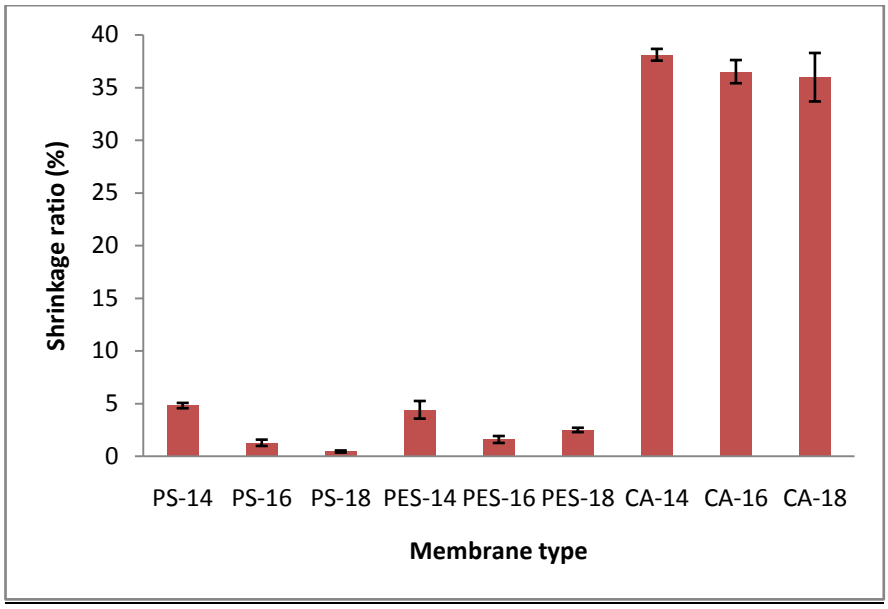

Figure 4. 21. Measured shrinkage ratios of the bare polymeric membranes.

Results of the shrinkage experiment for nanomaterial containing membranes are given in Figure 4. 22. Measured shrinkage values of the nanomaterial containing membranes were less then that of the bare polymeric membranes. Thus it can be said that, nanomaterial addition was beneficial to preserve the membrane form after drying process. Shrinkage values are measured relatively as; AgNP<TiNP<AlONP<CNT<SiNP. Results prove that, AgNP addition provided the highest performance for preserving membrane size while SiNP addition provided the poorest performance. Results did not change much for the membranes with higher nanomaterial contents.

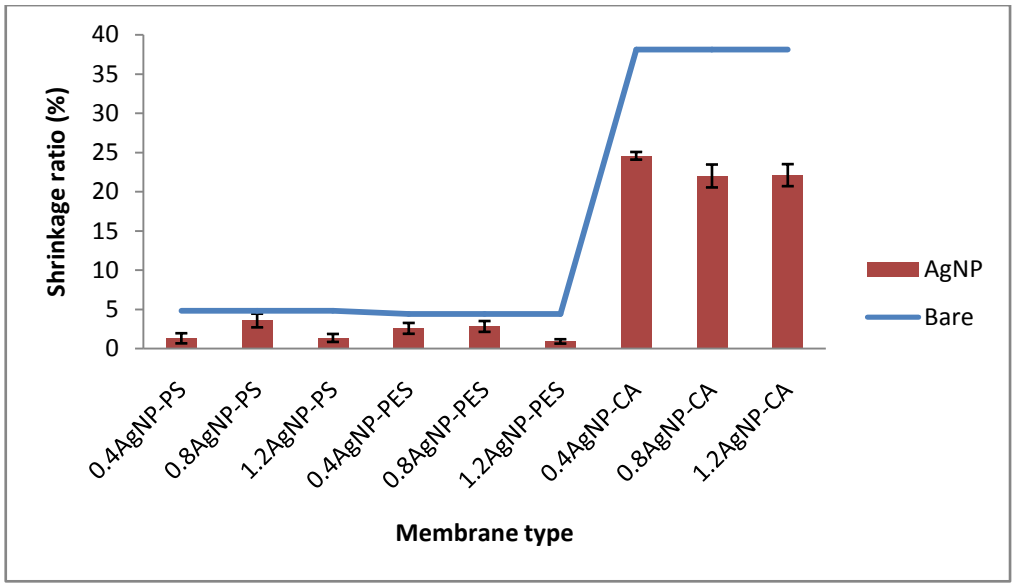

(a)

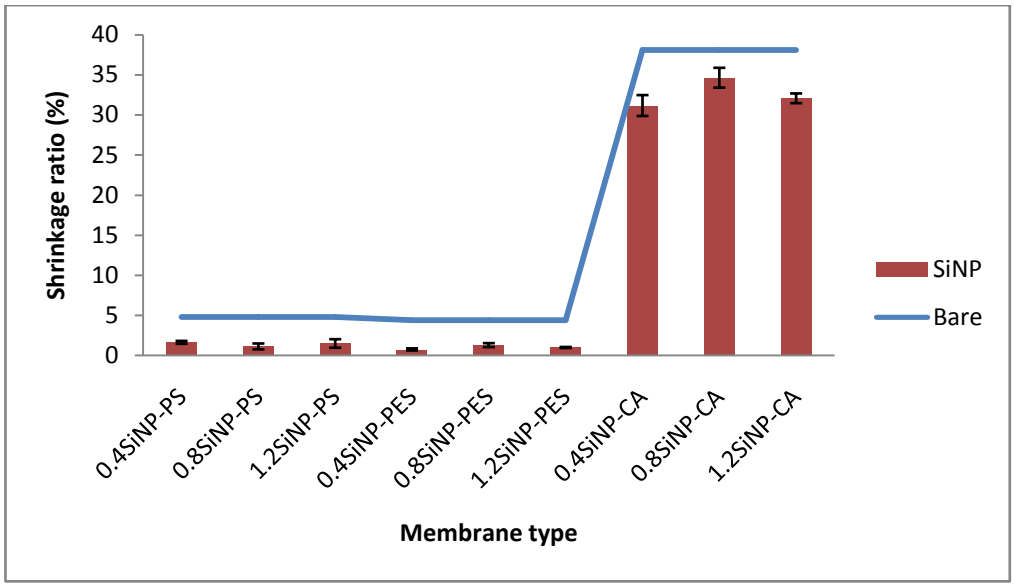
Shrinkage ratio (%)
40
35
30
25
20
15
10
5
0
0.4SiNP-PS
0.8SiNP-PS
1.2SiNP-PS
0.4SiNP-PES
0.8SiNP-PES
1.2SiNP-PES
0.4SiNP-CA
0.8SiNP-CA
1.2SiNP-CA
Membrane type
SiNP
Bare

(b)

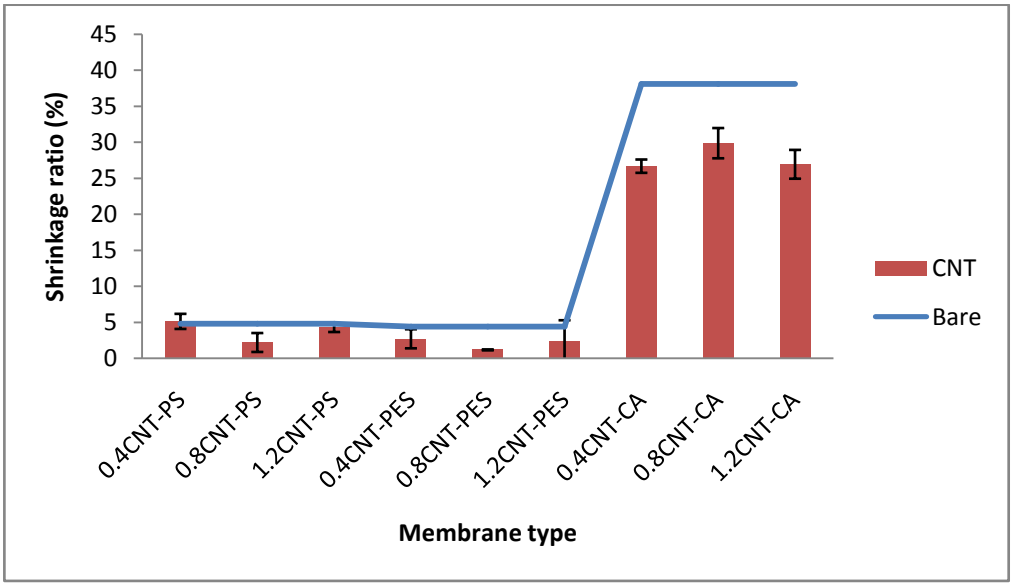
Shrinkage ratio (%)
45
40
35
30
25
20
15
10
5
0
0.4CNT-PS
0.8CNT-PS
1.2CNT-PS
0.4CNT-PES
0.8CNT-PES
1.2CNT-PES
0.4CNT-CA
0.8CNT-CA
1.2CNT-CA
Membrane type
CNT
Bare

(c)

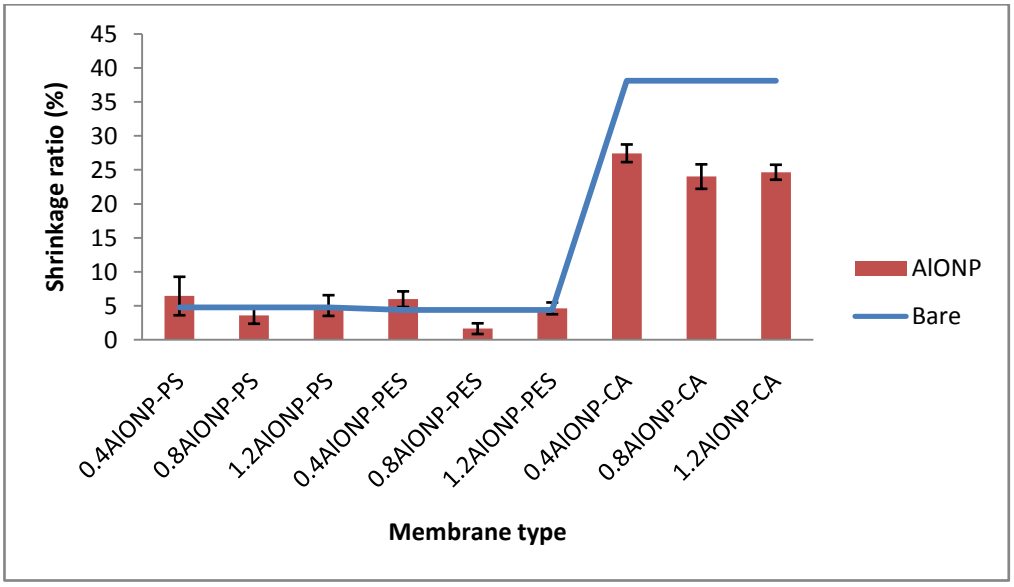
Shrinkage ratio (%)
45
40
35
30
25
20
15
10
5
0
0.4AlONP-PS
0.8AlONP-PS
1.2AlONP-PS
0.4AlONP-PES
0.8AlONP-PES
1.2AlONP-PES
0.4AlONP-CA
0.8AlONP-CA
1.2AlONP-CA
Membrane type
AlONP
Bare

(d)

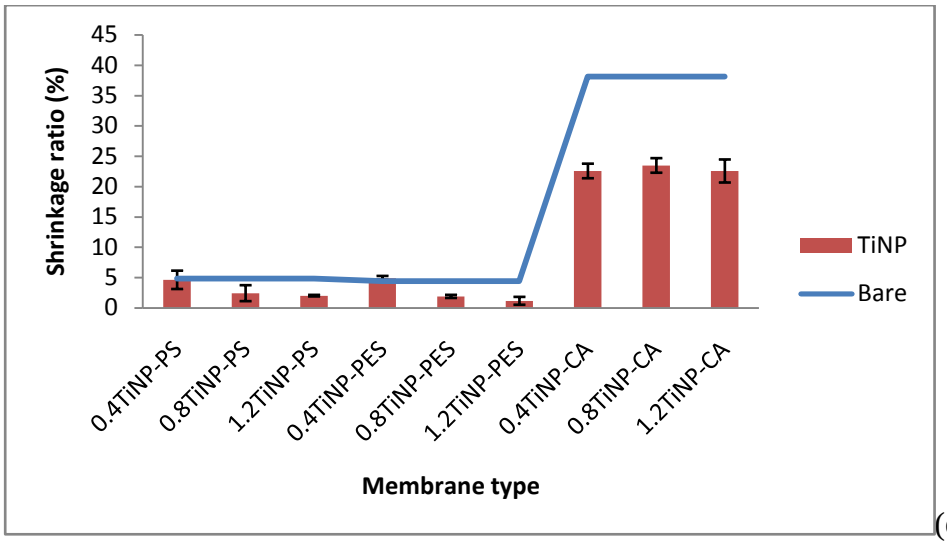

(e)

Figure 4. 22. Measured shrinkage rates for the nanocomposite membranes (a) AgNP (b) SiNP (c) CNT (d) AlONP (e) TiNP.

4.6 Contact Angle Results

Contact angles of the produced bare and nanocomposite polymeric membranes were measured in order to examine the hydrophilicity and hydrophobicity properties after drying process. Measured contact angle values for the bare polymeric membranes are given in Figure 4. 23. Measured contact angle values were decreased with the increase of polymer amount thus, hydrophilicity of the membranes were increased.

Nanomaterial containing membranes were produced by using nanomaterials and 14% polymer containing bare membranes. Contact angles of these 14% polymer containing membranes were measured as; 71±4° for PS-14 membrane, 71±4° for PES-14 membrane and 53±1° for CA-14 membrane.

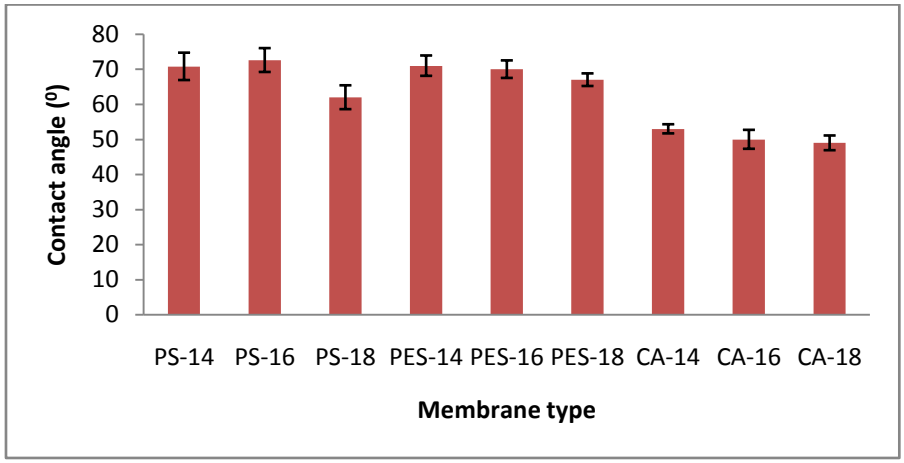

Figure 4. 23. Measured contact angles of the bare polymeric membranes.

Contact angle measurements for the nanomaterial containing membranes are shown inFigure 4. 24. Nanomaterials had different effects on the contact angles of membranes. Contact angle values were decreased with the addition of AgNP nanomaterials for all membranes. Hydrophilicity was measured higher especially for the AgNP-PES membranes. Measured contact angle values for SiNP containing membranes, were not changed significantly for PS membranes but decreased for PES membranes and increased for CA membranes. Measured contact angle values were decreased for all membranes with the addition of CNT nanomaterial. Hydrophilicity values of the membranes were also increased with the increase of CNT content. Measured contact angle values were decreased for all membranes with the addition of AlONP, especially for PES and CA membranes. Decreased contact angles might be reason of the performance increase of CA membranes, for protein and carbohydrate filtrations. Measured contact angle values were decreased for all membranes with the addition of TiNP nanomaterials. TiNP containing membranes were kept under UV light for 15 min and activated by using a 160W UV-A lamp. Contact angle of the membranes were especially decreased with the addition of AlONP and TiNP nanoparticles.

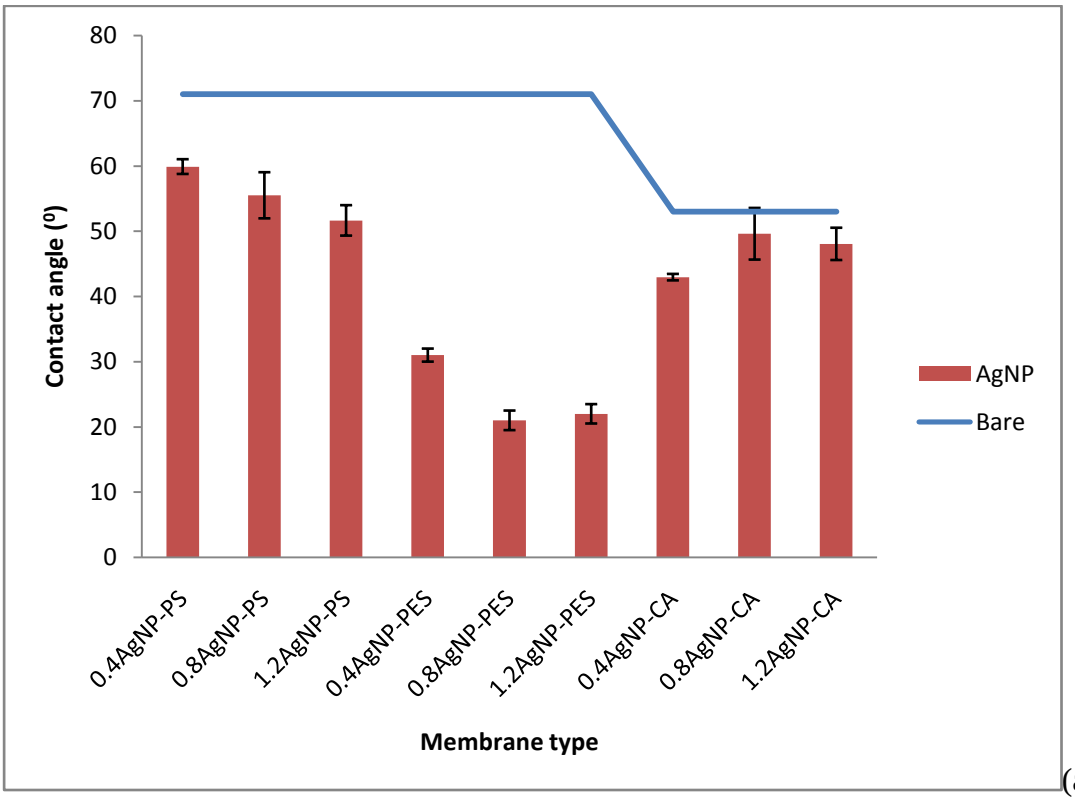

(a)

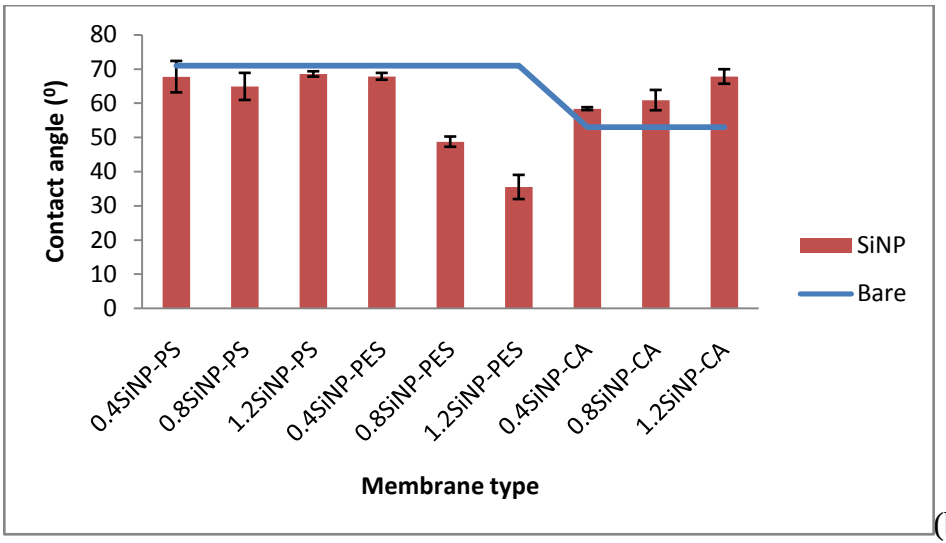
Contact angle (°)
80
70
60
50
40
30
20
10
0
0.4SiNP-PS
0.8SiNP-PS
1.2SiNP-PS
0.4SiNP-PES
0.8SiNP-PES
1.2SiNP-PES
0.4SiNP-CA
0.8SiNP-CA
1.2SiNP-CA
Membrane type
SiNP
Bare

(b)

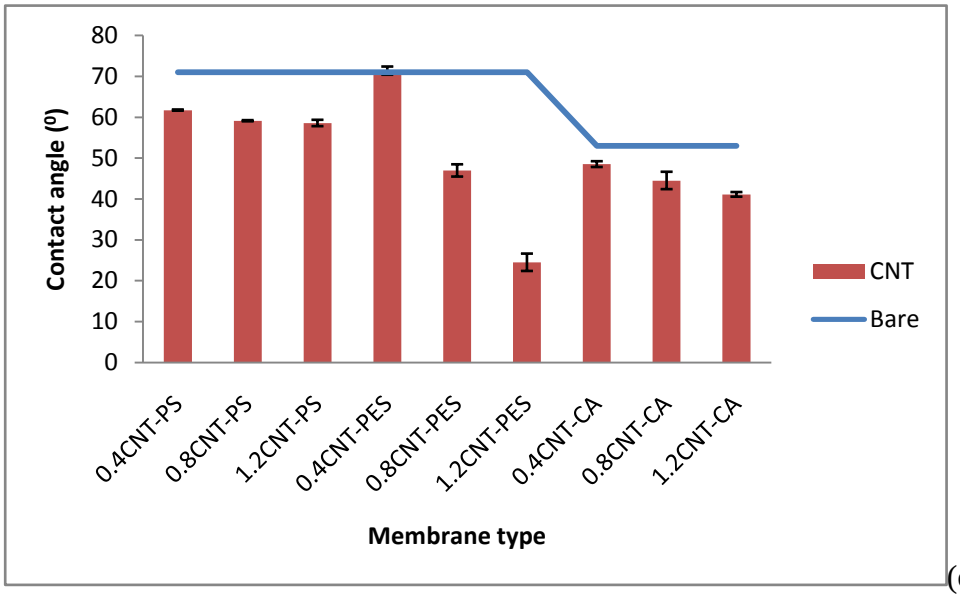
Contact angle (°)
80
70
60
50
40
30
20
10
0
0.4CNT-PS
0.8CNT-PS
1.2CNT-PS
0.4CNT-PES
0.8CNT-PES
1.2CNT-PES
0.4CNT-CA
0.8CNT-CA
1.2CNT-CA
Membrane type
CNT
Bare

(c)

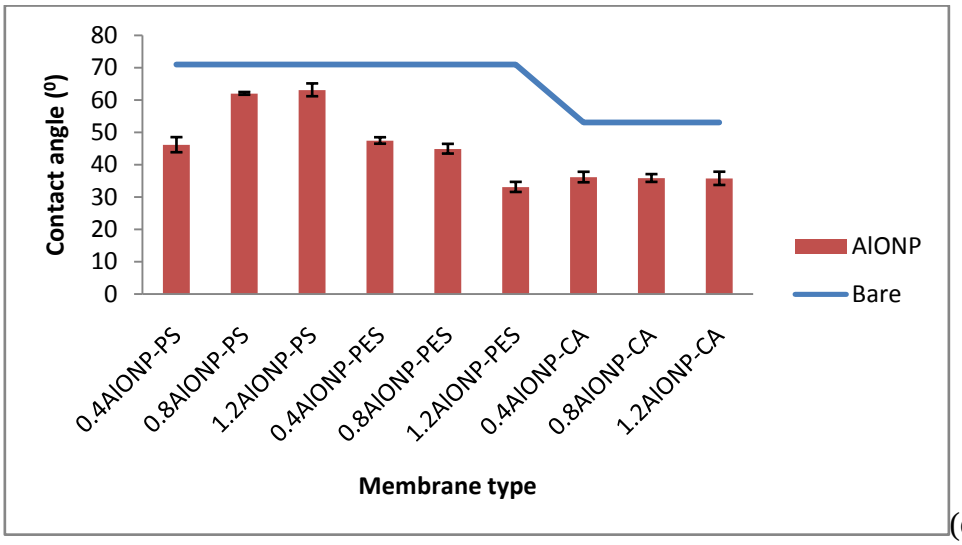
Contact angle (°)
80
70
60
50
40
30
20
10
0
0.4AlONP-PS
0.8AlONP-PS
1.2AlONP-PS
0.4AlONP-PES
0.8AlONP-PES
1.2AlONP-PES
0.4AlONP-CA
0.8AlONP-CA
1.2AlONP-CA
Membrane type
AlONP
Bare

(d)

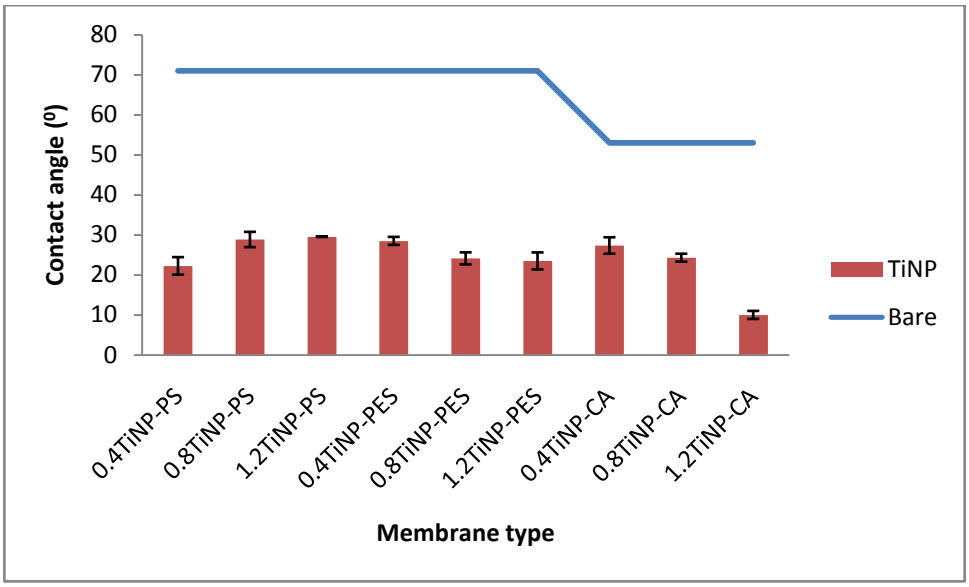

(e)

Figure 4. 24. Measured contact angles for the nanomaterial containing membranes (a) AgNP (b) SiNP (c) CNT (d) AlONP (e) TiNP.

4.7 Results of the Surface Charge Measurements

Measured surface charge values of the bare and nanomaterial containing polymeric membranes are given with the standard deviation values as a graph in Figure 4. 25(a-c). Surface charge measurements were done for the 14% polymer containing bare PS, PES and CA membranes, and for the 1.2% nanomaterial containing PS, PES and CA membranes for further comparison. As can be seen from Figure 4. 25(a), lowest surface charge values were obtained for the PS membranes having 1.2% SiNP or 1.2% AlONP nanoparticles. Surface charge of the bare PS membrane was also decreased with the NP addition.

Graph in the Figure 4. 25(b) shows that, lowest surface charge values were measured for 1.2% CNT containing PES membranes. Surface charges of the PES membranes were decreased with the NP addition.

Graph in the Figure 4. 25(c) shows that, lowest surface charge values were measured for 1.2% SiNP containing CA membranes. Surface charges of the CA membranes were increased with NP addition.

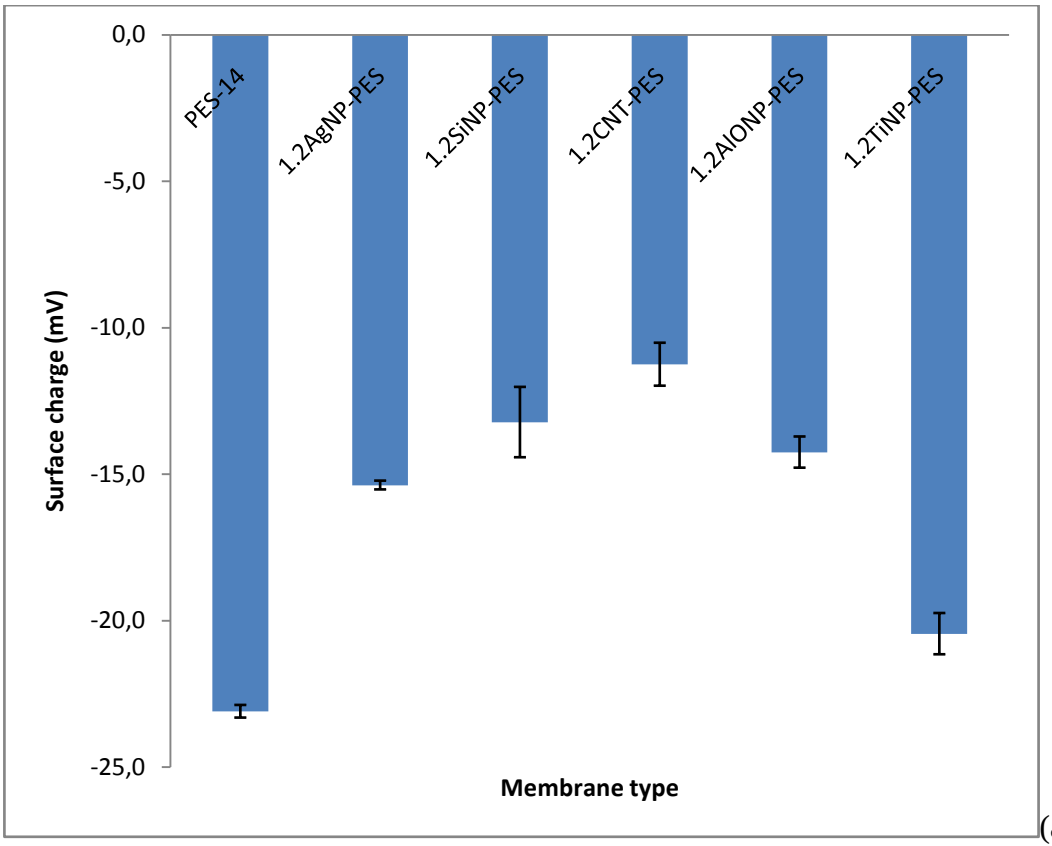
0,0
-5,0
-10,0
-15,0
-20,0
-25,0
Surface charge (mV)
PES-14
1.2AgNP-PES
1.2SiNP-PES
1.2CNT-PES
1.2AlONP-PES
1.2TiNP-PES
Membrane type

(a)

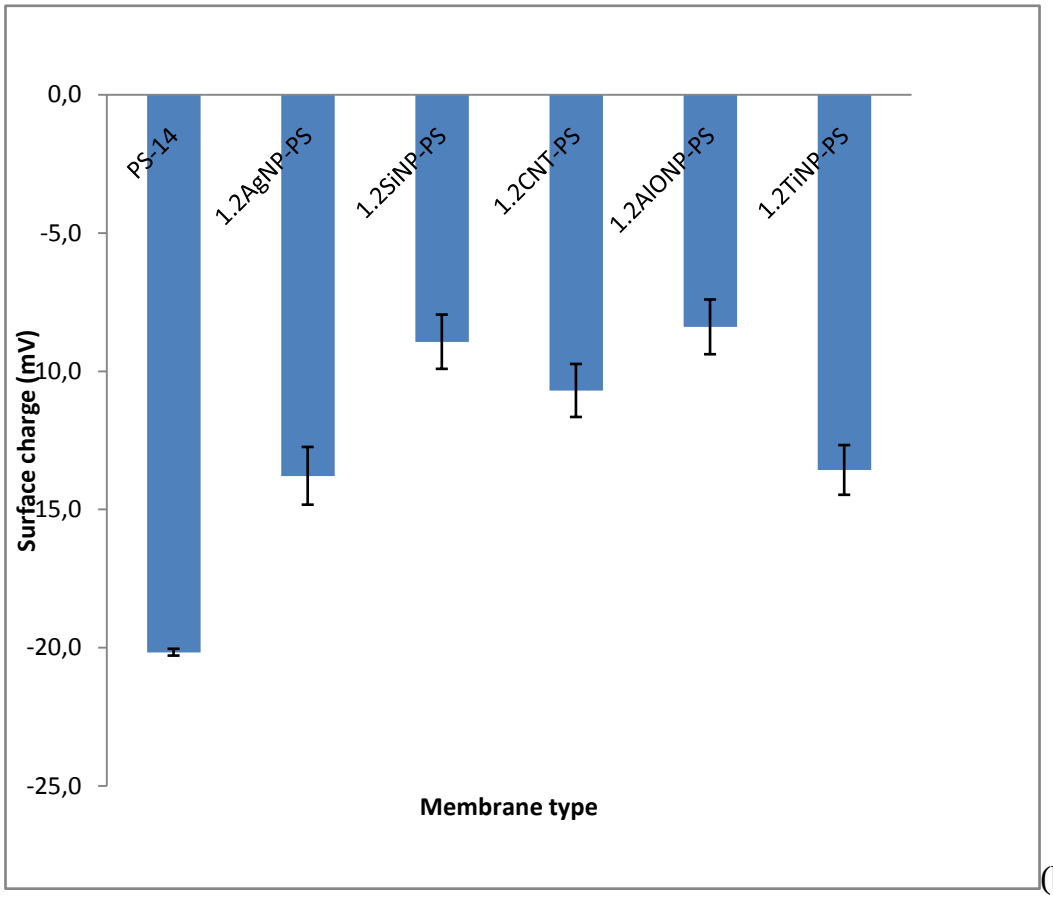
0,0
-5,0
-10,0
-15,0
-20,0
-25,0
Surface charge (mV)
PS-14
1.2AgNP-PS
1.2SiNP-PS
1.2CNT-PS
1.2AlONP-PS
1.2TiNP-PS
Membrane type

(b)

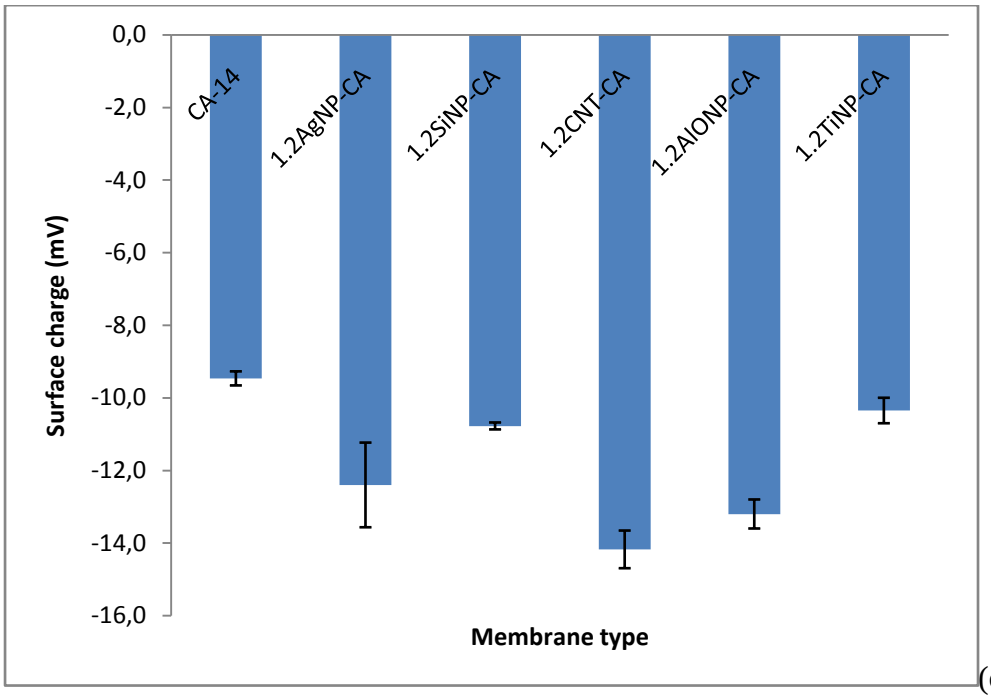

(c)

Figure 4. 25. Measured surface charge values of the bare and nanomaterial containing polymeric membranes (a) PS (b) PES (c) CA.

4.8 SEM-EDS and AFM Analysis

4.8.1 SEM analysis

Images obtained from the SEM-EDS analysis results of bare and nanomaterial containing membranes are shown in Figure 4. 26, Figure 4. 27, Figure 4. 28. SEM-EDS analysis were done for the 14% polymer containing bare PS, PES and CA membranes, and for the 1.2% nanomaterial containing PS, PES and CA membranes for further comparison. SEM images are shown on the left, while images of the peak distributions that are obtained from EDS analysis are shown on the right of the figure. EDS analysis were not useful for CNT containing membranes, because only peak of the C atom could be observed for both bare and CNT containing membranes. Thus, EDS analysis was only done and given for the 1.2% CNT-PES membrane just to have an example.

In Figure 4. 26(showing SEM images of bare and nanomaterial containing PS membranes), very small holes called pores can be seen for the bare PS membrane. White crystal-like structures were formed on the membrane surface with nanomaterial addition. As observed from the EDS analysis, nanoparticle distribution on the membrane surface was homogeneous for each nanomaterial. Furthermore,

observed elements in the EDS analysis were; C,S,O and Ag for the AgNP containing PS membrane, C,S,O and Si elements for the SiO_2NP containing PS membrane, C,S,O and Al for the Al_2O_3NP containing PS membrane and finally C,S,O and Ti for the TiO_2 NP containing PS membranes. EDS analysis was not done for the CNT containing PS membrane. C,S and O elements were observed with the EDS analysis for bare PS membrane.

In Figure 4. 27 (showing SEM images of bare and nanomaterial containing PES membranes), very small holes called pores can be seen for the bare PES membrane just like the SEM image of PS membrane.

White crystal-like structures were also formed on the surface of the PES membrane, with nanomaterial addition. As observed from the EDS analysis, nanoparticle distribution on the membrane surface was homogeneous for each nanomaterial. Furthermore, observed elements in the EDS analysis were; C,S,O and Ag for the AgNP containing PES membrane, C,S,O and Si elements for the SiO_2NP containing PES membrane, C,S,O and Al for the Al_2O_3NP containing PES membrane and finally C,S,O and Ti for the TiO_2 NP containing PES membranes. EDS analysis was also done for bare and CNT containing PES membranes just to have an example. Only C,S and O elements were observed for both bare and CNT containing PES membranes.

As can be seen from the Figure 4. 28 (showing SEM images of bare and nanomaterial containing CA membranes), there are not any pore on the surface of bare CA membranes unlike the PS and PES membranes. White crystal-like structures and also precipitates were formed on the surface of the PES membranes, with nanomaterial addition. CNT nanoparticles were agglomerated and covered the surface of membranes especially for the CNT-CA membranes. As observed from the EDS analysis, nanoparticle distribution on the membrane surface was homogeneous for each nanomaterial. Furthermore, observed elements in the EDS analysis were; C,O and Ag for the AgNP containing CA membrane, C,O and Si elements for the SiO_2NP containing CA membrane, C,O and Al for the Al_2O_3NP containing CA membrane and finally C,O and Ti for the TiO_2 NP containing CA membranes. C and O elements were observed from the elemental analysis of bare CA membrane.

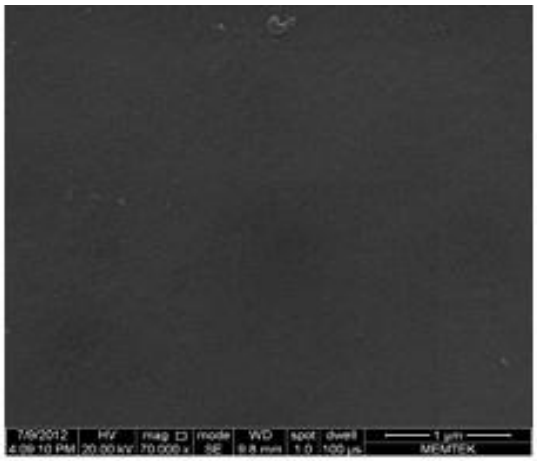

(a)

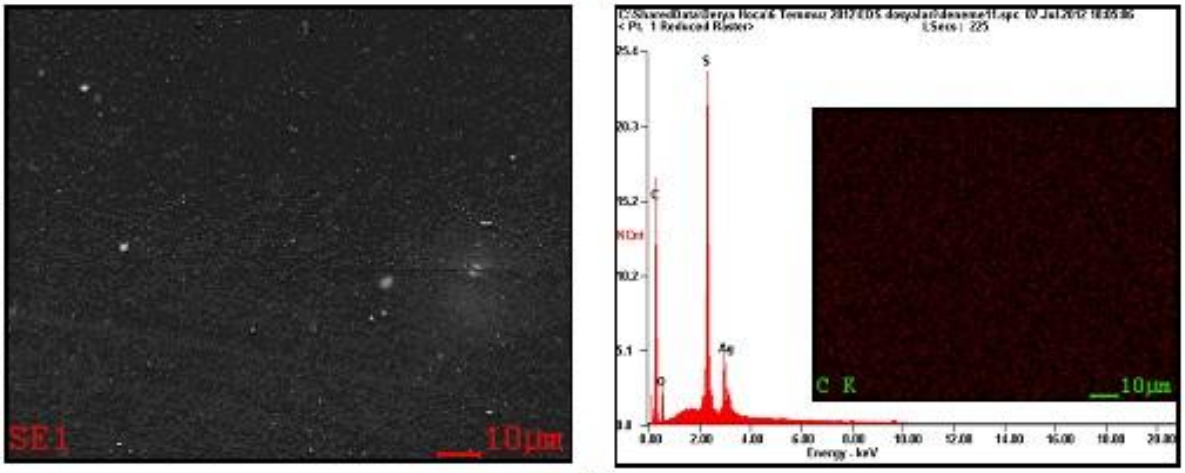
SE1
10µm
S
C
O
Au
C K
10µm
Energy - keV

(b)

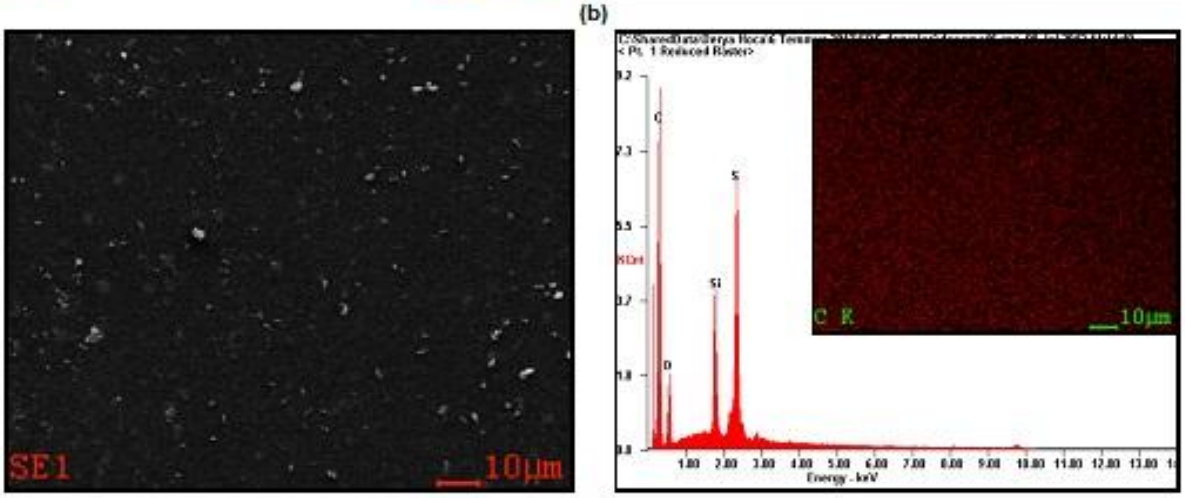
SE1
10µm
C
S
Si
O
C K
10µm
Energy - keV

(c)

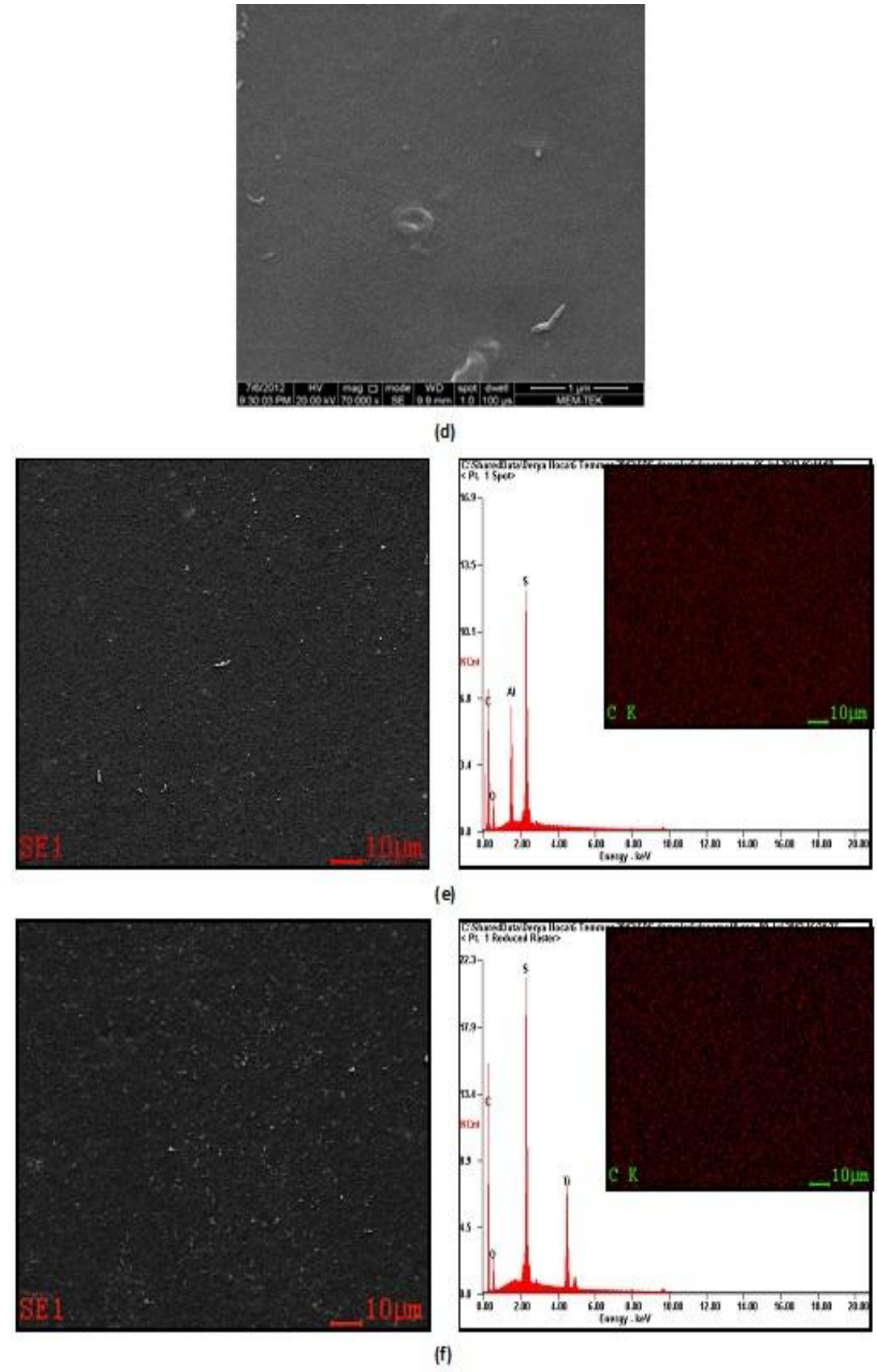

Figure 4. 26. SEM images of bare and nanocomposite PS membranes (a) Bare PS (b) 1.2AgNP-PS (c)1.2SiNP-PS (d) 1.2CNT-PS (e) 1.2AlONP-PS (f) 1.2TiNP-PS.

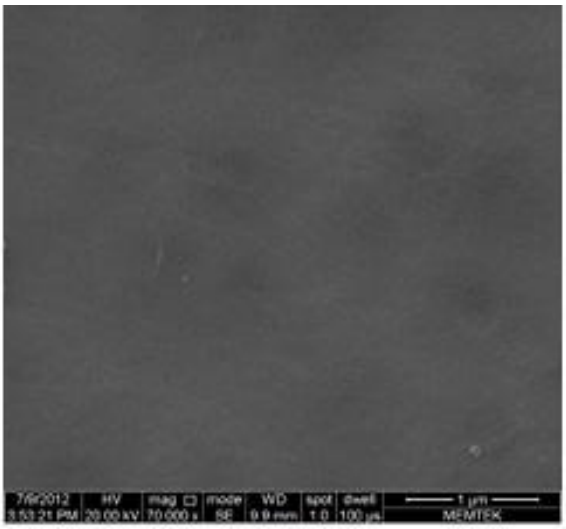

(a)

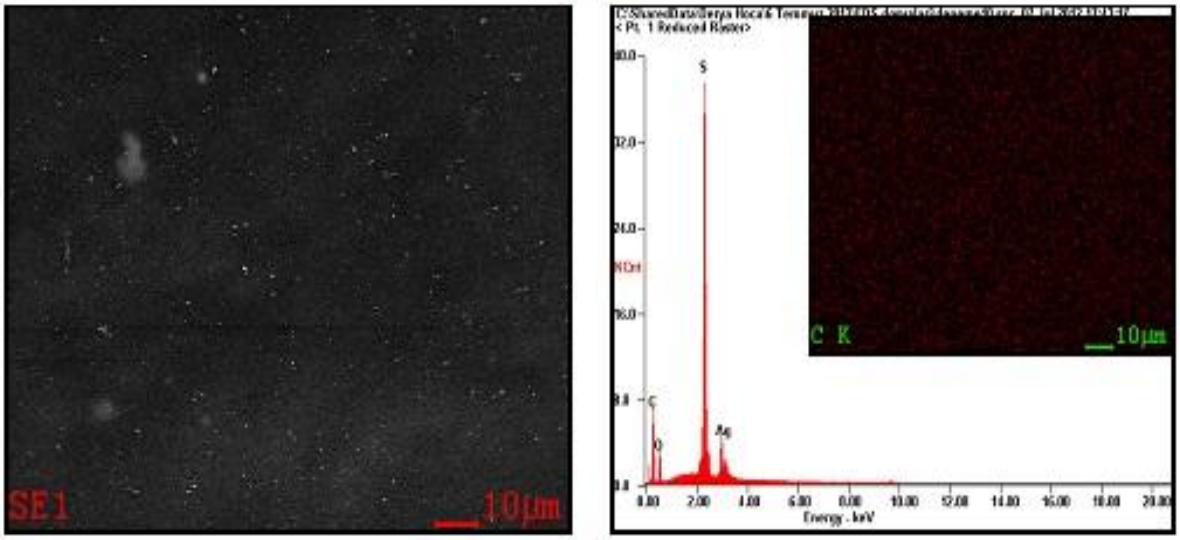

(b)

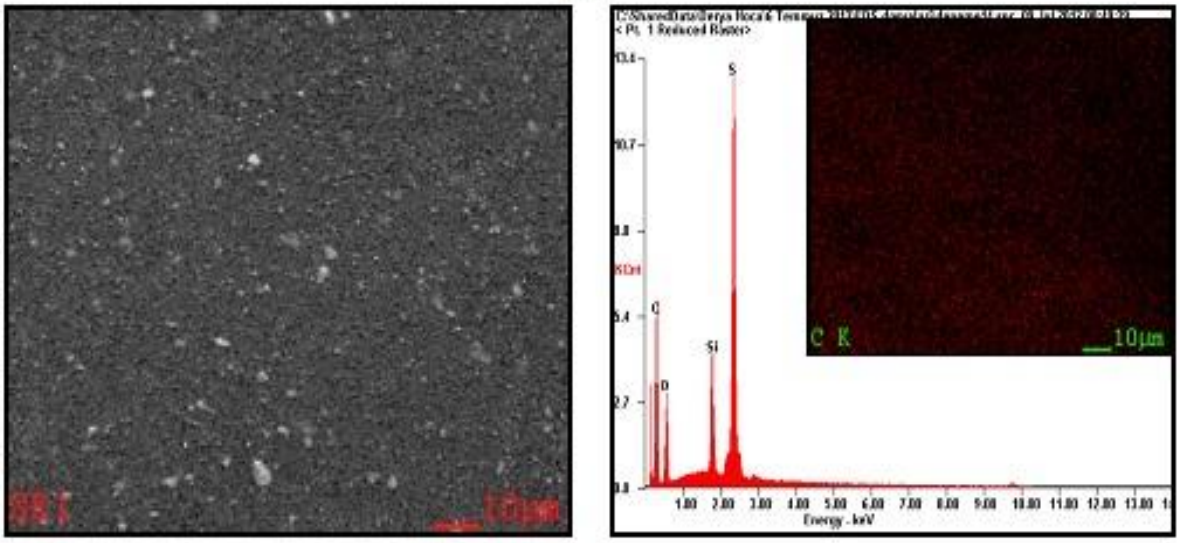

(c)

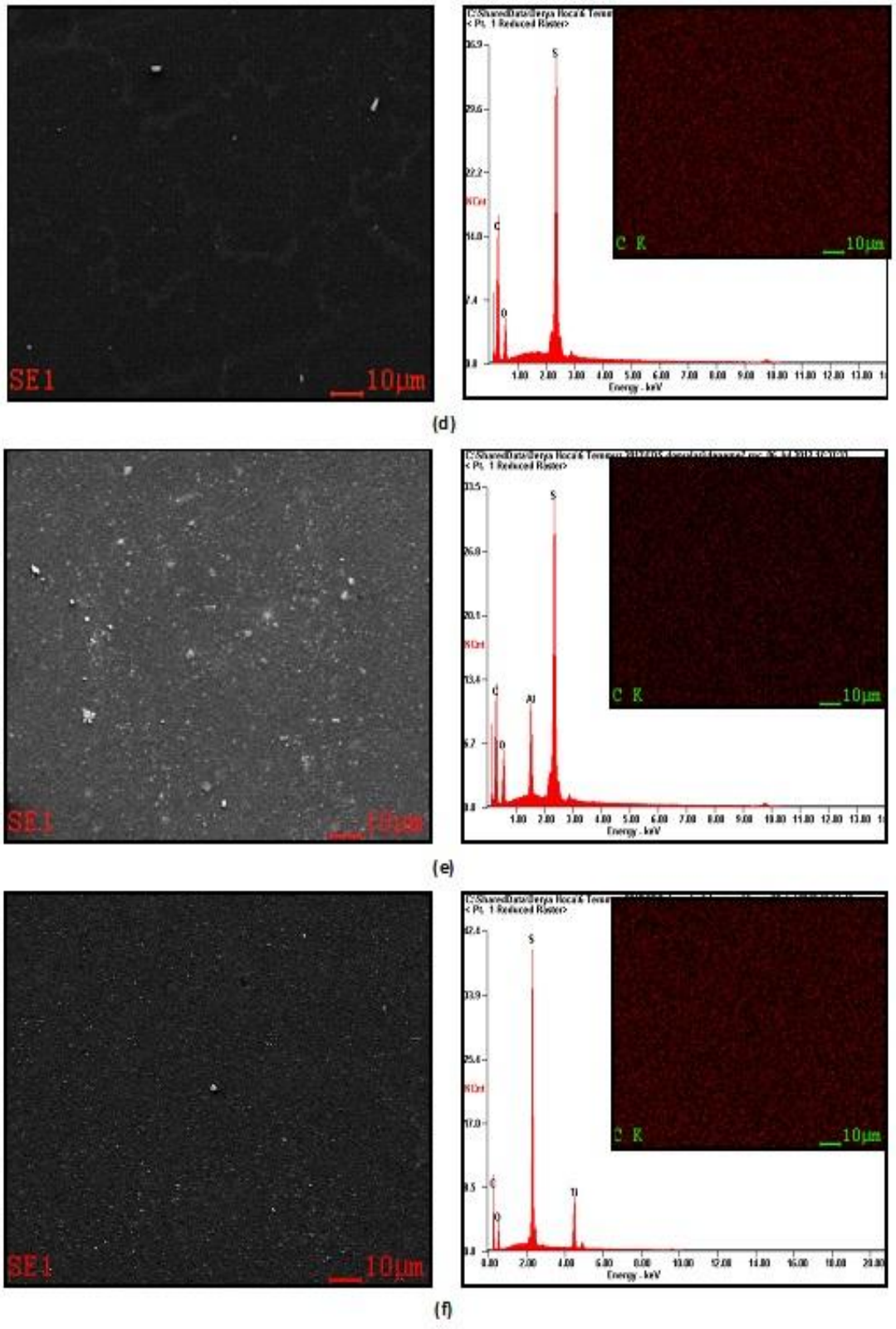

Figure 4. 27. SEM images of bare and nanocomposite PES membranes (a) Bare PES (b) 1.2AgNP-PES (c)1.2SiNP-PES (d) 1.2CNT-PES (e) 1.2AlONP-PES (f) 1.2TiNP-PES.

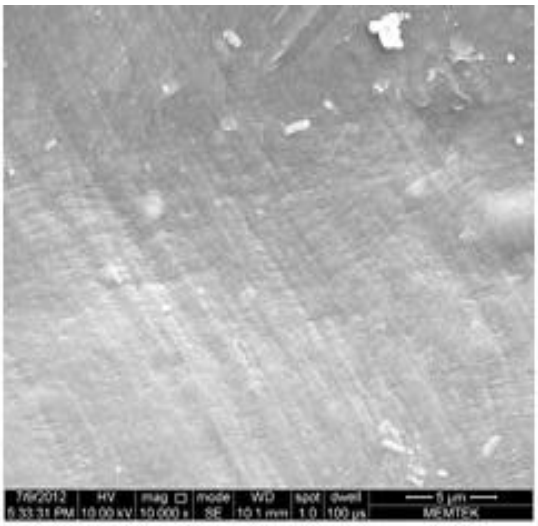

(a)

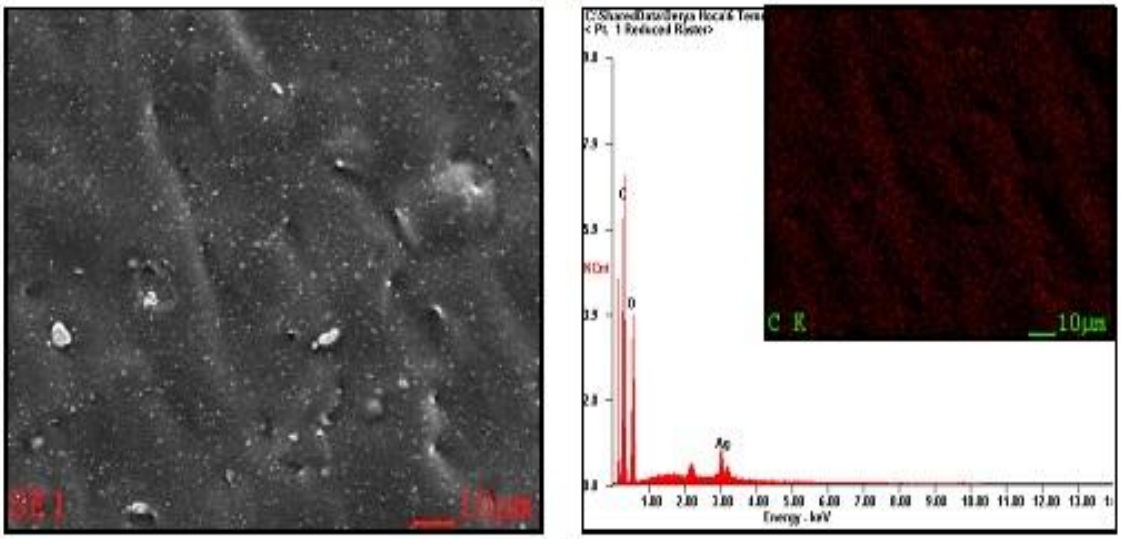
SE1
10µm
C K
10µm
O
Ag
Energy . keV

(b)

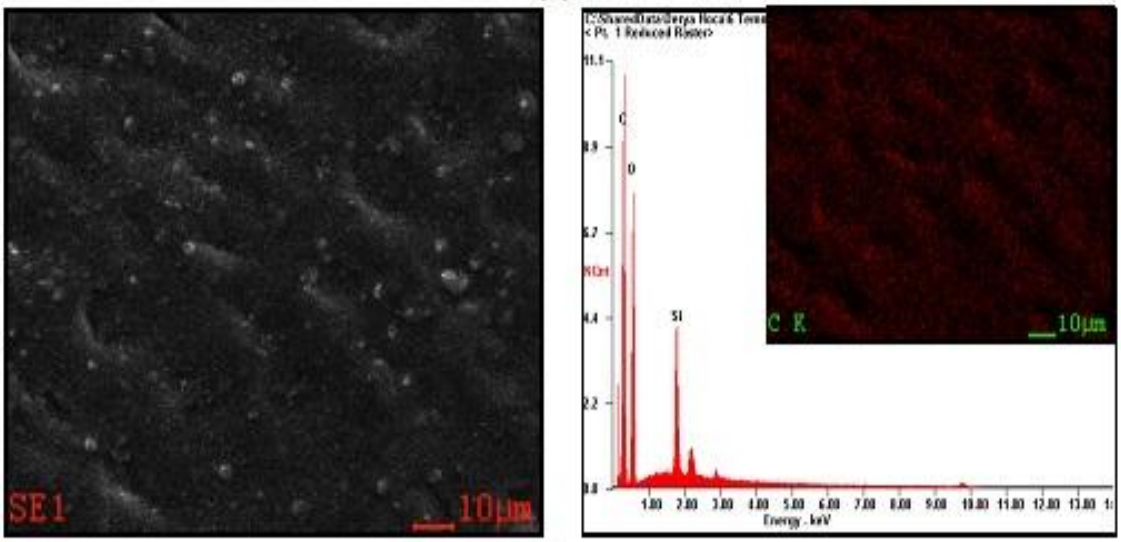
SE1
10µm
C K
10µm
O
Si
Energy . keV

(c)

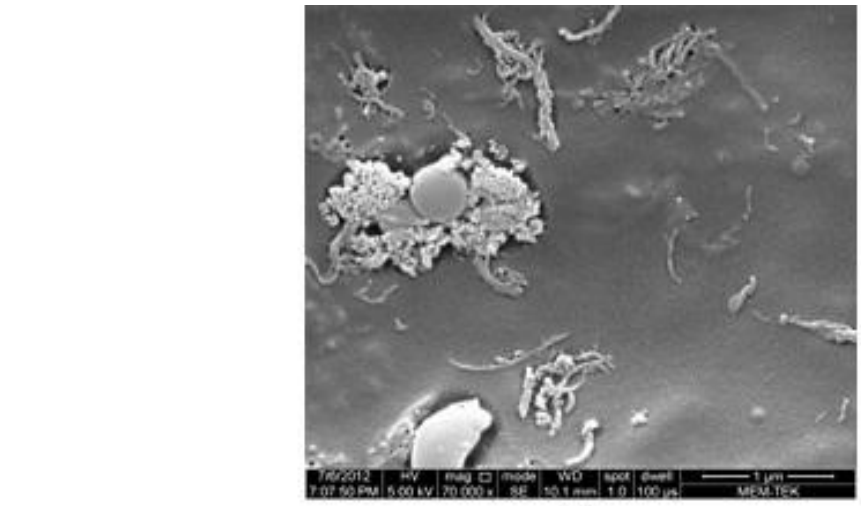

(d)

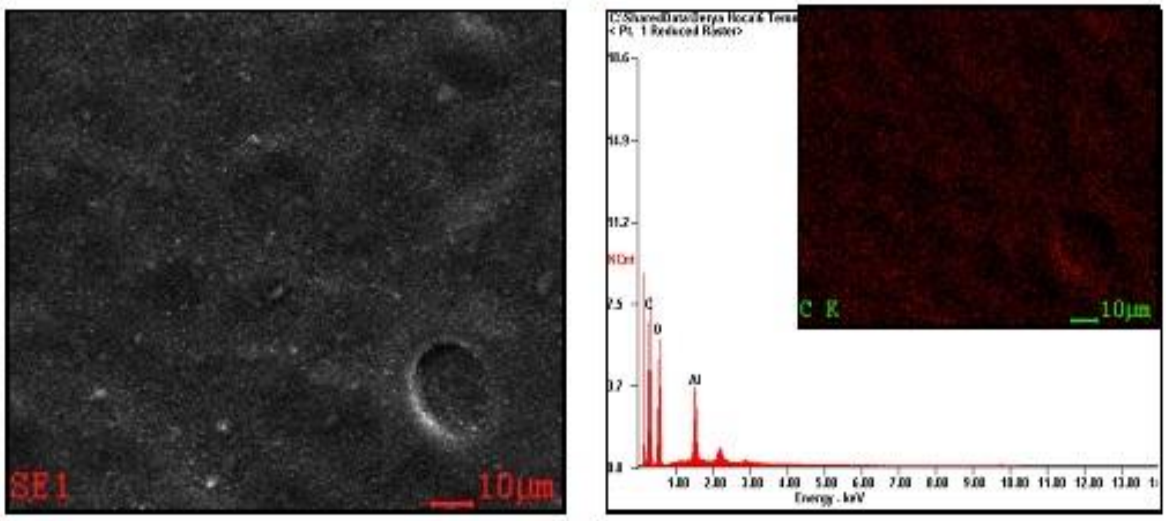

(e)

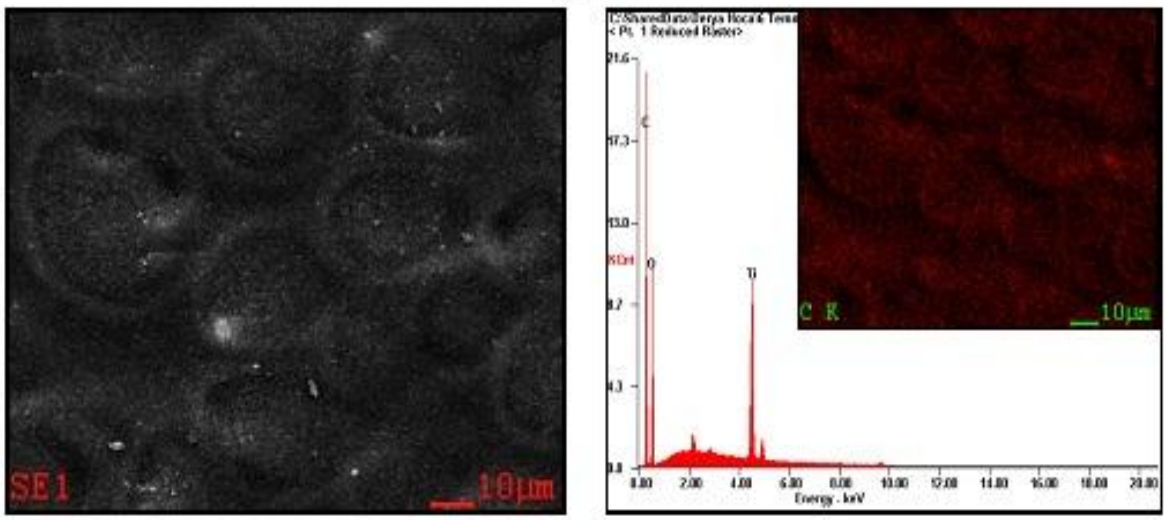

(f)

Figure 4. 28. SEM images of bare and nanomaterial containing CA membranes (a) Bare CA (b) 1.2AgNP-CA (c)1.2SiNP-CA (d) 1.2CNT-CA (e) 1.2AlONP-CA (f) 1.2TiNP-CA.

4.8.2 AFM analysis

AFM analyses were done for each produced membrane. Images obtained from the AFM measurements of bare membranes are shown according to the polymer ratios, in Figure 4. 29 (a-i).

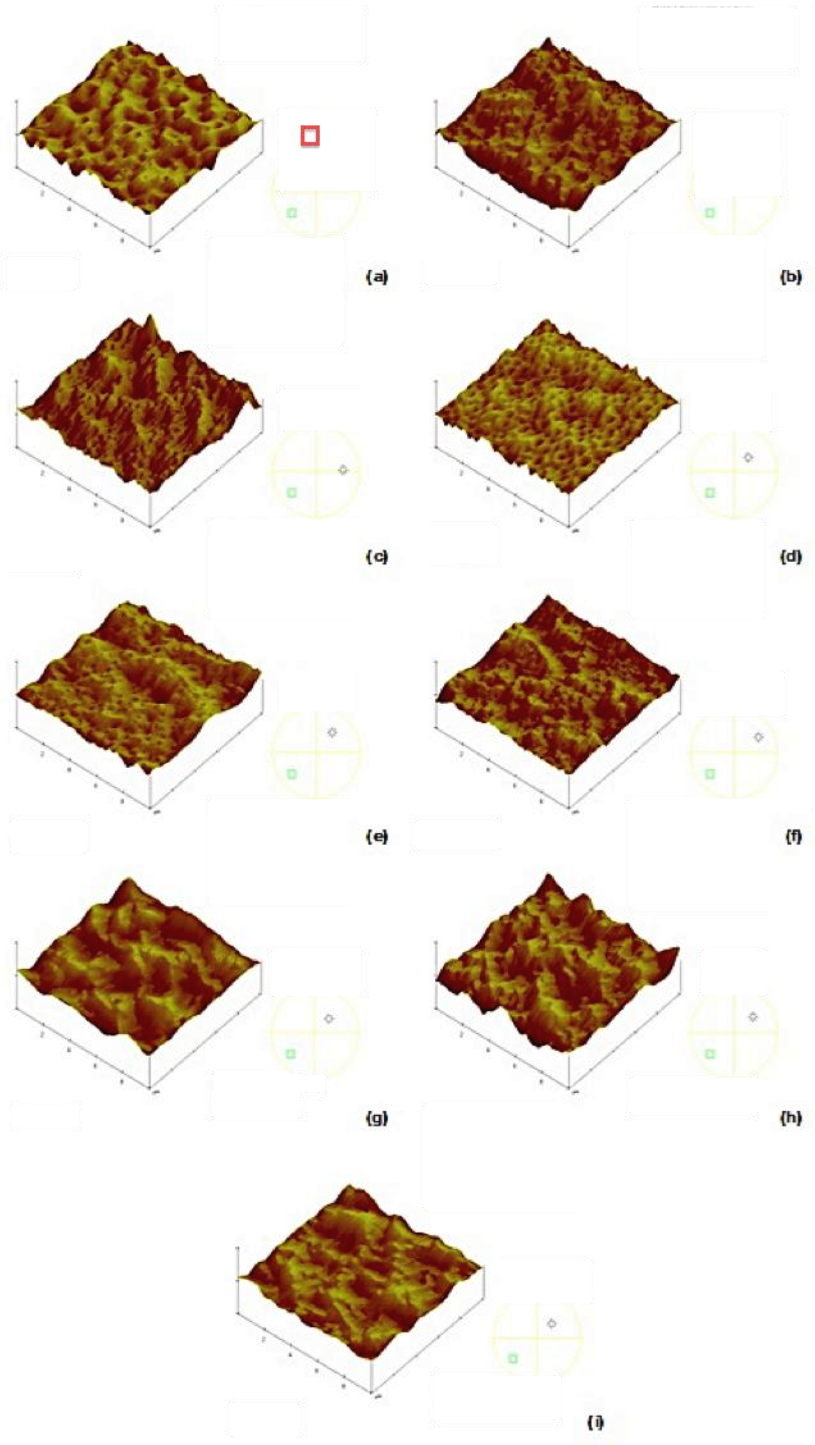

Figure 4. 29. Results of the AFM analysis for bare membranes having different polymer ratios (a) PS-14 (b) PS-16 (c) PS-18 (d) PES-14 (e) PES-16 (f) PES-18 (g) CA-14 (h) CA-16 (i) CA-18.

Average roughness (Ra) values, measured by the AFM analysis, are given for bare membranes in Table 4. 1. Measured Ra values were generally decreased as the polymer contents of membranes were increased. Lowest roughness value was measured for PES type membrane while highest roughness value was measured for the CA type membrane.

Table 4. 1. Ra values of the bare membranes.

Membrane type	Ra (nm)
PS-14	23.4
PS-16	11.6
PS-18	14.8
PES-14	15.0
PES-16	12.0
PES-18	8.3
CA-14	76.8
CA-16	63.6
CA-18	67.5

AFM images of AgNP containing membranes, as the second set of experiments, are shown in Figure 4. 30(a-i). Roughness values are shown in theTable 4. 2. Effects of the AgNP addition on the roughness values of PS-14, PES-14 and CA-14 membranes were investigated. Measured roughness values were similar for bare PS-14 membrane (23.4nm) and the AgNP containing PS membranes except for the 0.8 AgNP-PS membrane. Measured roughness values of AgNP containing membranes were increased, compared to bare PES-14 membrane (15.0nm), except for the 0.4 AgNP-PES membrane. Measured roughness values of the AgNP containing membranes were decreased, compared to bare CA-14 (76.8 nm). Lowest roughness value of the AgNP containin membranes was measured for the 0.4% AgNP containing membranes.

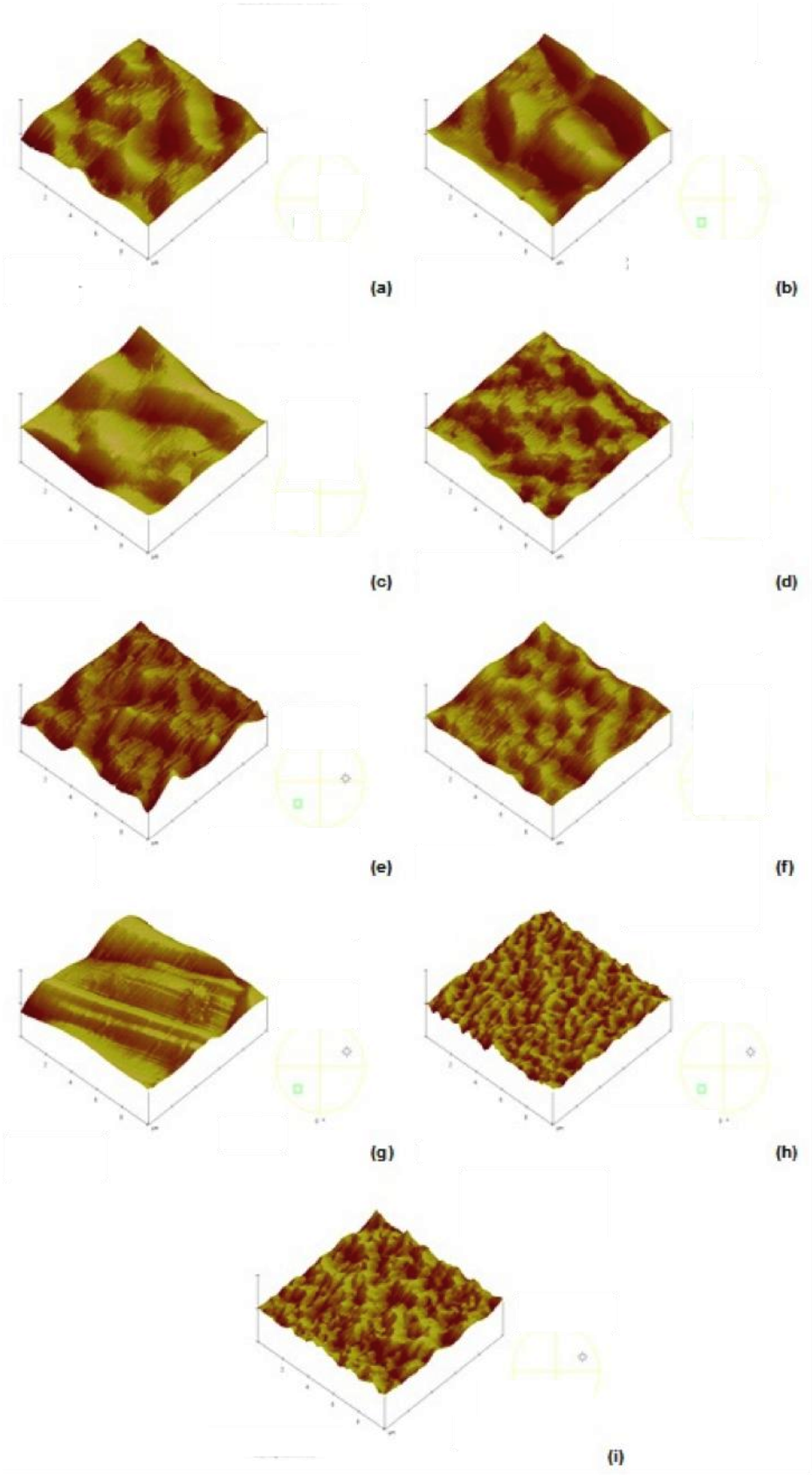

Figure 4. 30. Results of the AFM analysis for AgNP containing membranes (a) 0.4AgNP-PS (b) 0.8AgNP-PS (c) 1.2AgNP-PES (d) 0.4AgNP-PES (e) 0.8AgNP-PES (f) 1.2AgNP-PES (g) 0.4AgNP-CA (h) 0.8AgNP-CA (i) 1.2AgNP-CA.

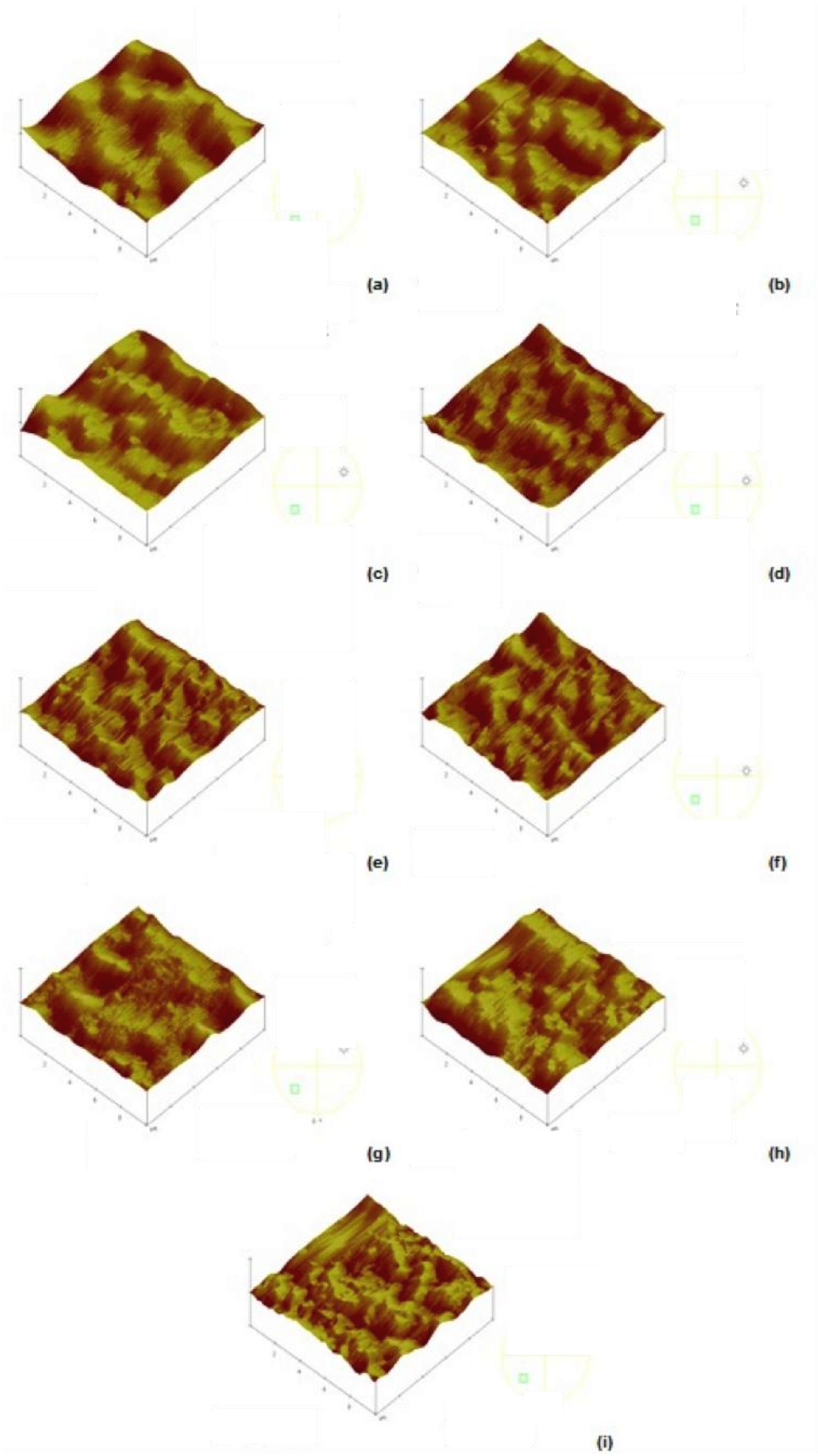

Figure 4. 31. Results of the AFM analysis for SiNP containing membranes (a) 0.4SiNP-PS (b) 0.8SiNP-PS (c) 1.2SiNP-PES (d) 0.4SiNP-PES (e) 0.8SiNP-PES (f) 1.2SiNP-PES (g) 0.4SiNP-CA (h) 0.8SiNP-CA (i) 1.2SiNP-CA.

Table 4. 2. Ra values of AgNP containing membranes.

Membrane type	Ra (nm)
0.4AgNP-PS	23.2
0.8AgNP-PS	28.5
1.2AgNP-PS	23.5
0.4AgNP-PES	16.0
0.8AgNP-PES	21.0
1.2AgNP-PES	18.8
0.4AgNP-CA	19.2
0.8AgNP-CA	52.0
1.2AgNP-CA	69.6

AFM images of SiNP containing membranes, as the third set of experiments, are shown in Figure 4. 31(a-i). SiNP addition decreased the roughness value of CA-14 membrane (76.8 nm) and increased the roughness values of bare PS-14 membrane (23.4 nm) and PES-14 membrane (15.0 nm). Lowest roughness values of SiNP containing membranes were measured for the 0.4% SiNP containing membrane.

Table 4. 3. Ra values for SiNP containing membranes.

Membrane type	Ra (nm)
0.4SiNP-PS	29.0
0.8SiNP-PS	43.7
1.2SiNP-PS	37.6
0.4SiNP-PES	21.0
0.8SiNP-PES	23.9
1.2SiNP-PES	27.9
0.4SiNP-CA	14.0
0.8SiNP-CA	27.9
1.2SiNP-CA	71.6

AFM images of CNT containing membranes, as the fourth set of experiments, are shown in Figure 4. 32(a-i). Roughness values are shown in theTable 4. 4. CNT addition decreased the roughness value of bare CA-14 membrane (76.8nm) but did not change significantly for bare PS-14 membrane (23.4nm) and bare PES-14 membrane (15.0nm). Measured roughness values were similar for all CNT containing membranes.

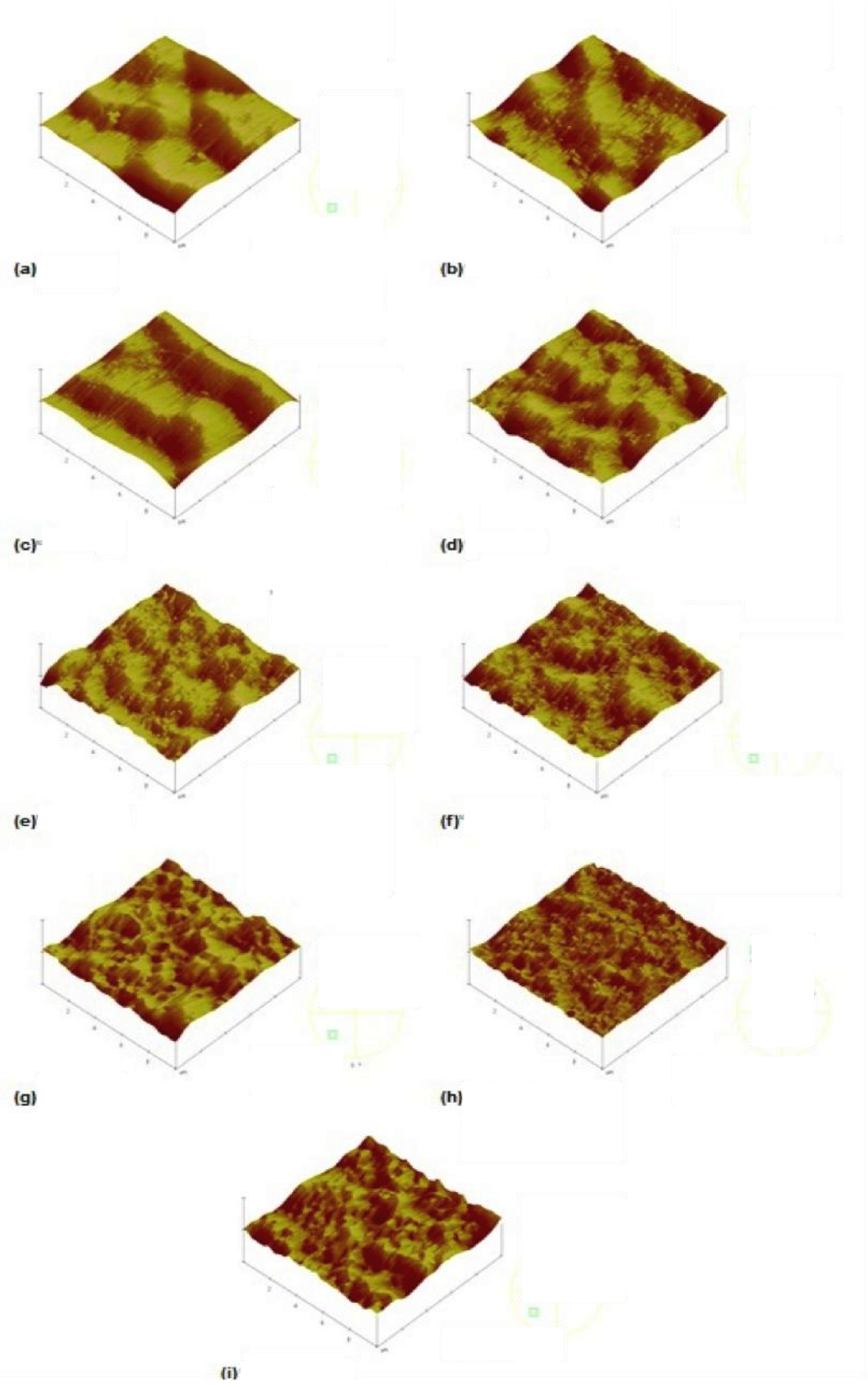

Figure 4. 32. AFM analyses for CNT containing membranes (a) 0.4CNT-PS (b) 0.8CNT-PS (c) 1.2CNT-PES (d) 0.4CNT-PES (e) 0.8CNT-PES (f) 1.2CNT-PES (g) 0.4CNT-CA (h) 0.8CNT-CA (i) 1.2CNT-CA.

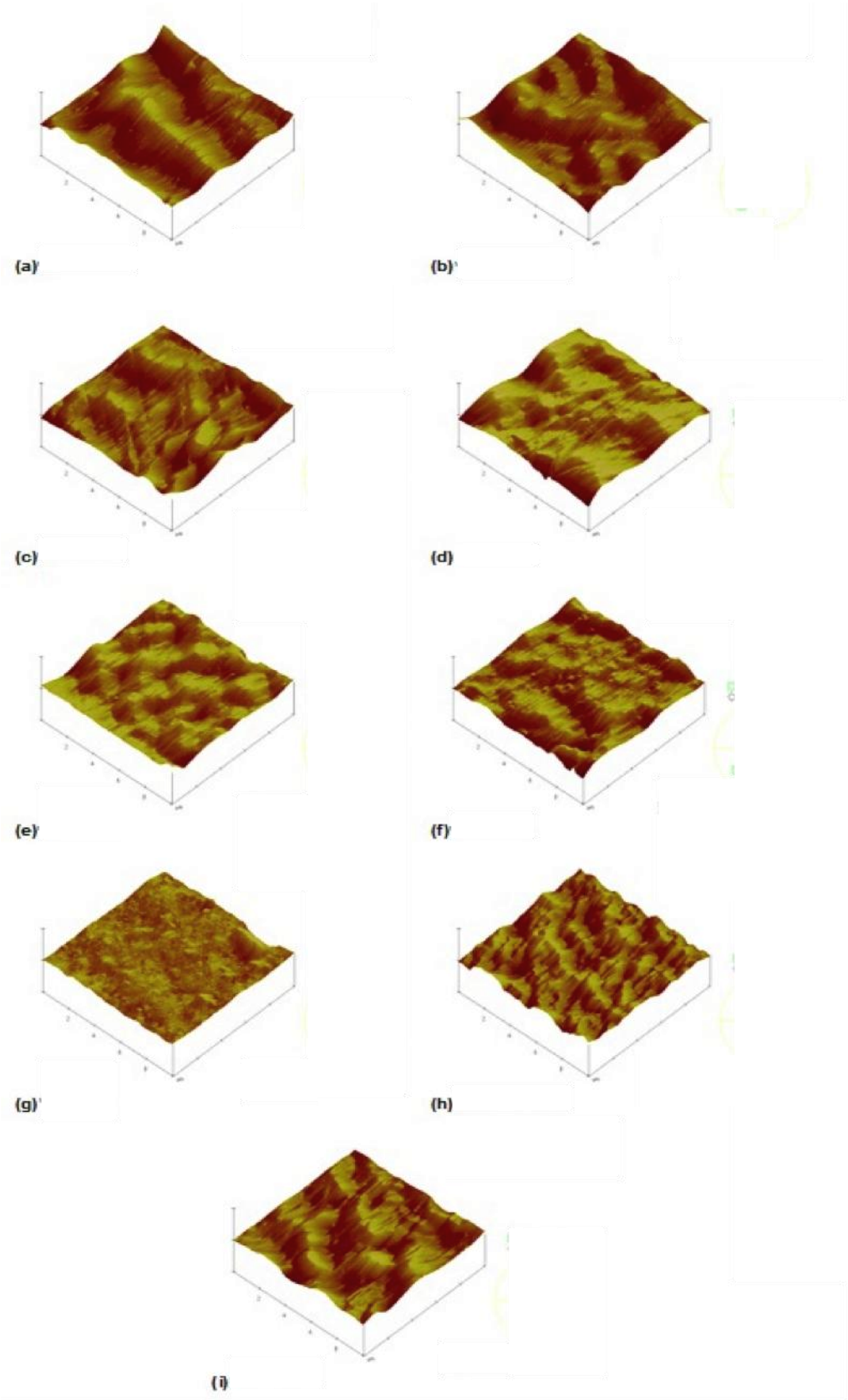

Figure 4. 33. AFM analysis results for AlONP containing membranes (a) 0.4AlONP-PS (b) 0.8AlONP-PS (c) 1.2AlONP-PES (d) 0.4AlONP-PES (e) 0.8AlONP-PES (f) 1.2AlONP-PES (g) 0.4AlONP-CA (h) 0.8AlONP-CA (i) 1.2AlONP-CA.

Table 4. 4. Ra values of CNT containing membranes.

Membrane type	Ra (nm)
0.4CNT-PS	26.6
0.8CNT-PS	20.8
1.2CNT-PS	26.1
0.4CNT-PES	18.6
0.8CNT-PES	16.6
1.2CNT-PES	17.3
0.4CNT-CA	66.0
0.8CNT-CA	66.9
1.2CNT-CA	66.5

AFM images of AlONP containing membranes, as the fifth set of experiments, are shown in Figure 4. 33(a-i). AlONP addition increased the roughness value of bare PS-14 (23.4nm) and bare PES-14 membrane (15.0nm) but decreased the roughness value of bare CA-14 membrane (76.8nm) except for the 0.4% AlONP containing CA-14. Lowest roughness value of AlONP containing membranes was measured for the 0.4% AlONP containing membrane.

Table 4. 5. Ra values of AlONP containing membranes.

Membrane type	Ra (nm)
0.4AlONP-PS	25.7
0.8AlONP-PS	33.0
1.2AlONP-PES	45.5
0.4AlONP-PES	20.5
0.8AlONP-PES	24.7
1.2AlONP-PES	21.1
0.4AlONP-CA	53
0.8AlONP-CA	93.2
1.2AlONP-CA	50.9

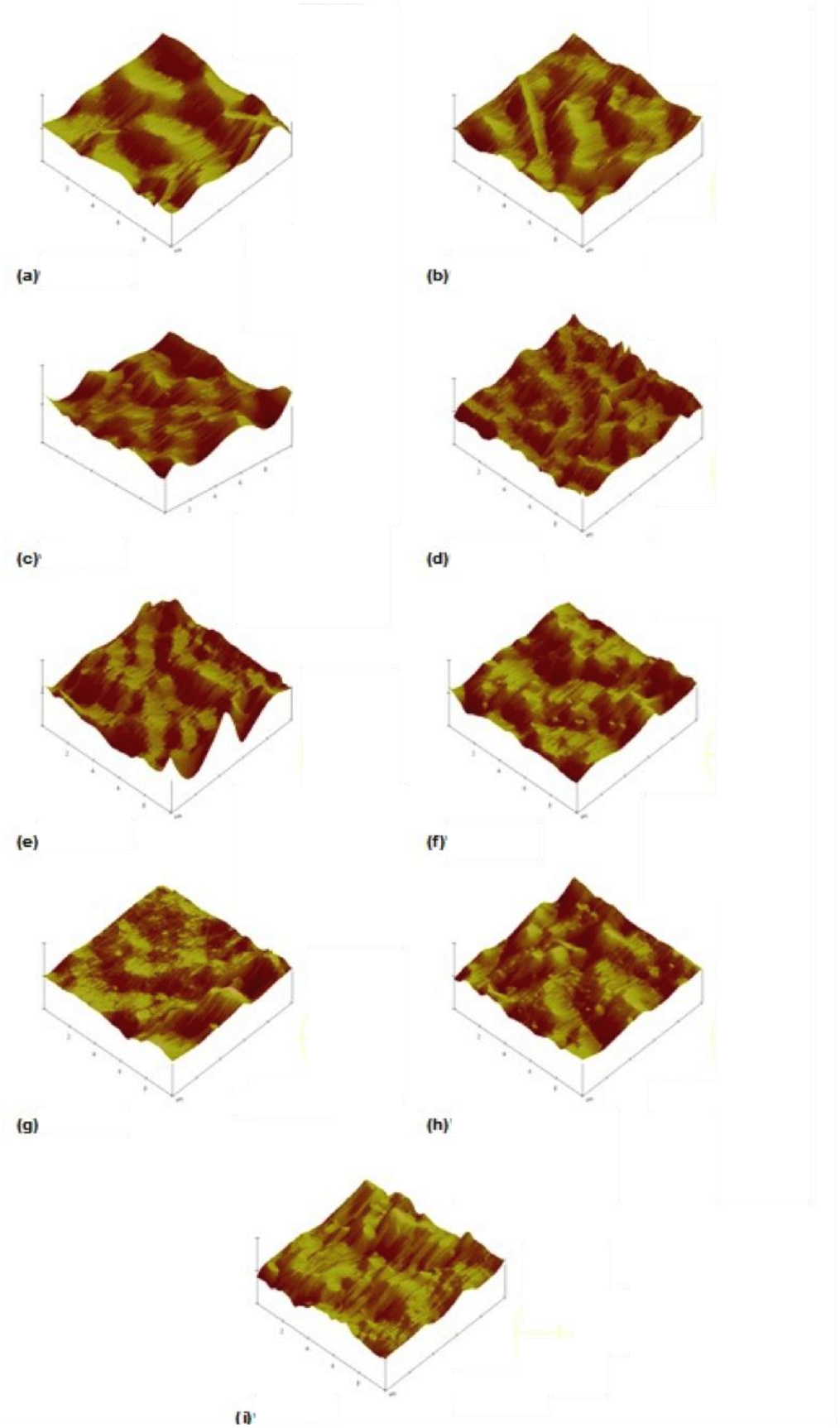

Figure 4. 34. AFM analysis results for TiNP contining membranes (a) 0.4TiNP-PS (b) 0.8TiNP-PS (c) 1.2TiNP-PS (d) 0.4TiNP-PES (e) 0.8TiNP-PES (f) 1.2TiNP-PES (g) 0.4TiNP-CA (h) 0.8TiNP-CA (i) 1.2TiNP-CA.

AFM images of TiNP containing membranes, as the sixth set of experiments, are shown in Figure 4. 34 (a-i). Roughness values are shown in the Table 4. 6. TiNP addition decreased the roughness value of bare CA-14 membrane (76.8 nm) but increased the roughness values of bare PS-14 (23.4 nm) and PES-14 (15.0 nm) membranes. Lowest roughness value of TiNP containing membranes was measured for the 0.4% TiNP containing membrane.

Table 4. 6. Ra values of TiNP containing membranes.

Membrane type	Ra (nm)
0.4TiNP-PS	37.0
0.8TiNP-PS	35.0
1.2TiNP-PS	54.0
0.4TiNP-PES	19.8
0.8TiNP-PES	25.0
1.2TiNP-PES	39.0
0.4TiNP-CA	32.4
0.8TiNP-CA	36.2
1.2TiNP-CA	35.3

4.8.3 Results of the XRD measurements

XRD measurements were done for 14% polymer containing bare PS, PES, CA membranes, and 1.2% nanomaterial containing PS, PES, CA membranes for further comparison. As can be seen from the XRD images of bare and nanomaterial containing PS membranes (Figure 4. 35), there is no peak on the surface of bare PS membrane. After the addition of nanoparticles, Ag and TiO_2 (anatase) peaks were observed only for the AgNP and TiNP containing PS membranes. But, there was no peak for the SiNP, CNT and Al_2O_3 containing membranes.

As can be seen from the XRD images of bare and nanomaterial containing PES membranes (Figure 4. 36), there is no peak on the surface of bare PES membrane similar with the bare PS membrane. After the addition of nanoparticles, Ag and TiO_2 (anatase) peaks were observed only for the AgNP and TiNP containing PES membranes. But, there was no peak for the SiNP, CNT and Al_2O_3 containing membranes.

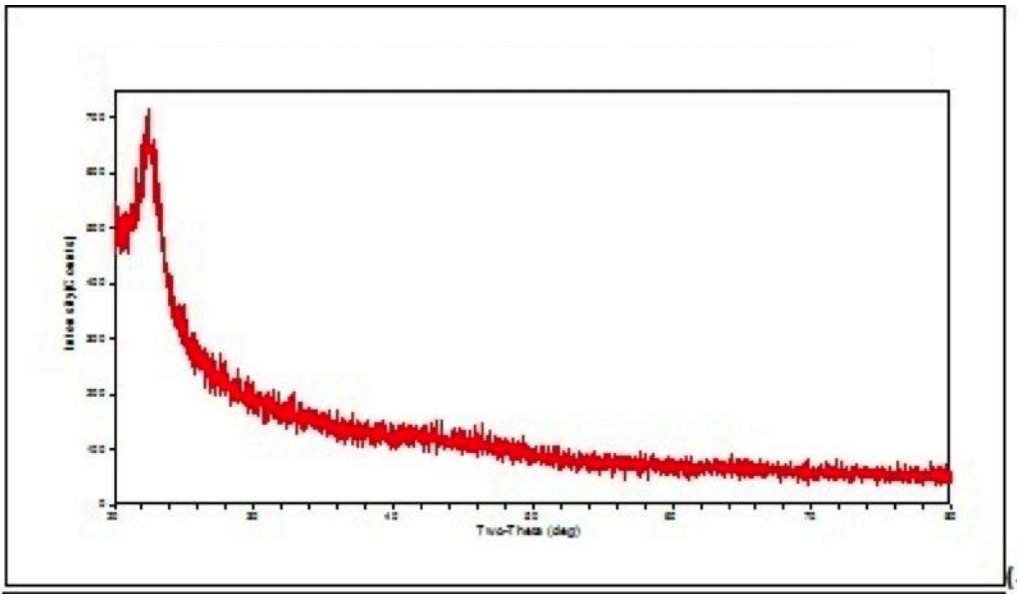

(a)

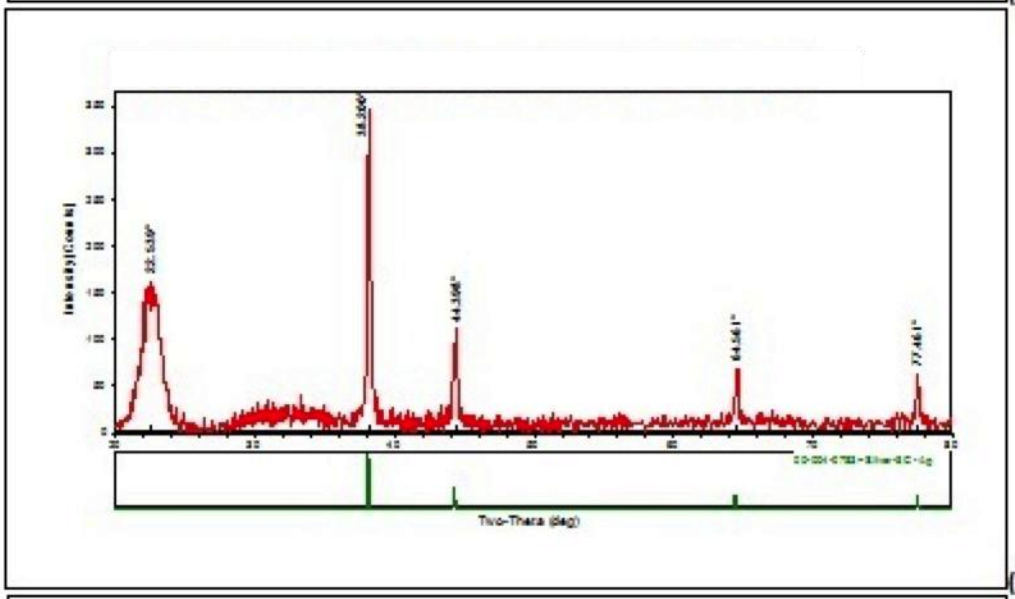

(b)

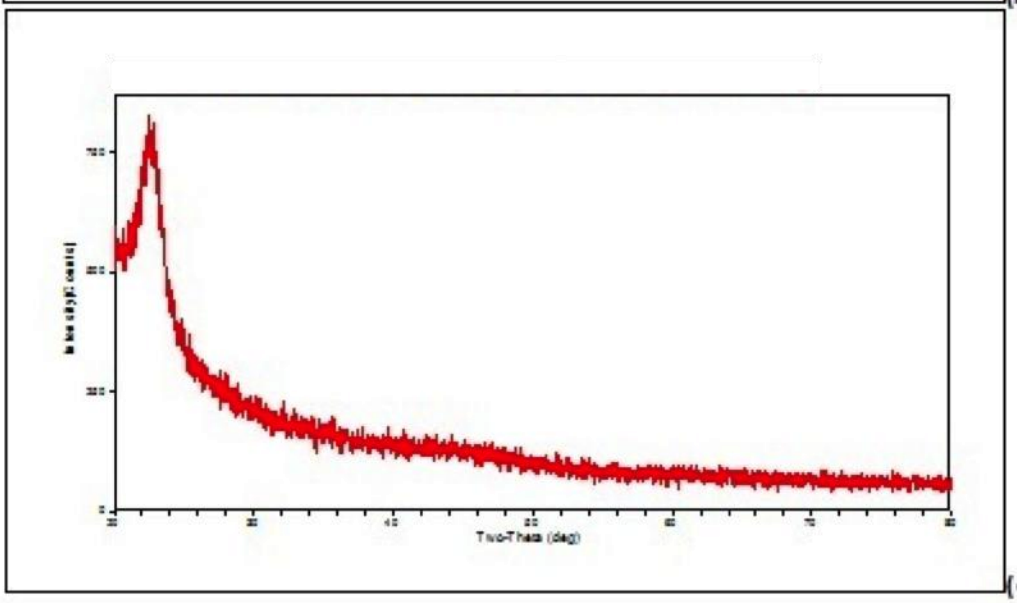

(c)

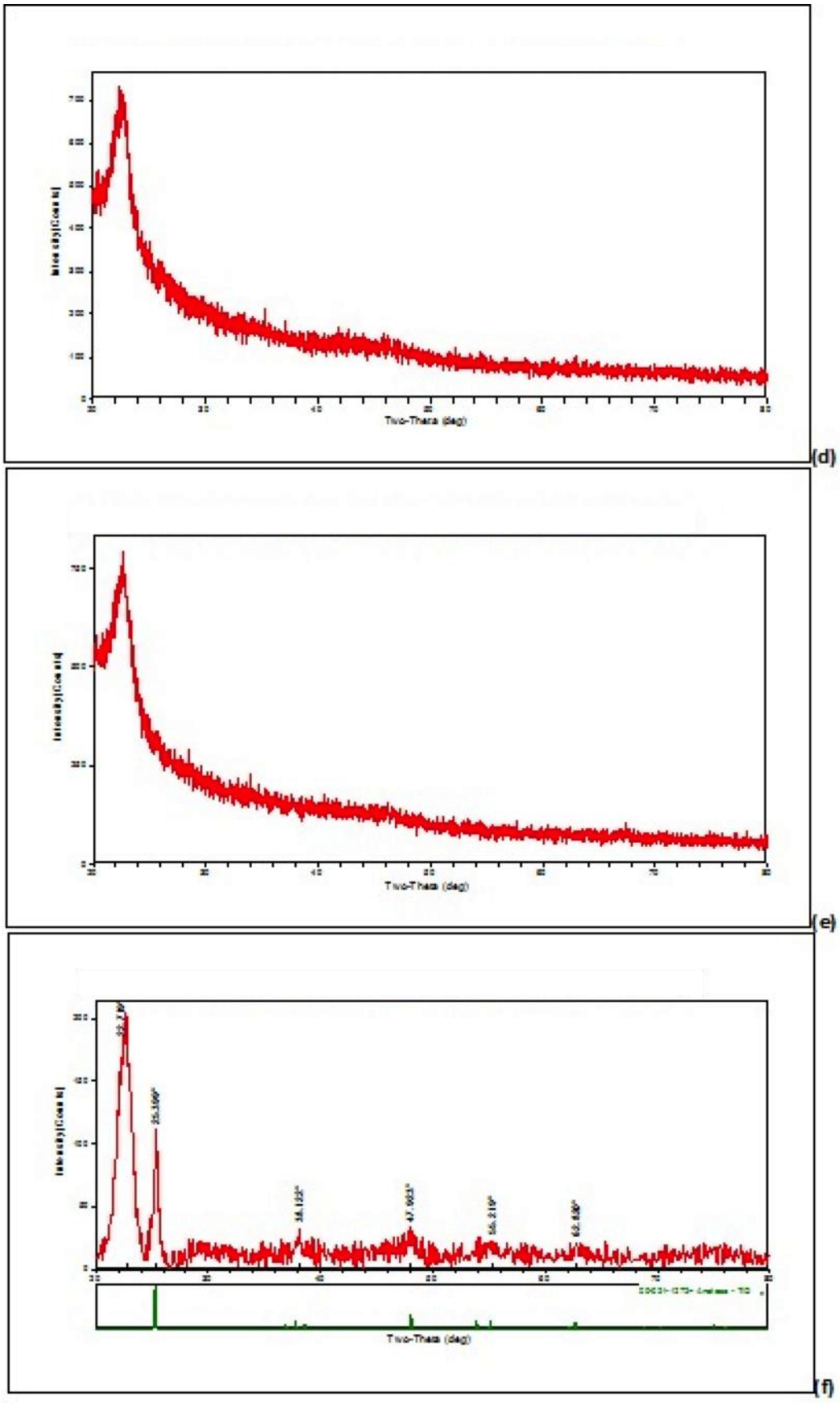

Figure 4. 35. XRD images of bare and nanocomposite PS membranes (a) Bare PS (b) 1.2AgNP-PS (c)1.2SiNP-PS (d) 1.2CNT-PS (e) 1.2AlONP-PS (f) 1.2TiNP-PS.

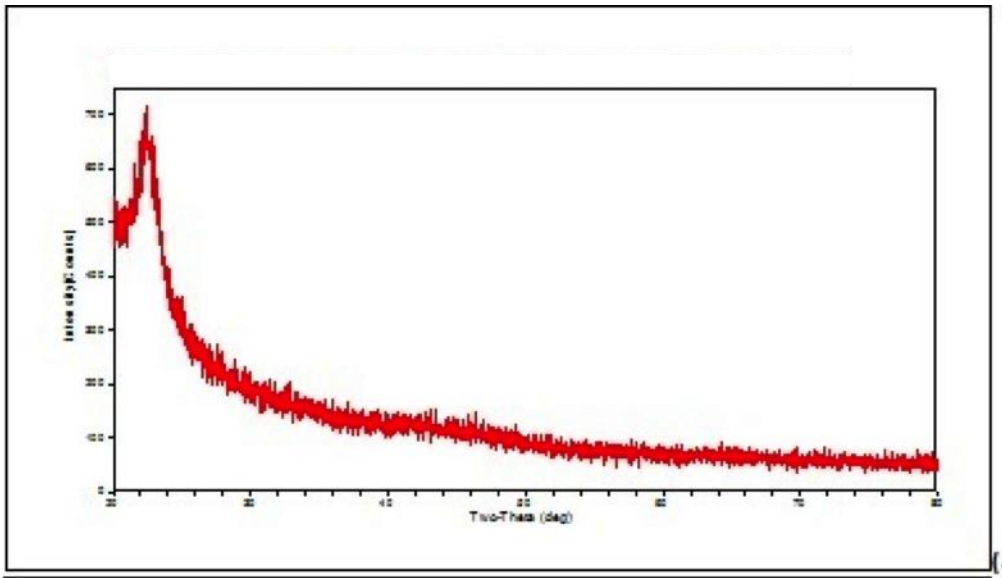

(a)

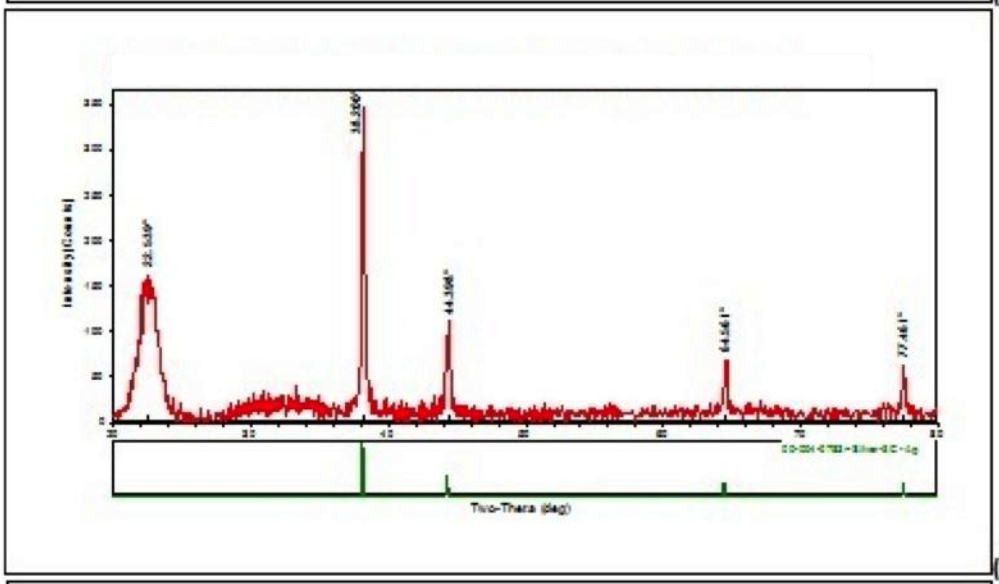

(b)

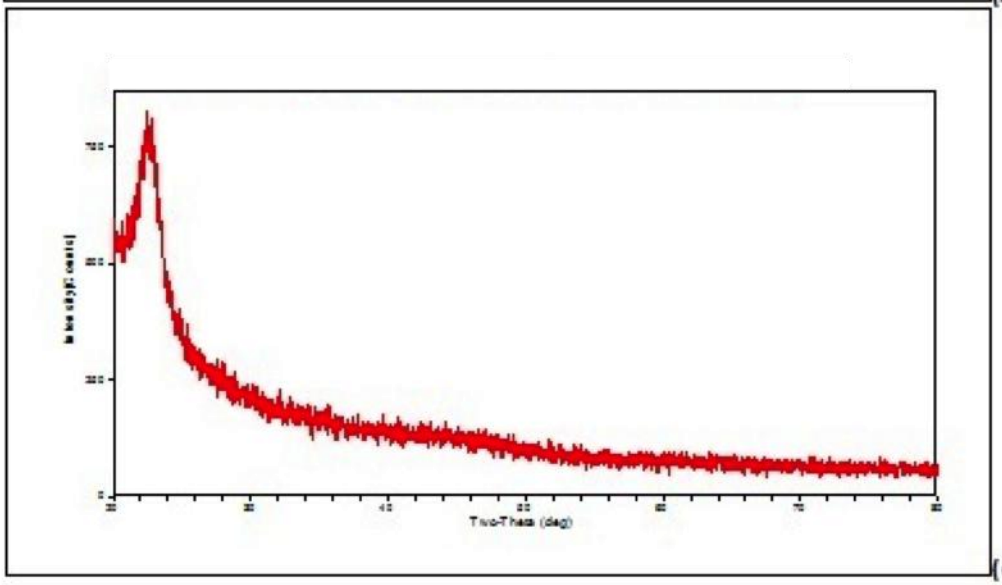

(c)

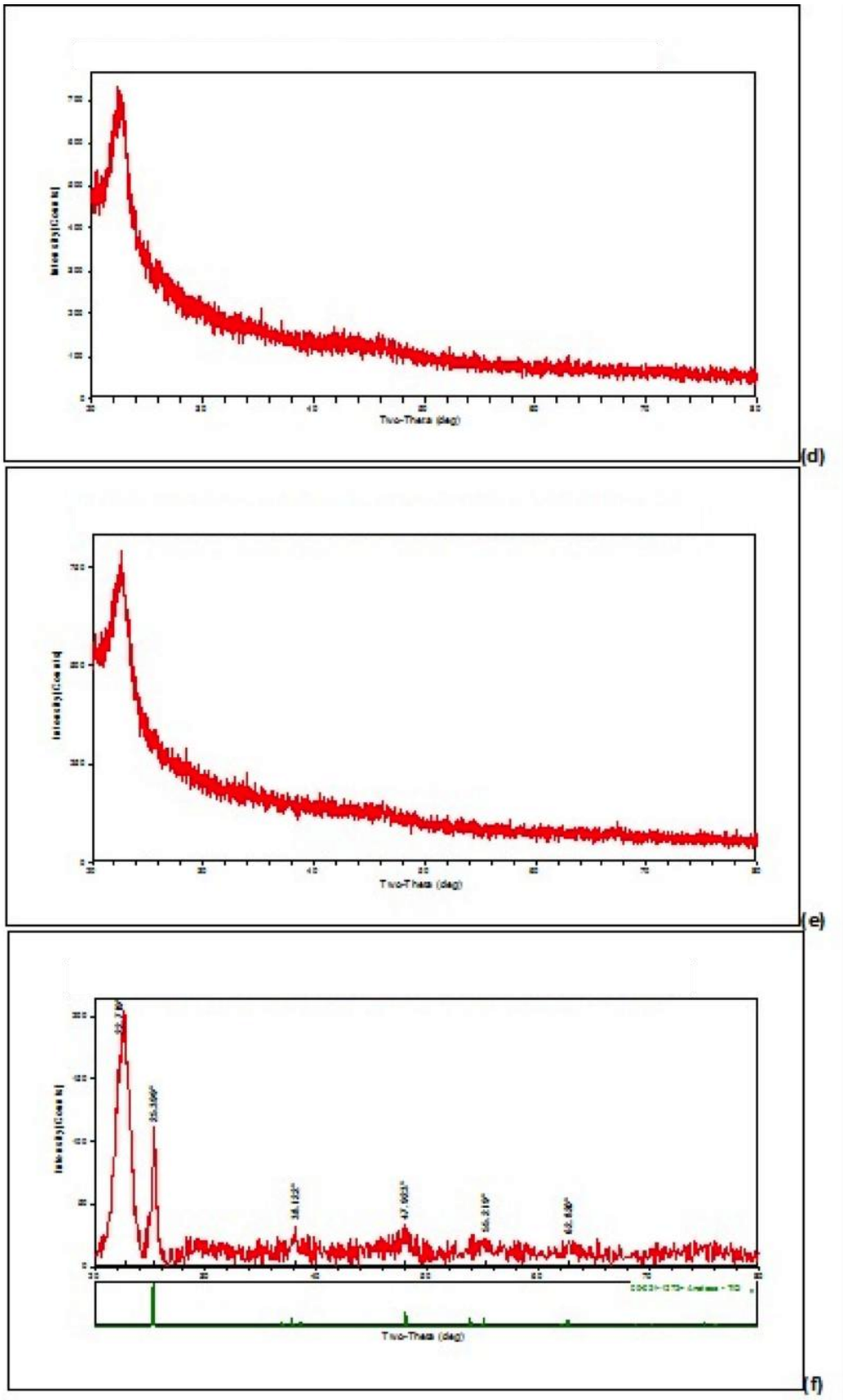

Figure 4. 36. XRD images of bare and nanocomposite PES membranes (a) Bare PES (b) 1.2AgNP-PES (c)1.2SiNP-PES (d) 1.2CNT-PES (e) 1.2AlONP-PES (f) 1.2TiNP-PES.

As can be seen from the XRD images of bare and nanomaterial containing CA membranes (Figure 4. 37), there is no peak on the surface of bare CA membrane similar with the bare PS and bare PES membranes. After the addition of nanoparticles, Ag and TiO_2 (anatase) peaks were observed only for the AgNP and TiNP containing CA membranes. But, there was no peak for the SiNP, CNT and Al_2O_3 containing membranes.

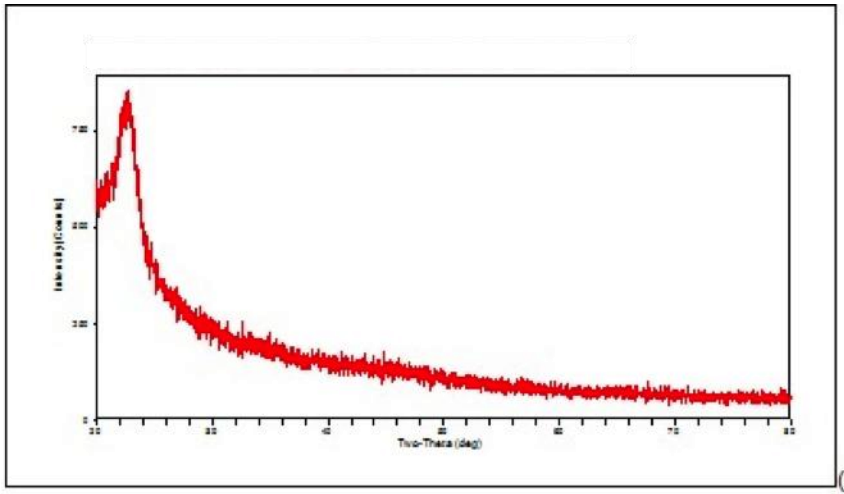

(a)

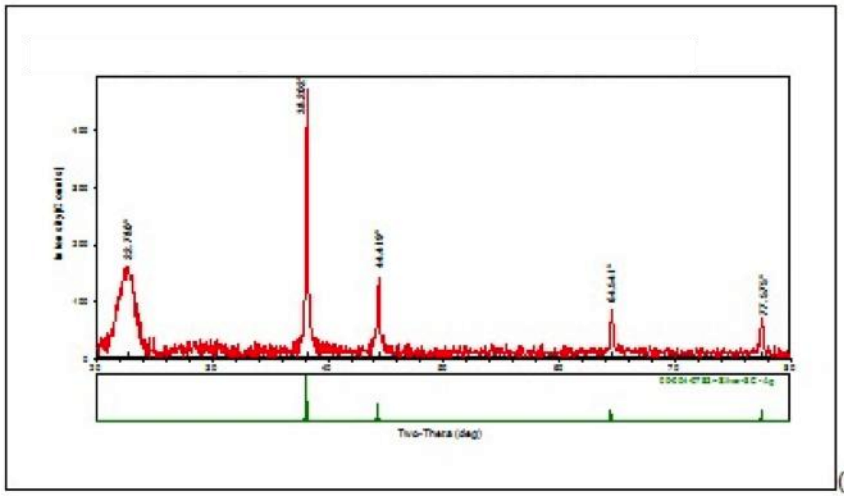

(b)

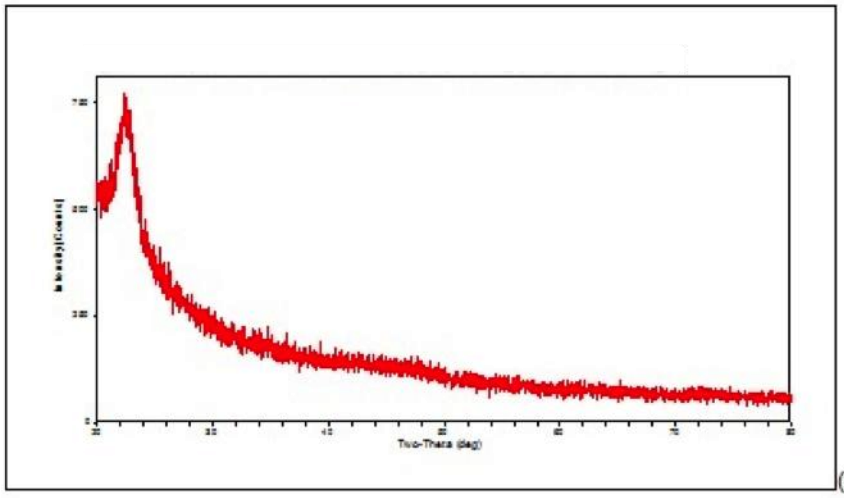

(c)

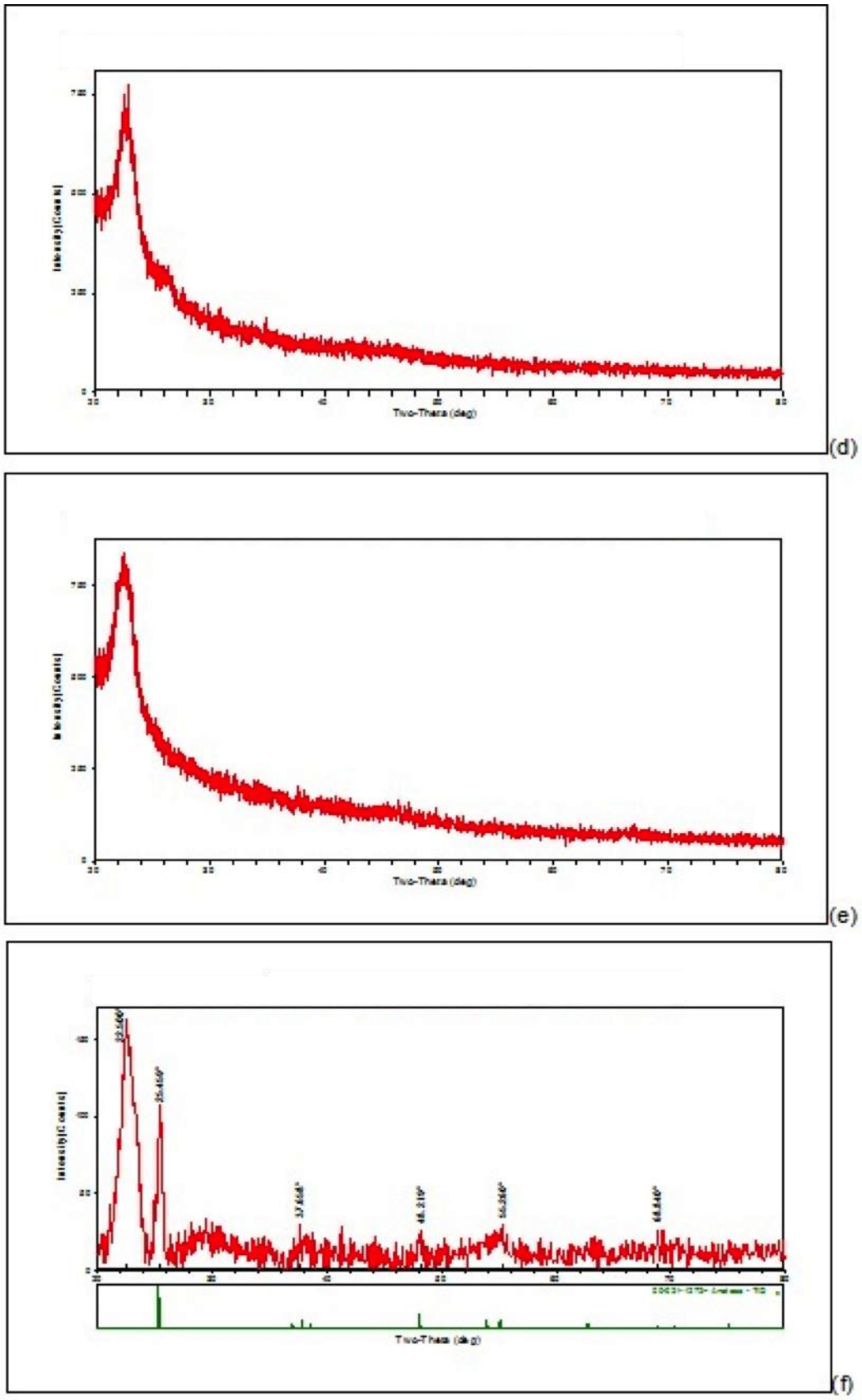

Figure 4. 37. XRD images of bare and nanocomposite CA membranes (a)Bare CA (b)1.2AgNP- CA (c)1.2SiNP-CA (d)1.2CNT- CA (e)1.2AlONP- CA (f)1.2TiNP-CA.

4.9 Filtration Performance Results of the Membranes

4.9.1 Protein filtration

In the first set of experiments, filtrations of BSA proteins were carried out by using bare polymeric membranes and results are shown as time-volume graph in Figure 4. 38(a-c). Results are evaluated separately for the membrane types. It is clearly seen from Figure 4. 38(a) that, filtrate volumes obtained after the protein filtrations were decreased with the increase of polymer amount in PS membranes. After solutions were filtrated for 1 h; 53 ml filtrate was obtained for PS-14, 30 ml filtrate was obtained for PS-16 and 23 ml filtrate was obtained for PS-18 membranes. Protein filtration results of the PES membranes are given as a graph in Figure 4. 38 (b). As can be seen from the graph, obtained filtrate volumes were similar for PES-14 and PES-16 while performance of the PES-18 was very poor compared with other membranes. After solutions were filtrated for 1 h; 113 ml filtrate was obtained for PES-14, 117 ml filtrate was obtained for PES-16 and 61 ml filtrate was obtained for PES-18 membranes. Protein filtration results of the CA membranes are given as a graph inFigure 4. 38 (c). Filtrate volumes obtained after the protein filtrations were decreased dramatically with the increase of polymer amount in CA membranes. After solutions were filtrated for 1 h; 93 ml filtrate was obtained for CA-14, 51 ml filtrate was obtained for CA-16 and 29 ml filtrate was obtained for CA-18 membranes. When membranes were compared with each other, highest performance result was obtained for 14% polymer containing membranes and PES type. Measured permeability values were higher for PS membranes than CA membranes, but higher filtrate volumes were obtained by using CA membranes.

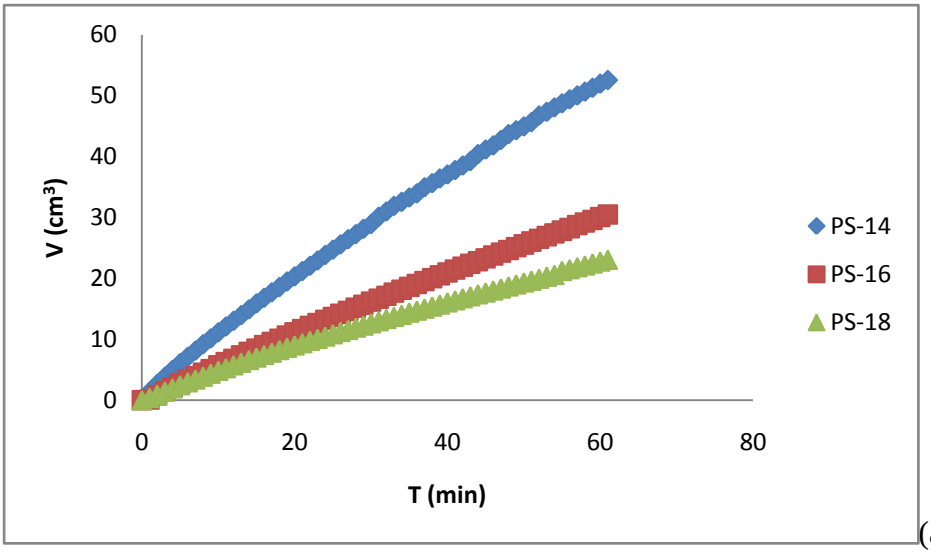

(a)

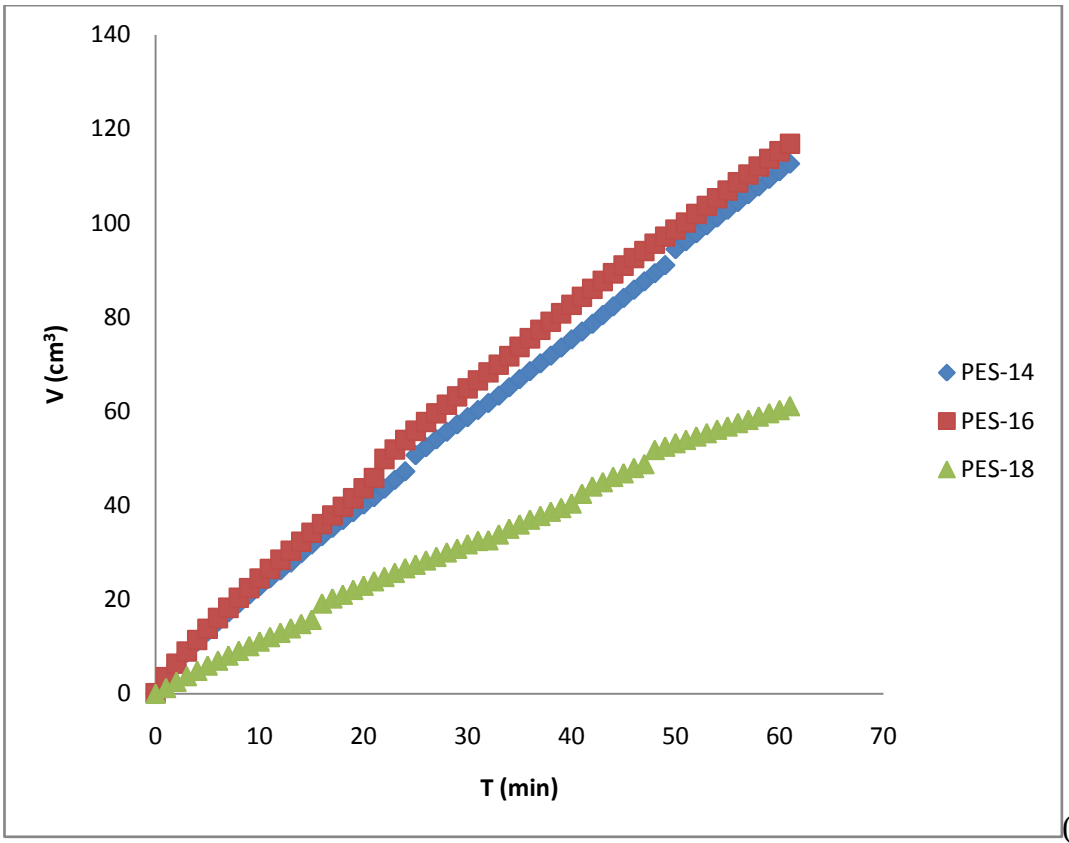

(b)

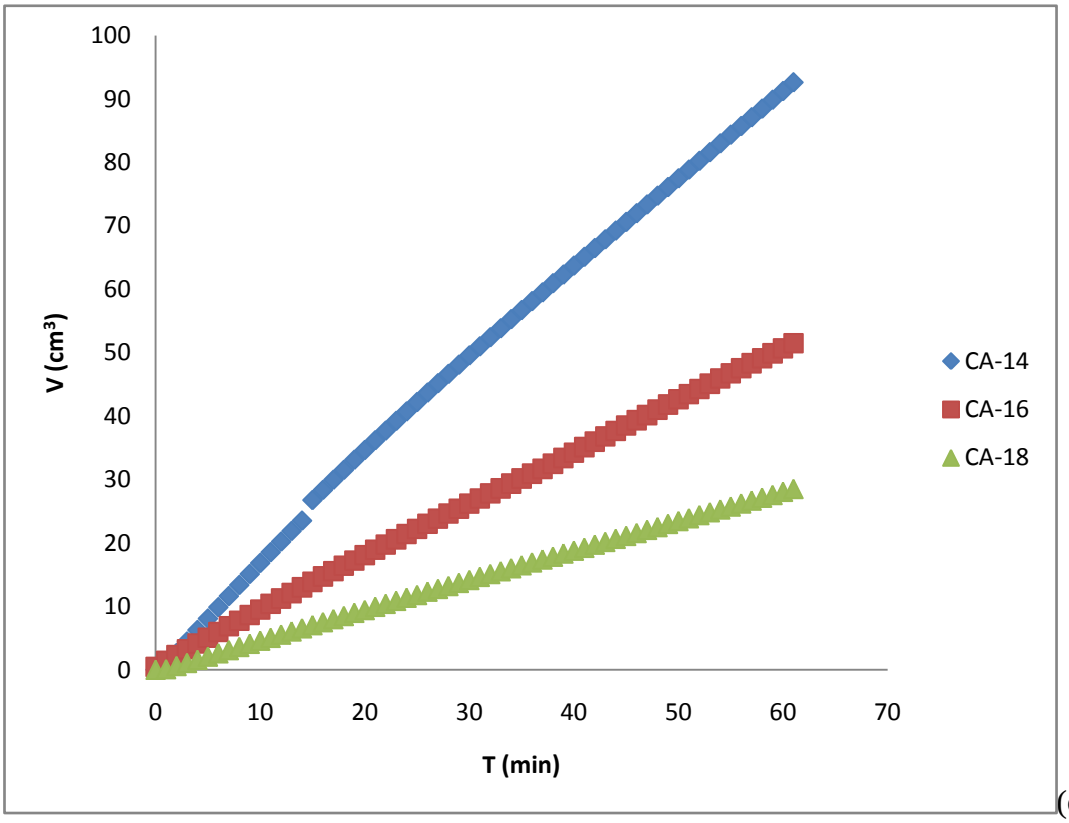

(c)

Figure 4. 38. Time-volume graphs of bare membranes obtained from the protein filtration process (a) PS membranes (b) PES membranes (c) CA membranes.

Equilibrium flux values and flux reduction rates, obtained from the protein filtration of bare membranes are given in Table 4. 7. As can be seen from the Table 4. 7, highest flux values were measured for PS-14, PES-14 and CA-14 membranes. However, highest flux reduction rates (FRR) were also measured for PS-14, PES-14 and CA-14 membranes. When membrane types were compared with each other, highest flux rate was measured for PES membranes. Lowest flux rates and highest flux reduction rates (FRR) were measured for PS membranes. Results proved that, contamination after the protein filtration was higher for PS membranes than other types of membranes. Lowest flux reduction rates (FRR) were measured for CA membranes.

Table 4. 7. Measured flux values and flux reduction rates for the bare membranes after protein filtration process.

Membrane type	**$J_{ss(protein)}$ (L/m^2hr)**	**FRR* (%)**
PS-14	27	82
PS-16	18	80
PS-18	14	72
PES-14	68	82
PES-16	68	67
PES-18	29	81
CA-14	57	21
CA-16	33	9
CA-18	8	12

FRR*: Flux reduction rate was measured as the ratio of flux values of distilled water and protein filtration. $FRR=[1-(J_{ss(protein)}/J_{ds})]_x100$

Protein analysis were applied for the initial and filtrate solutions after the filtration process. Results were calculated as % rejection and given as a graph inFigure 4. 39. Calculated rejection values were higher than 90% for PES and PS membranes. Lowest protein rejection values were obtained for the CA membranes. Rejection rates were increased up to 81% with increasing polymer amounts in CA membranes. Lowest protein rejection efficiencies were calculated for the CA membranes.

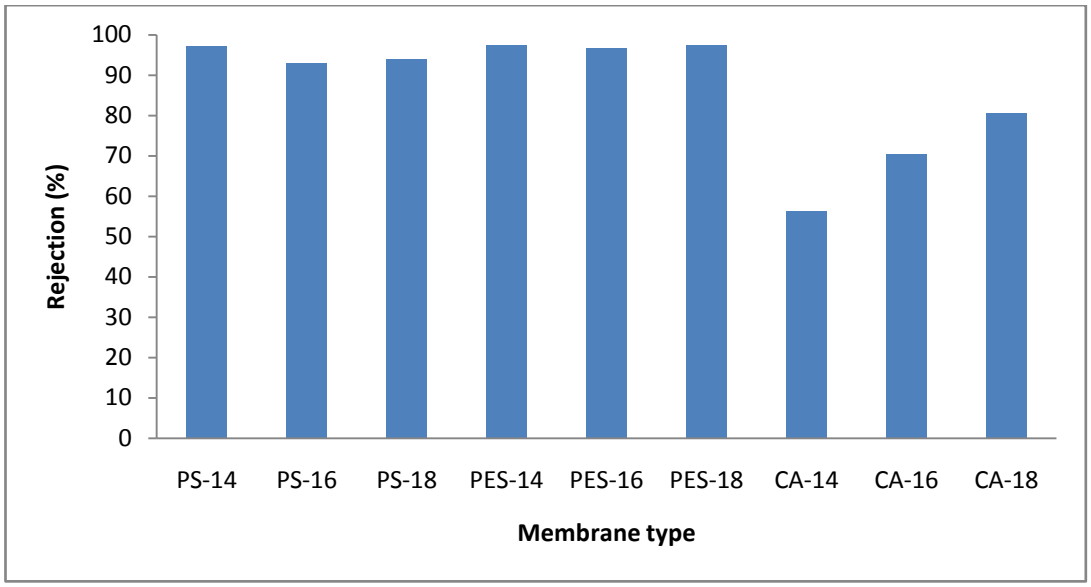

Figure 4. 39. % Rejection values for the protein filtration of bare membranes.

In the second set of experiments, filtrations of BSA proteins were carried out by using AgNP containing membranes and results are shown as time-volume graph in Figure 4. 40(a-c). With addition of AgNP, volume of the filtrate solutions were increased for PS membranes, decreased for CA membranes and did not change significantly for PES membranes. As can be seen from Figure 4. 40(a), after solutions were filtrated for 1 h; 53 ml filtrate was obtained for bare PS-14 membrane, 120 ml filtrate was obtained for 0.4AgNP-PS membrane, 89 ml filtrate was obtained for 0.8AgNP-PS membrane and 109 ml filtrate was obtained for 1.2AgNP-PS membrane. Volume of the filtrate solution was increased for PS membrane with the addition of AgNP. Varying AgNP amounts did not cause significant changes for the filtrate volumes but the highest filtrate volume was measured for 0.4% AgNP containing PS membrane. As can be seen from Figure 4. 40(b), after solutions were filtrated for 1 h; 113 ml filtrate was obtained for bare PES-14 membrane, 117 ml filtrate was obtained for 0.4AgNP-PES membrane, 81 ml filtrate was obtained for 0.8AgNP-PES membrane and 93 ml filtrate was obtained for 1.2AgNP-PES membrane. Filtrate volume of bare PES membrane was decreased with the addition of AgNP. Optimum performance was observed for the 0.4% AgNP containing PES membrane, similar with the first set of experiments.As can be seen from Figure 4. 40(c), after solutions were filtrated for 1 h; 93 ml filtrate was obtained for bare CA-14 membrane, 85 ml filtrate was obtained for 0.4AgNP-CA membrane, 66 ml filtrate was obtained for 0.8AgNP-CA membrane and 50 ml filtrate was obtained for

1.2AgNP-CA membrane. Filtrate volume of bare CA membrane was decreased with the addition of AgNP. Filtrate volumes were decreased with the increase of AgNP amount in membranes. Optimum performance was observed for the 0.4% AgNP containing CA membrane.

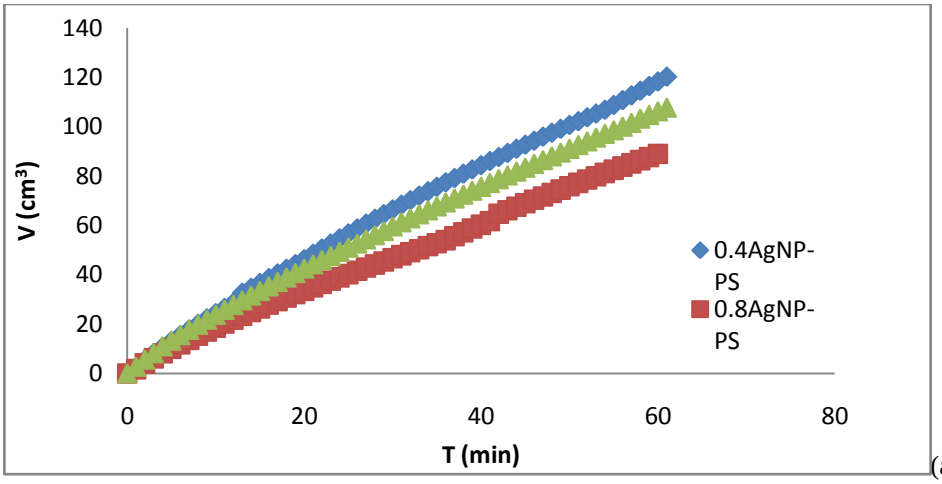

(a)

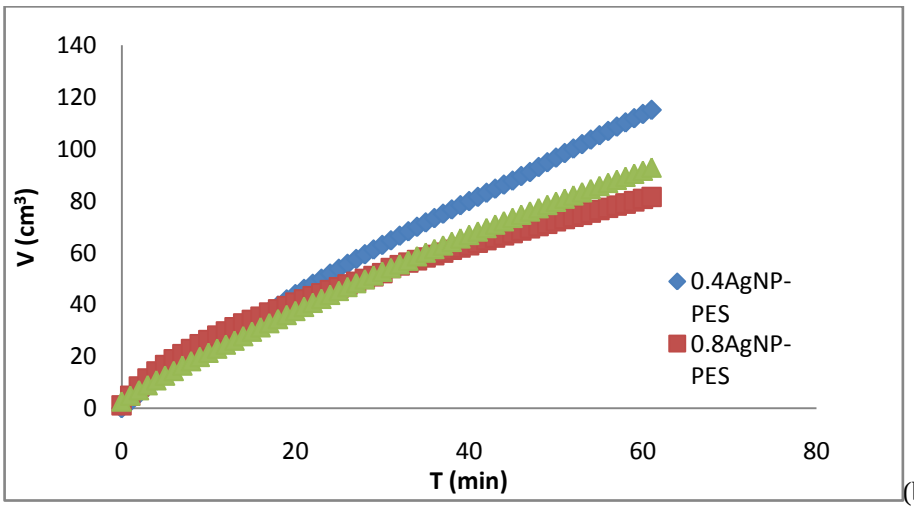

(b)

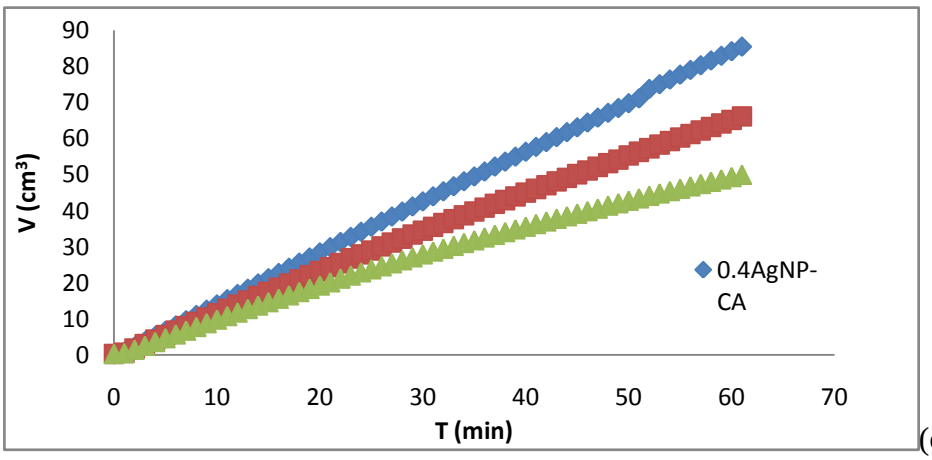

(c)

Figure 4. 40. Time-volume graphs of AgNP containing membranes obtained from the protein filtration process (a) PS membranes (b) PES membranes (c) CA membranes.

Equilibrium flux values and flux reduction rates, obtained from the protein filtration of AgNP containing membranes are given inTable 4. 8. As can be seen from theTable 4. 8, highest flux values were measured for 0.4% AgNP containing membranes. Measured flux values of PES and PS membranes were decreased for 0.8% AgNP containing membranes and increased again for 1.2% AgNP containing membranes. Measured flux values of CA membranes were decreased with the increase of AgNP amount. Highest flux reduction rates were measured for AgNP-PES membranes and lowest flux reduction rates were measured for AgNP-CA membranes.

Table 4. 8. Measured flux values and flux reduction rates for the AgNP containing membranes after protein filtration process.

Membrane type	$J_{ss(protein)}$ (L/m^{2}hr)	FRR* (%)
0.4AgNP-PS	79	63
0.8AgNP-PS	54	76
1.2AgNP-PS	62	69
0.4AgNP-PES	69	76
0.8AgNP-PES	36	87
1.2AgNP-PES	49	85
0.4AgNP-CA	54	24
0.8AgNP-CA	40	14
1.2AgNP-CA	27	33

*FRR: Flux reduction rate was measured as the ratio of flux values of distilled water and protein filtration. FRR=$[1-(J_{ss(protein)}/J_{ds})]_x100$

Protein analysis were applied for the initial and filtrate solutions after the filtration process. Results were calculated as % rejection and given as a graph inFigure 4. 41. Calculated rejection values were 90% for AgNP-PES membranes and within the range of 77-83% for AgNP-PS membranes. Lowest protein rejection values were obtained for AgNP-CA membranes similar with the bare CA membranes (24-38%). Protein rejection amounts were not affected significantly by the increase in AgNP amount. Optimum performance was obtained with 0.4% AgNP content for all membranes according to their filtrate volumes, equilibrium flux values, flux reduction rates and protein rejection rates.

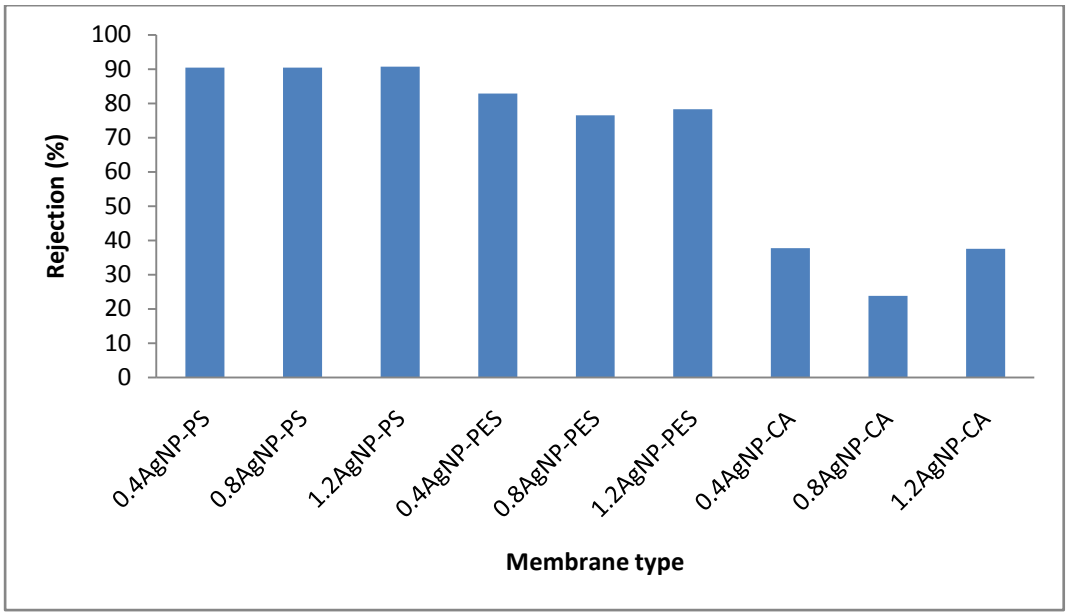

Figure 4. 41. % Rejection values for protein filtration of AgNP containing membranes.

In the third set of experiments, filtrations of BSA proteins were carried out by using SiNP containing membranes and results are shown as time-volume graph in Figure 4. 42 (a-c). With addition of SiNP; volume of the filrate solutions were increased for PS and PES membranes, compared to the filtrate volume of bare membranes, except for 0.4% SiNP containing membranes. SiNP addition dramatically decreased the filtrate volumes of CA membranes. As can be seen from Figure 4. 42(a), after solutions were filtrated for 1 h; 53 ml filtrate was obtained for bare PS-14 membrane, 38 ml filtrate was obtained for 0.4SiNP-PS membrane, 78 ml filtrate was obtained for 0.8SiNP-PS membrane and 104 ml filtrate was obtained for 1.2SiNP-PS membrane. Filtrate volumes were increased with the addition of SiNP. As can be seen from Figure 4. 42(b), after solutions were filtrated for 1 h; 113 ml filtrate was obtained for bare PES-14 membrane, 89 ml filtrate was obtained for 0.4SiNP-PES membrane, 123 ml filtrate was obtained for 0.8SiNP-PES membrane and 131 ml filtrate was obtained for 1.2SiNP-PES membrane. Filtrate volumes were also increased for PES membranes with the addition of SiNP. As can be seen from Figure 4. 42(c), after solutions were filtrated for 1 h; 93 ml filtrate was obtained for bare CA-14 membrane, 6 ml filtrate was obtained for 0.4SiNP-CA membrane, 8 ml filtrate was obtained for 0.8SiNP-CA membrane and 13 ml filtrate was obtained for 1.2SiNP-CA membrane. Filtrate volume of bare CA membrane was dramatically decreased with the addition of SiNP.

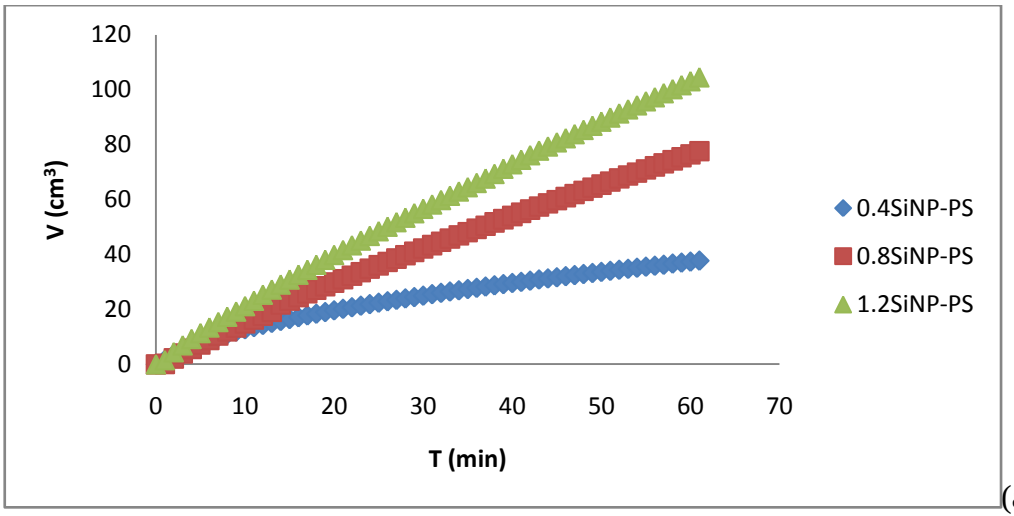

(a)

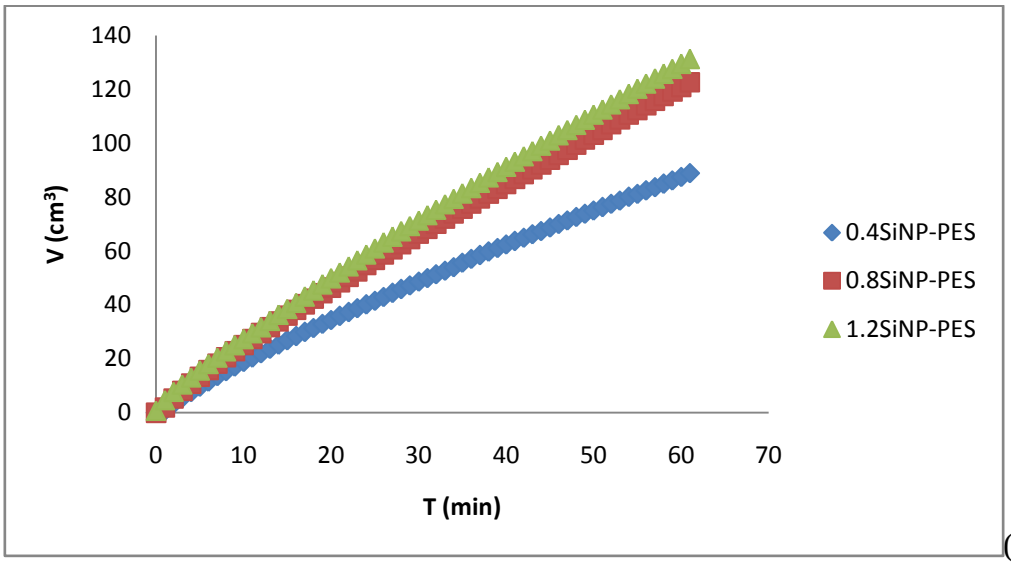

(b)

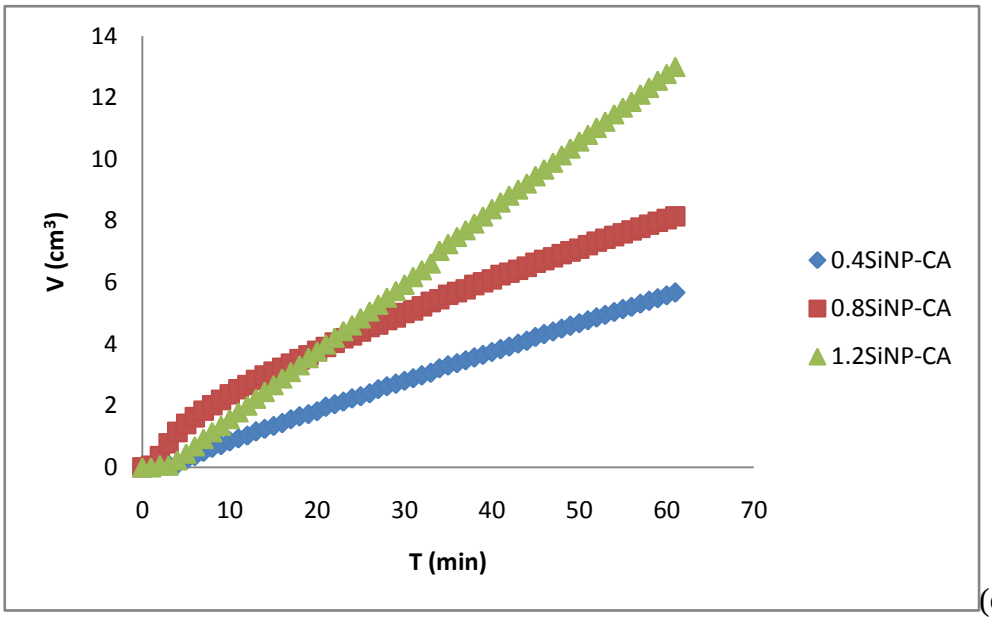

(c)

Figure 4. 42. Time-volume graphs of SiNP containing membranes obtained from the protein filtration process (a) PS membranes (b) PES membranes (c) CA membranes.

Equilibrium flux values and flux reduction rates, obtained from the protein filtration of SiNP containing membranes are given in Table 4. 9. As can be seen from theTable 4. 9, highest flux values were measured for 1.2% SiNP containing membranes. Furthermore, lowest flux reduction rates were also obtained for these membranes. When membrane types were compared to each other, highest flux values were obtained for the SiNP-PES type membranes. Besides that, measured flux values of SiNP-CA membranes were quite low.

Table 4. 9. Measured flux values and flux reduction rates for the SiNP containing membranes after protein filtration process.

Membrane type	**$J_{ss(protein)}$ (L/m^2hr)**	**FRR* (%)**
0.4SiNP-PS	15	85
0.8SiNP-PS	45	64
1.2SiNP-PS	60	69
0.4SiNP-PES	52	59
0.8SiNP-PES	71	73
1.2SiNP-PES	77	48
0.4SiNP-CA	4	67
0.8SiNP-CA	4	29
1.2SiNP-CA	9	6

*FRR: Flux reduction rate was measured as the ratio of flux values of distilled water and protein filtration. $FRR=[1-(J_{ss(protein)}/J_{ds})]_x100$

Protein analysis were applied for the initial and filtrate solutions after the filtration process. Results were calculated as % rejection and given as a graph in Figure 4. 43. Calculated rejection values were within the range of 45-59% for SiNP-CA membranes, and 80-85% for SiNP-PS and SiNP-PES membranes. Protein rejection rates were not affected significantly from SiNP addition. Optimum performance was obtained with 1.2% SiNP content for all membranes according to their filtrate volumes, equilibrium flux values, flux reduction rates and protein rejection rates.

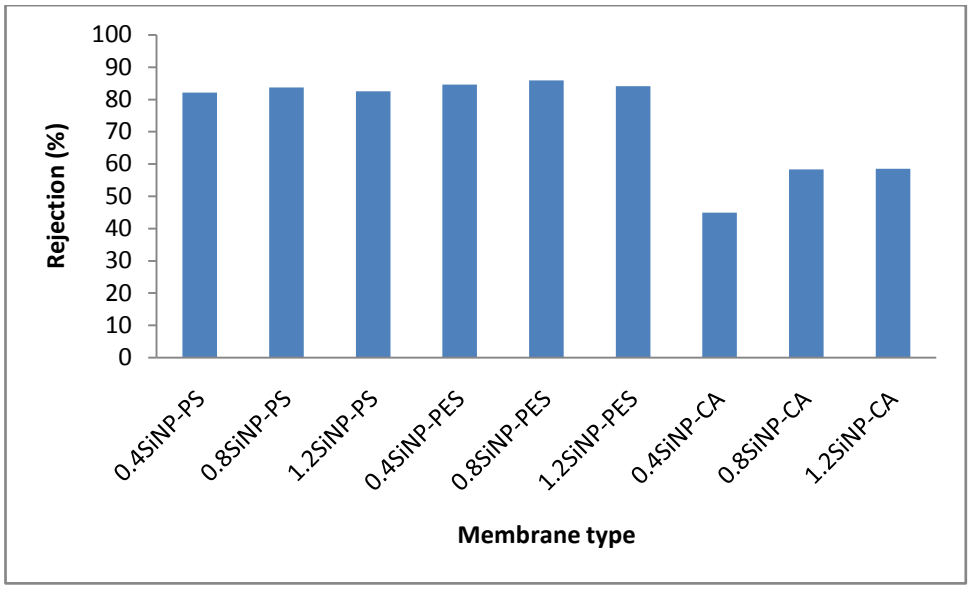

Figure 4. 43. % Rejection values for protein filtration of SiNP containing membranes.

In the fourth set of experiments, filtrations of BSA proteins were carried out by using CNT containing membranes and results are shown as time-volume graph in Figure 4. 44(a-c). With addition of CNT; volume of the filtrate solutions were increased for PS and PES membranes, and dramatically decreased for CA membranes. As can be seen from Figure 4. 44(a), after solutions were filtrated for 1 h; 53 ml filtrate was obtained for bare PS-14 membrane, 79 ml filtrate was obtained for 0.4CNT-PS membrane, 83 ml filtrate was obtained for 0.8CNT-PS membrane and 91 ml filtrate was obtained for 1.2CNT-PS membrane. Volume of the filtrate solutions were increased related with the increase in CNT amount. As can be seen from Figure 4. 44(b), after solutions were filtrated for 1 h; 113 ml filtrate was obtained for bare PES-14 membrane, 162 ml filtrate was obtained for 0.4CNT-PES membrane, 125 ml filtrate was obtained for 0.8CNT-PES membrane and 130 ml filtrate was obtained for 1.2CNT-PES membrane. Volume of the filtrate solutions were decreased related with the increase in CNT amount. As can be seen from Figure 4. 44(c), after solutions were filtrated for 1 h; 93 ml filtrate was obtained for bare CA-14 membrane, 12 ml filtrate was obtained for 0.4CNT-CA membrane, 14 ml filtrate was obtained for 0.8CNT-CA membrane and 11 ml filtrate was obtained for 1.2CNT-CA membrane. Addition af CNT dramatically decreased the filtrate volume of CA membrane.

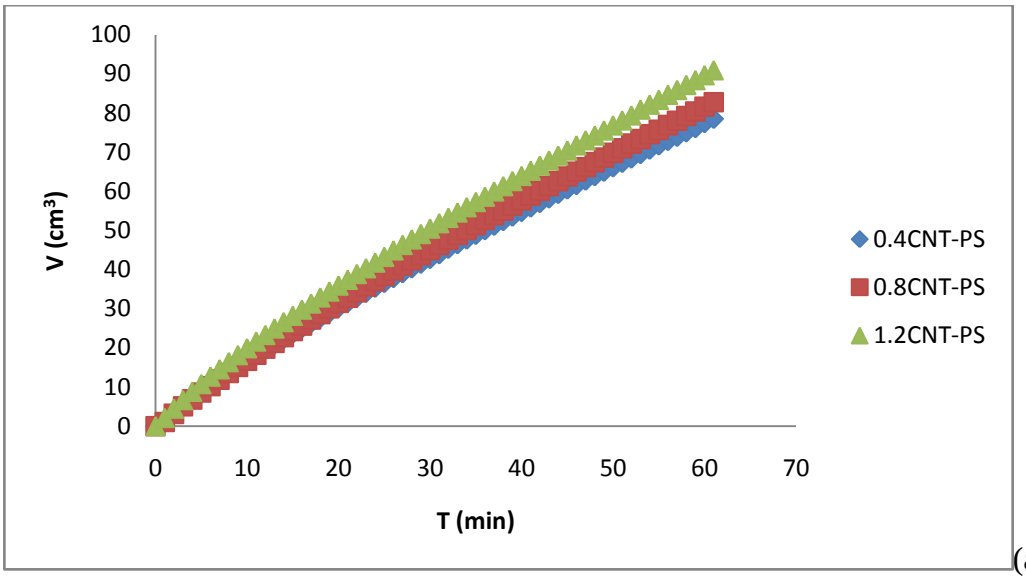

(a)

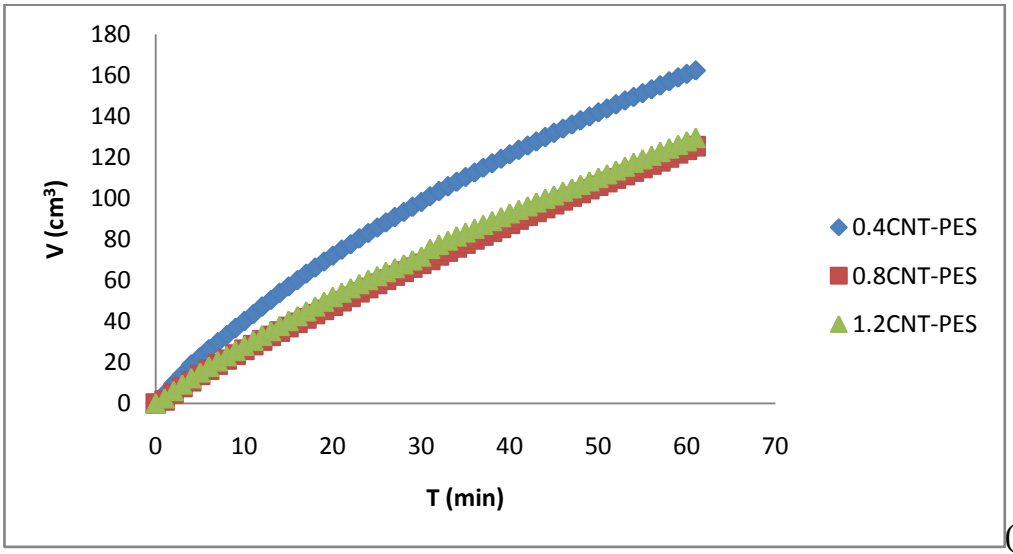

(b)

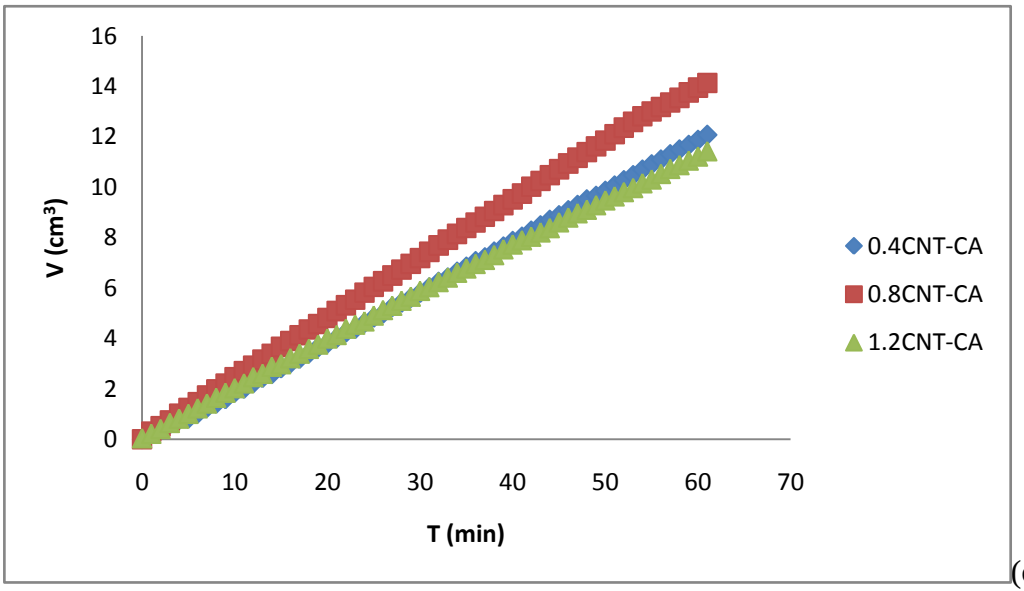

(c)

Figure 4. 44. Time-volume graphs of CNT containing membranes obtained from the protein filtration process (a) PS membranes (b) PES membranes (c) CA membranes.

Equilibrium flux values and flux reduction rates, obtained from the protein filtration of CNT containing membranes are given in Table 4. 10. As can be seen from Table 4. 10, when flux values of the same type of membranes were compared according to their CNT contents, measured flux values were similar for varying amounts of CNT. When flux values of all membranes were compared, highest flux values were measured for CNT-PES type membranes and lowest flux values were measured for CNT-CA type membranes.

Table 4. 10. Measured flux values and flux reduction rates for the CNT containing membranes after protein filtration process.

Membrane type	$J_{ss(protein)}$ (L/m^{2}hr)	FRR* (%)
0.4CNT-PS	46	67
0.8CNT-PS	48	55
1.2CNT-PS	53	55
0.4CNT-PES	75	72
0.8CNT-PES	71	82
1.2CNT-PES	73	81
0.4CNT-CA	6	19
0.8CNT-CA	8	18
1.2CNT-CA	7	20

*FRR: Flux reduction rate was measured as the ratio of flux values of distilled water and protein filtration. FRR=$[1-(J_{ss(protein)}/J_{ds})]_x100$

Protein analysis were applied for the initial and filtrate solutions after the filtration process. Results were calculated as % rejection and given as a graph in Figure 4. 45. Calculated rejection values were higher than 95% for all membranes. Performances of the same type of membranes were compared to each other. Even though the performances were similar for varying CNT contents, optimum performance was obtained with 1.2% CNT content for CNT-PS, 0.4% CNT content for CNT-PES and 0.8% CNT content for CNT-CA according to their filtrate volumes, equilibrium flux values, flux reduction rates and protein rejection rates.

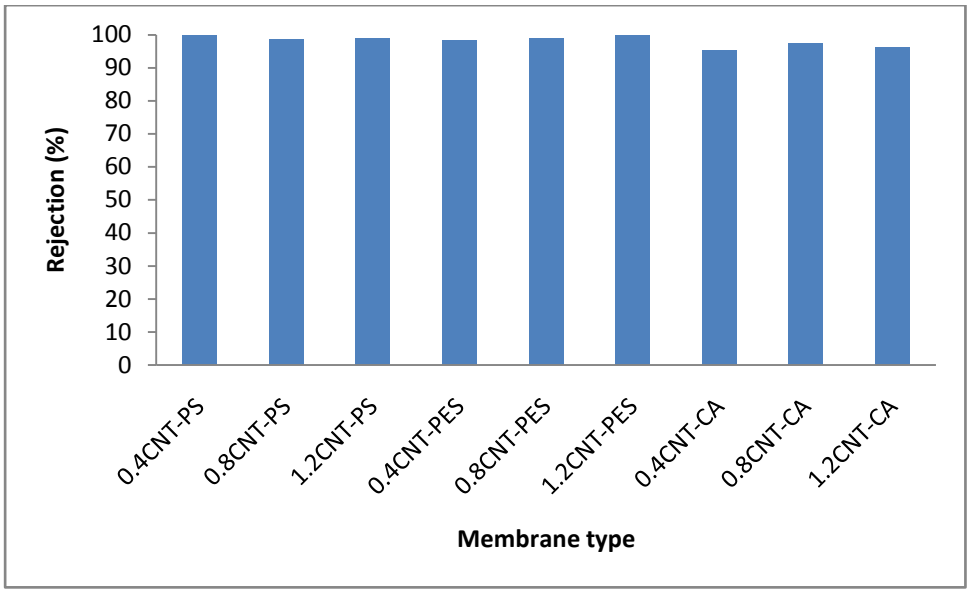

Figure 4. 45. % Rejection values for protein filtration of CNT containing membranes.

In the fifth set of experiments, filtrations of BSA proteins were carried out by using Al_2O_3 containing membranes and results are shown as time-volume graph in Figure 4. 46(a-c). With addition of Al_2O_3, volumes of the filtrate solutions were increased for all types of bare membranes. As can be seen from Figure 4. 46(a), after solutions were filtrated for 1 h; 53 ml filtrate was obtained for bare PS-14 membrane, 121 ml filtrate was obtained for 0.4AlONP-PS membrane, 93 ml filtrate was obtained for 0.8AlONP-PS membrane and 68 ml filtrate was obtained for 1.2AlONP-PS membrane. Filtrate volumes were increased with the increase in AlONP amount. As can be seen from Figure 4. 46(b), after solutions were filtrated for 1 h; 113 ml filtrate was obtained for bare PES-14 membrane, 140 ml filtrate was obtained for 0.4AlONP-PES membrane, 123 ml filtrate was obtained for 0.8AlONP-PES membrane and 121 ml filtrate was obtained for 1.2AlONP-PES membrane. Filtrate volumes were increased with the increase in AlONP amount. As can be seen from Figure 4. 46(c), after solutions were filtrated for 1 h; 93 ml filtrate was obtained for bare CA-14 membrane, 95 ml filtrate was obtained for 0.4AlONP-CA membrane, 99 ml filtrate was obtained for 0.8AlONP-CA membrane and 110 ml filtrate was obtained for 1.2AlONP-CA membrane. Similarly, filtrate volumes of CA membranes were increased with the increase in AlONP amount.

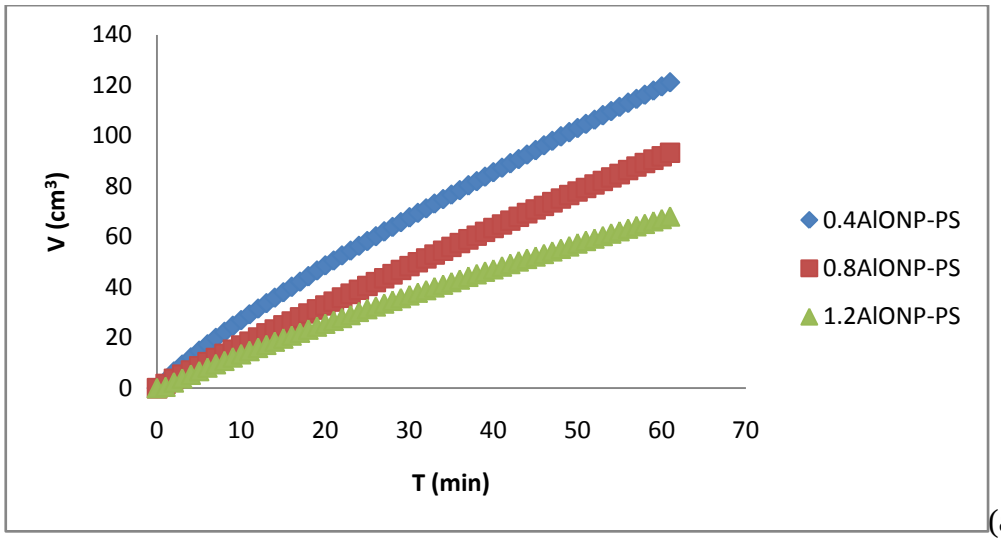

(a)

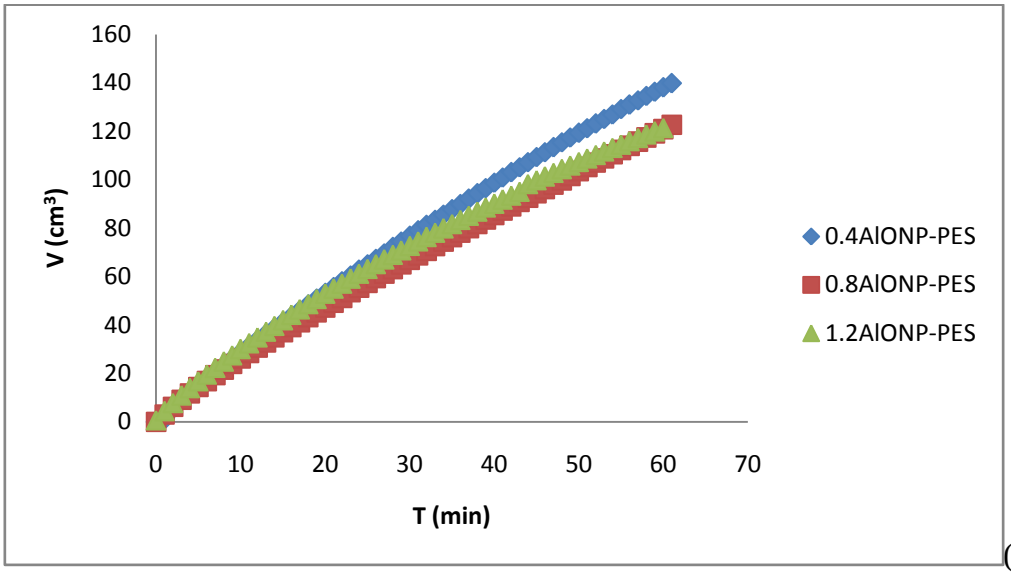

(b)

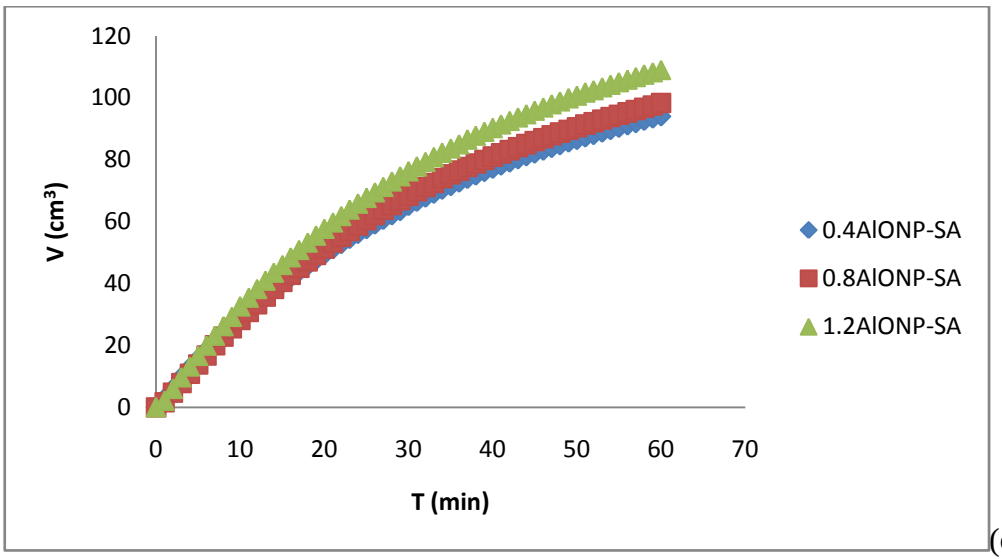

(c)

Figure 4. 46. Time-volume graphs of AlONP containing membranes obtained from the protein filtration process (a) PS membranes (b) PES membranes (c) CA membranes.

Equilibrium flux values and flux reduction rates, obtained from the protein filtration of AlONP containing membranes are given in Table 4. 11. As can be seen from Table 4.5; when flux values of the same type of membranes were compared according to their CNT contents, measured flux values were decreased with the increase in their CNT contents. When membrane types were compared to each other, highest flux values were measured for AlONP-PES type of membranes and lowest flux values were measured for AlONP-CA type of membranes.

Table 4. 11. Measured flux values and flux reduction rates for the AlONP containing membranes after protein filtration process.

Membrane type	**$J_{ss(protein)}$ (L/m^2hr)**	**FRR* (%)**
0.4AlONP-PS	68	69
0.8AlONP-PS	58	66
1.2AlONP-PS	40	72
0.4AlONP-PES	77	76
0.8AlONP-PES	71	71
1.2AlONP-PES	58	83
0.4AlONP-CA	31	82
0.8AlONP-CA	32	76
1.2AlONP-CA	34	78

*FRR: Flux reduction rate was measured as the ratio of flux values of distilled water and protein filtration. $FRR=[1-(J_{ss(protein)}/J_{ds})]_x100$

Protein analysis were applied for the initial and filtrate solutions after the filtration process. Results were calculated as % rejection and given as a graph in Figure 4. 47. Calculated rejection values were measured, within the range of 25-30%% for AlONP-CA membranes but higher than 90% for AlONP-PS and AlONP-PES membranes. Lowest protein rejection values were measured for AlONP-CA membranes compared with other membranes. Optimum performance was obtained with 1.2% AlONP content for CA membrane and 0.4% AlONP content for PES and PS membranes according to their filtrate volumes, equilibrium flux values, flux reduction rates and protein rejection rates.

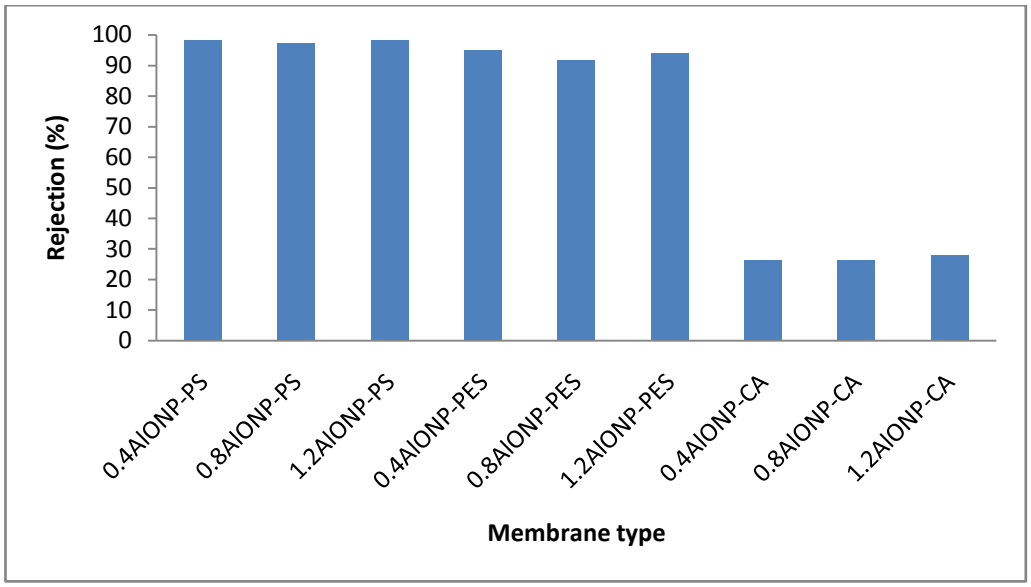

Figure 4. 47. % Rejection values for protein filtration of AlONP containing membranes.

In the sixth set of experiments, filtrations of BSA proteins were carried out by using TiO_2 containing membranes and results are shown as time-volume graph in Figure 4. 48(a-c). Membranes were kept under UV light for 15 minutes and activated by using a 160 W UV-A lamp. Filtrate volumes of PS and CA membranes were increased with TiO_2 addition but it did not affect the filtrate volume of PES membranes significantly. As can be seen from Figure 4. 48(a), after solutions were filtrated for 1 h; 53 ml filtrate was obtained for bare PS-14 membrane, 123 ml filtrate was obtained for 0.4TiNP-PS membrane, 82 ml filtrate was obtained for 0.8TiNP-PS membrane and 108 ml filtrate was obtained for 1.2TiNP-PS membrane. As can be seen from Figure 4. 48(b), after solutions were filtrated for 1 h; 113 ml filtrate was obtained for bare PES-14 membrane, 100 ml filtrate was obtained for 0.4TiNP-PES membrane, 113 ml filtrate was obtained for 0.8TiNP-PES membrane and 83 ml filtrate was obtained for 1.2TiNP-PES membrane. As can be seen from Figure 4. 48(c), after solutions were filtrated for 1 h; 93 ml filtrate was obtained for bare CA-14 membrane, 178 ml filtrate was obtained for 0.4TiNP-CA membrane, 127 ml filtrate was obtained for 0.8TiNP-CA membrane and 148 ml filtrate was obtained for 1.2TiNP-CA membrane. Filtrate volume for CA membrane was increased with the addition of TiNP much more than other membranes.

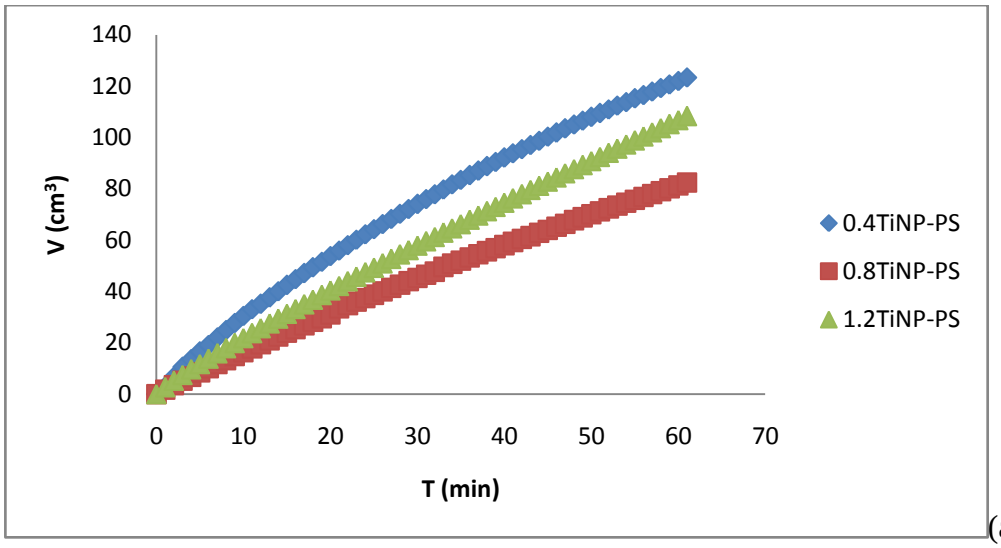

(a)

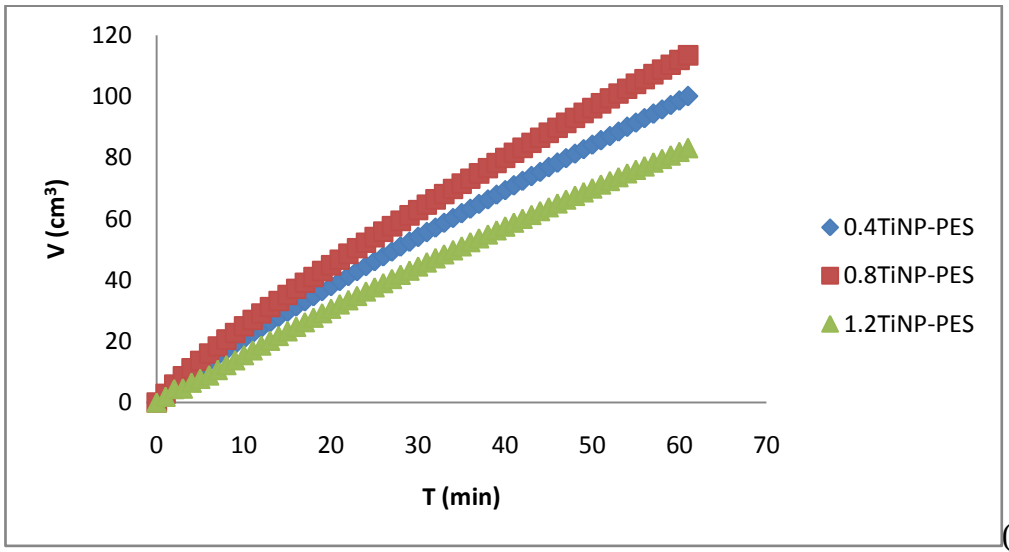

(b)

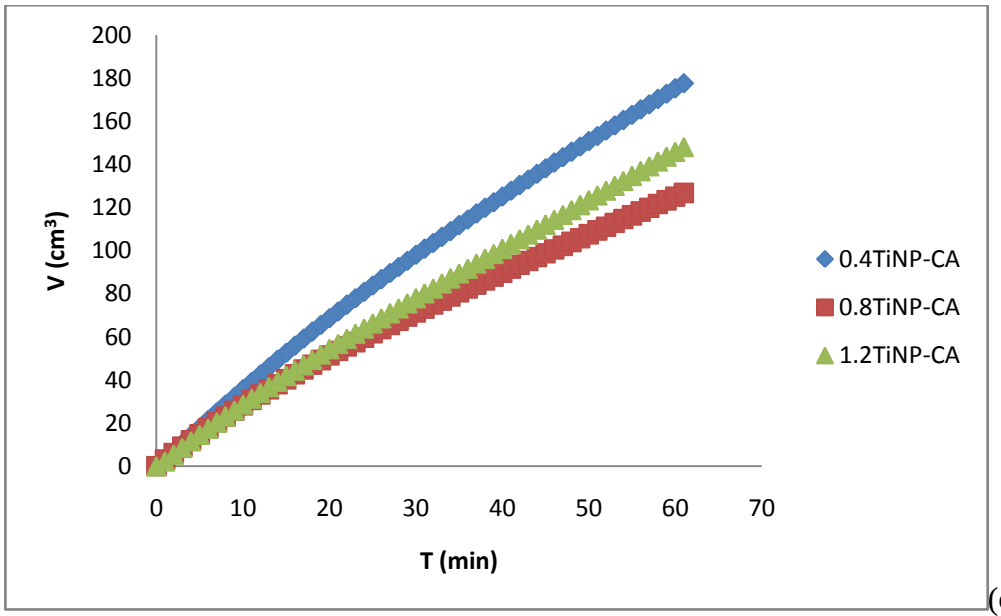

(c)

Figure 4. 48. Time-volume graphs of TiNP containing membranes obtained from the protein filtration process (a) PS membranes (b) PES membranes (c) CA membranes.

Equilibrium flux values and flux reduction rates, obtained from the protein filtration of TiNP containing membranes are given inTable 4. 12. As can be seen fromTable 4. 12; when flux values of the same type of membranes were compared, it was not possible to evaluate a relation between flux change and CNT concentration. When membrane types were compared to each other, highest flux values were measured for TiNP-CA membranes unlike the other experiments. Similar flux values were measured for TiNP-PS and TiNP-PES membranes.

Table 4. 12. Measured flux values and flux reduction rates for the TiNP containing membranes after protein filtration process.

Membrane type	**$J_{ss(protein)}$ (L/m^2hr)**	**FRR* (%)**
0.4TiNP-PS	58	74
0.8TiNP-PS	46	74
1.2TiNP-PS	65	67
0.4TiNP-PES	59	76
0.8TiNP-PES	64	79
1.2TiNP-PES	49	84
0.4TiNP-CA	101	33
0.8TiNP-CA	71	50
1.2TiNP-CA	92	33

*FRR: Flux reduction rate was measured as the ratio of flux values of distilled water and protein filtration. $FRR=[1-(J_{ss(protein)}/J_{ds})]_x100$

Protein analysis were applied for the initial and filtrate solutions after the filtration process. Results were calculated as % rejection and given as a graph in Figure 4. 49. Calculated rejection values were measured, higher than 80% for TiNP-PS membranes and higher than 95% for TiNP-PES but within the range of 25-45% for TiNP-CA membranes. Rejection rates were increased with the increase of TiNP amounts in membranes.Optimum performance was obtained with 1.2% TiNP content for PS membrane, 0.8% TiNP content for PES membrane and 0.4% TiNP content for CA membrane according to their filtrate volumes, equilibrium flux values, flux reduction rates and protein rejection rates.

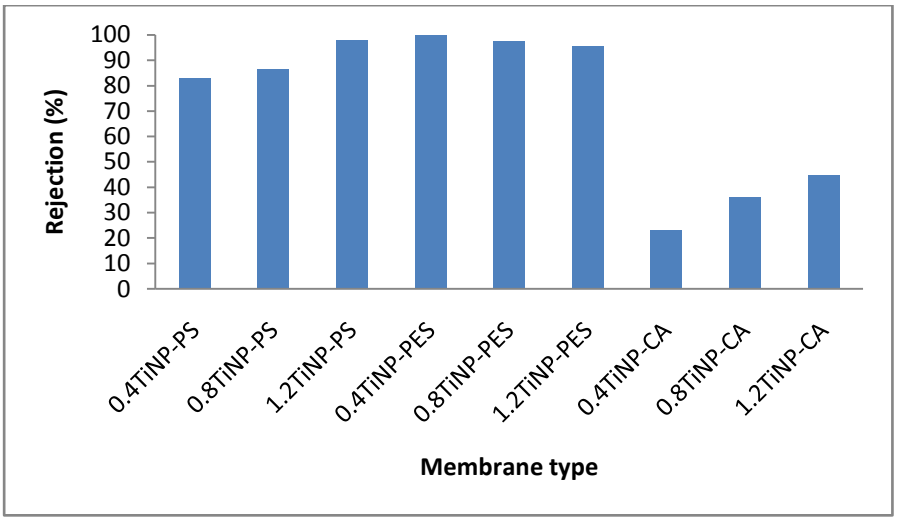

Figure 4. 49. % Rejection values for protein filtration of TiNP containing membranes.

4.9.2 Carbohydrate filtration

In the first set of experiments, filtrations of carbohydrates were carried out by using bare membranes and results are shown as time-volume graph in Figure 4. 50(a-c). Results are evaluated separately for the membrane types. It is clearly seen from Figure 4. 50(a) that, filtrate volumes obtained after the carbohydrate filtrations were decreased with the increase of polymer amount in PS membranes. After solutions were filtrated for 1 h; 91 ml filtrate was obtained for PS-14, 62 ml filtrate was obtained for PS-16 and 48 ml filtrate was obtained for PS-18 membranes. Carbohydrate filtration results of the PES membranes are given as a graph in Figure 4. 50(b). As can be seen from the graph; obtained filtrate volumes were 156 ml for PES-14 membrane, 108 ml for PES-16 membrane and 51 ml for PES-18 membrane. Volume of the filtrate solutions were decreased with the increase of polymer amount in PES membranes. Carbohydrate filtration results of the CA membranes are given as a graph in Figure 4. 50(c). Volume of the filtrate solutions were decreased with the increase of polymer amount in CA membranes like PES and PS membranes. After solutions were filtrated for 1 h; 91 ml filtrate was obtained for CA-14, 45 ml filtrate was obtained for CA-16 and 10 ml filtrate was obtained for CA-18 membranes. When membranes were compared to each other, optimum performance for the carbohydrate filtrations were obtained for PES type of membranes, similar to protein filtrations. Filtrate volumes obtained by the carbohydrate filtrations were twice of the filtrate volumes obtained by protein filtrations for PS membranes, while performances of PES and CA membranes were similar for both filtrations.

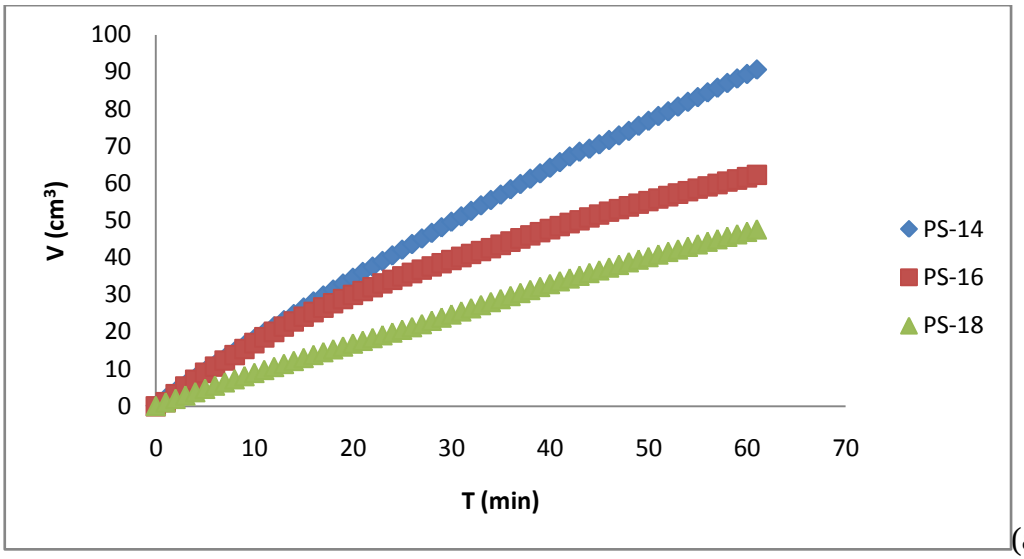

(a)

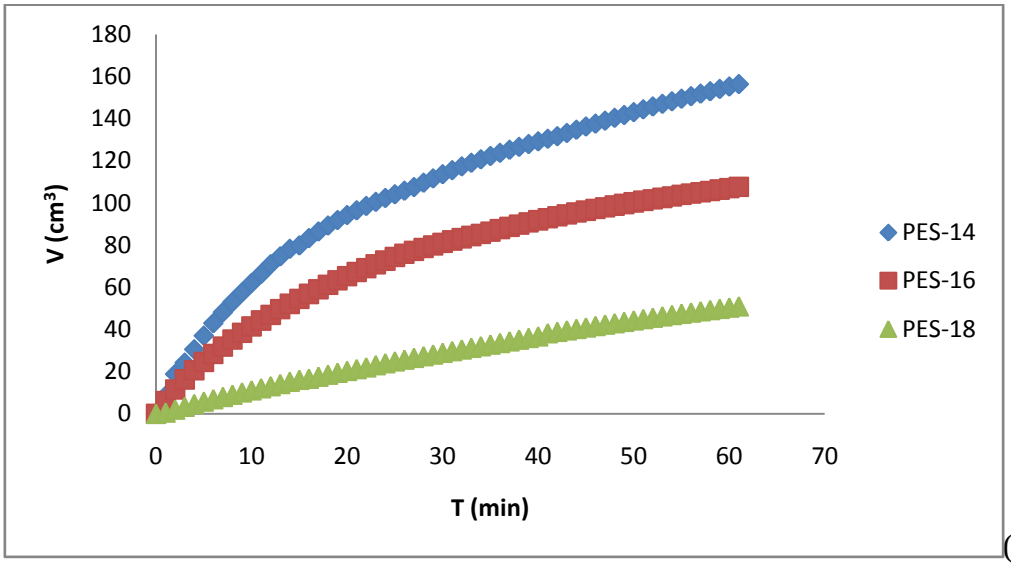

(b)

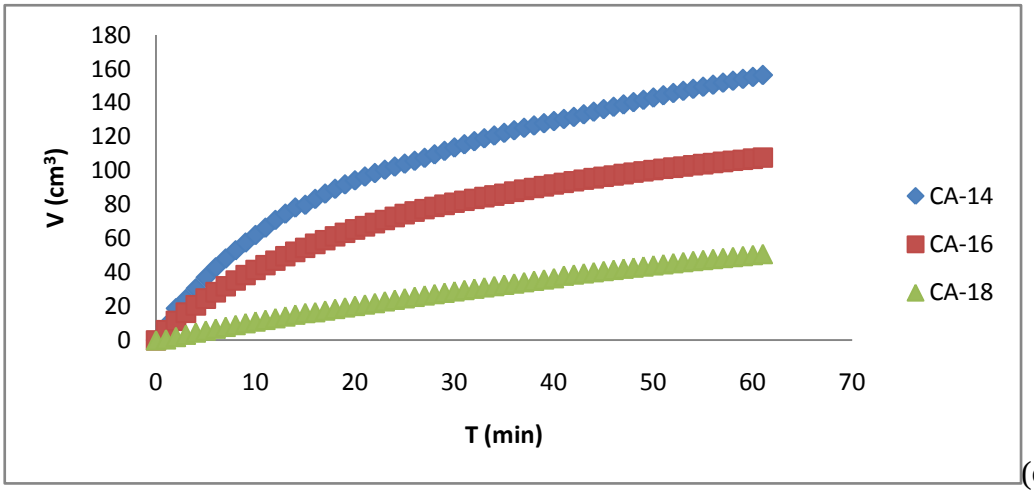

(c)

Figure 4. 50. Time-volume graphs of bare membranes obtained from the carbohydrate filtration process (a) PS membranes (b) PES membranes (c) CA membranes.

Equilibrium flux values and flux reduction rates, obtained from the carbohydrate filtration of bare membranes are given in Table 4. 13. As can be seen from Table 4. 13, highest flux values were measured for 14% polymer containing PS-14, PES-14 and CA-14 membranes. When membrane types were compared to each other, measured flux values were similar for the membranes that contain same amounts of polymers except for the CA-18 membrane. Lowest flux reduction rates (FRR) were measured for CA membranes similar to protein filtration experiments.

Table 4. 13. Measured flux values and flux reduction rates for bare membranes after carbohydrate filtration process.

Membrane type	$J_{ss(carbohydrate)}$ (L/m^{2}hr)	FRR* (%)
PS-14	52	65
PS-16	26	52
PS-18	28	43
PES-14	50	87
PES-16	28	87
PES-18	25	80
CA-14	54	25
CA-16	25	24
CA-18	6	25

*FRR: Flux reduction rate was measured as the ratio of flux values of distilled water and carbohydrate filtration. FRR=[1-(Jss(carbohydrate)/Jds)]x100

TOC analyses were applied for the initial and filtrate solutions after the filtration process, in order to find the carbohydrate rejection rates. Results were calculated as % rejection and given as a graph in Figure 4. 51. Measured carbohydrate rejection rates were lower than the protein rejection rates for all membranes. Carbohydrate rejection rates of PS membranes were measured as; 29% for PS-14 membrane, 14% for PS-16 membrane and 68% for PS-18 membrane. Carbohydrate rejection rates of PES membranes were measured as; 13% for PES-14 membrane, 19% for PES-16 membrane and 16% for PES-18 membrane. Carbohydrate rejection rates of CA membranes were measured as; 16% for CA-14 membrane, 45% for CA-16 membrane and 59% for CA-18 membrane. Carbohydrate addition rates were

increased relative with the polymer amounts for PS and CA membranes. But rejection rates were not changed with polymer addition for PES membrane.

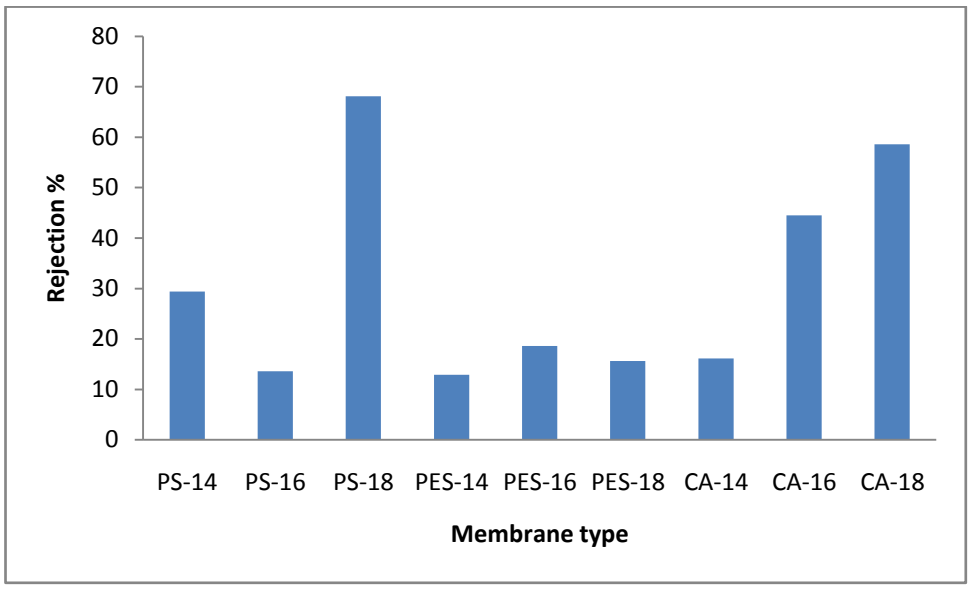

Figure 4. 51. % Rejection values for carbohydrate filtration of bare membranes.

In the second set of experiments, filtrations of carbohydrates were carried out by using AgNP containing membranes and results are shown as time-volume graph in Figure 4. 52(a-c). With the addition of AgNP, filtrate volumes were decreased for bare PES-14 and CA-14 membranes but increased for bare PS-14 membrane. As can be seen from Figure 4. 52(a), after solutions were filtrated for 1 h; 91 ml filtrate was obtained for bare PS-14 membrane, 142 ml filtrate was obtained for 0.4AgNP-PS membrane, 134 ml filtrate was obtained for 0.8AgNP-PS membrane and 123 ml filtrate was obtained for 1.2AgNP-PS membrane. Even though the filtrate volumes were not significantly different for varying AgNP amounts, highest filtrate volume was measured for 0.4% AgNP containing PS membrane. As can be seen from Figure 4. 52(b), after solutions were filtrated for 1 h; 156 ml filtrate was obtained for bare PES-14 membrane, 158 ml filtrate was obtained for 0.4AgNP-PES membrane, 129 ml filtrate was obtained for 0.8AgNP-PES membrane and 127 ml filtrate was obtained for 1.2AgNP-PES membrane. Filtrate volumes were decreased for varying AgNP amounts. As can be seen from Figure 4. 52(c), after solutions were filtrated for 1 h; 91ml filtrate was obtained for bare SA-14 membrane, 70 ml filtrate was obtained for 0.4AgNP-CA membrane, 73 ml filtrate was obtained for 0.8AgNP-CA membrane and 58 ml filtrate was obtained for 1.2AgNP-CA membrane. Filtrate volumes were decreased for varying AgNP amounts.

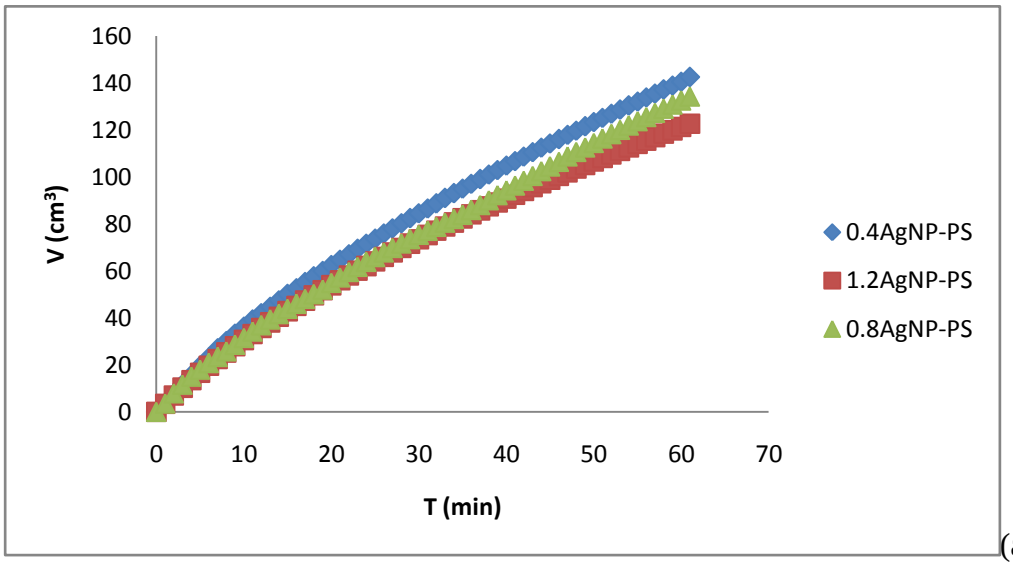

(a)

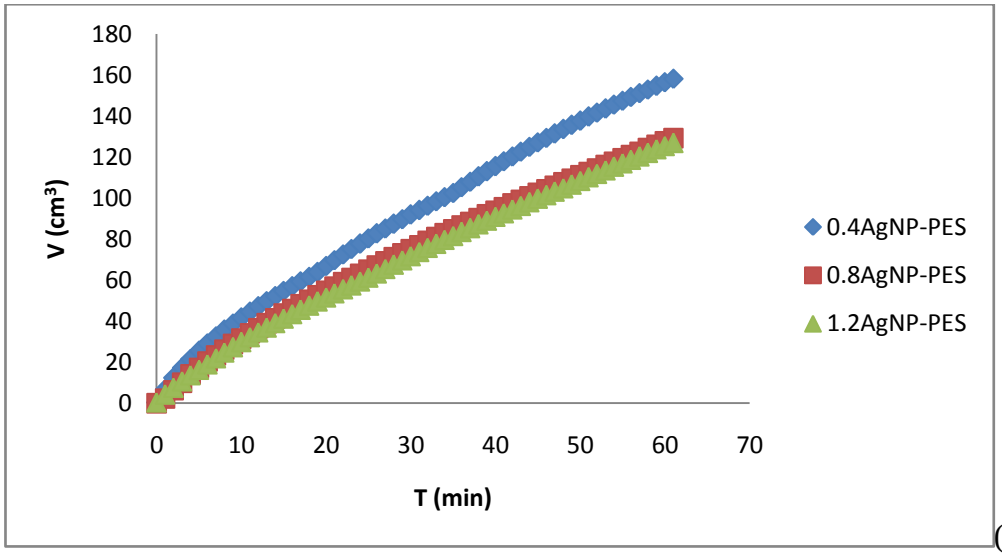

(b)

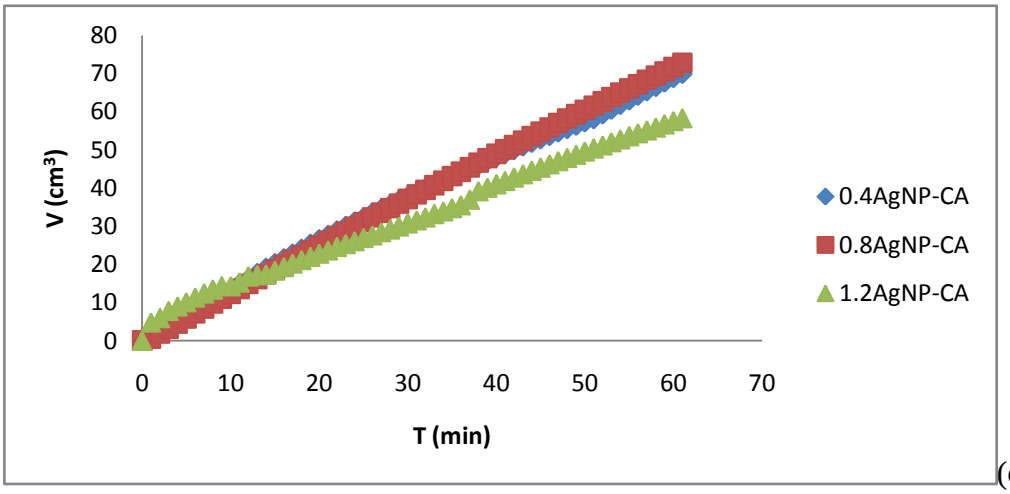

(c)

Figure 4. 52. Time-volume graphs of AgNP containing membranes obtained from the carbohydrate filtration process (a) PS membranes (b) PES membranes (c) CA membranes.

Equilibrium flux values and flux reduction rates, obtained from the carbohydrate filtration of AgNP containing membranes are given inTable 4. 14. As can be seen fromTable 4. 14, similar flux values were measured for AgNP-PS andAgNP-PES membranes while the lowest flux values were measured for AgNP-CA membranes. Lowest flux reduction rates (FRR) were measured for AgNP-CA membranes and highestflux reduction rates were measured for AgNP-PES membranes.

Table 4. 14. Measured flux values and flux reduction rates for AgNP containing membranes after carbohydrate filtration process.

Membrane type	$J_{ss(carbohydrate)}$ (L/m^{2}hr)	FRR* (%)
0.4AgNP-PS	71	67
0.8AgNP-PS	60	72
1.2AgNP-PS	74	51
0.4AgNP-PES	77	77
0.8AgNP-PES	68	73
1.2AgNP-PES	69	63
0.4AgNP-CA	49	34
0.8AgNP-CA	46	15
1.2AgNP-CA	33	27

*FRR: Flux reduction rate was measured as the ratio of flux values of distilled water and carbohydrate filtration. FRR=$[1-(J_{ss(carbohydrate)}/J_{ds})]_x100$

TOC analyses were applied for the initial and filtrate solutions after the filtration process, in order to find the carbohydrate rejection rates. Results were calculated as % rejection and given as a graph inFigure 4. 53. Carbohydrate rejection rates of AgNP-PS membranes were measured as; 25% for 0.4AgNP-PS membrane, 22% for 0.8AgNP-PSmembrane and 23% for 1.2AgNP-PS membrane.Carbohydrate rejection rates of AgNP-PES membranes were measured as; 24% for 0.4AgNP-PES membrane, 15% for 0.8AgNP-PES membrane and 44% for 1.2AgNP-PES membrane. Carbohydrate rejection rates of AgNP-CA membranes were measured as; 2% for 0.4AgNP-CA membrane, 1% for 0.8AgNP-CA membrane and 4% for 1.2AgNP-CA membrane. Carbohydrate rejection rates of the AgNP-CA membranes were quite low compared with other membranes. Optimum performance was obtained with 0.4% AgNP content for all membranes according to their filtrate

volumes, equilibrium flux values, flux reduction rates and carbohydraterejection rates.

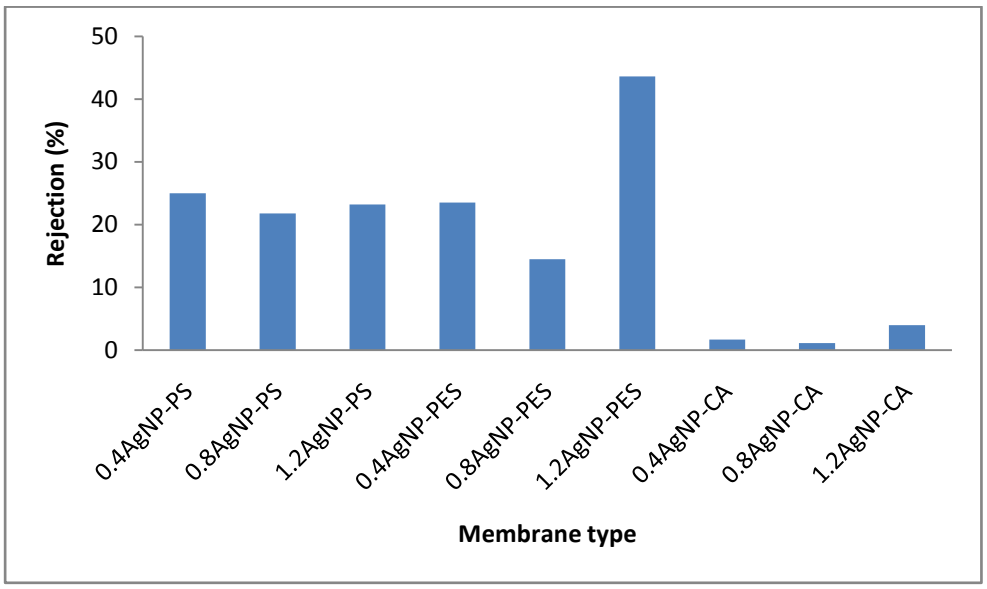

Figure 4. 53. % Rejection values for carbohydrate filtration of AgNP containing membranes.

In the third set of experiments, filtrations of carbohydrates were carried out by using SiNP containing membranes and results are shown as time-volume graph in Figure 4. 54(a-c).As can be seen from Figure 4. 54(a), after solutions were filtrated for 1 h; 91 ml filtrate was obtained for bare PS-14 membrane, 90 ml filtrate was obtained for 0.4SiNP-PS membrane, 89 ml filtrate was obtained for 0.8SiNP-PS membrane and 168 ml filtrate was obtained for 1.2SiNP-PS membrane.As can be seen from Figure 4. 54(b), after solutions were filtrated for 1 h; 156 ml filtrate was obtained for bare PES-14 membrane, 137 ml filtrate was obtained for 0.4SiNP-PES membrane, 185 ml filtrate was obtained for 0.8SiNP-PES membrane and 156 ml filtrate was obtained for 1.2SiNP-PES membrane.As can be seen from Figure 4. 54(c), after solutions were filtrated for 1 h;91 ml filtrate was obtained for bare CA-14 membrane, 24 ml filtrate was obtained for 0.4SiNP-CA membrane, 10 ml filtrate was obtained for 0.8SiNP-CA membrane and 7 ml filtrate was obtained for 1.2SiNP-PES membrane. Filtrate volume was dramatically decreased with SiNP addition for CA membrane, proportional to SiNP amount.

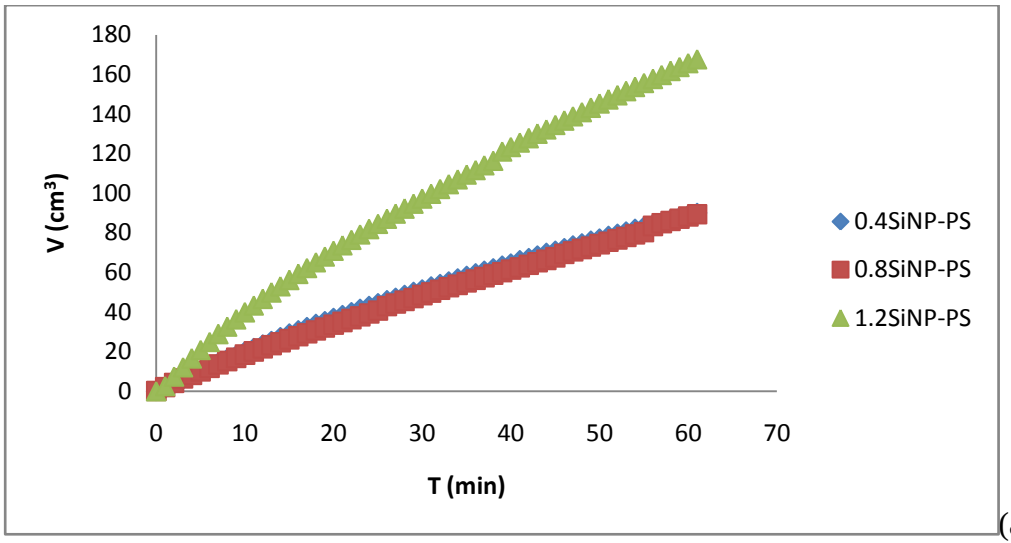

(a)

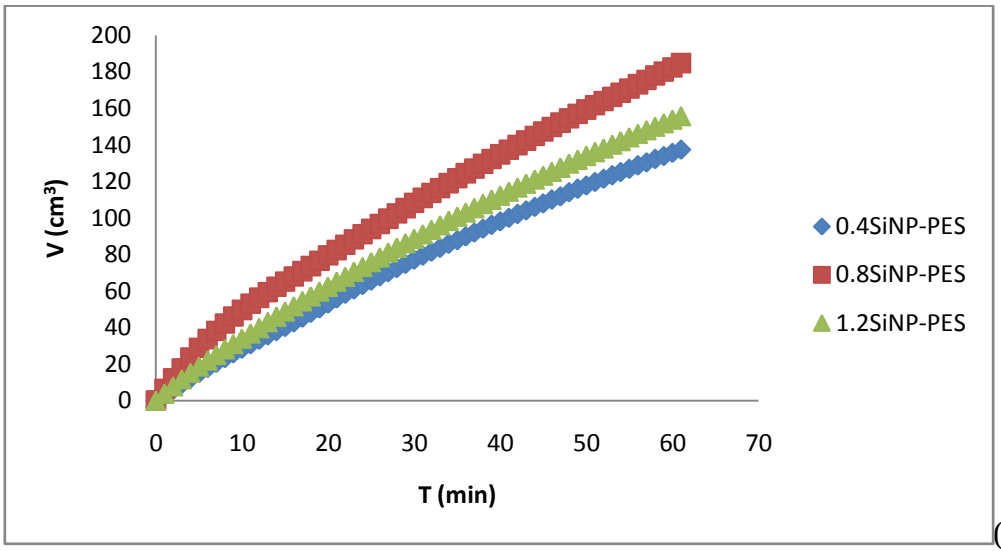

(b)

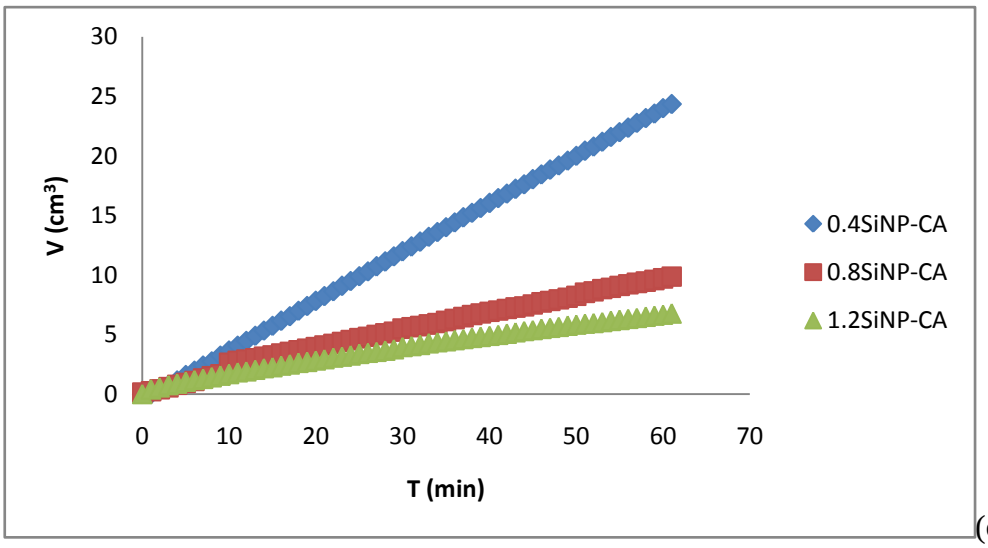

(c)

Figure 4. 54. Time-volume graphs of SiNP containing membranes obtained from the carbohydrate filtration process (a) PS membranes (b) PES membranes (c) CA membranes.

Equilibrium flux values and flux reduction rates, obtained from the carbohydrate filtration of SiNP containing membranes are given inTable 4. 15. As can be seen fromTable 4. 15, highest flux values were measured for SiNP-PES membranes while the measured flux values were very low for SiNP-CA membranes. Similar flux reduction rates (FRR) were measured for SiNP-PS and SiNP-PES membranes. Flux reduction rates were increased for SiNP-CA membranes, proportional to SiNP amount.

Table 4. 15. Measured flux values and flux reduction rates for SiNP containing membranes after carbohydrate filtration process.

Membrane type	**$J_{ss(carbohydrate)}$ (L/m^2hr)**	**FRR* (%)**
0.4SiNP-PS	48	53
0.8SiNP-PS	49	51
1.2SiNP-PS	84	50
0.4SiNP-PES	73	42
0.8SiNP-PES	95	65
1.2SiNP-PES	82	44
0.4SiNP-CA	16	7
0.8SiNP-CA	6	14
1.2SiNP-CA	3	50

*FRR: Flux reduction rate was measured as the ratio of flux values of distilled water and carbohydrate filtration. $FRR=[1-(J_{ss(carbohydrate)}/J_{ds})]_x100$

TOC analyses were applied for the initial and filtrate solutions after the filtration process, in order to find the carbohydrate rejection rates. Results were calculated as % rejection and given as a graph inFigure 4. 55. Carbohydrate rejection rates of SiNP-PS membranes were measured as; 50% for 0.4SiNP-PS membrane, 36% for 0.8SiNP-PS membrane and 25% for 1.2SiNP-PS membrane.Carbohydrate rejection rates of SiNP-PES membranes were measured as; 1% for 0.4SiNP-PES membrane, 10% for 0.8SiNP-PES membrane and 12% for 1.2SiNP-PES membrane.Carbohydrate rejection rates of SiNP-CA membranes were measured as; 57% for 0.4SiNP-CA membrane, 77% for 0.8SiNP-CA membrane and 77% for 1.2SiNP-CA membrane. For SiNP-PS and SiNP-CA membranes, measured carbohydrate rejection rates were higher than that of the bare and AgNP containing

membranes. With SiNP addition, measured carbohydrate rejection rates were dramatically decreased for SiNP-PES membranes compared to bare and AgNP containing membranes. Optimum performance was obtained with 1.2% SiNP content for PS membrane, 0.8% SiNP content for PES membrane, and 0.4% SiNP content for CA membrane according to their filtrate volumes, equilibrium flux values, flux reduction rates and carbohydrate rejection rates.

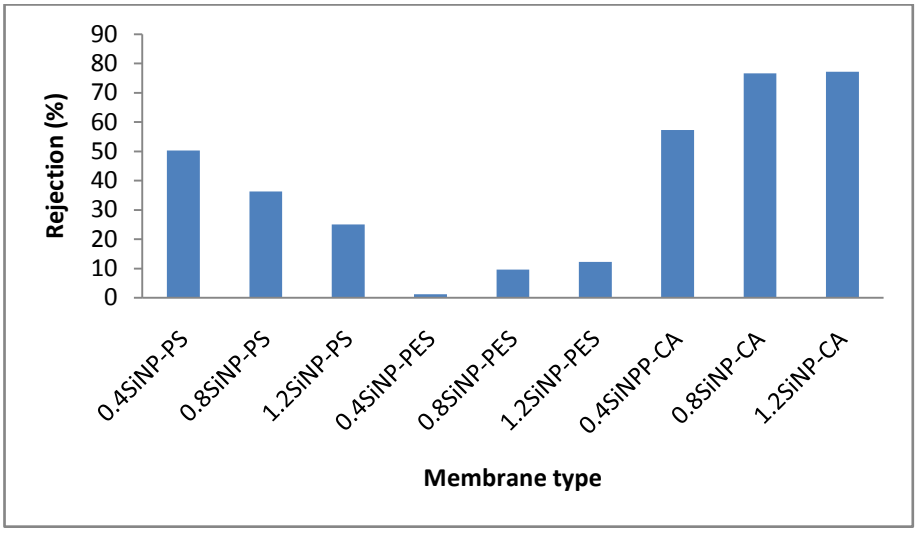

Figure 4. 55. % Rejection values for carbohydrate filtration of SiNP containing membranes.

In the fourth set of experiments, filtrations of carbohydrates were carried out by using CNT containing membranes and results are shown as time-volume graph inFigure 4. 56 (a-c).As can be seen from Figure 4. 56(a), after solutions were filtrated for 1 h; 91 ml filtrate was obtained for bare PS-14 membrane, 102 ml filtrate was obtained for 0.4CNT-PS membrane, 84 ml filtrate was obtained for 0.8CNT-PS membrane and 119 ml filtrate was obtained for 1.2CNT-PS membrane.As can be seen from Figure 4. 56(b), after solutions were filtrated for 1 h; 156 ml filtrate was obtained for bare PES-14 membrane, 192 ml filtrate was obtained for 0.4CNT-PES membrane, 164 ml filtrate was obtained for 0.8CNT-PES membrane and 166 ml filtrate was obtained for 1.2CNT-PES membrane.As can be seen from Figure 4. 56(c), after solutions were filtrated for 1 h;91 ml filtrate was obtained for bare CA-14 membrane, 13 ml filtrate was obtained for 0.4CNT-CA membrane, 6 ml filtrate was obtained for 0.8CNT-CA membrane and 14 ml filtrate was obtained for 1.2CNT-CA membrane.Addition of CNT dramatically decreased the filtrate volumes of CA membranes.

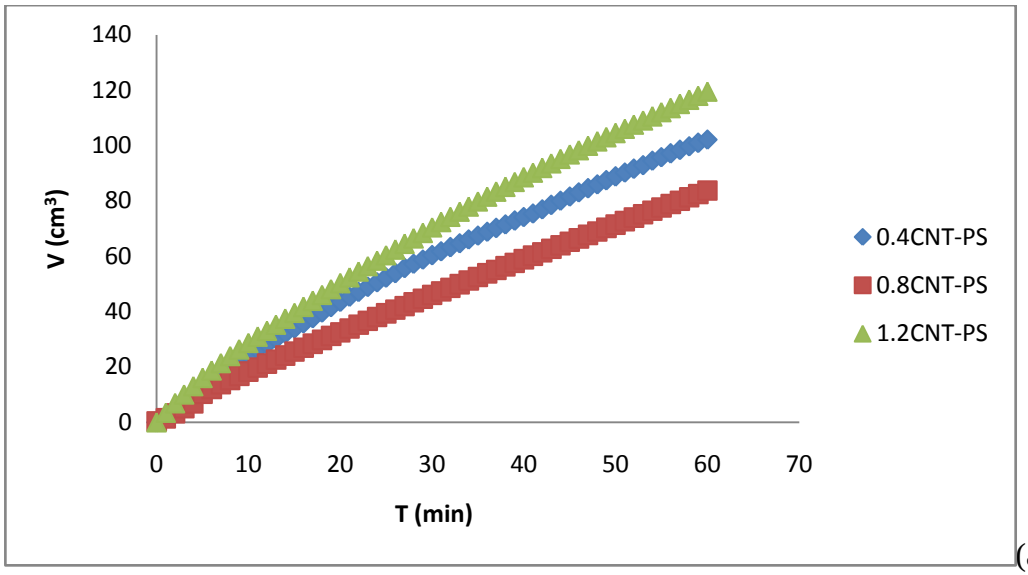

(a)

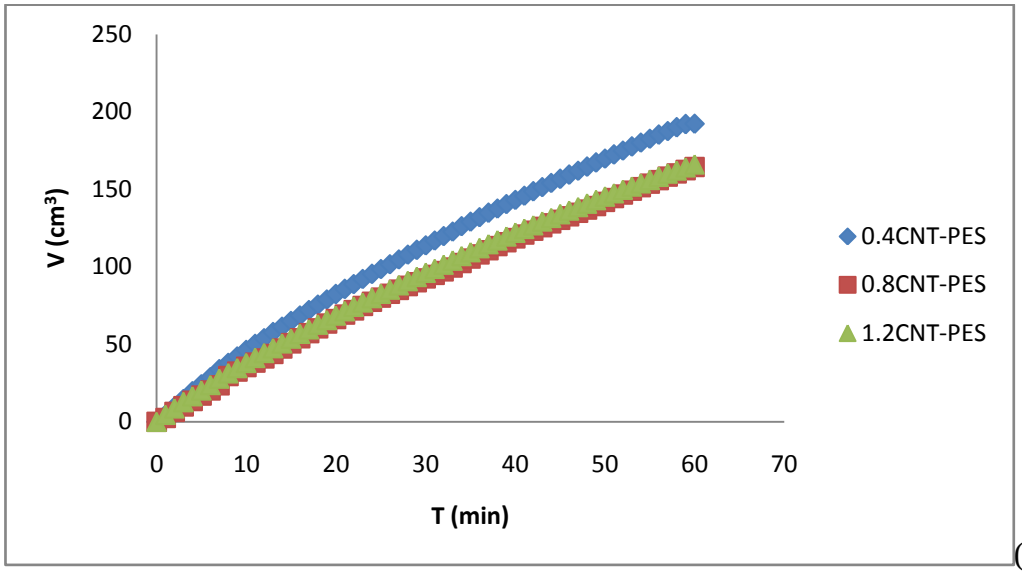

(b)

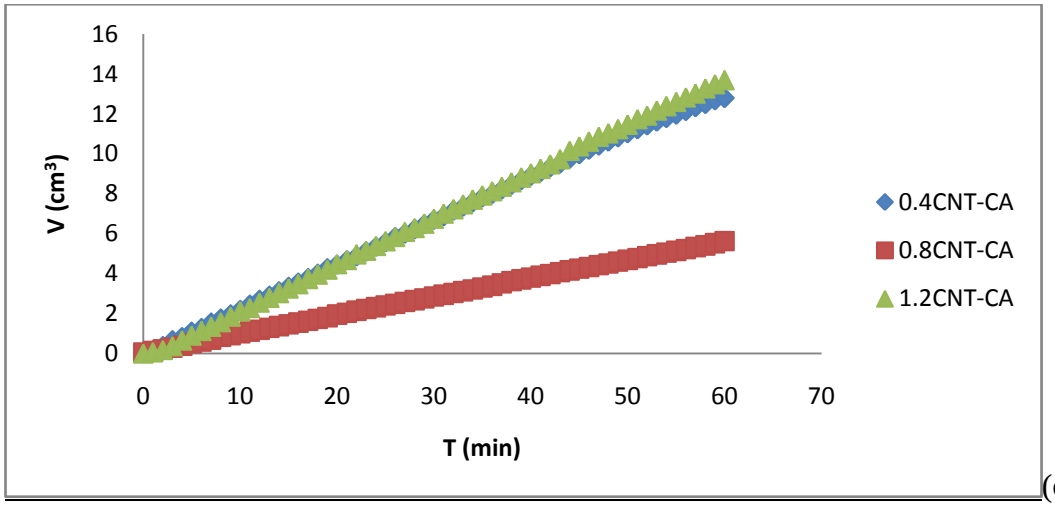

(c)

Figure 4. 56. Time-volume graphs of CNT containing membranes obtained from the carbohydrate filtration process (a) PS membranes (b) PES membranes (c) CA membranes.

Equilibrium flux values and flux reduction rates, obtained from the carbohydrate filtration of CNT containing membranes are given inTable 4. 16. As can be seen fromTable 4. 16, highest flux values were measured for CNT-PES membranes while the measured flux values were very low for CNT-CA membranes. Highest flux reduction rates (FRR) were measured for CNT-PES membranes and lowest flux reduction rates were measured for CNT-CA membranes.

Table 4. 16. Measured flux values and flux reduction rates for CNT containing membranes after carbohydrate filtration process.

Membrane type	$J_{ss(carbohydrate)}$ (L/m^{2}hr)	FRR* (%)
0.4CNT-PS	55	58
0.8CNT-PS	50	52
1.2CNT-PS	62	59
0.4CNT-PES	104	61
0.8CNT-PES	94	73
1.2CNT-PES	86	78
0.4CNT-CA	8	11
0.8CNT-CA	4	33
1.2CNT-CA	9	4

*FRR: Flux reduction rate was measured as the ratio of flux values of distilled water and carbohydrate filtration. FRR=$[1-(J_{ss(carbohydrate)}/J_{ds})]_x100$

TOC analyses were applied for the initial and filtrate solutions after the filtration process, in order to find the carbohydrate rejection rates. Results were calculated as % rejection and given as a graph inFigure 4. 57. Carbohydrate rejection rates of CNT-PS membranes were measured as; 23% for 0.4CNT-PS membrane, 10% for 0.8CNT-PS membrane and 25% for 1.2CNT-PS membrane.Carbohydrate rejection rates of CNT-PES membranes were measured as; 5% for 0.4CNT-PES membrane, 15% for 0.8CNT-PES membrane and 25% for 1.2CNT-PES membrane.Carbohydrate rejection rates of CNT-CA membranes were measured as; 18% for 0.4CNT-CA membrane, 25% for 0.8CNT-CA membrane and 25% for 1.2CNT-CA membrane.Optimum performance was obtained with 1.2% CNT content for PS and CA membranes and 0.4% CNT content for PES membrane according to their filtrate

volumes, equilibrium flux values, flux reduction rates and carbohydrate rejection rates.

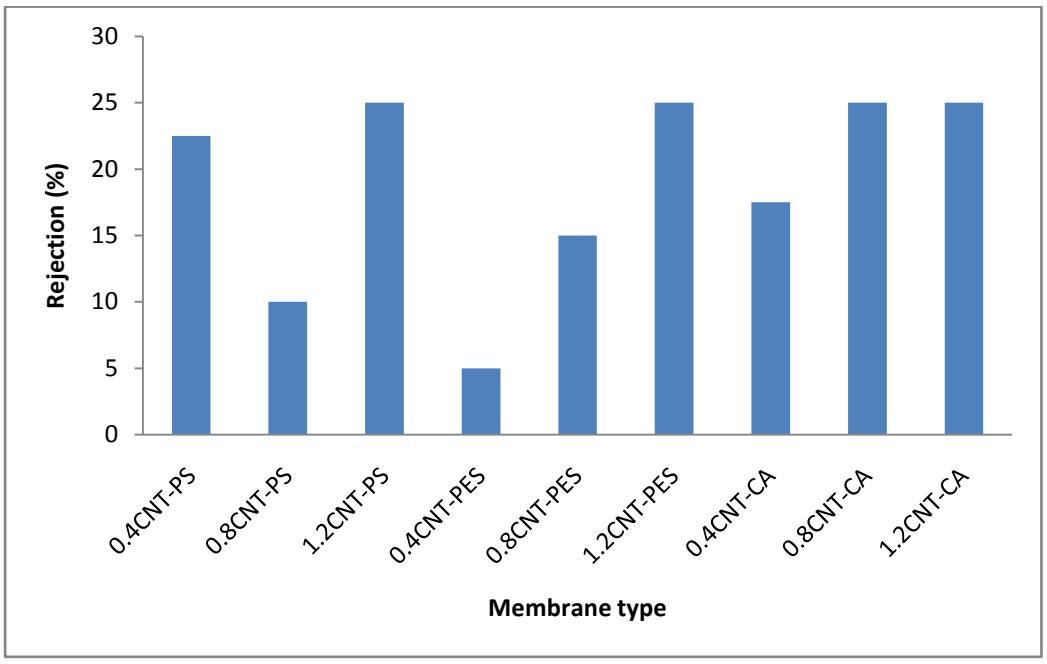

Figure 4. 57. % Rejection values for carbohydrate filtration of CNT containing membranes.

In the fifth set of experiments, filtrations of carbohydrates were carried out by using Al_2O_3 containing membranes and results are shown as time-volume graph in Figure 4. 58(a-c). As can be seen from Figure 4. 58(a), after solutions were filtrated for 1 h; 91 ml filtrate was obtained for bare PS-14 membrane, 139 ml filtrate was obtained for 0.4AlONP-PS membrane, 179 ml filtrate was obtained for 0.8AlONP-PS membrane and 133 ml filtrate was obtained for 1.2AlONP-PS membrane. As can be seen from Figure 4. 58(b), after solutions were filtrated for 1 h; 156 ml filtrate was obtained for bare PES-14 membrane, 243 ml filtrate was obtained for 0.4AlONP-PES membrane, 231 ml filtrate was obtained for 0.8AlONP-PES membrane and 239 ml filtrate was obtained for 1.2AlONP-PES membrane. As can be seen from Figure 4. 58(c), after solutions were filtrated for 1 h; 91 ml filtrate was obtained for bare CA-14 membrane, 147 ml filtrate was obtained for 0.4AlONP-CA membrane, 164 ml filtrate was obtained for 0.8AlONP-CA membrane and 144 ml filtrate was obtained for 1.2AlONP-CA membrane.

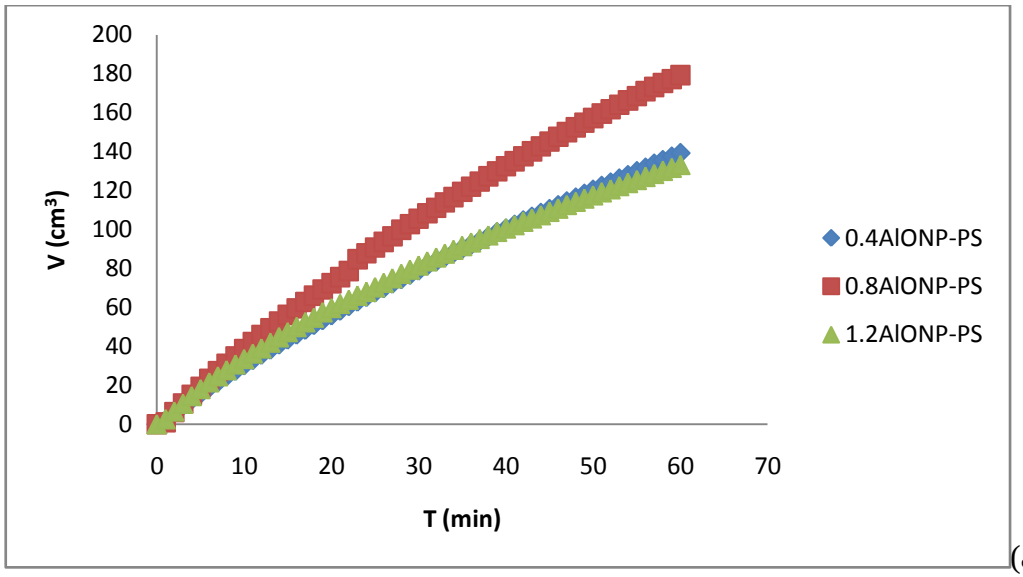

(a)

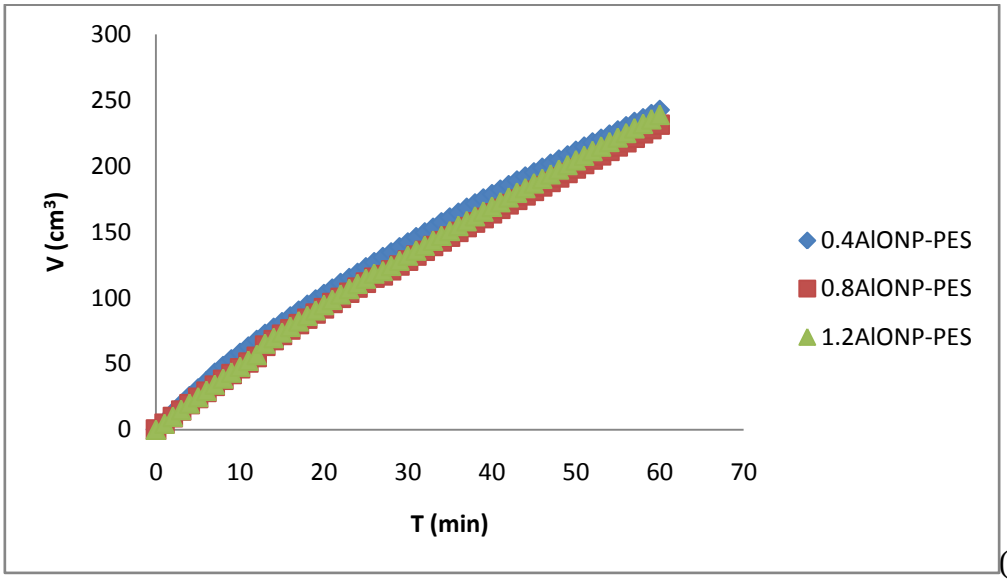

(b)

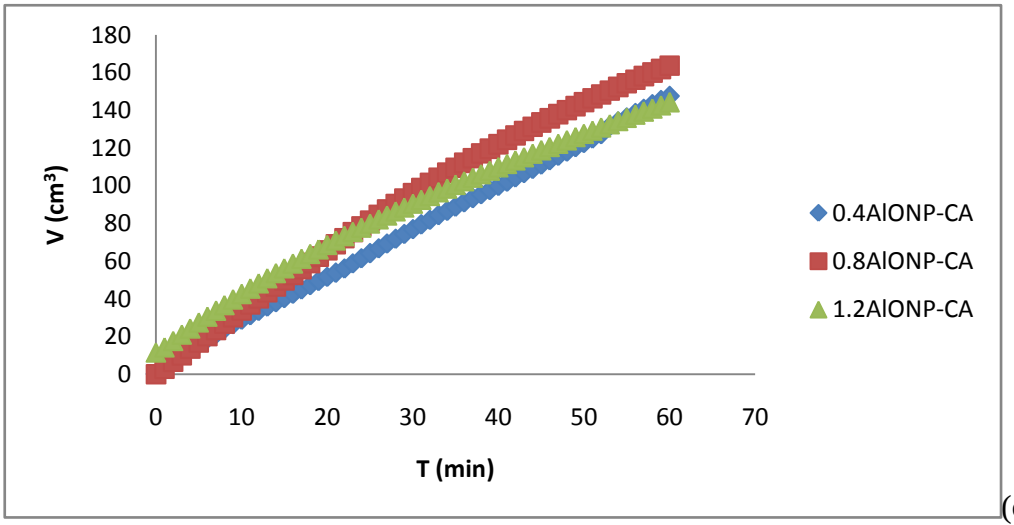

(c)

Figure 4. 58. Time-volume graphs of AlONP containing membranes obtained from the carbohydrate filtration process (a) PS membranes (b) PES membranes (c) CA membranes.

Equilibrium flux values and flux reduction rates, obtained from the carbohydrate filtration of AlONP containing membranes are given in Table 4. 17. As can be seen from Table 4. 17, highest flux values were measured for AlONP-PES membranes while the measured flux values were similar for AlONP-CA and AlONP-PS membranes. Carbohydrate filtration flux values of the CA membranes were measured higher for AlONP-CA membranes than SiNP-CA and CNT-CA membranes. Measured flux reduction rates were similar for AlONP-PES and AlONP-PS membranes while the lowest flux reduction rates were measured for AlONP-CA membranes.

Table 4. 17. Measured flux values and flux reduction rates for AlONP containing membranes after carbohydrate filtration process.

Membrane type	$J_{ss(carbohydrate)}$ (L/m^{2}hr)	FRR* (%)
0.4AlO-PS	77	61
0.8AlO-PS	88	49
1.2AlO-PS	64	56
0.4AlO-PES	128	61
0.8AlO-PES	137	52
1.2AlO-PES	142	54
0.4AlO-CA	94	24
0.8AlO-CA	80	40
1.2AlO-CA	69	48

*FRR: Flux reduction rate was measured as the ratio of flux values of distilled water and carbohydrate filtration. FRR=$[1-(J_{ss(carbohydrate)}/J_{ds})]_x100$

TOC analyses were applied for the initial and filtrate solutions after the filtration process, in order to find the carbohydrate rejection rates. Results were calculated as % rejection and given as a graph in Figure 4. 59. Carbohydrate rejection rates of AlONP-PS membranes were measured as; 20% for 0.4AlONP-PS membrane, 16% for 0.8AlONP-PS membrane and 15% for 1.2AlONP-PS membrane. Carbohydrate rejection rates of AlONP-PES membranes were measured as; 10% for 0.4AlONP-PES membrane, 7% for 0.8AlONP-PES membrane and 5% for 1.2AlONP-PES membrane. Carbohydrate rejection rates of AlONP-CA membranes were measured as; 4% for 0.4AlONP-CA membrane, 12% for 0.8AlONP-CA membrane and 32%

for 1.2AlONP-CA membrane. Optimum performance was obtained with 1.2% AlONP content for PES membrane and 0.4% AlONP content for PS and CA membranes according to their filtrate volumes, equilibrium flux values, flux reduction rates and carbohydrate rejection rates.

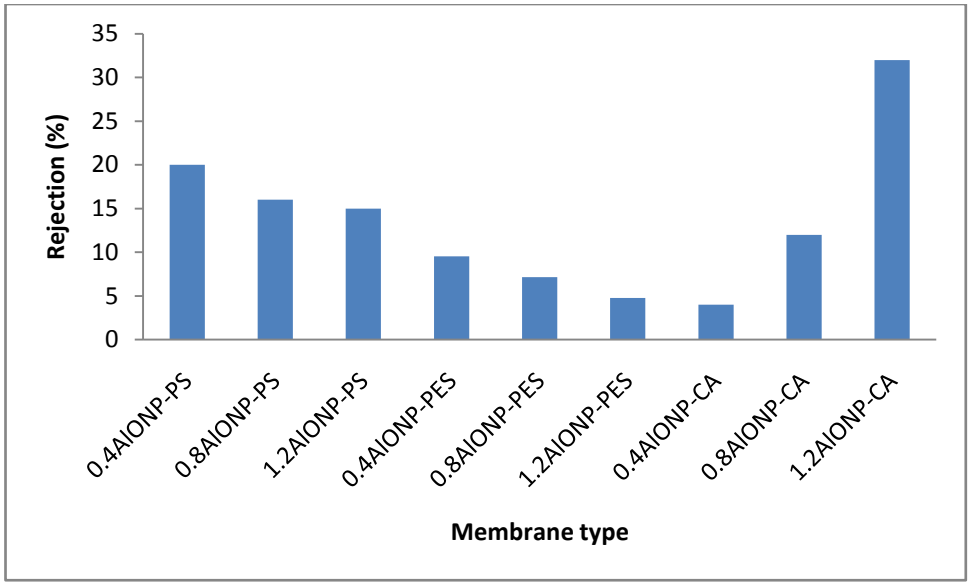

Figure 4. 59. % Rejection values for carbohydrate filtration of AlONP containing membranes.

In the sixth set of experiments, filtrations of carbohydrates were carried out by using TiO_2 containing membranes and results are shown as time-volume graph in Figure 4. 60(a-c). Membranes were kept under UV light for 15 minutes and activated before the carbohydrate filtration by using a 160W UV-A lamp. As can be seen from Figure 4. 60(a), after solutions were filtrated for 1 h; 91 ml filtrate was obtained for bare PS-14 membrane, 201 ml filtrate was obtained for 0.4TiNP-PS membrane, 205 ml filtrate was obtained for 0.8TiNP-PS membrane and 256 ml filtrate was obtained for 1.2TiNP-PS membrane. As can be seen from Figure 4. 60(b), after solutions were filtrated for 1 h; 156 ml filtrate was obtained for bare PES-14 membrane, 183 ml filtrate was obtained for 0.4TiNP-PES membrane, 204 ml filtrate was obtained for 0.8TiNP-PES membrane and 249 ml filtrate was obtained for 1.2TiNP-PES membrane. As can be seen from Figure 4. 60(c), after solutions were filtrated for 1 h; 91 ml filtrate was obtained for bare CA-14 membrane, 166 ml filtrate was obtained for 0.4TiNP-CA membrane, 222 ml filtrate was obtained for 0.8TiNP-CA membrane and 189 ml filtrate was obtained for 1.2TiNP-CA membrane.

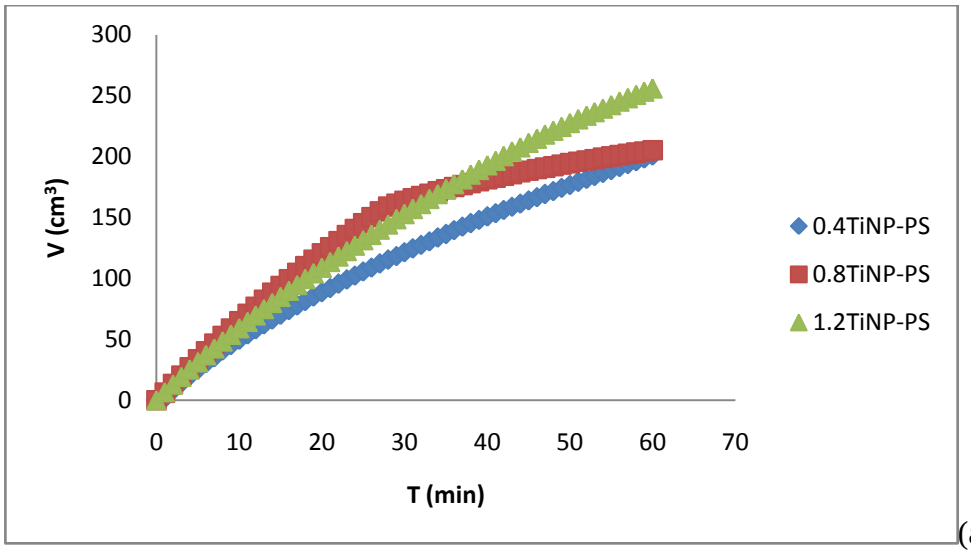

(a)

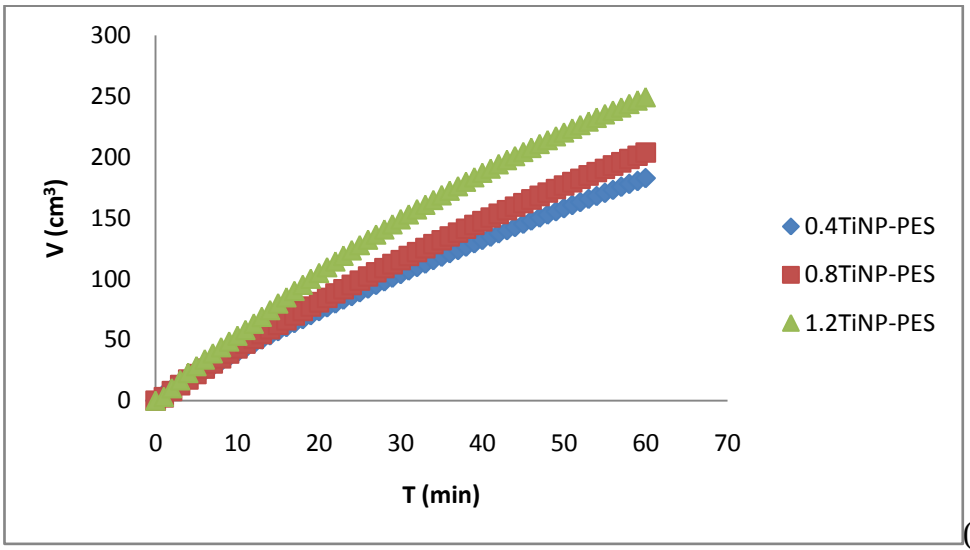

(b)

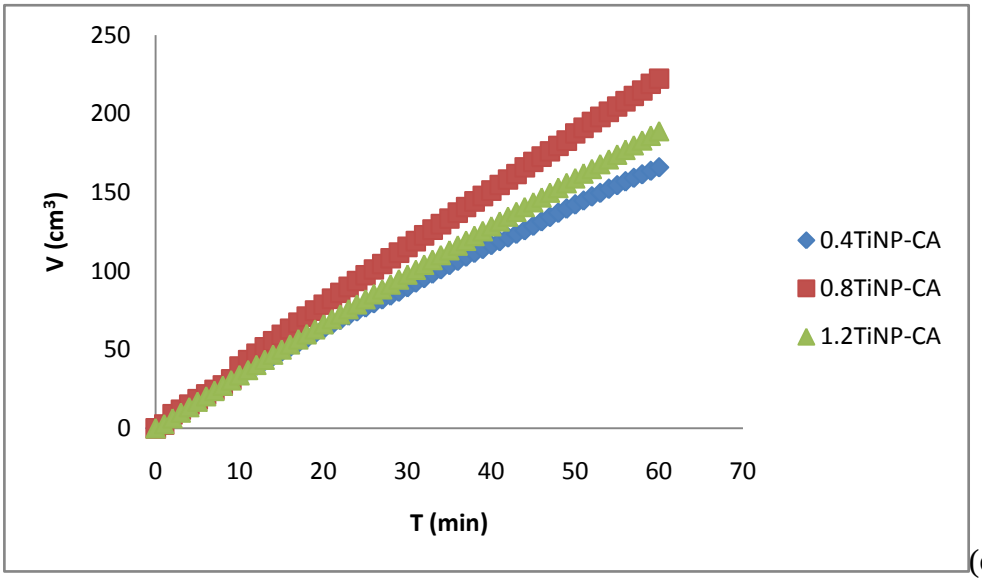

(c)

Figure 4. 60. Time-volume graphs of TiNP containing membranes obtained from the carbohydrate filtration process (a) PS membranes (b) PES membranes (c) CA membranes.

Equilibrium flux values and flux reduction rates, obtained from the carbohydrate filtration of TiNP containing membranes are given in Table 4. 18. As can be seen from Table 4. 18, highest flux values were measured for TiNP-CA membranes and the lowest flux values were measured for TiNP-PS membranes. Lowest flux reduction rates were measured for TiO_2 containing membranes, compared with other nanoparticle containing membranes.

Table 4. 18. Measured flux values and flux reduction rates for TiNP containing membranes after carbohydrate filtration process.

Membrane type	$J_{ss(carbohydrate)}$ (L/m^{2}hr)	FRR* (%)
0.4TiNP-PS	99	55
0.8TiNP-PS	86	35
1.2TiNP-PS	116	14
0.4TiNP-PES	102	52
0.8TiNP-PES	112	59
1.2TiNP-PES	118	62
0.4TiNP-CA	99	29
0.8TiNP-CA	136	13
1.2TiNP-CA	123	10

*FRR: Flux reduction rate was measured as the ratio of flux values of distilled water and carbohydrate filtration. $FRR=[1-(J_{ss(carbohydrate)}/J_{ds})]_x100$

TOC analyses were applied for the initial and filtrate solutions after the filtration process, in order to find the carbohydrate rejection rates. Results were calculated as % rejection and given as a graph in Figure 4. 61. Carbohydrate rejection rates of TiNP-PS membranes were measured as; 8% for 0.4TiNP-PS membrane, 13% for 0.8TiNP-PS membrane and 17% for 1.2TiNP-PS membrane. Carbohydrate rejection rates of TiNP-PES membranes were measured as; 3% for 0.4TiNP-PES membrane, 11% for 0.8TiNP-PES membrane and 13% for 1.2TiNP-PES membrane. Carbohydrate rejection rates of TiNP-CA membranes were measured as; 5% for 0.4TiNP-CA membrane, 5% for 0.8TiNP-CA membrane and 2% for 1.2TiNP-CA membrane. Optimum performance was obtained with 1.2% TiNP content for PES and PS membranes, and 0.8 % TiNP content for CA membranes according to their

filtrate volumes, equilibrium flux values, flux reduction rates and carbohydrate rejection rates.

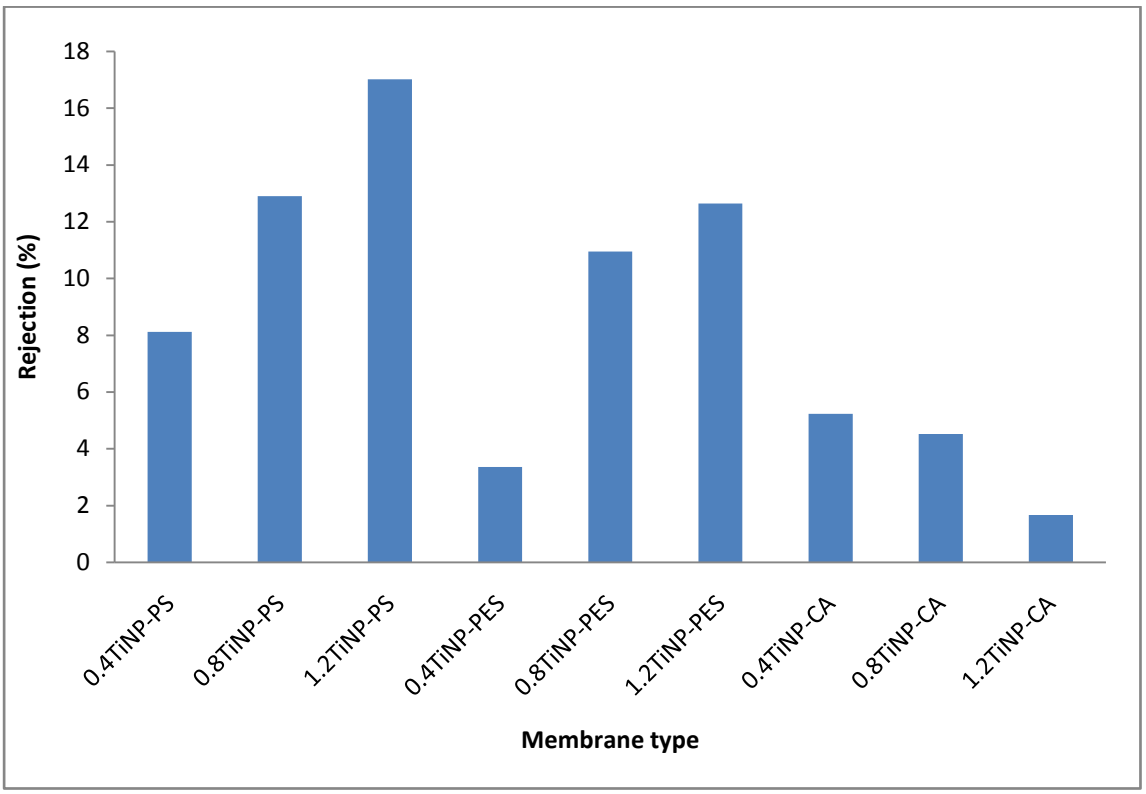

Figure 4. 61. % Rejection values for carbohydrate filtration of TiNP containing membranes.

4.9.3 Model EPS filtration

Model EPS solutions (having 100 mg/L concentration) were filtrated for an hour and graphical results are given below as a table, seperately for each polymer. First set of EPS experiments were carried out for the bare and nanoparticle containing membranes, prepared by using PS polymer, and results are given as a time-volume graph in Figure 4. 62. After solutions were filtrated for an hour, obtained filtrate volumes were; 96 ml for bare PS membrane, 72 ml for 0.4AgNP-PS membrane, 89 ml for 1.2SiNP-PS membrane, 71 ml for 1.2CNT-PS membrane, 101 ml for 0.4AlONP-PS membrane and 89 ml for 1.2TiNP-PS membrane as can be seen from the figure. When compared to the bare PS membrane, filtrate volumes were decreased with nanoparticle addition except for the AlONP. Filtrate volume was increased for bare PS membrane with the addition of AlONP.

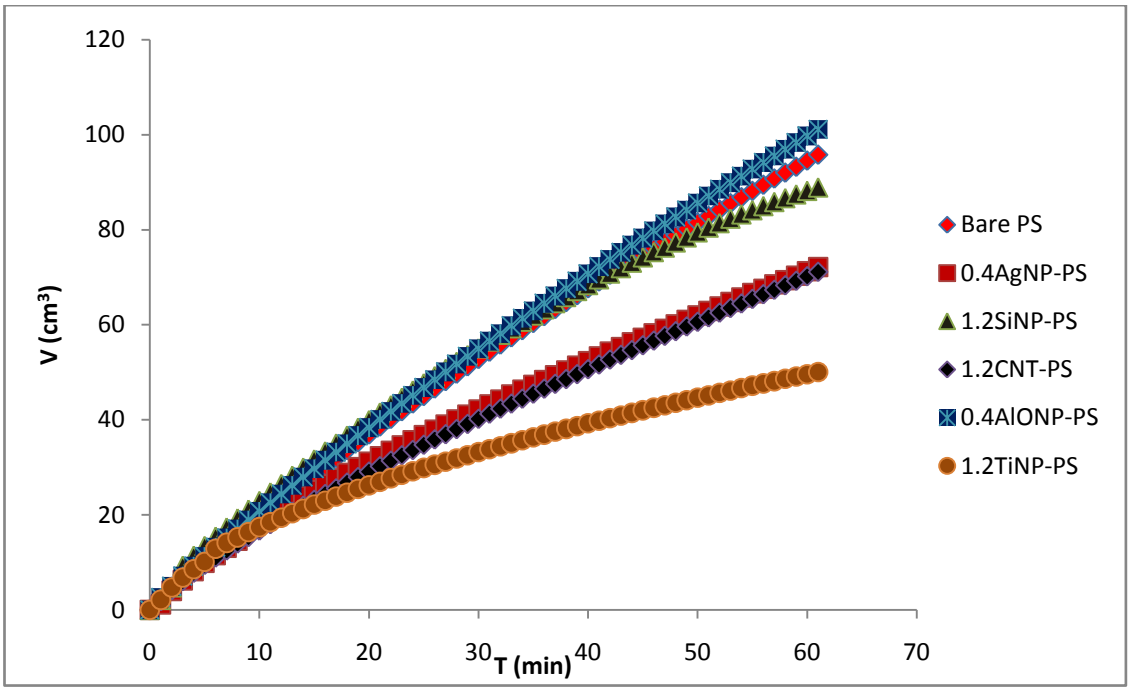

Figure 4. 62. Time – Volume graphs of PS membranes obtained from the EPS filtration processes.

Protein and carbohydrate analyses were applied for the initial and filtrate solutions. Results were calculated as % rejection and given as a graph in Figure 4. 63. Protein rejection rates were higher than the carbohydrate rejection rates and measured within the range of 85-90% for all membranes. Measured carbohydrate rejection rates were within the range of 45-60%.

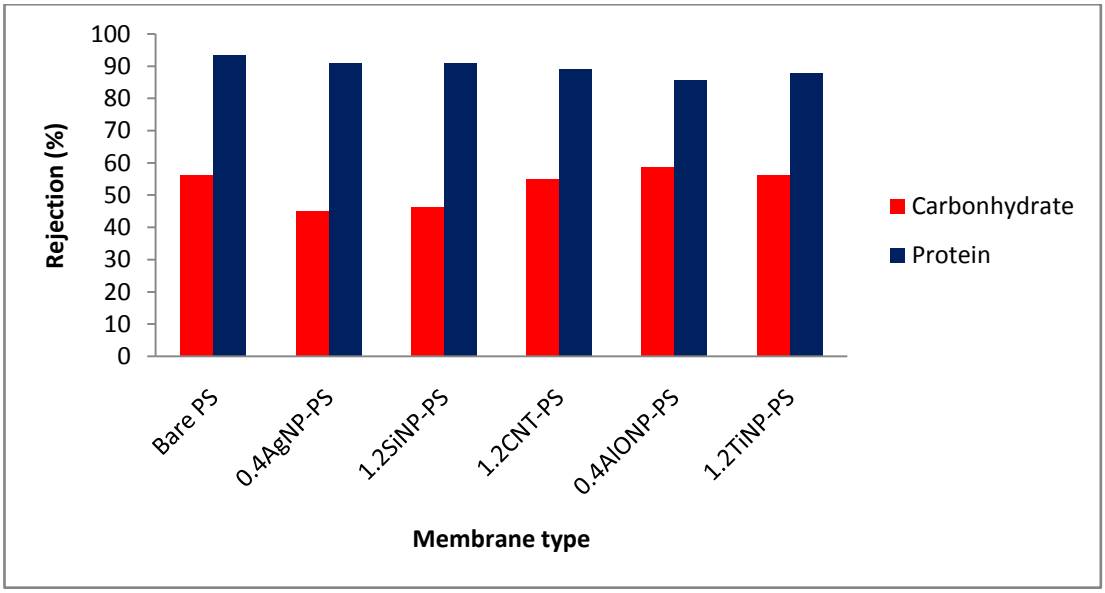

Figure 4. 63. Protein – Carbohydrate rejection rates of PS membranes obtained from the EPS filtration processes (%).

Second set of EPS experiments were carried out for the bare and nanoparticle containing membranes, prepared by using PES polymer, and results are given as a time-volume graph in Figure 4. 64. After solutions were filtrated for an hour obtained filtrate volumes were; 70 ml for bare PES membrane, 121 ml for 0.4AgNP-PES membrane, 67 ml for 1.2SiNP-PES membrane, 48 ml for 1.2CNT-PES membrane, 88 ml for 0.4AlONP-PES membrane and 41 ml for 1.2TiNP-PES membrane, as can be seen from the figure. When compared to the bare PES membrane, filtrate volumes of PES membranes were increased with the addition of AgNP and AlONP. However, filtrate volumes were decreased with the addition of other nanoparticles.

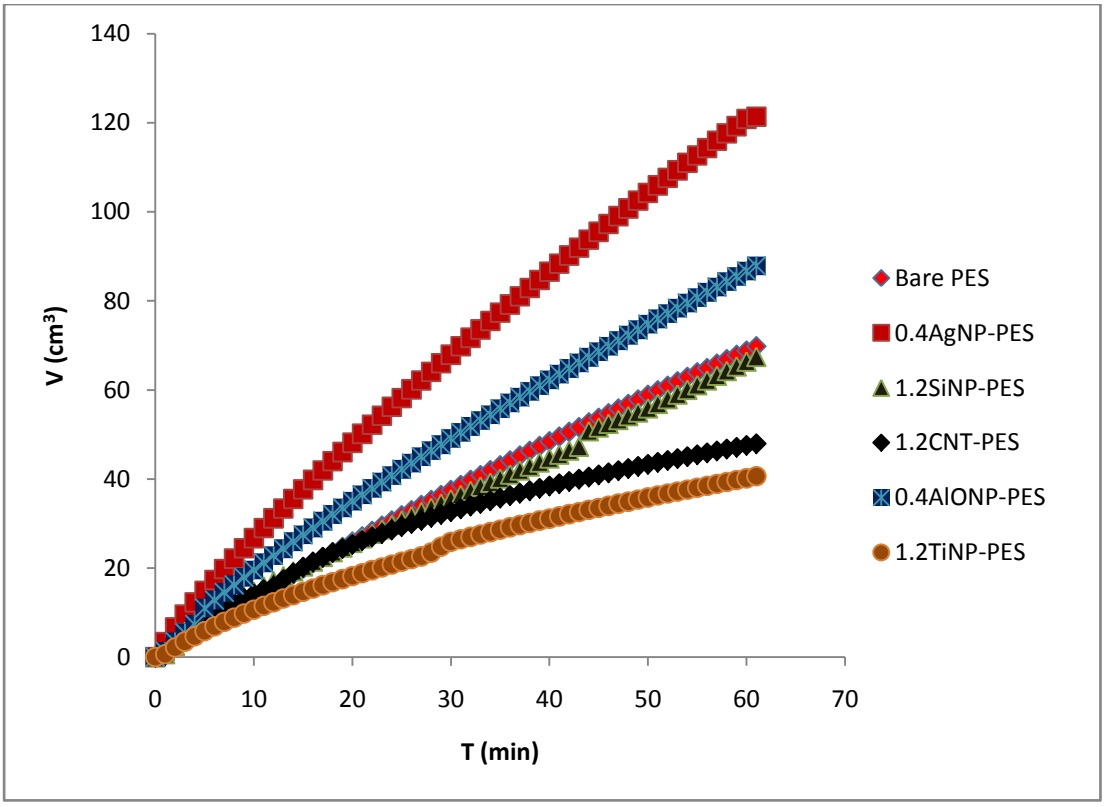

Figure 4. 64. Time – Volume graphs of PES membranes obtained from the EPS filtration processes.

Protein and carbohydrate analyses were applied for the initial and filtrate solutions. Results were calculated as % rejection and given as a graph in Figure 4. 65. Protein rejection rates were higher than the carbohydrate rejection rates and measured within the range of 85-90% for all membranes. Measured carbohydrate rejection rates were within the range of 30-60%.

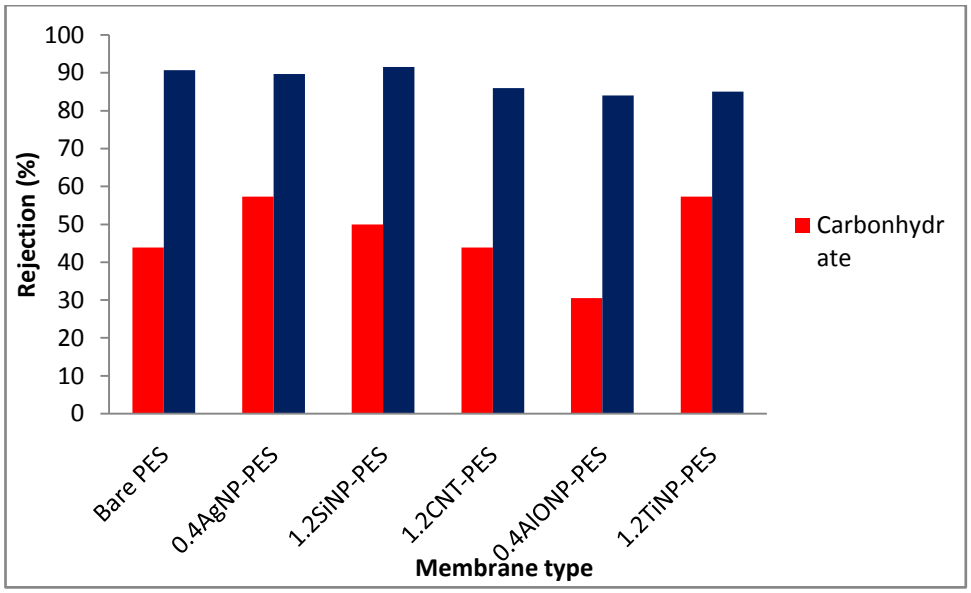

Figure 4. 65. Protein – Carbohydrate rejection rates of PES membranes obtained from the EPS filtration processes (%).

Third set of EPS experiments were carried out for the bare and nanoparticle containing membranes, prepared by using CA polymer, and results are given as a time-volume graph in Figure 4. 66. After solutions were filtrated for an hour obtained filtrate volumes were; 46 ml for bare CA membrane, 77 ml for 0.4AgNP-CA membrane, 9 ml for 1.2SiNP-CA membrane, 10 ml for 1.2CNT-CA membrane, 36 ml for 0.4AlONP-CA membrane and 38 ml for 1.2TiNP-CA membrane, as can be seen from the figure. When compared to the bare CA membrane, filtrate volumes of CA membranes were increased with the addition of AgNP. However, filtrate volumes were decreased with the addition of other nanoparticles, especially with the addition of SiNP and CNT nanoparticles.

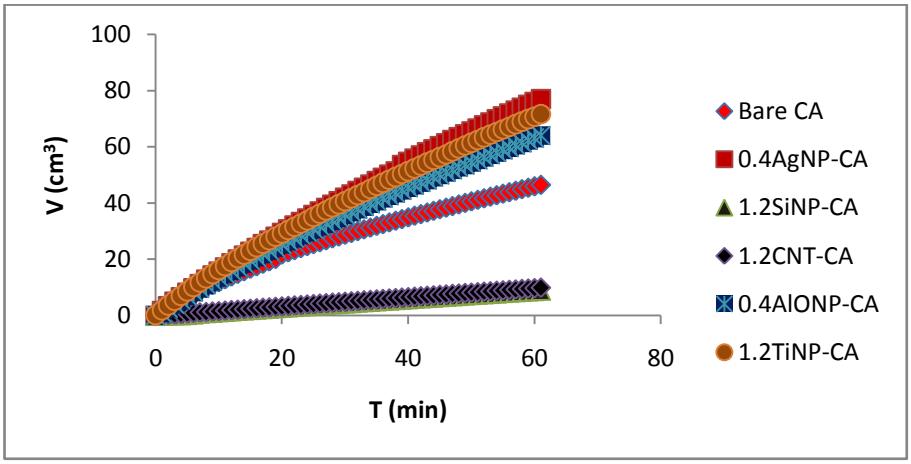

Figure 4. 66. Time – Volume graphs of CA membranes obtained from the EPS filtration processes.

Protein and carbohydrate analyses were applied for the initial and filtrate solutions. Results were calculated as % rejection and given as a graph in Figure 4. 67. Similar with the previous results, protein rejection rates were higher than the carbohydrate rejection rates and measured within the range of 80-95% for all membranes. Measured carbohydrate rejection rates were within the range of 30-60%.

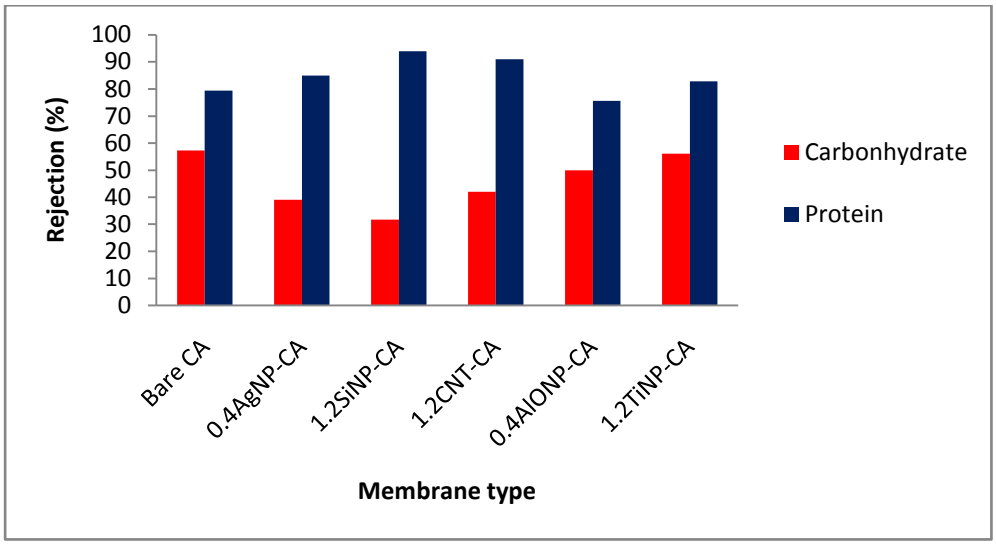

Figure 4. 67. Protein – Carbohydrate rejection rates of CA membranes obtained from the EPS filtration processes (%).

Equilibrium flux values of PS, PES and CA membranes, obtained from the model EPS filtration process, are shown in theTable 4. 19. For bare, CNT containing and AlONP containing membranes, highest flux values were measured for PS membranes. For AgNP and SiNP containing membranes, highest flux values were measured for PES membranes. And for TiNP containing membranes, highest flux values were measured for CA membranes.

Table 4. 19. Equilibrium flux values of PS, PES and CA membranes obtained from the model EPS filtration process.

	J_{EPS} (L/m^{2}h)		
Membrane	**PS**	**PES**	**CA**
Bare	**53**	41	22
0.4AgNP	40	**64**	43
1.2SiNP	35	**43**	6
1.2CNT	**39**	20	7
0.4AlONP	**58**	49	36
1.2TiNP	20	18	**38**

A medium that do not contain any living material but the bacterial products, is called the Model EPS. Hereby it can be expected that, obtained flux values were important to estimate how the flux values of EPS coated membrane surfaces would change. For EPS filtration, flux reduction or increase is directly proportional to the accumulation of gel layer on the surface. If a high flux value is obtained from the EPS filtration, it can be understood that the accumulated gel layer was thin thus, the permeability of the membrane was not affected much. Similarly, if a low flux value is obtained from the EPS filtration, it can be understood that the accumulated gel layer was thick thus, the permeability of the membrane was affected significantly and water could not pass through the membrane. It is thought that, reason of the flux increase of PES membrane after AgNP addition, is related with this mechanism. When permeability values and model EPS flux values are compared, a significant correlation cannot be observed. Thus it can be said that, EPS filtrations were not affected significantly by the membrane porosity. Therefore a correlation could not be observed between the EPS flux values and the measured MWCO values.A correlation between, hydrophilicity/hydrophobicity of the membrane surfaces and the flux values, could not be observed. So far from the estimations it can be said that, there is not any correlation between the EPS filtration performance, permeability (showing the membrane porosity), MWCO (showing the rejection efficiency related to molecular weight distribution of solutions) and surface hydrophilicity. On the contrary, a correlation between the measured surface roughness values (Ra) and EPS flux changes can be observed. For example; roughness differences of the PS membranes can be shown as TiNP-PS>SiNP-PS>CNT-PS>AlONP-PS=BarePS=AgNP-PS. And EPS flux differences can be shown as AlONP-PS>BarePS>AgPS>CNT-PS>SiNP-PS>TiNP-PS. As can be seen from the comparison, flux values were decreased with the increase of roughness values.

4.9.4 *E.coli* bacteria suspension filtration

Solutions were filtrated for an hour by using *E.coli* suspension and graphical results are given as a table. Results are evaluated separately for the polymer types.

In the first set of experiments, filtrations were carried out for bare and nanoparticle containing PS membranes and results are shown as time-volume graph inFigure 4. 68. After solutions were filtrated for 1 h; 177 ml filtrate was obtained for bare PS,

213 ml filtrate was obtained for 0.4AgNP-PS, 169 ml filtrate was obtained for 1.2SiNP-PS, 174 ml for 1.2CNT-PS, 149 ml for 0.4AlONP-PS and 206 ml for 1.2TiNP-PS membranes. Compared to bare PS membrane, higher filtrate volumes were obtained for the AgNP and TiNP containing PS membranes.

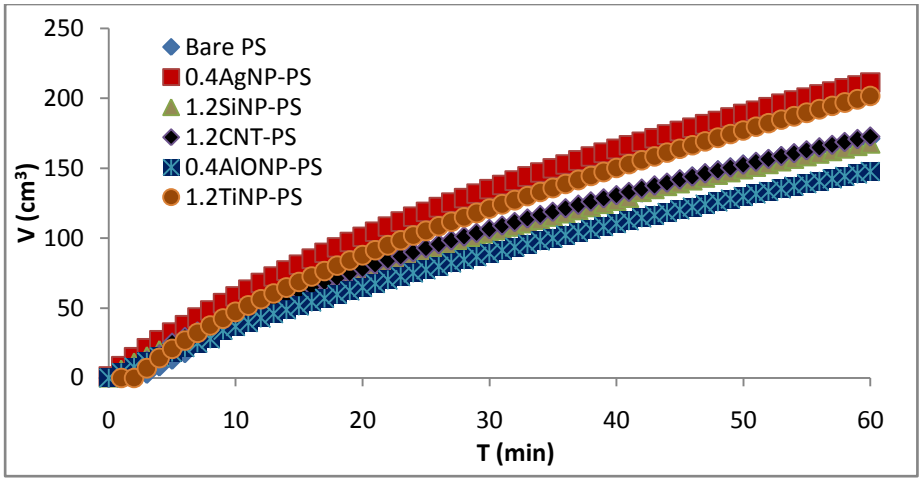

Figure 4. 68. Time – Volume graphs of PS membranes obtained from the *E.coli* suspension filtration processes.

Protein and carbohydrate analyses were applied for the initial and filtrate solutions of bacterial products (SMP). Results were calculated as % rejection and given as a graph in Figure 4. 69.

As can be seen from the graph, different rejection properties were exhibited by the membranes while the infiltration. Highest carbohydrate rejection rates were measured for bare PS membranes. Measured protein rejection rates were generally lower than 20% for all membranes.

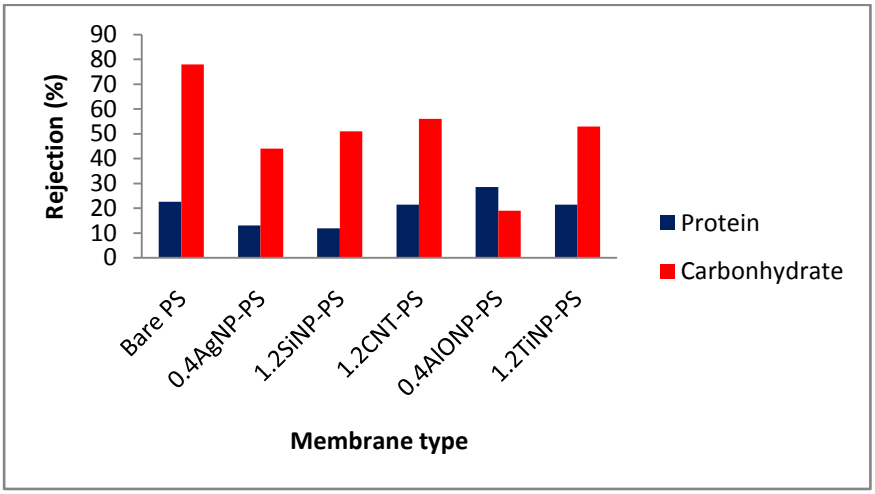

Figure 4. 69. Protein – Carbohydrate rejection rates of PS membranes obtained from the *E.coli* filtration processes (%).

In the second set of experiments, *E.coli* filtrations were carried out for bare and nanoparticle containing PES membranes and results are shown as time-volume graph inFigure 4. 70. After solutions were filtrated for 1 h; 181 ml filtrate was obtained for bare PES, 175 ml filtrate was obtained for 0.4AgNP-PES, 186 ml filtrate was obtained for 1.2SiNP-PES, 218 ml for 1.2CNT-PES, 221 ml for 0.4AlONP-PES and 222 ml for 1.2TiNP-PES membranes. Compared to bare PES membrane, higher filtrate volumes were obtained for the AlONP, CNT and TiNP containing PES membranes. But, filtrate volumes were not affected significantly from the addition of other nanoparticles.

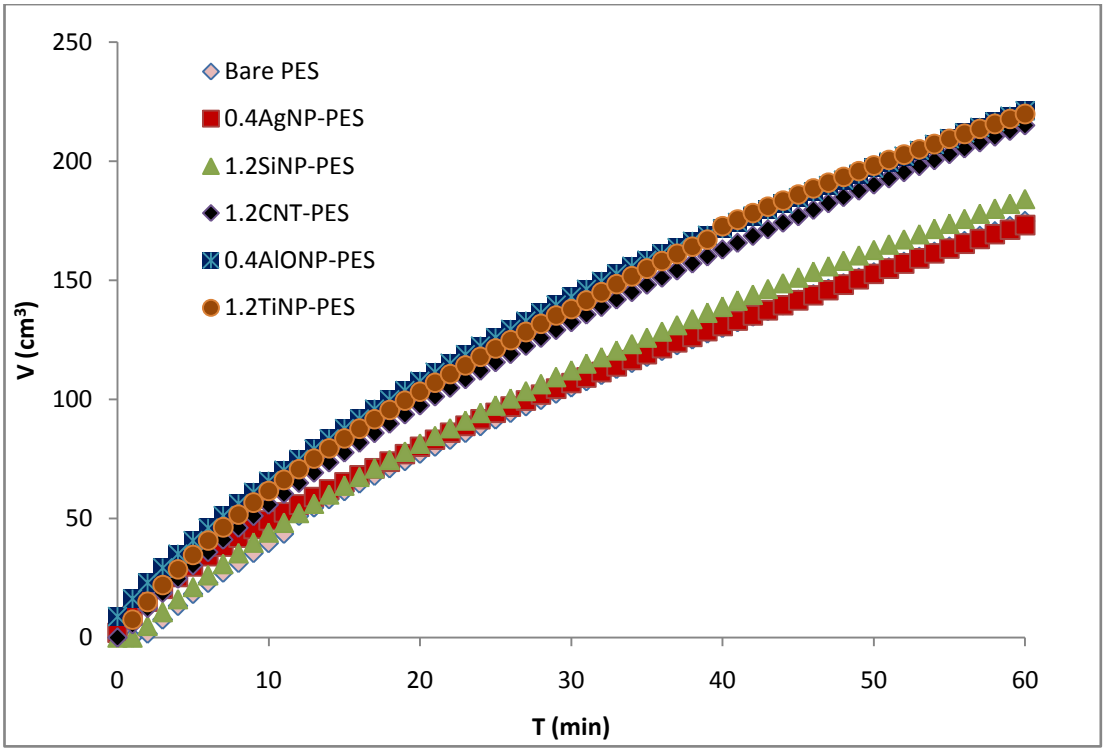

Figure 4. 70. Time – Volume graphs of PES membranes obtained from the *E.coli* suspension filtration processes.

Protein and carbohydrate analyses were applied for the initial and filtrate solutions of bacterial products (SMP). Results were calculated as % rejection and given as a graph in Figure 4. 71.

As can be seen from the graph, similar to PS membranes, different rejection properties were exhibited by PES membranes while the infiltration.

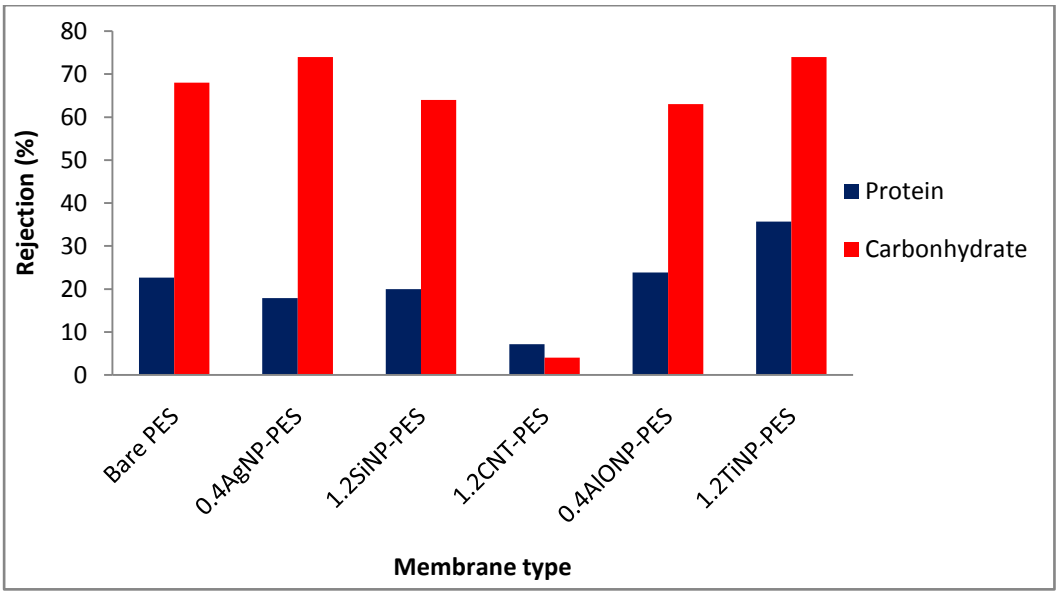

Figure 4. 71. Protein – Carbohydrate rejection rates of PES membranes obtained from the *E.coli* filtration processes (%).

In the third set of experiments, *E.coli* filtrations were carried out for bare and nanoparticle containing CA membranes and results are shown as time-volume graph inFigure 4. 72. After solutions were filtrated for 1 h; 112 ml filtrate was obtained for bare CA, 113 ml filtrate was obtained for 0.4AgNP-CA, 11 ml filtrate was obtained for 1.2SiNP-CA, 12 ml for 1.2CNT-CA, 119 ml for 0.4AlONP-CA and 140 ml for 1.2TiNP-CA membranes. Filtrate volume of CA membrane was dramatically increased with the addition of TiNP. However, filtrate volume of CA membrane was dramatically decreased with the addition of SiNP and CNT.

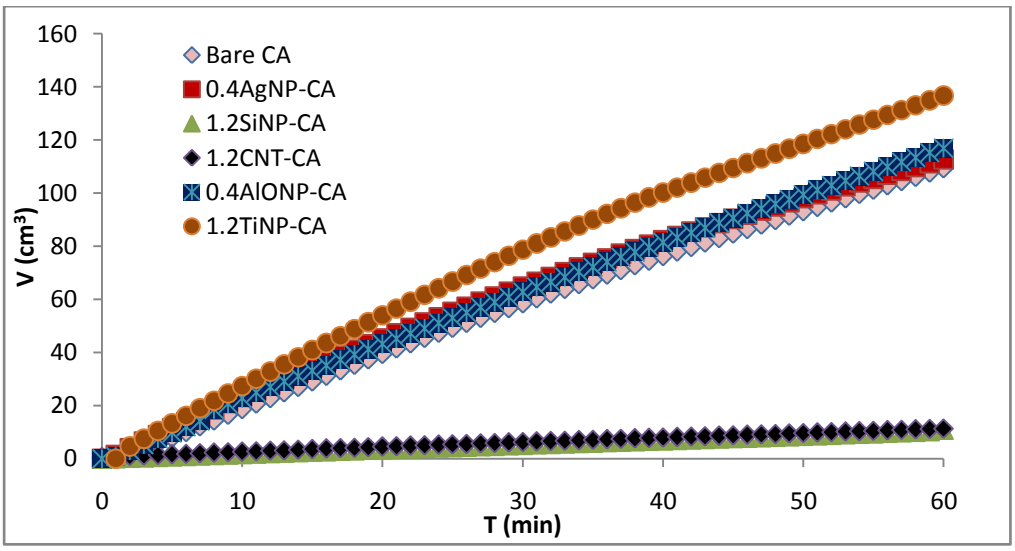

Figure 4. 72. Time – Volume graphs of CA membranes obtained from the *E.coli* suspension filtration processes.

Protein and carbohydrate analyses were applied for the initial and filtrate solutions of bacterial products (SMP). Results were calculated as % rejection and given as a graph in Figure 4. 73.As can be seen from the graph, similar to PES and PS membranes, different rejection properties were exhibited by CA membranes while the infiltration, especially for the carbohydrate filtration.

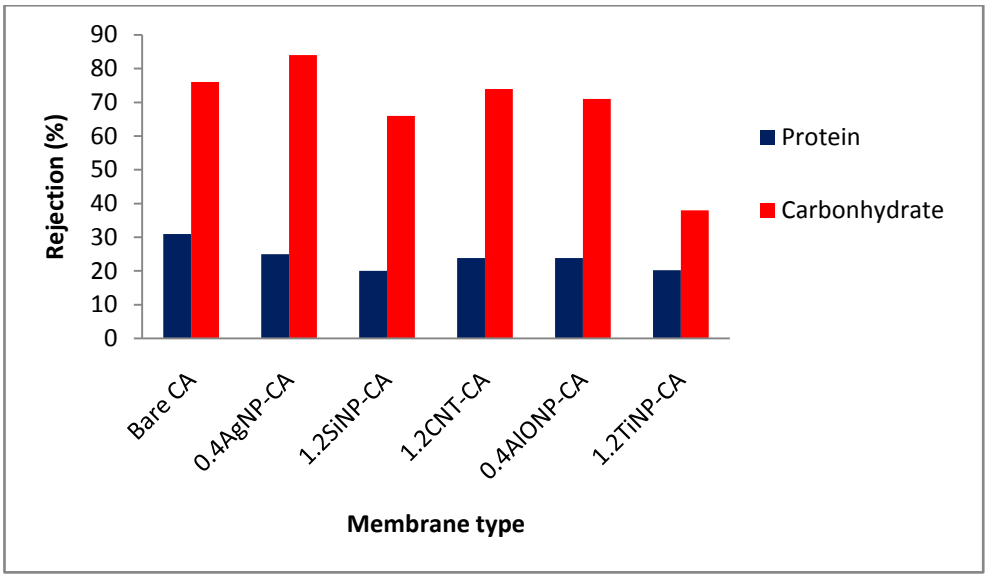

Figure 4. 73. Protein – Carbohydrate rejection rates of CA membranes obtained from the *E.coli* filtration processes (%).

Equilibrium flux values of PS, PES and CA membranes, obtained from the *E.coli* filtration processes, are given in the Table 4. 20. For bare, CNT containing, AlONP containing and SiNP containing membranes, highest flux values were measured for PES membranes. For AgNP and TiNP containing membranes, highest flux values were measured for PS membranes. Worst *E.coli* filtration performance was obtained with the CA membranes. Measured flux values were generally higher than that of the model EPS filtration because density of the *E.coli* suspension was lower than that of the model EPS. Thus, accumulation on membrane surfaces was less for the *E.coli* suspension process. Using model EPS was provided to examine the membrane performances in a medium containing only bacterial products while using *E.coli* suspension was provided to examine the membrane performances in a medium containing only one type of bacterium. As a result it can be said that, reason of the membrane performance decrement was contamination because membranes were contaminated more in an only bacterial product containing medium.

Table 4. 20. Equilibrium flux values of PS, PES and CA membranes obtained from the *E.coli* filtration processes.

	$J_{E.coli}$ (L/m^{2}hr)		
Membrane	**PS**	**PES**	**CA**
Bare	77	**88**	67
0.4AgNP	**92**	84	56
1.2SiNP	76	**87**	8
1.2CNT	82	**102**	7
0.4AlONP	73	**99**	76
1.2TiNP	**100**	89	75

It is known that, a large number of living bacteria was also existed in*E.coli* medium along with the bacterial products. Thus, flux values obtained from these experiments have a high importance especially to examine the antibacterial properties of nanoparticle containing membrane surfaces. High flux values can be explained with the low accumulation on the membrane surfaces. It can also be estimated from the high flux values that, membrane pores were not blocked by the bacteria significantly. It is possible that nanoparticles on the surfaces were directly killed the *E.coli* cells or electrostatically inhibited them from conglutination on the surfaces. For PS and CA membranes, highest *E.coli* flux values were obtained with the addition of AgNP, CNT and TiNP nanoparticles, which are known for their antibacterial properties. Furthermore, for PES membranes having very high *E.coli* flux values, highest flux values were measured for PES membranes containing CNT and AlONP nanoparticles. In order to determine the mechanism completely, superior techniques are required.

4.9.4.1 Viability test results obtained from the *E.coli* filtration processes

Thephotographs of viability test of suspended *E.coli* cells are given at Figure 4.74.When bare membranes were compared, obtained growth rates were high for CA membranes but significant growth rates were not obtained for PS and PES membranes.

When nanoparticle containing membranes were compared, growth circles around the membrane surfaces were smaller for AgNP and AlONP containing membranes while there was almost no growth for the 0.4 AgNP-PS membranes.

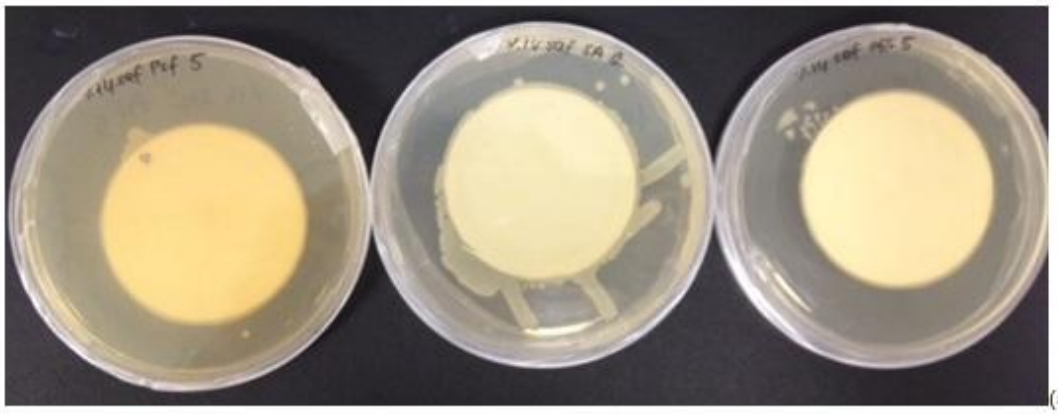

(a)

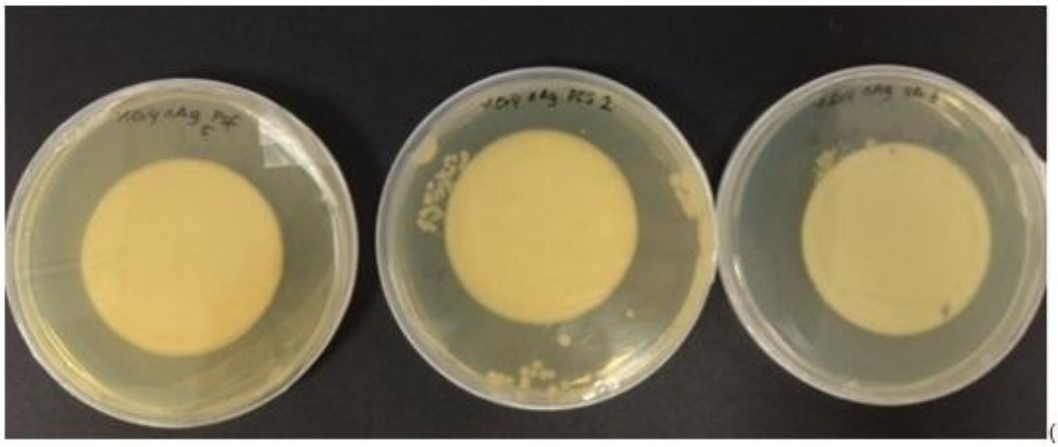

(b)

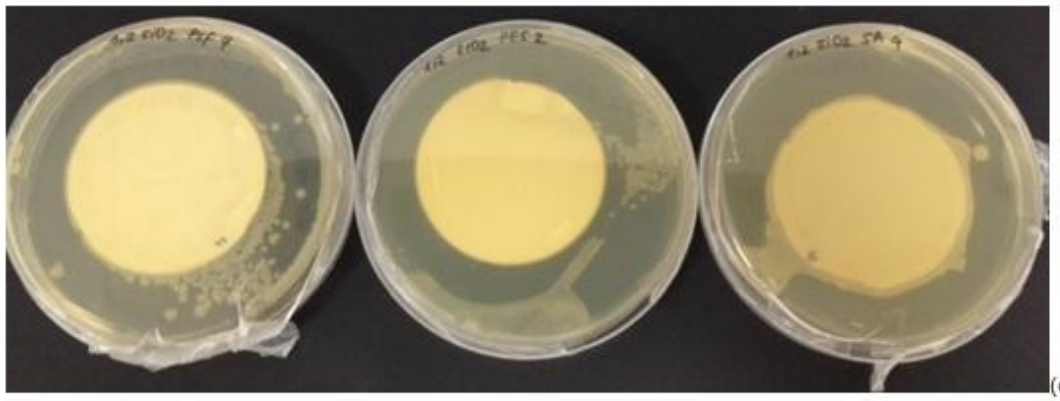

(c)

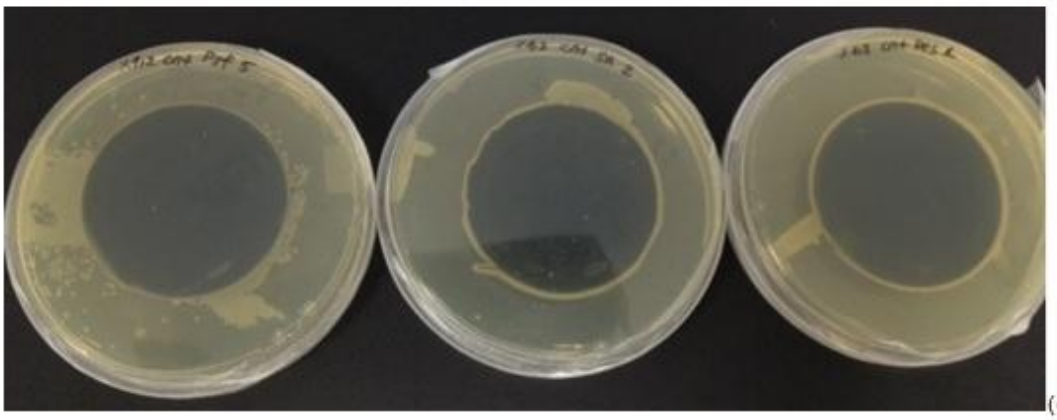

(d)

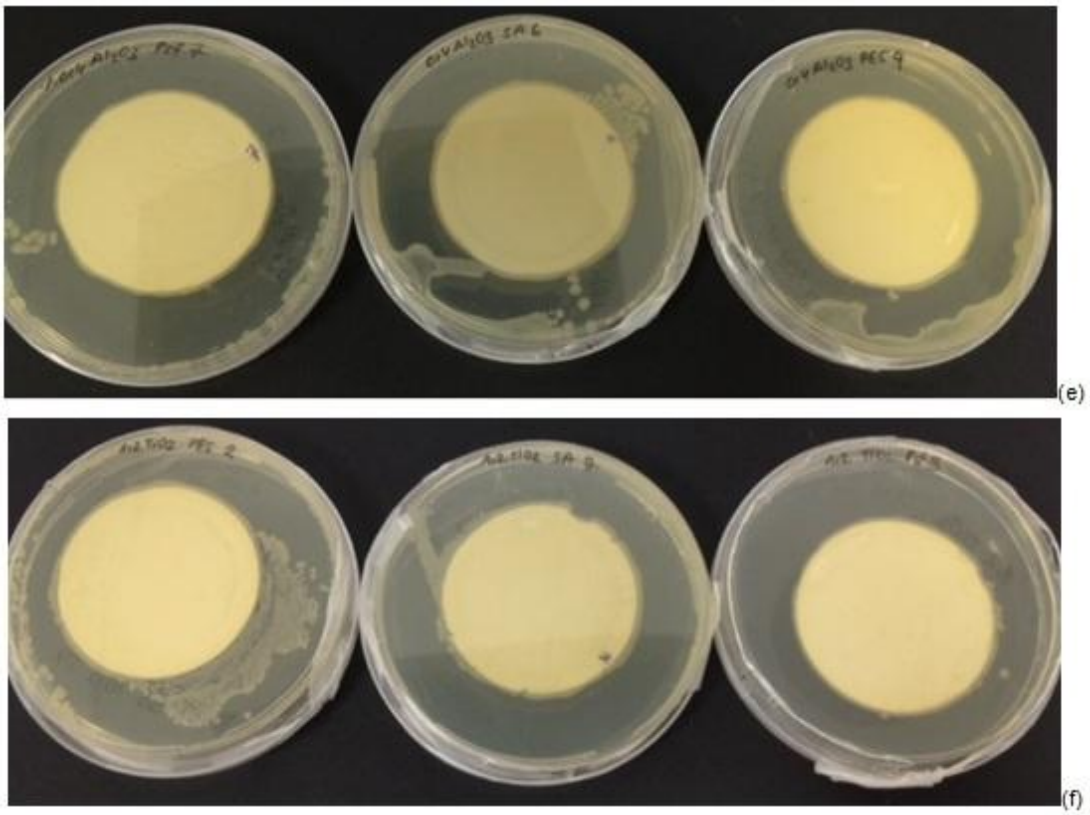

Figure 4. 74. The photographs of viability test of suspended *E.coli* cells.

5. CONCLUSIONS

Results of the performance and characterization tests for bare membranes containing PS, PES and CA polymers; and for the composite membranes containing bothPS, PES and CA polymers and AgNP, SiNP, CNT, AlONP and TiNP nanoparticles are given below as tables comparatively in order to determine the ingredient ratios for further studies. Results for the bare PS and composite PS membranes are given in theTable 5. 1. To prevent confusion, average numbers are given without the standard deviation values for each parameter. Optimum nanomaterial ratios were determined by taking the majority into account and optimum values were marked with a darker color for each parameter. For example; even though the highest $R_{carbohydrate}$ value and the smallest contact angle value were measured for 1.2% AgNP containing PS membrane, optimum values for most of the parameters were obtained for the 0.4% AgNP containing membrane. Consequently, optimum ratio was determined as 0.4% for the AgNP-PS composite membrane. Similarly, optimum nanomaterial ratios were determined as 1.2% for SiNP, CNT and TiNP nanoparticles and 0.4% for AlONP nanoparticle. Results for the bare PES and composite PES membranes are given in theTable 5. 2. Similar to the PS composite membranes, optimum nanomaterial ratios were determined as 1.2% for SiNP, CNT and TiNP nanoparticles and 0.4% for AlONP nanoparticle. But the optimum AgNP ratio was determined as 0.4% for PES membrane. Results for the bare CA and composite CA membranes are given in the Table 5. 3. For CA membranes, optimum nanomaterial ratios were determined as 0.4% for AgNP, SiNP and TiNP nanoparticles and 0.8% for CNT and AlONP nanoparticles.

From the all results, major findings are listed as follows:

1. Bare polymeric membrane production experiments (as the rate of polymer increases);

- Viscosity of dope solutions increased,
- Permeability values decreased,

- MWCO values decreased,
- Protein and carbohydrate filtration performances decreased (Flux, volume of permeate decreased), protein rejection rates for PS and PES membranes aresimilar, but for CA membranes it is increased. Carbohydraterejection rates are very low compared to protein rejection rates,
- Membrane porosity did not change much,
- Shrinkage ratios decreased, (Shrinkage ratios of CA membranes are very high compared to other membranes)
- Contact angle value decreased a little,
- Roughness value decreased a little,
- 14% polymer ratio was chosen at the end of the experiments.

2. Nanocomposite membrane production experiments;

- Viscosities of the polymer dope solutions increased as the addition of NP, but increasing NP ratio did not make too much change,
- New properties provided by nanomaterial addition varied for different polymer types. For example; addition of CNT was increased permeability of PES membranes but decreased for PS and CA membranes. In addition, addition of TiNP improved filtration performances of CA membranes but did not affect much to other polymer types.
- MWCO values differ for different NPs and NP ratios even for same polymer type and ratio. Therefore, it was thought that addition of NPs change membranes pore sizes and distribution.
- Values of membrane porosity experiments did not change much for various NPs and polymers so membranes porosities were similar for membranes.
- Addition of NPs decreased the contact angle value for most of the membranes. Therefore, NP addition make membranes surface more hydrophilic. However, increased hyrophlicity did not affect the permeabilities as expected. Accordingly, it could not said that increased hydrophlicity caused by NP addition is directly affectingthe permeability by itself.

- Roughness was decreased by the addition of NP for CA membranes, but for PS and PES membranes,it was generally increased. It is also hard to say that roughness value directly affect the permeability and filtration performances.

3. Membrane filtration experiments;

- Filtration of model EPS solution showed that filtration performance did not relate with permeability values so it also did not relate with porosity, MWCO values and hydrophilicity but it was related with roughness values.
- For *E.coli* filtrations, high fluxes were observed for PS and CA membranes with the addition of AgNP, CNT and TiNP as indicated in literature as antibacterial properties. For PES membranes, higher fluxes were observed for CNT and AlNP nanocomposites.
- At the end of viability experiments, nanocomposite membranes were compared and resulted that membranes produced with AgNP and AlONP had a smaller growing ring around the membrane, especially 0.4AgNP-PS membrane had no growth at all.

Table 5. 1. Filtration performances of bare and nanocomposite PS membranes.

	Bare	**AgNP**			**SiNP**			**CNT**			**AlONP**			**TiNP**		
Parameter	**14%**	**0.4%**	**0.8%**	**1.2%**	**0.4%**	**0.8%**	**1.2%**	**0.4%**	**0.8%**	**1.2%**	**0.4%**	**0.8%**	**1.2%**	**0.4%**	**0.8%**	**1.2%**
Permeability ($L/m^2h.bar$)	154	218	210	**225**	95	108	**193**	140	109	**150**	**213**	180	144	**234**	160	176
MWCO(kDa)	254	**423**	428	415	**121**	113	118	329	403	**511**	735	528	925	641	844	1624
$J_{protein}$ (L/m^2h) (%FRR)	27 (82)	**79 (63)**	54 (76)	62 (69)	15 (85)	45 (64)	**60 (69)**	46 (67)	48 (55)	**53 (55)**	**68 (69)**	58 (66)	40 (72)	58 (74)	46 (74)	**65 (67)**
$R_{protein}$(%)	97	90	90	**91**	82	**84**	82	99	99	**99**	**98**	97	**98**	83	87	**98**
$J_{carbohydrate}$ (L/m^2h) (%FRR)	52 (65)	71 (67)	60 (72)	**74 (51)**	48 (53)	49 (51)	**84 (50)**	55 (58)	50 (52)	**62 (59)**	**77 (61)**	88 (49)	64 (56)	99 (55)	86 (35)	**116 (14)**
$R_{carbohydrate}$(%)	29	**25**	22	23	**50**	36	25	23	10	**25**	**20**	16	15	8	13	17
Porosity (%)	85	85	86	**87**	**89**	88	**89**	90	90	**90**	90	**91**	89	87	87	**88**
Shrinkage(%)	5	1	4	**1**	2	**1**	**1**	5	**2**	4	6	**4**	5	5	**2**	**2**
Contact angle (^{0})	71	60	56	**52**	68	**65**	69	62	**59**	**59**	**46**	62	63	**22**	29	30
R_a(nm)	23.4	23.2	28.5	23.5	29.0	43.7	37.6	26.6	20.8	26.1	25.7	33.0	45.5	37.0	35.0	54.0
Surface charge (mV)	-20.2±0.1	-	-	-13.8±1.0	-	-	-8.9±1.0	-	-	-10.7±1.0	-	-	-8.4±1.0	-	-	-13.6±1.0

Table 5. 2. Filtration performances of bare and nanocomposite PES membranes.

	Bare	**AgNP**			**SiNP**			**CNT**			**AlONP**			**TiNP**		
Parameter	**14%**	**0.4%**	**0.8%**	**1.2%**	**0.4%**	**0.8%**	**1.2%**	**0.4%**	**0.8%**	**1.2%**	**0.4%**	**0.8%**	**1.2%**	**0.4%**	**0.8%**	**1.2%**
Permeability ($L/m^2h.bar$)	365	**327**	248	220	110	260	**297**	277	371	**401**	324	257	**338**	235	307	**321**
MWCO(kDa)	307	252	**264**	232	82	153	**188**	694	**797**	707	487	504	702	367	503	2900
$J_{protein}$ (L/m^2h) (%FRR)	68 (82)	**69 (76)**	36 (87)	49 (85)	52 (59)	71 (73)	**77 (48)**	**75 (72)**	71 (82)	73 (81)	**77 (76)**	71 (71)	58 (83)	59 (76)	**64 (79)**	49 (84)
$R_{protein}$(%)	98	**83**	77	78	85	**86**	84	98	**99**	**99**	**95**	92	94	**99**	97	96
$J_{carbohydrate}$ (L/m^2h) (%FRR)	50 (87)	**77 (77)**	68 (73)	69 (63)	73 (42)	**95 (65)**	82 (44)	**104 (61)**	94 (73)	86 (78)	128 (61)	137 (52)	**142 (54)**	102 (52)	112 (59)	**118 (62)**
$R_{carbohydrate}$(%)	13	24	15	**44**	1	10	**12**	5	15	**25**	**10**	7	5	3	11	13
Porosity(%)	85	**86**	**86**	**86**	**89**	**89**	**89**	**89**	88	88	89	90	**91**	85	**86**	85
Shrinkage(%)	4	3	3	**1**	**1**	**1**	**1**	3	**1**	2	6	**2**	5	5	2	**1**
Contact angle (^{0})	71	31	**21**	22	68	49	**36**	71	47	**25**	47	45	**33**	29	24	**24**
R_a(nm)	15.0	16	21	18.8	21.0	23.9	27.9	18.6	16.6	17.3	20.5	24.7	21.1	19.8	25.0	39.0
Surface charge (mV)	-23±0.2	-	-	-15±0.2	-	-	-13±1.2	-	-	-11±0.7	-	-	-14±0.5	-	-	-21±0.7

Table 5. 3. Filtration performances of bare and nanocomposite CA membranes.

	Bare	**AgNP**			**SiNP**			**CNT**			**AlONP**			**TiNP**		
Parameter	**14%**	**0.4%**	**0.8%**	**1.2%**	**0.4%**	**0.8%**	**1.2%**	**0.4%**	**0.8%**	**1.2%**	**0.4%**	**0.8%**	**1.2%**	**0.4%**	**0.8%**	**1.2%**
Permeability ($L/m^2h.bar$)	79	**67**	49	40	**14**	7	7	7	**10**	9	111	**143**	132	**148**	146	144
MWCO(kDa)	203	**177**	129	136	**121**	42	31	81	101	**133**	145	169	180	294	490	1770
$J_{protein}$ (L/m^2h) (%FRR)	57 (21)	**54 (24)**	40 (14)	27 (33)	4 (67)	4 (29)	**9 (6)**	6 (19)	**8 (18)**	7 (20)	31 (82)	32 (76)	**34 (78)**	**101 (33)**	71 (50)	92 (33)
$R_{protein}$(%)	56	**38**	24	**38**	45	**58**	**58**	95	**97**	96	27	**26**	**28**	23	36	**45**
$J_{carbohydrate}$ (L/m^2h) (%FRR)	54 (25)	**49 (34)**	46 (15)	33 (27)	**16 (7)**	6 (14)	3 (50)	8 (11)	4 (33)	**9 (4)**	**94 (26)**	80 (40)	69 (48)	99 (29)	**136 (13)**	123 (10)
$R_{carbohydrate}$(%)	16	2	1	**4**	57	**77**	**77**	18	**25**	**25**	4	12	**32**	**5**	5	2
Porosity (%)	89	87	**88**	87	**92**	91	89	90	**91**	**91**	**92**	**92**	91	**88**	**88**	87
Shrinkage(%)	38	25	**22**	**22**	**31**	35	32	27	30	**27**	27	**24**	25	**23**	**23**	**23**
Contact angle (^{0})	53	**43**	50	48	**58**	61	68	49	45	**41**	**36**	**36**	**36**	27	24	**10**
R_a(nm)	76.8	19.2	52.0	69.6	14.0	27.9	71.6	66.0	66.9	66.5	53	93.2	50.9	32.4	36.2	35.3
Surface charge (mV)	-10±0..2	-	-	-12±1.2	-	-	-11±0.1	-	-	-14±0.5	-	-	-13±0.4	-	-	-10±0.4

REFERENCES

AWWA Membrane Technology Research Committee, (2005). Recent advances and research need in membrane fouling. J. AWWA 97(8), 79-89.

Ba, C., Ladner, D.A., Economy, J., (2010) Using polyelectrolyte coatings to improve fouling resistance of a positively charged nanofiltration membrane, J. Membr. Sci. 347, 250–259.

Babu, V.R., Kim, C., Kim, S., Ahn, C., Lee, Y.I., (2010). Development of semi-interpenetrating carbohydrate polymeric hydrogels embedded silver nanoparticles and its facile studies on *E. coli*, Carbohydr. Polym. 81, 196–202.

Bae, T.H., Tak, T.M., (2005). Effect of TiO_2 nanoparticles on fouling mitigation of ultrafiltration membranes for activated sludge filtration. J. Membr. Sci. 249,1-8.

Bae, T.H., Kim, I.C., Tak, T.M., (2006). Preparation and characterization of fouling resistant TiO_2 self-assembled nanocomposite membranes. J. Membr. Sci. 275, 1-5.

Baker, R.W., (2004). Membrane Technology and Applications. (2th ed). NewYork: McGraw-Hill

Basri, H., Ismail, A.F., Aziz, M., (2011). Polyethersulfone (PES)–silver composite UF membrane: Effect of silver loading and PVP molecular weight on membrane morphology and antibacterial activity, Desalination 273, 72–80.

Bottino, A., Capannelli, G., Comite, A., (2002). Preparation and characterization of novel porous PVDF-ZrO_2 composite membranes. Desalination 146, 35-40.

Chae, S., Wang, S., Hendren, Z.D., Wiesner, M.R., Watanabe, Y., Gunsch, C.K., (2009). Effects of fullerene nanoparticles on *Escherichia coli* K-12 respiratory activity in aqueous suspension and potential use for membrane biofouling control. J. Membr. Sci. 329, 68-74.

Choi, W., Termin, A., Hoffmann, M.R., (1994). The role of metal ion dopants in quantum-sized TiO_2: correlation between photoreactivity and charge carrier recombination dynamics. J. Phys. Chem. 98, 13669-13672.

Chou, W.L., Yu, D.G., Yang, M.C., (2005). The preparation and characterization of silver loading cellulose acetate hollow fiber membrane for water treatment, Polym. Adv. Technol. 16, 600–607.

Cortalezzi, M.M., Rose, J., Barron, A.R., Wiesner, M.R., (2002). Characteristics of ultrafiltration ceramic membranes derived from alumoxane nanoparticles. J. Membr. Sci. 205, 33-43.

Cortalezzi, M.M., Rose, J., Wells, G.F., Bottero, J.Y., Barron, A.R., Wiesner, M.R., (2003). Ceramic membranes derived from ferroxane nanoparticles; a new route for the fabrication of iron oxide ultrafiltration membranes. J. Membr. Sci. 227, 207-217.

Drioli, E., Giorno, L., (2010). Comprehensive Membrane Science and Engineering. United Kingdom: Elseiver

Dubois, M., Gilles, K.A., Hamilton, J.K., Rebers, P.A., Smith, F., (1956). Colorimetric Method for Determination of Sugarsand Related Substances Analytical Chemistry, 28 : 3.

Helin, H., Na, Li, Linlin, W., Hui, Z., Guangxia, W., Zonghuan, Y., Xiangwei, L., Lianyi, T., (2008). Anti-fouling ultrafiltration prepared from polysulfone-graft-methylacrylate compolyers by UV-induced grafting method. J. Environ. Sci. 20, 565-570.

Hirano, S., Wakasa, Y., Saka, A., Yoshizawa, S., Oya-Seimiya, Y., Hishinuma, Y., Nishimura, A., Matsumoto, A., Kumakura, H., (2003). Preparation of Bi-2223 bulk composed with silver-alloy wire, Phys. C (392–396), 458–462.

Holister, P., (2002). *Nanotech - the tiny revolution*. CMP Cientifica [Online]. Available: http://www.cientifica.com/html/Whitepapers/wpfiles/nanotech_WP.pdf [2013, April 02]

Holister, P., Weener, J.W., Vas, C. R., & Harper, T., (2003). *Nanoparticles; Technology White Papers nr. 3*.Cientifica [Online]. Available: http://www.cientifica.com/html/Whitepapers/whitepapers.htm [2013, April 05]

Jadav, G.L., Singh, P.S., (2009). Synthesis of novel silica-polyamide nanocomposite membrane with enhanced properties. J. Membr. Sci. 328, 257-267.

Kim, J., Davies, S.H.R., Baumann, M.J., Tarabara, V.V., Masten, S.J., (2008). Effects of ozone dosage and hydrodynamic conditions on the permeate flux in a hybrid ozonation-ceramic ultrafiltration system treating natural waters. J. Membr. Sci. 311, 165-172.

Kim, K.S., Lee, K.H., Cho, K., Park, C.E., (2002). Surface modification of polysulfone ultrafiltration membrane by oxygen plasma treatment, J. Membr. Sci. 199, 135–145.

Kim, S.H., Kwak, S.Y., Sohn, B.H., Park, T.H., (2003). Design of TiO_2 nanoparticle self- assembled aromatic polyamide thin-film-composite (TFC) membrane as an approach to solve biofouling problem. J. Membr. Sci. 211, 157-165.

Kochkodan, V.M., Hilal, N., Goncharuk, V.V., Al-Khatib, L., Levadna, T.I., (2006). Effect of the Surface Modification of Polymer Membranes on Their Microbiological Fouling, Colloid Journal. 68, 267–273.

Li, J.B., Zhu, J.W., Zheng, M.S., (2007). Morphologies and properties of poly(phthala- zinone ether sulfone ketone) matrix ultrafiltration

membranes with entrapped TiO_2 nanoparticles. J. Appl. Polym. Sci. 103(6), 3623-3629.

Li, J.F., Xu,Z.-L., Yang, H., Yu, L.-Y., Liu, M., (2009a). Effect of TiO_2 nanoparticles on the surface morphology and performance of microporous PES membrane. Appl. Surf. Sci. 255, 4725-4732.

Li, J.H., Xu, Y.Y., Zhu, L.P., Wang, J.H., Du, C.H., (2009b). Fabrication and characterization of a novel TiO_2 nanoparticle self-assembly membrane with improved fouling resistance. J. Membr. Sci. 326, 659-666.

Liu, F., Xu, Y.Y., Zhu, B.K., Zhang, F., Zhu, L.P., (2009). Preparation of hydrophilic and fouling resistant poly(vinylidene fluoride) hollow fiber membranes, J. Membr. Sci. 345, 331–339.

Luo, M.J., Zhao, J.Q., Tang, W., Pu, C.S., (2005). Hydrophilic modification of poly (ether sulfone) ultrafiltration membrane surface by self-assembly of TiO_2 nanoparticles. Appl. Surf. Sci. 249, 76-84.

Mansourpanah, Y., Madaeni, S.S., Rahimpour, A., Farhadian, A., Taheri, A.H., (2009). Formation of appropriate sites on nanofiltration membrane surface for binding TiO_2 photo-catalyst: performance, characterization, and fouling-resistant capability. J. Membr. Sci. 330, 297-306.

Mayer, M., Braun, R., Fuchs, W., (2006) Comparison of various aeration devices for air sparging in crossflow membrane filtration. J. Membr. Sci. 277, 258–269

Mulder, M., (1996). Basic Principles of Membrane Technology. Boston: Kluwer Academic Publishers, Netherlands, pp.6.

NathK., (2008). Membrane Separation Processes. Prentice-Hall, India, pp.30-33.

Prud Homme, R.K., Froiman, G., A., Haogland, D., (1982) Molecular sice determination of xanthan polysaccharide. Carbohydrate Research, 106, 225-233.

Rahimpour, A., Madaeni, S.S., Taheri, A.H., Mansourpanah, Y., (2008). Coupling TiO_2 nanoparticles with UV irradiation for modification of polyether sulfone ultra- filtration membranes. J. Membr. Sci. 313, 158-169.

Rana, D., Matsuura, T., (2010). Surface Modifications for Antifouling Membranes, Chem. Rev., 110, 2448–2471.

Sae-Khow, O., Mitra, S., (2009). Fabrication and characterization of carbon nanotubes immobilized inporous polymeric membranes. J. Mater. Chem. 19 (22), 3713-3718.

Scott, K., (1999) Membrane Materials, Preparation and Characterisation, Handbook of Industrial Membranes, Elsevier Science & Technology Books, UK, 1999, pp 201.

Su, Y., Cheng, W., Li, Chao, Jiang, Z., (2009). Preparation of antifouling ultrafiltration membranes with poly(ethyleneglucose)-graft-copolymers. J. Membr. Sci. 329, 246-252.

Susanto, H., Ulbricht, M., (2009). Characteristics, performance and stability of polyethersulfone ultrafiltration membranes prepared by phase separation method using different macromolecular additives, J. Membr. Sci. 327, 125–135.

Takao, S., (1983). Process for Producing Acrylonitrile Separation Membranes in Fibrous Form, US Patent 4,409,162.

Taurozzi, J.S., Arul, H., Bosak, V.Z., Burban, A.F., Voice, T.C., Bruening, M.L., Tarabara, V.V., (2008). Effect of filler incorporation route on the properties of polysulfone-silver nanocomposite membranes of different porosities. J. Membr. Sci. 325, 58-68.

The Royal Society, & The Royal Academy of Engineering., (2004). Nanoscience and nanotechnologies: opportunities and uncertainties: The Royal Society & The Royal Academy of Engineering.

Twist, J., (2004). *Myths and realities of nano futures*. BBC News Online UK edition [Online]. Available: http://news.bbc.co.uk/1/hi/sci/tech/3920685.stm [2013, April 11]

Verweji, H., Schillo, M.C., Li, J., (2007). Fast mass transport through carbonnanotube membranes. Small 12, 1996-2004.

Wang L.K, Chen, J. P., Hung, Y.T., Shammas, N. K.,(2011). Membrane and Desalination Technologies. NewYork: Springer, pp.4.

Wang, Y., Yang, Q., Shan, G., Wang, C., Du, J., Wang, S., Li, Y., Chen, X., Jing, X., Wei, Y., (2005). Preparation of silver nanoparticles dispersed in polyacrylonitrile nanofiber film spun by electrospinning, Mater. Lett. 59, 3046–3049.

Wood, S., Jones, R., & Geldart, A., (2003). *The Social and Economic Challenges of Nanotechnology* (No. 0-86226-294-1). Swindon, UK: The Economic and Social Research Council.

Wu, G., Gan, S., Cui, L., Xu, Y., (2008). Preparation and characterization of PES/TiO_2 composite membranes. Appl. Surf. Sci. 254, 7080-7086.

Yan, L., Li, Y.S., Xiang, C.B., (2005). Preparation of poly (vinylidene fluoride) (PVDF) ultrafiltration membrane modified by nano-sized alumina (Al_2O_3) and its antifouling research. Polymer 46, 7701-7706.

Yang, H.L., Lin, J.C.T., Huang, C., (2009). Application of nanosilver surface modification to RO membrane and spacer for mitigating biofouling in seawater desalination, Water Research 43, 3777 – 3786.

Yang, Y., Zhang, H., Wang, P., Zheng, Q., Li, J., (2007). The influence of nano-sized TiO2 fillers on the morphologies and properties of PSF UF membrane. J. Membr. Sci. 288, 231-238.

Yu, H.Y., Hu, M.X., Xu, Z.K, Wang, J.L., Wang, S.Y., (2005). Surface modification of polypropylene microporous membranes to improve their antifouling property in MBR: NH_3 plasma treatment, Separation and Purification Technology.45, 8–15.

Zodrow, K., Brunet, L., Mahendra, S., Li, D., Zhang, A., Li, Q.L., Alvarez, P.J.J., (2009). Polysulfone ultrafiltration membranes impregnated

with silver nanoparticles show improved biofouling resistance and virus removal. Water Research 43 (3), 715-723.

CURRICULUM VITAE

Name Surname:	Merve Şile
Place and Date of Birth:	04.06.1988, Istanbul
Address:	Büyükdere mah., Bostan sk., No:2/6 Sarıyer/IST
E-Mail:	mervesile@gmail.com
B.Sc.:	I.T.U. Environmental Engineering